NASA/TM—2014-218384

Investigation of Spiral Bevel Gear Condition Indicator Validation Via AC–29–2C Using Damage Progression Tests

Paula J. Dempsey
Glenn Research Center, Cleveland, Ohio

September 2014

NASA STI Program . . . in Profile

Since its founding, NASA has been dedicated to the advancement of aeronautics and space science. The NASA Scientific and Technical Information (STI) program plays a key part in helping NASA maintain this important role.

The NASA STI Program operates under the auspices of the Agency Chief Information Officer. It collects, organizes, provides for archiving, and disseminates NASA's STI. The NASA STI program provides access to the NASA Aeronautics and Space Database and its public interface, the NASA Technical Reports Server, thus providing one of the largest collections of aeronautical and space science STI in the world. Results are published in both non-NASA channels and by NASA in the NASA STI Report Series, which includes the following report types:

- TECHNICAL PUBLICATION. Reports of completed research or a major significant phase of research that present the results of NASA programs and include extensive data or theoretical analysis. Includes compilations of significant scientific and technical data and information deemed to be of continuing reference value. NASA counterpart of peer-reviewed formal professional papers but has less stringent limitations on manuscript length and extent of graphic presentations.

- TECHNICAL MEMORANDUM. Scientific and technical findings that are preliminary or of specialized interest, e.g., quick release reports, working papers, and bibliographies that contain minimal annotation. Does not contain extensive analysis.

- CONTRACTOR REPORT. Scientific and technical findings by NASA-sponsored contractors and grantees.

- CONFERENCE PUBLICATION. Collected papers from scientific and technical conferences, symposia, seminars, or other meetings sponsored or cosponsored by NASA.

- SPECIAL PUBLICATION. Scientific, technical, or historical information from NASA programs, projects, and missions, often concerned with subjects having substantial public interest.

- TECHNICAL TRANSLATION. English-language translations of foreign scientific and technical material pertinent to NASA's mission.

Specialized services also include creating custom thesauri, building customized databases, organizing and publishing research results.

For more information about the NASA STI program, see the following:

- Access the NASA STI program home page at *http://www.sti.nasa.gov*

- E-mail your question to *help@sti.nasa.gov*

- Fax your question to the NASA STI Information Desk at 443–757–5803

- Phone the NASA STI Information Desk at 443–757–5802

- Write to:
  STI Information Desk
  NASA Center for AeroSpace Information
  7115 Standard Drive
  Hanover, MD 21076–1320

NASA/TM—2014-218384

Investigation of Spiral Bevel Gear Condition Indicator Validation Via AC–29–2C Using Damage Progression Tests

Paula J. Dempsey
Glenn Research Center, Cleveland, Ohio

National Aeronautics and
Space Administration

Glenn Research Center
Cleveland, Ohio 44135

September 2014

This work was sponsored by the Fundamental Aeronautics Program at the NASA Glenn Research Center.

Level of Review: This material has been technically reviewed by technical management.

Available from

NASA Center for Aerospace Information
7115 Standard Drive
Hanover, MD 21076–1320

National Technical Information Service
5301 Shawnee Road
Alexandria, VA 22312

Available electronically at http://www.sti.nasa.gov

Investigation of Spiral Bevel Gear Condition Indicator Validation Via AC–29–2C Using Damage Progression Tests

Paula J. Dempsey
National Aeronautics and Space Administration
Glenn Research Center
Cleveland, Ohio 44135

Executive Summary

This report documents the results of spiral bevel gear rig tests performed under a NASA Space Act Agreement with the Federal Aviation Administration (FAA) to support validation and demonstration of rotorcraft Health and Usage Monitoring Systems (HUMS) for maintenance credits via FAA Advisory Circular (AC) 29–2C, Section MG–15, Airworthiness Approval of Rotorcraft (HUMS) (Ref. 1). The overarching goal of this work was to determine a method to validate condition indicators in the lab that better represent their response to faults in the field.

Using existing in-service helicopter HUMS flight data from faulted spiral bevel gears as a "Case Study," to better understand the differences between both systems, and the availability of the NASA Glenn Spiral Bevel Gear Fatigue Rig, a plan was put in place to design, fabricate and test comparable gear sets with comparable failure modes within the constraints of the test rig. The research objectives of the rig tests were to evaluate the capability of detecting gear surface pitting fatigue and other generated failure modes on spiral bevel gear teeth using gear condition indicators currently used in fielded HUMS.

Nineteen final design gear sets were tested. Tables were generated for each test, summarizing the failure modes observed on the gear teeth for each test during each inspection interval and color coded based on damage mode per inspection photos. Gear condition indicators (CI) Figure of Merit 4 (FM4), Root Mean Square (RMS), ±1 Sideband Index (SI1) and ±3 Sideband Index (SI3) were plotted along with rig operational parameters. Statistical tables of the means and standard deviations were calculated within inspection intervals for each CI. As testing progressed, it became clear that certain condition indicators were more sensitive to a specific component and failure mode. These tests were clustered together for further analysis. Maintenance actions during testing were also documented. Correlation coefficients were calculated between each CI, component, damage state and torque.

Results found test rig and gear design, type of fault and data acquisition can affect CI performance. Results found FM4, SI1 and SI3 can be used to detect macro pitting on two more gear or pinion teeth as long as it is detected prior to progressing to other components or transitioning to another failure mode. The sensitivity of RMS to system and operational conditions limit its reliability for systems that are not maintained at steady state. Failure modes that occurred due to scuffing or fretting were challenging to detect with current gear diagnostic tools, since the damage is distributed across all the gear and pinion teeth, smearing the impacting signatures typically used to differentiate between a healthy and damaged tooth contact.

This is one of three final reports published on the results of this project. In the second report, damage modes experienced in the field will be mapped to the failure modes created in the test rig. The helicopter CI data will then be re-processed with the same analysis techniques applied to spiral bevel rig test data. In the third report, results from the rig and helicopter data analysis will be correlated. Observations, findings and lessons learned using sub-scale rig failure progression tests to validate helicopter gear condition indicators will be presented.

Contents

1.0 Background

This report documents the results of spiral bevel gear rig tests performed under a NASA Space Act Agreement with the Federal Aviation Administration (FAA). These tests were performed to support validation and demonstration of rotorcraft Health and Usage Monitoring Systems (HUMS) for maintenance credits via FAA Advisory Circular (AC) 29–2C, Section MG–15, Airworthiness Approval of Rotorcraft (HUMS) (Ref. 1). Maintenance credits are modified inspection and removal criteria of components based on HUMS measured condition and actual usage. Maintenance credit validation includes providing evidence of damage detection algorithm effectiveness using acceptance limits, trending methods, tests and demonstration methods. These methods can include using data from naturally occurring aircraft faults and component fault testing on a test stand (Ref. 2). Due to time, cost and safety concerns, direct evidence via actual service on aircraft is typically replaced with rig tests where a measurable and known component fault is checked against the algorithm and its thresholds.

The Civil Aviation Authority (CAA) also published a document to provide guidance using vibration health monitoring (VHM), defined as "data generated by processing vibration signals to detect incipient failures or degradation of mechanical integrity," for maintaining helicopter rotor and drive systems (Ref. 3). These vibration signatures are referred to as "condition indicators" (CI) that develop when a fault occurs on a component and interacts with its operational environment. Within this CAA document, fault testing is also mentioned as a validation method to demonstrate algorithm damage detection effectiveness for specific faults.

The goal of this work was to determine a method to validate condition indicators in the lab that better represent their response to faults in the field. Due to differences in both systems and their operational environments, response of a CI to a fault in a test stand may not be representative of a CI response in a helicopter. For these situations, CI performance limitations must be defined to understand the risks in using a test rig validated CI on a helicopter. One obstacle in determining if CI response to a fault in a test rig is comparable to its response when measured on a helicopter is the limited availability of CI data from a faulted component flying on a helicopter.

Previous analyses were performed on rotorcraft spiral bevel gear condition indicator performance in support of the U.S. Army's Condition-Based Maintenance (CBM) program (Refs. 4 and 5). CI performance was evaluated using fielded helicopter datasets recorded when damage occurred on spiral bevel gear (pinion/gear) teeth located in helicopter nose gearboxes. In addition to thousands of hours of CI data collected before and after spiral bevel gear replacement, tear down analyses were performed documenting the extent of damage to the gear and pinion teeth. Within the timeframe when the faulted components were occurring in the helicopters, NASA Glenn Research Center had an existing available Spiral Bevel Gear Fatigue Test Rig.

Using this existing in-service HUMS flight data from faulted spiral bevel gears as a "Case Study," to better understand the differences between both systems, a plan was put in place to design and test comparable gear sets within the constraints of the test rig. The rationale for testing in the component test rig, as opposed to a full-scale system, were based on the cost and time it would take to design, develop and build testing capabilities combined with the time required to initiate and progress a defect in the actual helicopter component. The availability of fielded helicopter HUMS CI data when spiral bevel gear damage occurred, the availability of the NASA Glenn Spiral Bevel Gear Fatigue Rig and the availability of the same HUMS installed on the helicopters for use in the rig made this a cost effective proposition within a reasonable timeframe.

The requirements for spiral bevel gear damage progression tests to be performed in the NASA Glenn Spiral Bevel Gear Fatigue Test Rig are outlined in Reference 6. Results of these tests will be discussed in this report. This is one of three final reports published on the results of this project. In the second report titled, "Investigation of Spiral Bevel Gear Condition Indicator Validation via AC–29–2C Using Fielded Rotorcraft HUMS Data," the helicopter data will be re-processed with same analysis techniques applied to spiral bevel rig test data. The damage modes experienced in the field will be mapped to the failure

modes created in the test rig. In the third report titled, "Investigation of Spiral Bevel Gear Condition Indicator Validation Via AC–29–2C Combining Test Rig Damage Progression Data with Fielded Rotorcraft Data," results from the rig and helicopter data published in reports 1 and 2 will be correlated and observations, findings and lessons learned using sub-scale rig failure progression tests to validate helicopter gear condition indicators will be discussed.

2.0 Objectives and Approach

Tests were performed on 19 spiral bevel gear sets in the NASA Glenn Spiral Bevel Gear Fatigue Test Rig to simulate the fielded failures of spiral bevel gears installed in a helicopter. Gear sets were tested until damage initiated and progressed on two or more gear or pinion teeth. During testing, gear health monitoring data and operational parameters were measured and recorded and tooth damage progression was documented. The specific objectives of the tests are as follows:

a) Generate "naturally occurring" accelerated helicopter failure modes on gear sets tested in the Spiral Bevel Gear Fatigue Rig.
b) Summarize gear tooth damage modes and magnitude using damage progression photographs.
c) Collect gear vibration condition indicator data during damage progression tests.
d) Correlate CI response, damage magnitude and progression time intervals.
e) Evaluate the capability of detecting gear surface pitting fatigue and other generated failure modes on spiral bevel gear teeth using condition indicators.
f) Evaluate the effect of operational and environmental conditions on CI performance.
g) Group or cluster comparable damage modes from different gear tests.

3.0 Test Rig Description

Tests were performed in the Spiral Bevel Gear Fatigue Test Rig at NASA Glenn Research Center. A detailed description of this test facility is provided in References 7 and 8. The Spiral Bevel Gear Fatigue Test Rig is illustrated in Figure 1. A cross sectional view is shown in Figure 2. The facility operates as a closed-loop torque regenerative system, where the drive motor only needs enough power to overcome power losses within the system. The load is locked into the loop via a split shaft and a thrust piston that forces a floating helical gear axially into mesh. The one hundred horsepower drive motor supplies the facility with rotation and loop losses via v-belts to the axially stationary helical gear.

Two sets of spiral bevel gears are installed in the test rig and tested simultaneously. Facing the gearboxes, per Figure 1, the left gear set (pinion/gear) is referenced as left and the right gear set (pinion/gear) is referenced as right within the paper. The spiral bevel gears on the left side operate where the pinion drives the gear in the normal speed reducer mode and the right side of the facility acts as a speed increaser. However, the concave side of the pinion is always in contact with the convex side of the gear on either side of the test facility.

Qualified helicopter transmission oil, AEROSHELL Turbine Oil 555, was used in the test rig during testing. Both gear sets are lubricated with oil jets pumped from an oil reservoir. The lubrication is gravity drained from the gearbox then exits the gearbox and flows through an inductance type in-line oil debris sensor, then past a magnetic chip detector. A strainer and a 3μm filter are located downstream of the oil debris (OD) sensor to capture any debris before returning to the sensor and gearbox.

As a precursor to these tests, preliminary checkout tests were performed in the Spiral Bevel Gear Fatigue Rig with a different gear design to check out the rig operation, facility instrumentation, facility data acquisition, research instrumentation and research data acquisition. Results of these preliminary checkout tests can be found in References 9 to 12.

Damage progression tests were also performed on eight prototype gear sets (pinion/gear) prior to testing of the final gear set design. The eight gear sets tested differed from the final design in that they were not shot peened, copper plating used for masking parts prior to heat treatment was not removed, had higher measured surface roughness and gear tooth edges were not broken to design specifications. Results of these tests can be found in References 13 and 14.

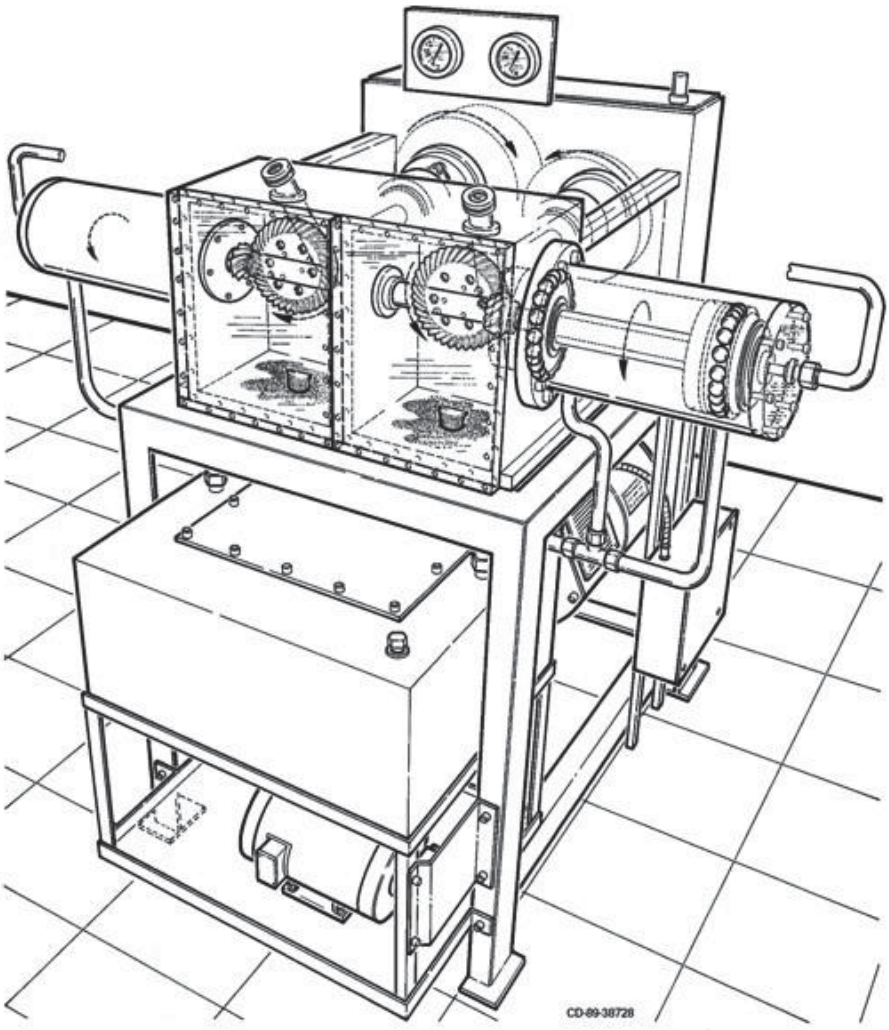

Figure 1.—Spiral Bevel Gear Fatigue Test Rig.

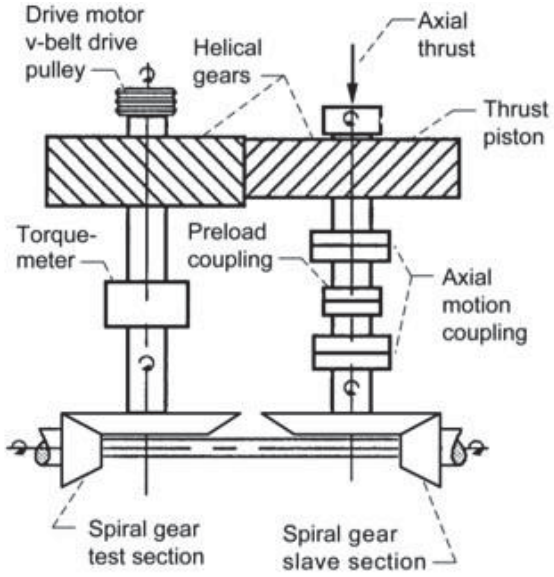

Figure 2.—Cross section of Spiral Bevel Gear Fatigue Rig.

4.0 Instrumentation and Data Acquisition

During these tests, three data acquisition systems were used. Vibration, oil debris, torque and speed data were collected once every minute with the NASA Glenn research data acquisition system (DAQ), referred to as the Mechanical Diagnostic System Software (MDSS). Vibration and speed data were collected from a second set of sensors with a helicopter HUMS referred to as the Modern Signal Processing Unit (MSPU). Operational parameters were collected with a third system referred to as the facility DAQ. These operational parameters included torque, speed, and right and left gearbox oil temperatures and pressures. Details of the instrumentation capabilities and installation will be discussed in the following sections. Transfer paths of the signal transmission from the gear mesh inside the gear box to the accelerometer installed on the gearbox external housing were also measured to verify the structure didn't filter accelerometer response from the vibration signatures at mesh to its installation location (Ref. 15).

4.1 Mechanical Diagnostic System Software (MDSS)

The NASA MDSS system acquires, digitizes and processes the tachometer pulses and accelerometer data. Acquisition was performed at a 200 KHz sample rate for one second duration every minute during rig rotation. Torque and oil debris sensor data were also recorded every minute with this system. A new experiment is set-up when a new gear set is installed on the test rig

For the MDSS system, accelerometers were installed on the right and left side of the test rig pinion support housings. Accelerometer frequency range was 0.7 to 20 KHz with a resonant frequency of ≥70 KHz. The MDSS accelerometers were mounted on the pinion support housing, radially and vertically with respect to the pinion, as shown in Figure 3. Facing the gearboxes, the left gear set (pinion/gear) and right gear set (pinion/gear) accelerometers were referenced as such in the MDSS system. Speed was measured with optical tachometers mounted on the left pinion shaft and left gear shaft to produce a separate once-per-revolution tachometer pulse for the pinion and gears.

An inductance type oil debris sensor was used to measure the ferrous debris generated during fatigue damage to the gear teeth. The MDSS records the particle counts measured by the oil debris sensor, their approximate size and an approximate mass. The sensor measures the number of particles and their approximate size based on user defined particle size ranges or bins. Based on the bin configuration, the average particle size for each bin is used to calculate the cumulative mass by assuming the average particle size as the diameter that is spherical in shape and multiplying it by the density of steel. Table 1 lists the 14 particle size ranges and the average particle size used to calculate accumulated mass during spiral bevel gear tests.

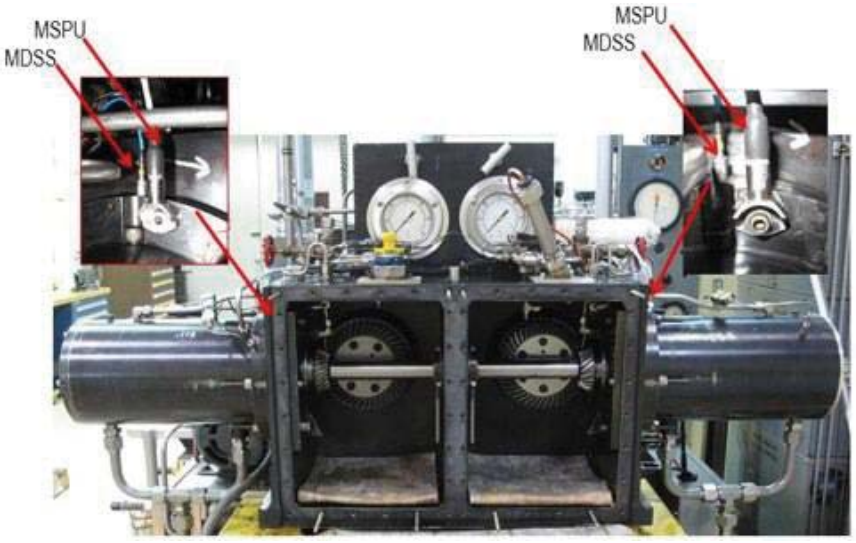

Figure 3.—Location of MDSS and MSPU Accelerometers.

TABLE 1.—SPIRAL BEVEL RIG OIL DEBRIS PARTICLE SIZE RANGES

Bin	Bin range, μm	Average Bin size	Bin	Bin range, μm	Average Bin size
1	225–275	250	8	575–625	600
2	275–325	300	9	625–675	650
3	325–375	350	10	675–725	700
4	375–425	400	11	725–775	750
5	425–475	450	12	775–825	800
6	475–525	500	13	825–900	863
7	525–575	550	14	900–1016	958

Figure 4.—Photograph of chip detector with captured debris.

Chip indications from the magnetic chip detector, when the gap was closed with debris, were also measured. For this magnetic chip detector, the MDSS records a voltage output from the chip detector until enough debris is collected on the magnet to close the gap. Then, the voltage output drops down to zero. The chip detector is a fuzz burn-off type. The operational principle of the fuzz burn-off chip detector involves the automatic discharge of a capacitor network after debris particles have bridged the gap of the two magnetic electrodes of the detector. A rapidly decaying pulse of energy controlled by capacitor size and operating voltage is applied to the debris bridging the gap. A photograph of debris captured on the chip detector is shown in Figure 4.

A commercially available non-contact rotary transformer shaft mounted torque sensor was used to measure torque during testing. A transformer transmits the AC excitation voltage to the strain gage bridge and another transfers signal output to the non-rotating part of the transducer. The facility DAQ provides the strain gage signal conditioning for the sensor.

4.2 Modern Signal Processing Unit (MSPU)

The MSPU system is an on-board rotorcraft HUMS system that acquires digitizes and processes the tachometer pulses and accelerometer data. The data is then downloaded to a ground station for further analysis. The configuration file used for the helicopter was modified for use in the test rig, limiting the components to those in the nose gearbox of the helicopter. Automatic acquisitions are set-up for every 30 min

when the rig is rotating. Due to the limited on-board storage capability of the MSPU system (80 MB), data must be downloaded daily. A new "tail" was defined when a new gear set was installed in the test rig.

For the MSPU system, accelerometers are also installed on the right and left side of the test rig. Accelerometer frequency range is 0.5 to 5 KHz with a resonant frequency of 26 KHz. A magnetic tachometer is installed on the right pinion and measures pinion pulses per tooth pass. The gear ratio is used to process the data at the correct speed for the gear. The MSPU accelerometers were mounted on the housing, in close proximity to the MDSS accelerometers, radially and vertically with respect to the pinion, as shown in Figure 3.

5.0 Test Gear Design

Prior to testing, design and fabrication of new gears was required. The gears tested were designed to represent a rotorcraft drive system gear mesh and fit within the space available in the Spiral Bevel Gear Fatigue Test Rig. The gear sets were fabricated under contract with an aerospace gear manufacturer. The gears were made from a steel alloy CEVM 9310, carburized, hardened and ground to AGMA quality 12. The gears were designed with the following requirements:

1. The gear set design was constrained to the space available in the Spiral Bevel Gear Fatigue Test Rig within its speed and load limitations.
2. The gear sets were designed to fail in a manner comparable to the failure modes observed on the helicopters. This required review of the tear down analysis (TDAs) available from the field units and on-site inspection of several of the gearboxes.
3. The gear sets were designed to insure rapid failures, within rig operating conditions, to limit overall test time.

A preliminary design was developed by NASA Glenn. A helicopter manufacturer was then tasked to evaluate our in-house bevel gear design and modify the design to better match helicopter gears. The helicopter gear design could not be directly adapted into the test rig due to the size of the gear set, the speed in which it runs, and the test stand loading capacity. Several design iterations were completed to provide a high chance of failure in a surface contact fatigue failure mode within a reasonable number of cycles. The process used to design the gears for test is summarized in References 16 and 17.

The final design was selected on the basis of a significant positive fatigue margin (low probability of failure) in bending coupled with a significantly negative fatigue margin (high probability of failure) in pitting. The gear set design specifications are: Ratio: 2.158 (41 gear teeth/19 pinion teeth); Diametral Pitch: 6.4; Pressure angle: 20°; Spiral Angle: 25°. The test gears were designed to operate at a gear speed of 3500 rpm and gear torque of 8000 in-lb, pinion speed of 7553 rpm and torque of 3707 in-lb and 240 to 265 °F inlet oil temperatures with an American Gear Manufacturers Association (AGMA) calculated contact stress of 237 ksi. Design code cannot identify a specific fatigue life, but was estimated to be between 100 to 200 hr at the operating conditions.

6.0 Failure Modes

The failure modes to be investigated for this study were defined by class (contact fatigue), general mode (macro pitting) and degree (progressive) per American Gear Manufacturers Association (AGMA) standards for gear wear terminology (Ref. 18). Table 2 illustrates the types of damage observed during these tests. The tests ran until progressive macro pitting/spalling larger than 1 mm in diameter covered a significant area of two or more gear or pinion tooth surfaces. Definitions for tooth surface pitting modes (Ref. 18) are summarized as follows:

- Initial—Pits less than 1 mm in diameter.
- Progressive—Pits in different shapes/sizes greater than 1 mm in diameter.
- Flaking—Pits that are shallow thin flakes.
- Spalling—Pits that cover tooth contact surfaces that exceed progressive pitting.

TABLE 2.—GEAR FAILURE MODES (REF. 18)

Class	Mode	Degree
Contact Fatigue	Subcase Fatigue	
	Micropitting	
	Macropitting	Initial
		Progressive
		Flaking
		Spalling
Scuffing	Scuffing	Mild
		Moderate
		Severe

Estimating fatigue failures in gears is not an exact science and very probabilistic in nature. In addition, these estimates are used to predict when a flaw will initiate, not once initiated, how will it progress. Forcing a particular failure mode on a specific component within a known timeframe is impossible. The test gears were designed to an estimated service life using fatigue strength S-N (stress-cycles) curves that relate component design, stress, number of cycles, usage loads, operating conditions and reliability. Design and manufacturing defects and some environmental and operational conditions were not taken into consideration.

During testing of the prototype gears (Ref. 14) and the first two gear sets of the final design, scuffing occurred to the gear sets installed on the right side of the test rig prior to contact fatigue damage. Scuffing causes transfer of metal from one tooth surface to another. Scuffing occurred to the right gear set during run-in making it impossible to get a baseline data set for this gear set. This failure class is also listed in Table 2. To minimize scuffing, and force a failure on the left side gear set, several gear sets were isotropic super-finished (ISF) and installed on the right side of the gearbox. ISF is a process applied to the gears that improves gear surface and extends gear life. Surface roughness improved by a factor of four on average after applying this process.

7.0 Test Procedures

For this study, all gear sets were tested at a gear speed of 3500 rpm or pinion speed of 7553 rpm. A speed sweep was performed that determined this speed was free of rig resonances. At the start of each test, a run-in was performed for a minimum of 1 hr at 4000 in-lb gear torque/3500 rpm gear speed or 1854 in-lb pinion torque/7553 rpm pinion speed. For some tests, the gear torque was increased to 8000 in-lb or pinion torque was increased to 3707 in-lb for the remainder of the test. For some tests, the rig ran a minimum of 1 hr at 4000 in-lb gear torque and a minimum of 1 hr at 6000 in-lb gear torque then at 8000 in-lb gear torque for the remainder of the test. Contact cycles accumulated at a rate of 210,000 per hour for the gear and 453,180 per hour for the pinion.

Each time a new gear set was installed, shim size was adjusted for an optimum contact pattern. The shim sizes and the backlash were measured and recorded. A representative photograph of the contact patterns on the gear and pinion teeth was also photographed. Photographs were taken of all the left and right gear and pinion teeth prior to rotation. At completion of the run-in, inspection photos were again taken of all the left and right gear and pinion teeth. Inspection photos were also taken periodically throughout the test of all the gear and pinion teeth to document damage progression and at test completion.

The gear sets were tested at four test conditions: I) Initiation and progression of gear contact fatigue tooth damage during naturally occurring fault tests; II) Initiation and progression of gear tooth damage due to poor design, assembly errors and improper shimming; III) Initiation and progression of gear tooth damage due to temperature related scuffing; and IV) Effects of torque changes to condition indicator response. Several gear sets were tested at multiple conditions.

The number of gear sets tested at each condition was determined by defining a hypothesis and applying a test statistic based on assumptions of the data set. Three different questions needed to be answered at the completion of the experimental investigation:

1. Do the CI values respond to the failure mode in the spiral bevel gear fatigue rig?
2. Do the CI values respond to the failure mode in the helicopter?
3. Do the CI values in the spiral bevel rig respond the same as the CI values in the helicopter to the same failure mode?

Determining the number of gears to test to answer question one above requires definition of a hypothesis and applying a statistical method to test the hypothesis. For this application, differences between two *populations* were investigated. The *hypothesis* was defined to determine if the CI for the "damaged" component (*pitting damage on two or more pinion teeth)* are *significantly different* than the CI values of an "undamaged" *(no pinion teeth damage)* component. Details of the statistical methods applied to determine the sample size can be found in References 19 and 20. Through this process a sample size of 10 gear sets for each test condition was determined to be an optimum sample size.

8.0 Summary of Gears Tested

Table 3 is a test log of the nineteen final design gear sets tested. The test name identifies the gear sets tested. For example, L4545R5050, identifies the Left (L) pinion (45) and gear (45) number and the Right (R) pinion (50) and gear (50) number. These gear sets were tested in the test rig with varying damage modes and levels. Damage modes and levels were determined by visual inspection and examination of inspection photographs. Photographs of all the damaged teeth, a total of 120 pictures, for each inspection were reviewed and summarized per inspection interval for each test. These photos and there corresponding inspection date are located in Appendix A titled, "Representative Photos of Gear and Pinion Teeth Damage."

TABLE 3.—GEAR TEST LOG

Test	Gear Set Left	Gear Set Right	RDGS Hours	Test	Gear Set Left	Gear Set Right	RDGS Hours
L2222R4646	Pinion: 22 Gear: 22	Pinion: 46 Gear: 46	7810 130	L1818R1616	Pinion: 18 Gear: 18	Pinion: 16 Gear: 16	9062 146
L4545R5050	Pinion: 45 Gear: 45	Pinion: 50 Gear: 50	2833 47	L2121R1919	Pinion: 21 Gear: 21	Pinion: 19 Gear: 19	1905 32
L3030R5050	Pinion: 30 Gear: 30	Pinion: 50 Gear: 50	6037 101	L1616R1919	Pinion: 16 Gear: 16	Pinion: 19 Gear: 19	445 7
L1515R5050	Pinion: 15 Gear: 15	Pinion: 50 Gear: 50	1291 22	L3737R2424	Pinion: 37 Gear: 37	Pinion: 24 Gear: 24	7072 118
L2020R5050	Pinion: 20 Gear: 20	Pinion: 50 Gear: 50	217 4	L3737R5036	Pinion: 37 Gear: 37	Pinion: 50 Gear: 36	7072 118
L4040R5050	Pinion: 40 Gear: 40	Pinion: 50 Gear: 50	370 6	L1414R1616	Pinion: 14 Gear: 14	Pinion: 16 Gear: 16	705 11
L3535R5050	Pinion: 35 Gear: 35	Pinion: 50 Gear: 50	9578 160	L4444R5252	Pinion: 44 Gear: 44	Pinion: 52 Gear: 52	970 16

Tables were generated for each test, summarizing the failure modes observed on the gear teeth for each test during each inspection interval and color coded based on damage mode. Test L22R4646 was not included due to scuffing occurring during run-in, comparable to damage modes of prototype gear tests (Ref. 14). The inspection tables for all the tests and the color codes are shown in Table 4. The first three columns of each table indicate the number, date and time of the inspection and the inspection interval in minutes. The next four columns indicate the damage for each component observed at each inspection interval. The color coded damage scale is shown in the top right of the table. The test number is shown in the first row of each test inspection table. Comparable failure modes are color coded for further analysis. For example, for tests L4545R5050 and L1515R5050 the left pinion was damaged at the end of the test. This is highlighted by purple.

An example of the interpretation of the gear tooth photographs for determination of the color codes used in the inspection tables will be discussed for Test L4545R5050. Refer to Appendix A for damage progression photographs taken during other tests.

During Test L4545R5050, macro pitting was first observed on left pinion tooth 10 at inspection 5 (2120 min). Figure 5 and Appendix A, Figure A.1.1 shows the pictures from the left hand side (LHS) pinion tooth 10 and tooth 13 from inspection 1 through inspection 7, left to right. At inspection 6, macro pitting was observed on tooth 10 and tooth 13. This is highlighted in yellow for PL for this test in Table 4. At test completion, the pit on tooth 13 increased in size from inspection 6 to inspection 7. This is highlighted in red for PL in Table 4.

TABLE 4.—INSPECTION TABLES AND DAMAGE SCALES FOR ALL TESTS

Inspection	Date	L4545R5050	GL	GR	PL	PR
1	2013-03-21	Inspection(min)				
2	2013-03-22	1 - 76				
3	2013-03-26	76 - 324				
4	2013-04-02	324 - 1370				
5	2013-04-11	1370 - 2120			1	
6	2013-04-15	2120 - 2403			2	
7	2013-04-17	2403 - 2833			2	

Inspection	Date	L1818R1616	GL	GR	PL	PR
1	2013-11-06	Inspection(min)				
2	2013-11-12	1 - 277				
3	2013-11-13	277 - 546				
4	2013-11-19	546 - 3603				edge
5	2013-11-25	3603 - 5249			1	edge
6	2013-12-06	5249 - 7065			1	edge
7	2014-01-23	7065 - 9062	4		3	edge

Damage Scale
No damage
micro pitting or edge wear
scuffing
1 tooth macropitting
2 or more teeth macropitting

Inspection	Date	L3030R5050	GL	GR	PL	PR
1	2013-04-22	Inspection(min)				
2	2013-04-23	1 - 70				
3	2013-04-30	70 - 1784			micro	
4	2013-05-07	1784 - 3270			micro	
5	2013-05-15	3270 - 4633	1		micro	
6	2013-05-22	4633 - 5359	1		micro	
7	2013-05-29	5359 - 5962	2		1	
8	2013-06-05	5962 - 6037	2		1	

Inspection	Date	L2121R1919	GL	GR	PL	PR
1	2014-02-21	Inspection(min)				
2	2014-02-25	1 - 127				
3	2014-02-26	127 - 307	s-all		s-all	edge
4	2014-02-27	307 - 1122	s-all		5	edge
5	2014-03-07	1122 - 1393	s-all		6	edge
6	2014-03-11	1393 - 1568	s-all		8	edge
7	2014-03-17	1568 - 1905	4		10	edge

Inspection	Date	L1515R5050	GL	GR	PL	PR
1	2013-06-05	Inspection(min)				
2	2013-06-06	1 - 63				
3	2013-06-27	63 - 705			1	
4	2013-07-02	705 - 1022			2	
5	2013-07-08	1022 - 1291			2	

Inspection	Date	L1616R1919	GL	GR	PL	PR
1	2014-03-19	Inspection(min)				
2	2014-03-25	1-445			edge	edge

Inspection	Date	L2020R5050	GL	GR	PL	PR
1	2013-07-10	Inspection(min)				
2	2013-07-12	1 - 70				
3	2013-07-17	70 - 217	s-all		s-all, pit	

Inspection	Date	L3737R2424	GL	GR	PL	PR
1	2014-04-08	Inspection(min)				
2	2014-04-23	1 - 214				
3	2014-04-25	214 - 427				
4	2014-05-02	427 - 4945				edge
5	2014-05-13	4945 - 6493				edge
6	2014-05-20	6493 - 7072				edge
7	2014-06-17	7072 - 7394	micro			1

Inspection	Date	L4040R5050	GL	GR	PL	PR
1	2013-07-26	Inspection(min)				
2	2013-07-30	1 - 63				
3	2013-07-31	63 - 370	s-all		s-all	

Inspection	Date	L3737R5036	GL	GR	PL	PR
1	2014-06-24	Inspection(min)				
2	2014-07-07	1 - 4730	micro			1

Inspection	Date	L3535R5050	GL	GR	PL	PR
1	2013-08-12	Inspection(min)				
2	2013-08-13	1 - 178				
3	2013-08-15	178 - 636				
4	2013-09-06	636 - 6276				
5	2013-09-10	6276 - 6818	2			
6	2013-09-11	6818 - 7617	2			
7	2013-09-16	7617 - 9358	2		1	
8	2013-11-04	9358 - 9578	2		1	

Inspection	Date	L1414R1616	GL	GR	PL	PR
1	2014-07-14	Inspection(min)				
2	2014-07-17	1-705				edge

Inspection	Date	L4444R5252	GL	GR	PL	PR
1	2014-07-23	Inspection(min)				
2	2014-07-31	1 - 273				
3	2014-08-04	273 - 602		root		edge
4	2014-08-11	602 - 970		root		edge

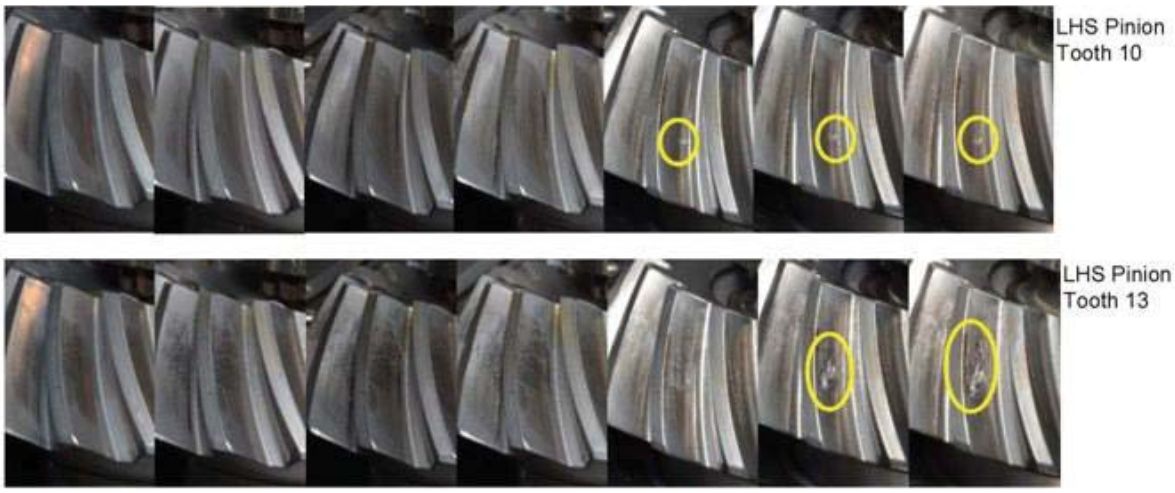

Figure 5.—Test L4545R5050 Pinion Damage Modes.

TABLE 5.—GEAR SETS MAPPED TO TEST CONDITIONS

Test Condition	Fault Condition	Final Design Gear Sets	Gear Set Number	Fit Check Gear Sets	Gear Set Number
I	Naturally occurring contact fatigue	10	45, 50, 30, 15, 20, 35, 18, 21, 37, 24	8	*
II	Assembly errors/Maintenance	11	35, 50, 18, 16, 21, 19, 37, 24, 14, 44, 52	8	*
III	Temperatures related scuffing	5	22, 46, 20, 40, 21	8	*
IV	Torque Effects	13	45, 50, 15, 35, 18, 16, 21, 19, 37, 24, 14, 44, 52	8	*

*All fit check gears had design errors , scuffing and surface fatigue damage

Table 5 lists the gear test conditions and the gear set number tested at each condition. Note that some gear sets were tested under two different conditions. Also note that when the eight prototype gears were tested per Reference 14, they met all four conditions. Refer to Reference 14 for results of these tests.

9.0 Analyses of Condition Indicators and Operational Data

Vibration data was collected at sample rates that provided sufficient vibration data for calculating time synchronous averaged data (TSA). TSA refers to techniques for averaging vibration signals over several revolutions of the shaft, in the time domain, to improve signal-to-noise ratio (Ref. 21). Using a once-per-revolution signal or tachometer, the vibration signal is interpolated into a fixed number of points per shaft revolution. Vibration signals synchronous with the shaft speed intensify relative to non-periodic signals which become weaker.

Since helicopter gears generate vibration signals synchronous with gear rotational speed, most current helicopter gear CIs are calculated from TSA data. All the gear CIs in the MSPU system use TSA data. Many CIs are based on statistical measurements of vibration energy. Signal processing techniques used to extract useful information to calculate a gear CI from the vibration signal are discussed in detail in Reference 22. Some gear CIs are calculated directly from the TSA signal, such as Root Mean Square (RMS). Some are calculated from the TSA converted to the frequency domain, such as Sideband Index (SI). Some convert the TSA signal to the frequency domain, filter specific frequencies, convert it back to the time domain, then calculate a statistical parameter from this data (Refs. 21 to 23).

Figure 6 illustrates the information used to calculate the TSA for the right gear and pinion. Using the sample rate of 200 KHz for 1 sec duration and the speed of both shafts, the number of TSA revolutions averaged for each acquisition is determined. To calculate the TSA, the accelerometer data is divided into segments equivalent to 1 revolution of the shaft. Each segment is then linearly interpolated into equal

numbers of points that have been rounded down to a power of two. A power of two is used because it eases the future use of the Fast Fourier Transform (FFT) to transform the TSA to the frequency domain. Per Figure 6, the right accelerometer raw data is plotted in the top plot. The two lowest plots are the TSA signal calculated from the 1/rev and vibration data for the right gear and pinion. Pulses from the 41 tooth gear and the 19 tooth pinion can easily be seen within these two plots.

FM4 is one CI used to indicate gear tooth damage. Figure 7, on the left, shows a block diagram of the steps required to calculate FM4 (Figure of Merit 4), a common vibration algorithm used in commercial HUMS (Ref. 21). RMS, also referred to as DA1, is another CI used to indicate gear tooth damage. Figure 7, on the right, shows is a block diagram of the steps required to calculate RMS.

TSA Info	Pinion	Gear
Test Gear Teeth	19	41
Max Speed (RPM)	7553	3500
Max Speed (Hz)	126	58
Gear Mesh (Hz)	2392	2392
Sample rate	200000	200000
Sample Duration (sec)	1	1
Revs per Acq	126	58
TSA int. points/rev	1024	2048

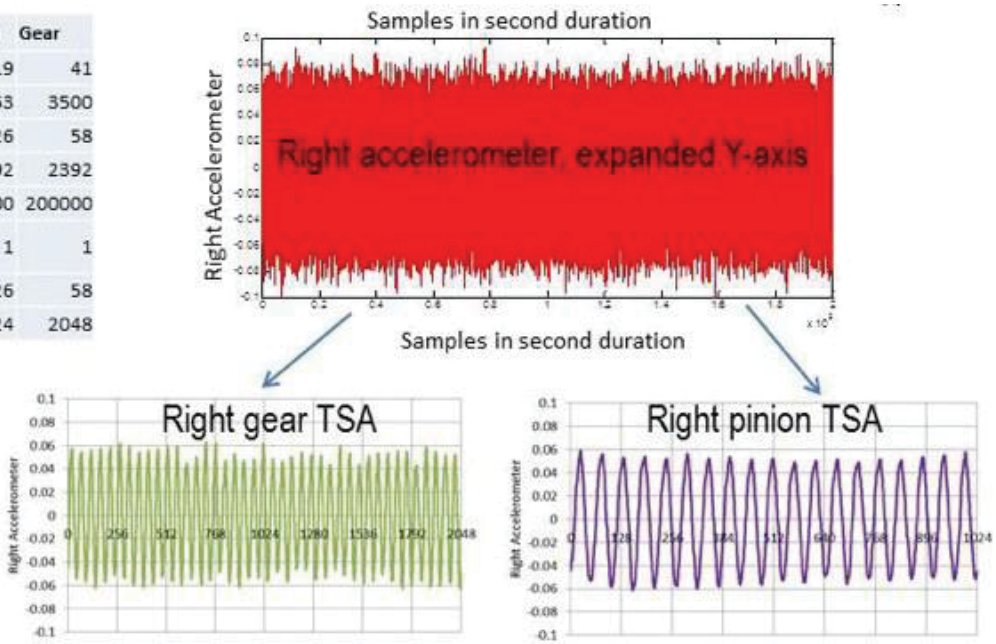

Figure 6.—Information Used to Calculate TSA.

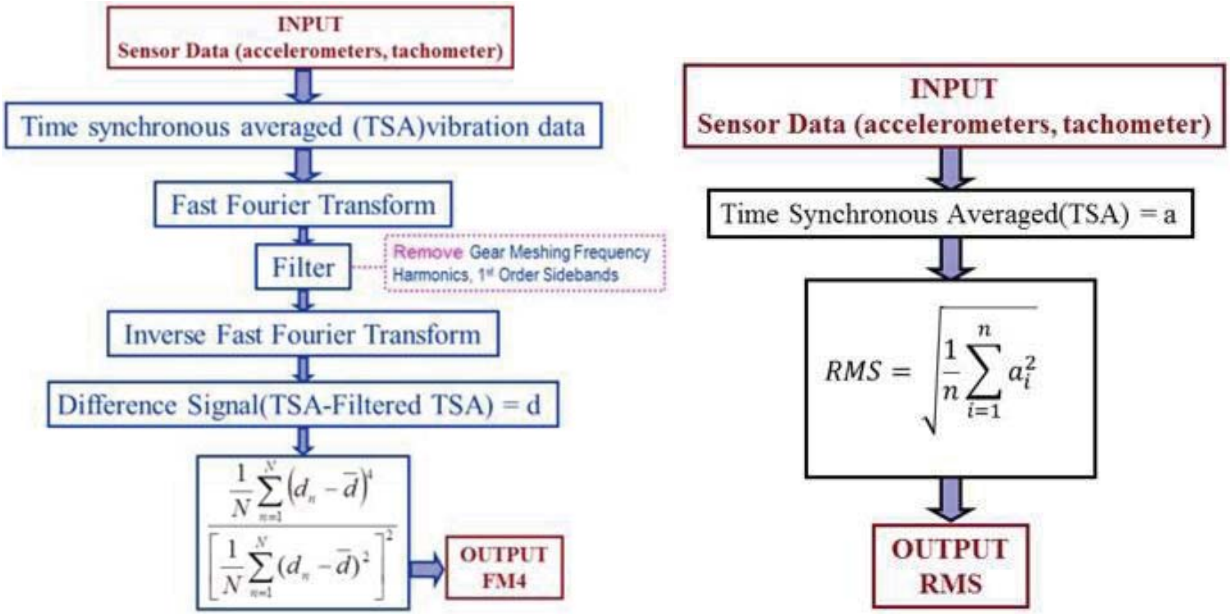

Figure 7.—FM4 and RMS Calculation.

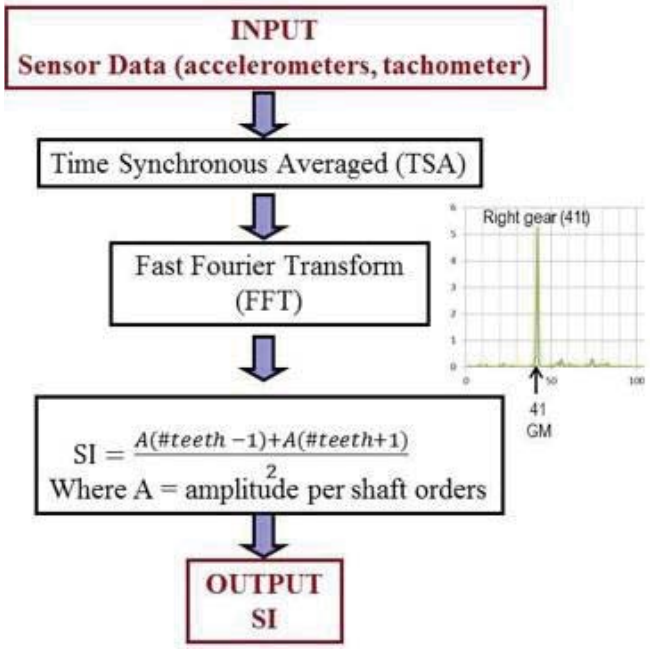

Figure 8.—SI1 calculation.

Sideband index (SI) is another CI used to indicate gear tooth damage (Ref. 5). SI is a frequency domain based CI. The CI value is an average value of sideband amplitudes about the fundamental gear mesh frequency. All gears generate a dominant gear mesh (GM) frequency in the vibration signature due to each tooth impacting the gear it is driving as the pinion and gear mesh. The gear (or pinion) mesh frequency is equal to the number of teeth multiplied by its speed. The number of sidebands included in the calculation of the sideband CI can vary with different health monitoring systems. Averages of ±1 SI (SI1) and ±3 SI (SI3) were used for this analysis. Figure 8 shows a block diagram of the steps required to calculate SI1.

Condition Indicators FM4, RMS, SI1 and SI3 for the left gear (GL), right gear (GR), left pinion (PL) and right pinion (PR) were plotted for all tests and are located in Appendix B titled “Plots of MDSS Condition Indicators and Operational Data.” Note that the color coded triangles on the x-axis correlate to inspections and observed damage during inspections per Table 4. Means and standard deviations for condition indicators FM4, RMS, SI1 and SI3 for the left gear (GL), right gear (GR), left pinion (PL) and right pinion (PR) are located in Appendix C, “Condition Indicator Inspection Statistical Parameters.” An example of the data contained in the Appendix B and Appendix C for Test L4545R5050 will be discussed.

Condition Indicators FM4, RMS, SI1 and SI3 for the left gear (GL), right gear (GR), left pinion (PL) and right pinion (PR) are plotted in Figure 9. These plots correspond to Appendix B Figure B.1.1. Note that the triangles on the x-axis correlate to inspections and observed damage during inspections. Left pinion FM4, SI1 and SI3 significantly increased in value as damage progressed from one to two pinion teeth. RMS showed a slight increase. However, RMS was very sensitive to changes in operational conditions. In addition, the right side the RMS values were significantly higher in amplitudes than the left for this and every test performed in the test rig. This is due to its documented sensitivity to operational and environmental conditions that include the gear and test rig design. This will be discussed further in Section 10.0, Correlation of MDSS, MSPU and Operational Parameters.

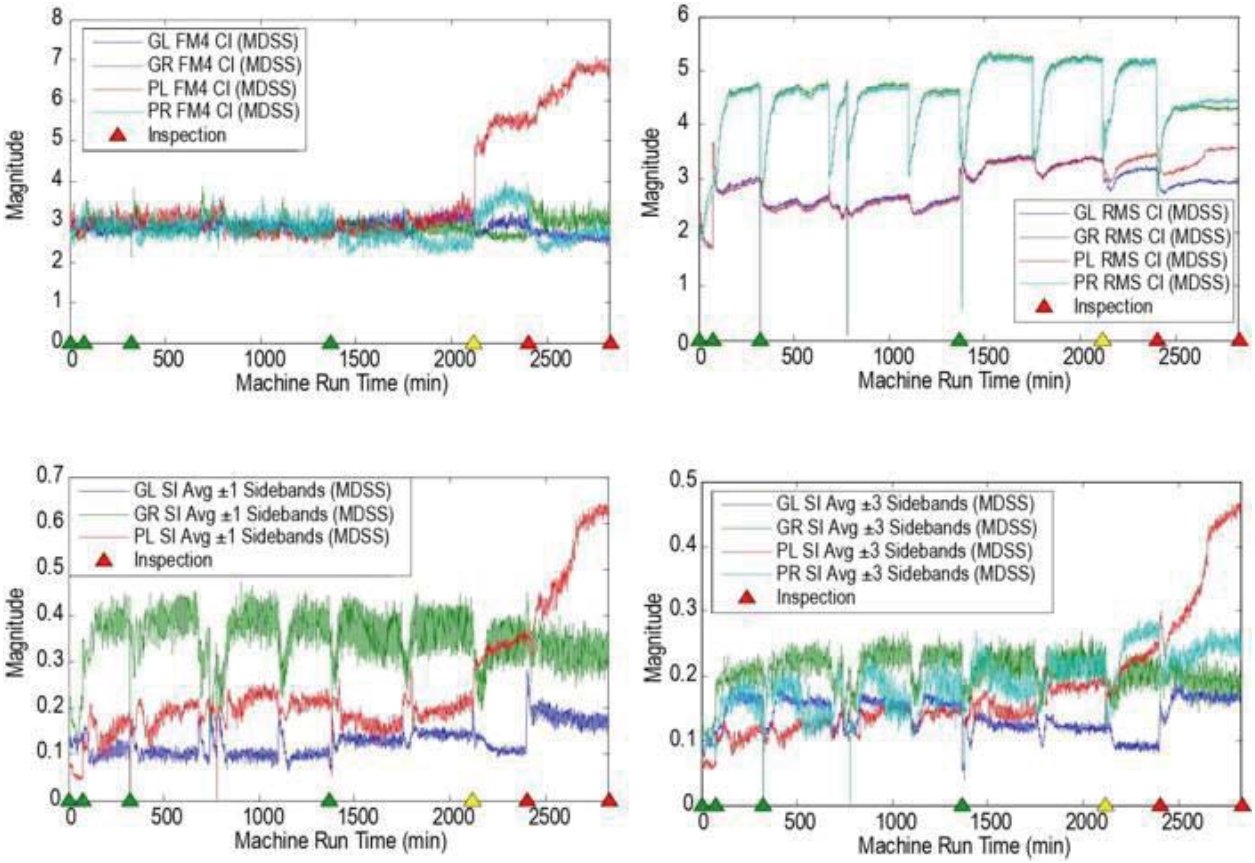

Figure 9.—Test L4545R5050 Plots of FM4, RMS, SI1 and SI3.

Operational parameters are plotted in Figure 10. These plots correspond to Appendix B, Figure B.1.3. These include oil temperatures (°F), oil pressures (psi), gear and pinion torque (in-lb) and speed (rpm). The oil temperatures measured were Left Oil Inlet (LOI), Left Oil Outlet (LOO), Left Fling Off (LFO), Right Oil Inlet (ROI), Right Oil Outlet (ROO) and Right Fling Off (RFO). Note, oil inlet temperature is controlled with a heat exchanger. Oil inlet temperatures were adjusted for several tests to minimize gear tooth scuffing. For this test, the right side oil inlet temperature was 50 °F lower than the left side. Due to rig lubrication system design, this limited oil jet pressure to 60 psi. Gear torque was 4000 in-lb for a 1 hr run-in (inspection 2), increased to 6000 in-lb until inspection 4, increased to 8000 in-lb until inspection 6, then dropped back to 6000 in-lb until test completion. Gear speed was maintained at 3500 rpm for the entire test. The negative spikes on all the plots are indications of rig shutdowns.

Mean and standard deviation values for Condition Indicators FM4, RMS, SI1 and SI3 for the left gear (GL), right gear (GR), left pinion (PL) and right pinion (PR) are listed in Table 6 and in Appendix C, Table C.1.1. Average torque values are also included. This table also indicates left pinion FM4 significantly increased in value as damage progressed from one to two pinion teeth. SI1 and SI3 values increased when damage on the second tooth increased in size.

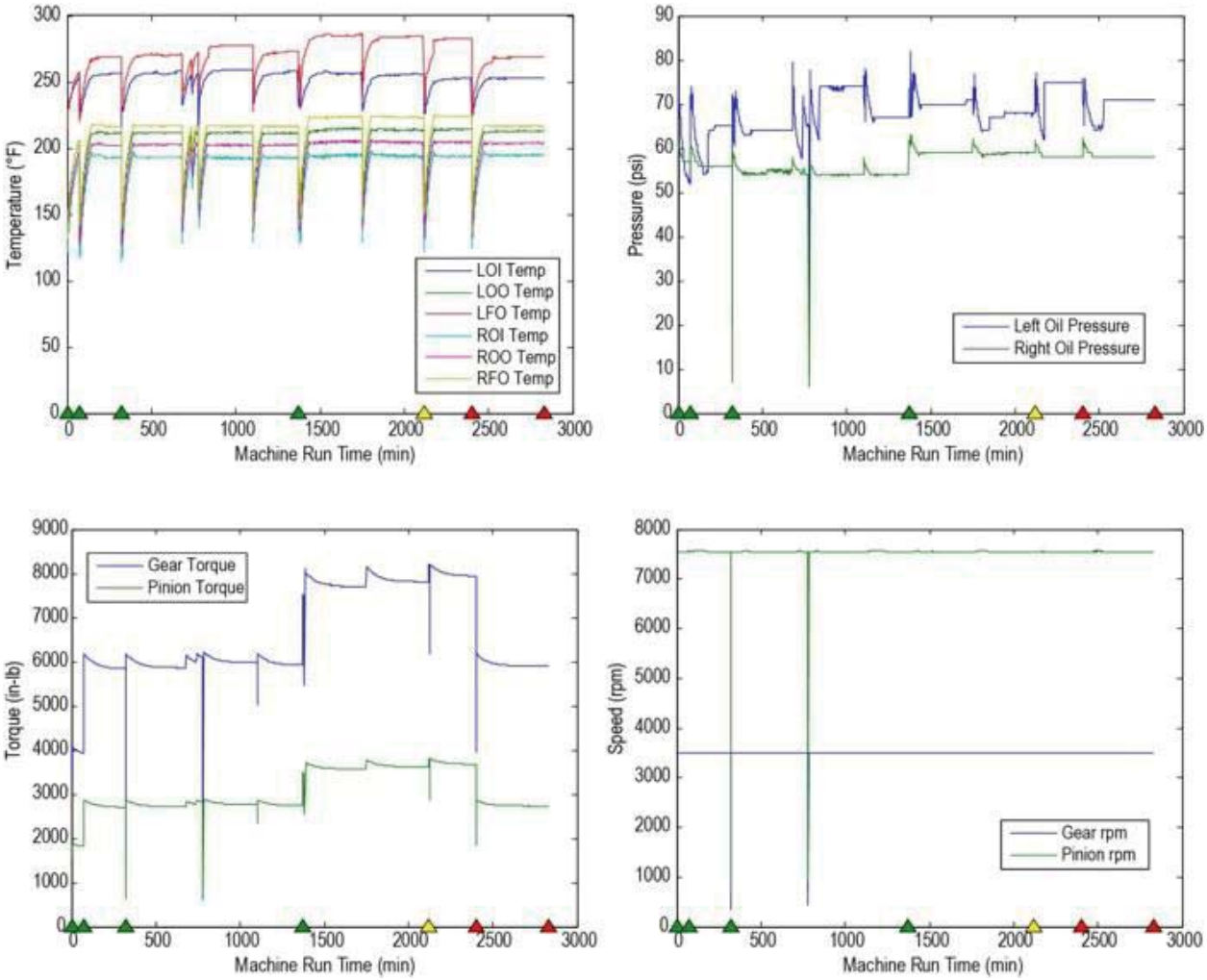

Figure 10.—Test L4545R5050 Plots of Oil Temperatures, Pressures, Torque and Speed.

TABLE 6.—MEAN AND STANDARD DEVIATION VALUES

L4545R5050

MDSS RMS	Mean	STDEV	Mean	STDEV	Mean	STDEV	Mean	STDEV
Inspection	GL	GL	GR	GR	PL	PL	PR	PR
1 - 76	1.93	0.21	2.46	0.27	1.88	0.22	2.29	0.26
76 - 324	2.90	0.24	4.34	0.60	2.84	0.24	4.29	0.61
324 - 1370	2.53	0.14	4.42	0.48	2.48	0.15	4.36	0.48
1370 - 2120	3.26	0.16	4.97	0.55	3.24	0.16	4.92	0.57
2120 - 2403	3.08	0.13	4.85	0.51	3.28	0.15	4.83	0.52
2403 - 2833	2.91	0.07	4.19	0.30	3.35	0.19	4.28	0.31
MDSS FM4	Mean	STDEV	Mean	STDEV	Mean	STDEV	Mean	STDEV
Inspection	GL	GL	GR	GR	PL	PL	PR	PR
1 - 76	2.84	0.11	2.64	0.09	2.90	0.16	2.85	0.22
76 - 324	2.79	0.09	2.91	0.20	2.98	0.16	2.90	0.19
324 - 1370	2.88	0.09	2.89	0.22	2.88	0.22	2.87	0.21
1370 - 2120	2.98	0.15	2.84	0.13	2.95	0.22	2.57	0.22
2120 - 2403	2.91	0.13	2.67	0.10	**5.29**	0.40	3.47	0.23
2403 - 2833	2.65	0.10	3.07	0.20	**6.37**	0.46	2.62	0.19
MDSS ±1 SI	Mean	STDEV	Mean	STDEV	Mean	STDEV	Mean	STDEV
Inspection	GL	GL	GR	GR	PL	PL	PR	PR
1 - 76	0.13	0.01	0.18	0.03	0.06	0.01	0.10	0.03
76 - 324	0.11	0.02	0.37	0.04	0.15	0.03	0.20	0.05
324 - 1370	0.11	0.02	0.36	0.06	0.20	0.03	0.18	0.05
1370 - 2120	0.14	0.01	0.36	0.04	0.19	0.03	0.16	0.03
2120 - 2403	0.12	0.02	0.33	0.05	0.33	0.03	0.30	0.06
2403 - 2833	0.18	0.02	0.33	0.03	**0.51**	0.10	0.22	0.04
MDSS ±3 SI	Mean	STDEV	Mean	STDEV	Mean	STDEV	Mean	STDEV
Inspection	GL	GL	GR	GR	PL	PL	PR	PR
1 - 76	0.09	0.01	0.12	0.01	0.06	0.00	0.10	0.01
76 - 324	0.15	0.02	0.20	0.02	0.11	0.01	0.16	0.02
324 - 1370	0.15	0.02	0.22	0.03	0.13	0.02	0.16	0.03
1370 - 2120	0.12	0.01	0.21	0.02	0.16	0.02	0.20	0.03
2120 - 2403	0.10	0.01	0.20	0.02	0.22	0.03	0.24	0.04
2403 - 2833	0.16	0.01	0.20	0.02	**0.36**	0.08	0.24	0.02

Operational Parameters

	Mean	STDEV	Mean	STDEV	Mean	STDEV
Inspection	Torque	Torque	LOO	LOO	ROO	ROO
1 - 76	4115	45	166	27	142	40
76 - 324	5961	317	201	20	189	27
324 - 1370	6037	215	198	24	185	33
1370 - 2120	7801	271	199	29	187	34
2120 - 2403	7995	127	196	25	179	37
2403 - 2833	6011	64	207	15	198	16

As testing progressed it became clear that certain Condition Indicators were more sensitive to a specific component and failure mode. Per the color codes of the tests listed in Table 4, the mean values for tests with comparable failure modes were also plotted. These plots are located in Appendix D titled, “Clustering of Condition Indicators and Damage Modes between Inspections.” For example, Figure 11,

Appendix D, Figure D.1.1 and Figure D.3.3, compares RMS, FM4, SI1 and SI3 for tests L4545R5050 and L1515R4545. During these two tests, two pinion teeth had macro pitting at test completion.

Reviewing Figure 11, it is clear that FM4 and SI1 increased in value as damage progressed to several pinion teeth. Additional comparisons between component, failure mode and testing environment will be further discussed in Section 11.0, Discussion of Results.

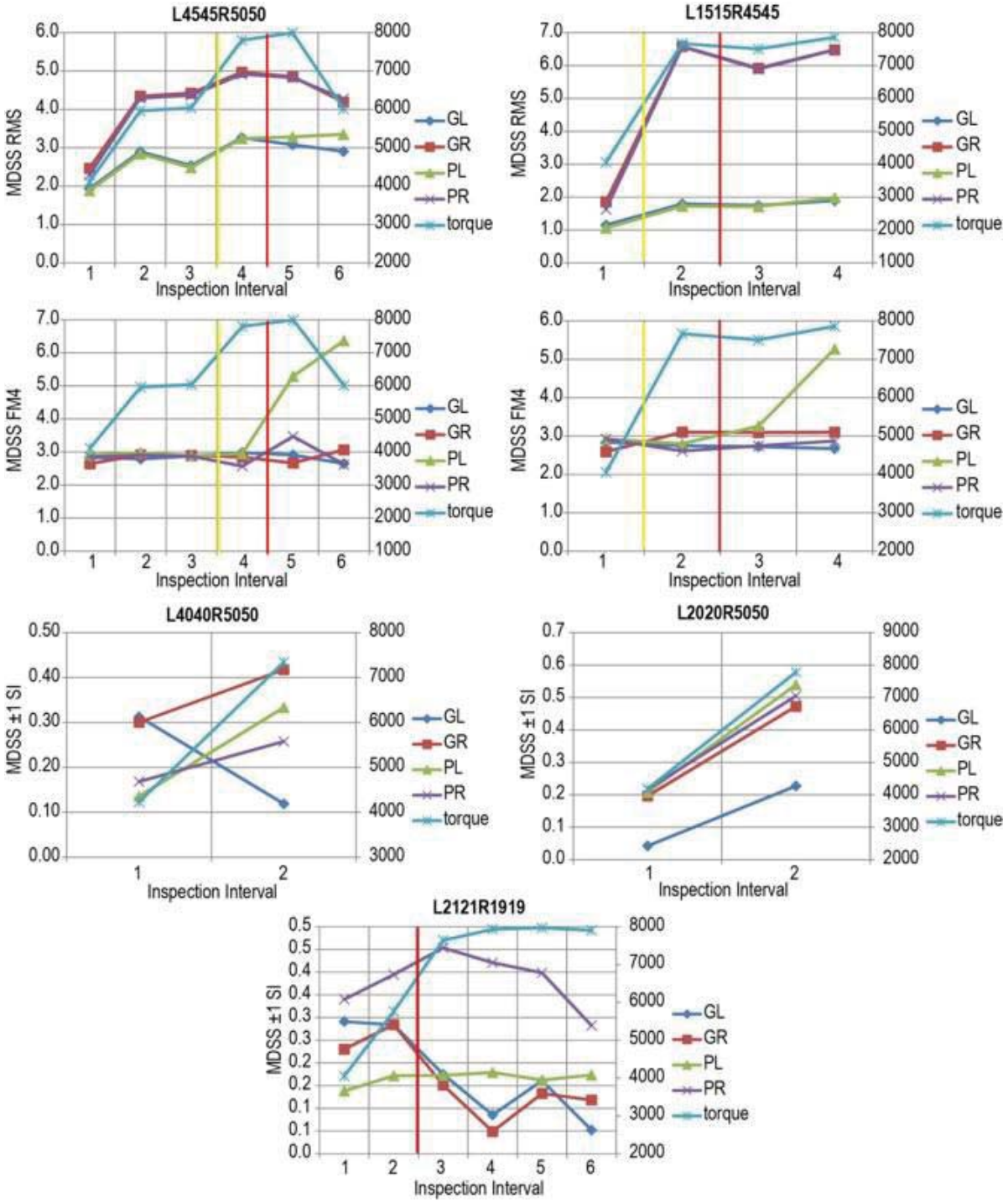

Figure 11.—Compare CIs to damage modes for Test L4545R5050 and Test L1515R4545.

10.0 Correlation of MDSS, MSPU and Operational Parameters

Many factors can affect a condition indicator's ability to respond to tooth damage through vibration response. The response of the accelerometer to a specific fault can depend on the sensor specifications, the signal processing of the raw signal, mounting and its location. The CI method of calculation, operational conditions and type of failure mode can also affect its response. Assessing whether a change in any particular condition indicator was due solely to a change in damage level, a change in operating condition or some combination of both was a challenge due to three data acquisitions systems with different measured parameters and acquisition rates. To assess the relationship between the different parameters, a software tool was developed to combine the three systems. The tool provided a means to analyze the data generated during gear damage initiation and progression from the MDSS, MSPU and facility data acquisition systems and the damage modes (Ref. 24).

The initial analysis will focus on the MDSS CI values compared to torque and outlet or output oil temperatures. Oil debris mass and speed is also plotted. An example of the data contained in the Appendix B for Test L4545R5050 will be discussed. Refer to Appendix B for similar data generated and plotted during the other tests. Figure 12, Appendix B Figure B.1.2, contains plots of RMS, oil debris, gear torque, gear speed, and left and right oil output temperatures. RMS plots are the same on the top and right in Figure 12. Their x-axes are lined up with the corresponding operational parameters plotted below them. RMS values for the right side were significantly higher than the left and were sensitive to torque and oil outlet temperature transients. RMS values for the left side were sensitive to torque. However, once damage was observed on two pinion teeth, the RMS value for the left pinion did not drop when torque decreased.

To evaluate the relationship between CIs and operational conditions, Pearson Correlation Coefficients (r) (Ref. 25) were calculated for the parameters. Correlation coefficients measure the strength and direction of the linear relationship between two parameters (Ref. 25). Correlation coefficients are calculated by dividing the covariance of the two variables (x,y) by the product of their standard deviations as shown in Equation (1) (Ref. 25).

$$r = \frac{n\sum xy - \left(\sum x\right)\left(\sum y\right)}{\sqrt{n\left(\sum x^2\right) - \left(\sum x\right)^2}\sqrt{n\sum\left(y^2\right) - \left(\sum y\right)^2}} \tag{1}$$

Its value ranges between –1 and +1. A perfect linear relationship between two parameters will have a correlation coefficient of 1 or –1. A value close to zero indicates no linear relationship between the two parameters. Hypothesis tests can be used to assess the significance of the relationship between the two parameters; however, a good rule of thumb is that values greater than 0.7 indicate a strong correlation and values less than 0.5 indicate a weak correlation. A correlation matrix is generated for each test showing the linear relationship between CIs for the four components, torque, oil debris mass, and the damage state of the four components. The damage state was quantified with a numerical damage for each component. Per the color coded damage scale in Table 4, no damage equals (0), micro pitting (0.25), scuffing (0.5), 1 tooth macro pitting (0.5) and 2 or more teeth macro pitting 1.

Table 7 is a summary of the r values that were 0.7 or greater for test L4545R5050. All 4 left pinion (PL) CIs correlated to damage as highlighted in green. This is the response one would want from the monitoring CI. The blue highlights strong correlations most likely due to the sensor used and how the CI is calculated. If the amplitude of the GR first order sidebands dominated during this test, both SI1 and SI3 will respond. GR and PR RMS correlate and GL and PL RMS correlate due to using the same accelerometer/location for both gear and pinion calculations. Even though different tachometers are used for the pinion and gear shafts, the accelerometer amplitude dominates. This response illustrates the importance of knowing how a specific CI is calculated to minimize false alarms. Orange highlights correlations due to our system design and illustrating CI response that may cause false alarms if you are unfamiliar with the limitations of your system. GL RMS was sensitive to torque. PR SI3 is sensitive to damage. This is most likely due to our rig design. Not understanding the coupling between both pinions in the test rig may cause false alarms and make it difficult to isolate which component failed in the gearbox.

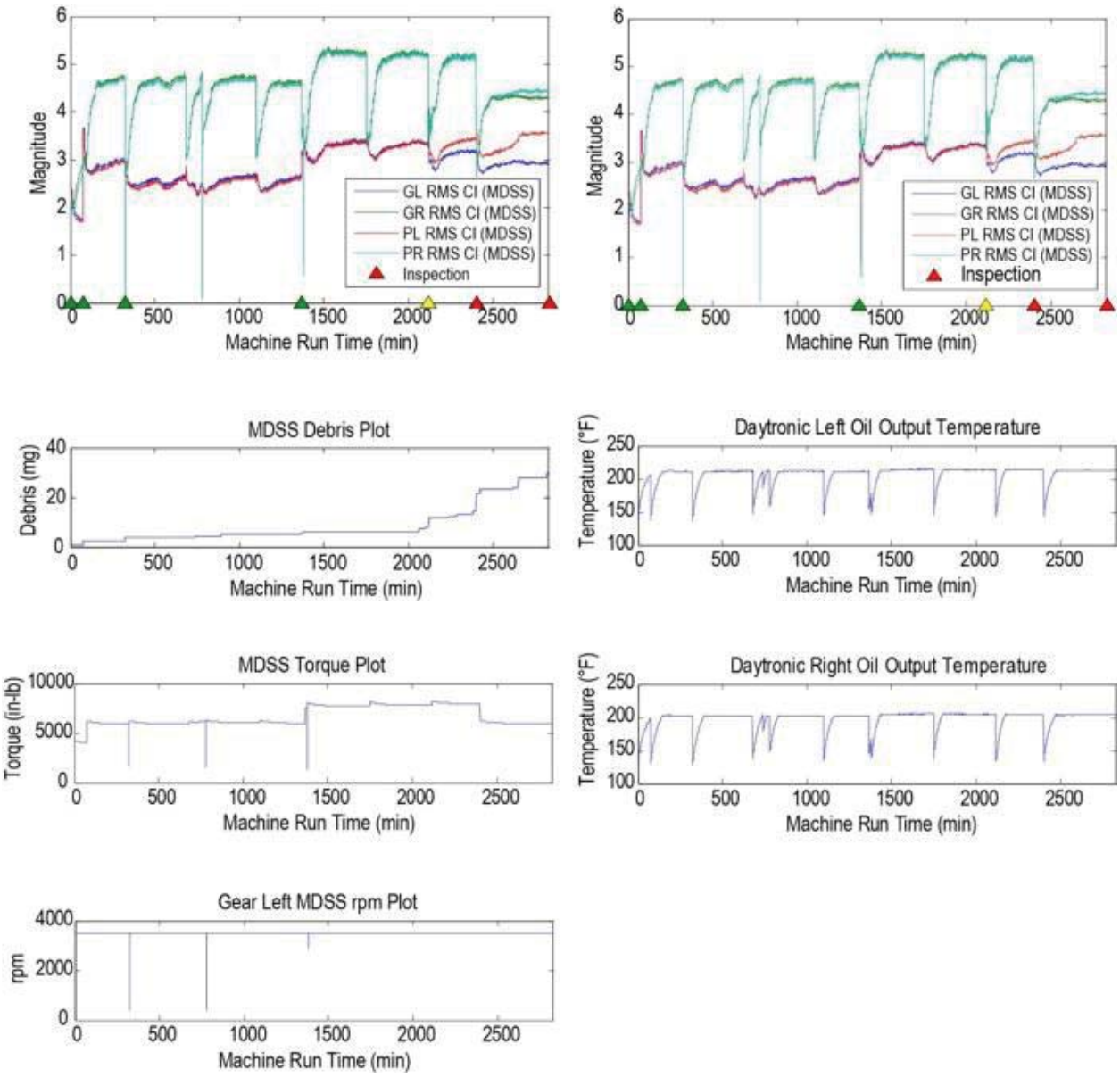

Figure 12.—Test L4545R5050 Plots of RMS and Operational Parameters.

TABLE 7.—TEST L4545R5050 CORRELATION MATRIX

	PL Damage	Torque (lb-in)	Debris (mg)	GL RMS CI	GR RMS CI	PL FM4 CI	GR SI1 CI	PL SI1 CI
Debris (mg)	0.82	-0.01	1.00					
GL RMS CI	0.56	0.82	0.22	1.00				
PL RMS CI	0.81	0.66	0.60	0.91	0.44			
PR RMS CI	0.22	0.58	0.04	0.61	1.00			
PL FM4 CI	0.84	0.00	0.94	0.18	-0.07	1.00		
PL SI1 CI	0.74	-0.03	0.96	0.17	0.00	0.92	-0.10	1.00
GR SI3 CI	-0.15	0.23	-0.14	0.29	0.64	-0.23	0.88	-0.08
PL SI3 CI	0.79	0.07	0.96	0.31	0.08	0.89	-0.08	0.97
PR SI3 CI	0.72	0.43	0.63	0.51	0.48	0.62	0.15	0.62

The next assessment will focus on comparing CIs calculated from the facility DAQ and MSPU system. When comparing data from several different data acquisition systems collected at varying acquisition

intervals, a method to align the timestamps and fill in the gaps of data for the systems recorded at a lower acquisition rates must be defined. This is required when applying statistical methods or data mining techniques to correlate relationships between variables across the systems. The MDSS and facility DAQ systems acquired data once per minute. The MSPU system acquired data once per 30 min. Since the MDSS, MSPU and facility DAQ systems collected data at varying acquisitions intervals, Nearest Neighbor Correlation Method was used to synch the data from the three systems. This method searches timestamps from the smaller to the larger dataset finding timestamps from the smaller data set closest to the same point in the larger dataset. A matched dataset the length of the smaller dataset is then correlated.

Condition Indicators FM4, RMS, SI1 and SI3 for the left gear (GL), right gear (GR), left pinion (PL) and right pinion (PR) from the MDSS system are compared to FM4, DA1, SI1 and SI3 from the MSPU system and located in Appendix E titled, “Correlation of MDSS CI Data to MSPU CI Data.” Note, RMS is referred to as DA1 is the MSPU system. An example of this data for Test L4545R5050 will be discussed. Figure E.1.1 and Figure E.2.2 contain plots of FM4, RMS/DA1, SI1 and SI3 for MDSS and MSPU. Figure E.1.4 to Figure E.1.6, demonstrate applying Nearest Time Correlation Methods to FM4, RMS, SI1 and SI3. Figure 13, Figure E.1.3 in Appendix E, illustrates this method applied to FM4. The top left figure is a plot of FM4 from MDSS and MSPU. The top right figure is a plot of FM4 from MDSS and MSPU after this method was applied. The bottom figure is a plot of MDSS FM4 versus MSPU FM4. There is a strong correlation between both condition indicators.

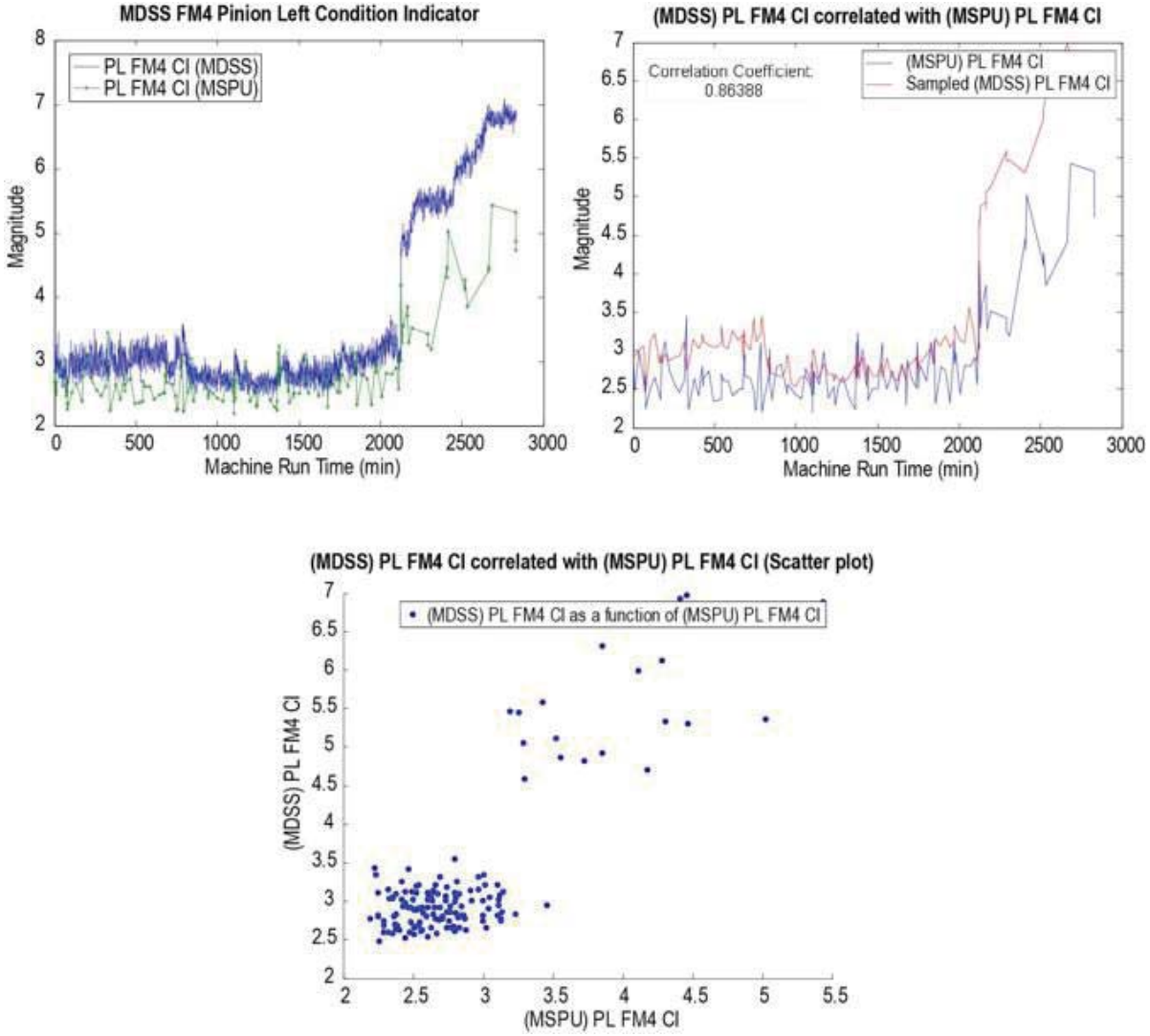

Figure 13.—Test L4545R5050 FM4 Nearest Time Correlation Methods.

TABLE 8.—APPENDIX TABLES AND FIGURES

Test	Appendix A	Appendix B	Appendix C	Appendix D	Appendix E
L4545R5050	A.1.1	B.1.1, B.1.2, B.1.3	C.1.1	D.1.1, D.1.2	E.1.1 through E.1.14
L3030R5050	A.1.2	B.2.1, B.2.2, B.2.3	C.1.3	D.2.1, D.2.2	E.2.1 through E.2.5
L1515R5050	A.1.3	B.3.1, B.3.2, B.3.3	C.1.2	D.1.1, D.1.2	E.3.1 through E.3.9
L2020R5050	A.1.4	B.4.1, B.4.2, B.4.3	C.1.6	D.3.1, D.3.2	
L4040R5050	A.1.5	B.5.1, B.5.2, B.5.3	C.1.7	D.3.1, D.3.2	
L3535R5050	A.1.6	B.6.1, B.6.2, B.6.3	C.1.4	D.2.1, D.2.2	E.4.1 through E.4.7
L1818R1616	A.1.7	B.7.1, B.7.2, B.7.3	C.1.5	D.2.1, D.2.2	E.5.1 through E.5.7
L2121R1919	A.1.8, A.1.9, A.1.10	B.8.1, B.8.2, B.8.3	C.1.8	D.3.1, D.3.2	
L1616R1919	A.1.11	B.9.1, B.9.2, B.9.3	C.1.9		
L3737R2424	A.1.12	B.10.1, B.10.2, B.10.3	C.1.10		E.6.1, E.6.2
L3737R5036	A.1.13	B.11.1, B.11.2, B.11.3	C.1.11		E.7.1, E.7.2
L1414R1616	A.1.14	B.12.1, B.12.2, B.12.3	C.1.12		
L4444R5252	A.1.15	B.13.1, B.13.2, B.13.3	C.1.13		

*Similar damage mode and components color coded

Appendix E also contains correlation plots of FM4, RMS, SI1 and SI3 correlated to torque and oil outlet temperatures for several of the tests.

For reference, Table 8 lists the appendix figures previously discussed for test L4545R5050 that correspond to the other tests listed in the Table 3 “Gear Test Log.” The tests are color coded, similar to Table 4, for comparable damage modes and components. The statistical tables in Appendix C and the clustered plots in Appendix D are paired together based on this factor. Correlation plots were not generated for all tests due to limited MSPU data available.

11.0 Discussion of Results

Gear sets with comparable damaged components and failure modes will be discussed together using correlation matrices. Plots and tables contained in appendices for each test should be referenced during the discussion. Table 4 should be referenced to identify the component with damage during each test. When viewing the correlation coefficient tables, green highlights CIs that responded well to damage. Blue highlights CIs that responded due to other factors such as system design or CI calculation methods. Orange indicates parameters that would be interpreted as false alarms.

During tests L4545R5050 and L1515R5050, macropitting was observed on two the left pinion teeth at test completion. Outlet oil temperatures averaged 215 °F for the left side and 205 °F for the right side for both tests. For test L1515R5050, torque was maintained at 8000 in-lb for the majority of the test. For test L4545R5050, torque was at 6000 in-lb until 1370 min, increased to 8000 in-lb until 2403 min, then dropped back down to 6000 in-lb until the end of the test.

The correlation matrix for test L4545R5050, shown in Table 9, was previously discussed. All four conditions indicators (RMS, FM4, SI1 and SI3) and debris correlated to the left pinion (PL) damage. For testL1515R5050, also shown in Table 9, only FM4 responded to left pinion damage. Note that two damage scale values were compared for test L1515R5050. The first “PL Damage” column used damage scale factors previously mentioned of no damage equals (0), micro pitting (0.25), scuffing (0.5), 1 tooth macro pitting (0.5) and 2 or more teeth macro pitting 1 per damage modes observed at inspections listed in Table 4. The second “PL Damage*” column only identifies damage during the final inspection interval 5. During this interval, the size of the pit on one tooth covered the entire tooth contact area and debris and PL FM4 both correlated to the damage scale.

TABLE 9.—TESTS L4545R5050 AND L1515R5050 CORRELATION COEFFICIENTS

L4545R5050

	PL Damage	Torque (in-lb)
Torque (in-lb)	0.47	1.00
Debris (mg)	0.82	-0.01
GL RMS CI	0.56	0.82
GR RMS CI	0.16	0.58
PL RMS CI	0.81	0.66
PR RMS CI	0.22	0.58
GL FM4 CI	-0.20	0.43
GR FM4 CI	0.02	-0.19
PL FM4 CI	0.84	0.00
PR FM4 CI	0.03	0.04
GL SI1 CI	0.63	0.08
GR SI1 CI	-0.18	0.17
PL SI1 CI	0.74	-0.03
PR SI1 CI	0.39	0.16
GL SI3 CI	-0.22	-0.53
GR SI3 CI	-0.15	0.23
PL SI3 CI	0.79	0.07
PR SI3 CI	0.72	0.43

L1515R5050

	PL Damage	PL Damage*	Torque (in-lb)
Torque (in-lb)	0.34	0.14	1.00
Debris (mg)	0.66	0.97	0.21
GL RMS CI	0.28	0.20	0.69
GR RMS CI	0.22	0.09	0.75
PL RMS CI	0.39	0.37	0.69
PR RMS CI	0.23	0.09	0.76
GL FM4 CI	-0.12	-0.10	-0.15
GR FM4 CI	0.18	0.04	0.41
PL FM4 CI	0.63	0.95	0.12
PR FM4 CI	0.20	0.31	-0.29
GL SI1 CI	-0.03	0.12	0.28
GR SI1 CI	0.08	0.04	0.34
PL SI1 CI	0.28	0.34	0.69
PR SI1 CI	0.21	0.24	0.70
GL SI3 CI	0.14	0.19	0.64
GR SI3 CI	0.35	0.28	0.57
PL SI3 CI	0.48	0.61	0.58
PR SI3 CI	0.13	0.05	0.68

PL Damage* = 1 for last inspection

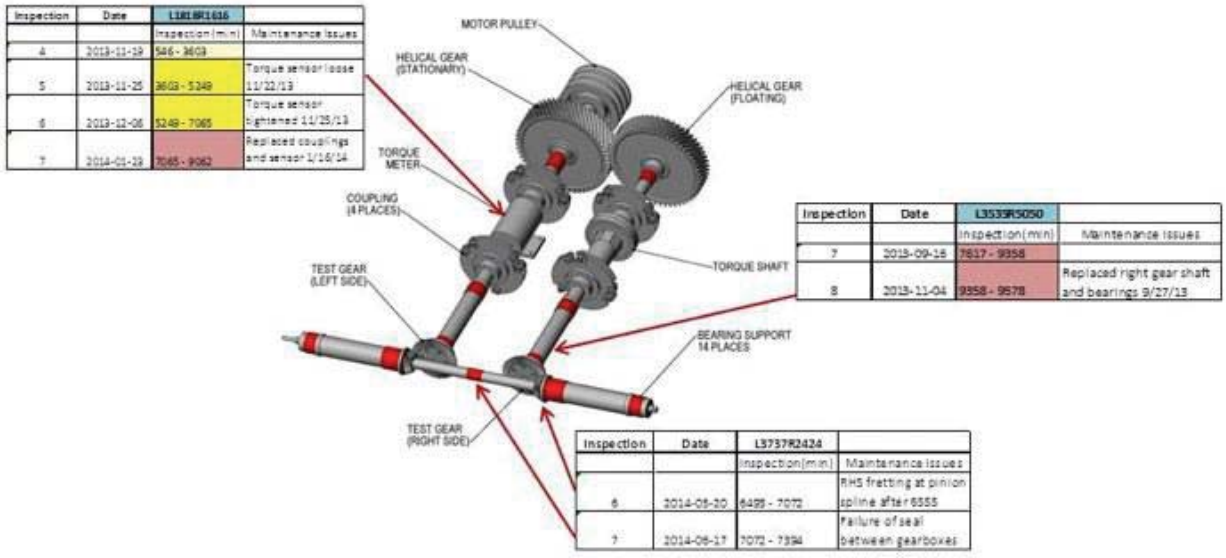

Figure 14.—Maintenance actions to the test rig drive train.

During tests L3030R5050 and L3535R5050 macropitting was observed on one left pinion tooth and two left gear teeth at test completion. During test L1818R1616, macropitting was observed on three left pinion and four left gear teeth at test completion. Edge wear was also observed on the right pinion teeth that was later found to be caused by minor fretting of the right pinion in the support shaft and will be discussed further later in this section. Maintenance actions to the system can affect condition indicator response. Figure 14 identifies maintenance issues to the test rig during testing correlated to the specific test and inspection interval when they occurred. These actions occurred during tests L3535R5050, L1818R1616 and L3737R2424. Maintenance actions must be taken into consideration when reviewing condition indicator response. At the completion of test L3535R5050, the right gear shaft and bearings were replaced. During test L1818R1616, the torque sensor came loose and had to be replaced with its couplings. Test L3737R2424 maintenance action will be discussed later in this section.

Test L3535R5050 outlet oil temperatures averaged 215 °F for the left side and 205 °F for the right side. Due to scuffing occurring in subsequent tests, the oil inlet temperature was reduced and the outlet oil temperatures for tests L3535R5050 and L1818R1616 averaged 180 °F for the right and left side. Torque was maintained at 8000 in-lb for the majority of the test for all three tests.

The correlation coefficients for the three tests are shown in Table 10. For test L3030R5050, GL FM4 correlated to left gear damage, PL SI1 correlated to left pinion damage and debris correlated to both components. For test L3535R5050, GL RMS, FM4, SI1, SI3 and debris correlated to left gear damage. PL RMS, SI1, SI3 and debris correlated to left pinion damage. However, a strong correlation between the right RMS CI values and torque was observed that continued into test L1818R1616. For test L1818R1616, GL SI3 correlated to left gear damage, PL SI1 and SI3 correlated to left pinion damage and debris correlated to both.

TABLE 10.—TESTS L3030R5050, L3535R5050 AND TEST L1818R1616 CORRELATION COEFFICIENTS

L3030R5050

	GL Damage	PL Damage	Torque (in-lb)
Torque (in-lb)	0.12	0.35	1.00
Debris (mg)	0.81	0.70	0.11
GL RMS CI	-0.23	0.03	0.54
GR RMS CI	0.15	0.12	0.29
PL RMS CI	0.18	0.35	0.64
PR RMS CI	0.17	0.13	0.30
GL FM4 CI	0.70	0.83	0.04
GR FM4 CI	0.01	0.12	0.16
PL FM4 CI	-0.63	-0.24	-0.09
PR FM4 CI	0.26	0.08	0.06
GL SI1 CI	0.59	0.35	0.18
GR SI1 CI	0.24	0.20	0.21
PL SI1 CI	0.77	0.74	0.16
PR SI1 CI	-0.41	-0.27	0.17
GL SI3 CI	0.55	0.48	0.45
GR SI3 CI	0.39	0.22	0.15
PL SI3 CI	0.88	0.60	0.15
PR SI3 CI	0.06	0.09	0.23

L3535R5050

	GL Damage	PL Damage	Torque (in-lb)
Torque (in-lb)	0.01	0.00	1.00
Debris (mg)	0.88	0.89	0.06
GL RMS CI	0.79	0.81	0.19
GR RMS CI	-0.20	-0.14	0.94
PL RMS CI	0.83	0.79	0.19
PR RMS CI	-0.19	-0.14	0.94
GL FM4 CI	0.77	0.95	0.03
GR FM4 CI	0.53	0.82	0.00
PL FM4 CI	0.69	0.49	-0.20
PR FM4 CI	0.46	0.35	-0.07
GL SI1 CI	0.77	0.54	0.27
GR SI1 CI	-0.33	-0.22	-0.63
PL SI1 CI	0.86	0.73	0.10
PR SI1 CI	0.39	0.47	0.41
GL SI3 CI	0.87	0.61	0.20
GR SI3 CI	0.35	0.20	-0.41
PL SI3 CI	0.88	0.73	0.11
PR SI3 CI	0.63	0.53	0.52

L1818R1616

	GL Damage	PL Damage	PR Damage	Torque (in-lb)
Torque (in-lb)	-0.09	0.01	0.52	1.00
Debris (mg)	0.79	0.91	0.46	0.20
GL RMS CI	-0.48	-0.75	0.08	0.32
GR RMS CI	-0.09	-0.21	0.30	0.83
PL RMS CI	-0.34	-0.62	0.22	0.38
PR RMS CI	-0.08	-0.18	0.33	0.84
GL FM4 CI	-0.38	-0.21	0.14	0.30
GR FM4 CI	0.11	0.46	0.40	0.35
PL FM4 CI	-0.07	-0.43	-0.48	-0.27
PR FM4 CI	0.58	0.78	0.26	0.32
GL SI1 CI	0.56	0.81	0.32	0.13
GR SI1 CI	0.85	0.79	0.16	0.25
PL SI1 CI	0.77	0.94	0.23	-0.02
PR SI1 CI	0.01	0.07	0.26	0.78
GL SI3 CI	0.75	0.88	0.40	0.32
GR SI3 CI	0.80	0.78	0.24	0.37
PL SI3 CI	0.75	0.94	0.29	-0.03
PR SI3 CI	0.78	0.90	0.39	0.30

During tests L2020R5050, L4040R5050 and L2121R1919 scuffing occurred on all the left gear and pinion teeth after run-in. During test L4040R5050, only scuffing was observed at test completion. During test mL2020R5050, macropitting occurred on all the pinion teeth at test completion. During test L2121R1919, macropitting was observed on four left gear teeth, ten left pinion teeth and edge wear was also observed on the right pinion teeth.

Test L2020R5050 outlet oil temperatures averaged 215 °F for the left side and 205 °F for the right side. Due to scuffing occurring, the oil inlet temperature was reduced and the outlet oil temperatures for tests L4040R5050 and L2121R1919 averaged 180 °F for the right and left side. Torque was maintained at 8000 in-lb after the 1 hr run-in at 4000 in-lb for test L2020R5050. Torque was maintained at 7800 in-lb after the 1 hr run-in at 4000 in-lb for test L4040R5050.

For test L2121R1919, the gears were run-in at 4000 in-lb for 3 hr, then increases to 6000 in-lb for one hr before reaching 8000 in-lb torque. The scuffing failure mode occurred as soon as load was increased for all three tests. It was indicated by a spike in the left oil fling off (LFO) temperature during all three tests as soon as load was applied. Reference plots Figure B.4.3, Figure B.5.3 and Figure B.8.3 located in in Appendix B.

The correlation coefficients for the three tests are shown in Table 11. For test L2020R5050, GL RMS, SI1 and SI3 correlated to left gear damage, PL RMS, SI1 and SI3 correlated to left pinion damage. All of them correlated with torque as did the right RMS, SI1 and SI3 values. For test L4040R5050, no CI positive correlation was observed, where a negative correlation was observed with GL CI SI1 and SI3 and torque. PL SI1 and SI3 correlated with left pinion damage. Debris correlated for gear and pinion damage. Similar to test L2020R5050, all of them correlated with torque as did the right RMS, PR SI1 and PR SI3 values. For test L2121R1919, only PL RMS correlated to left pinion damage and both GL and PL RMS values correlated to torque.

Beginning with test L2121R1919 through L44R5252 listed in Table 4, fretting on the right side pinion within its shaft dominated the dynamic response within the vibration signature. Fretting is a form of wear caused by the movement of two components in contact and subjected to small amplitude cyclic relative motion (Ref. 18). The only way to stop fretting is to stop the relative motion of the contacting parts under load (Ref. 26). Due to the finite life and schedule for this project, redesigning the shaft to tighten the fit was not an option. Several rig modifications were employed to try to eliminate this design issue, but proved to be unsuccessful. Since fretting is a common wear mechanism that occurs in geared systems (Ref. 27), and detection before critical components loosen would be of benefit, a decision was made to briefly discuss the effect of fretting on gear condition indicator response during these tests.

Fretting caused unusual wear patterns distributed across the contact surfaces on all the teeth making isolation of the gear mesh and signatures traditionally used for gear damage detection of limited use. Mild fretting was observed during several tests. During test L3737R2424 excessive fretting of the right pinion in the shaft caused an anomaly in the raw vibration data measured by the left accelerometer. Figure 15 is a snapshot of the raw vibration data before and after fretting was observed and photographs of where fretting occurred on the pinion, pinion shaft and splined shaft. Reference Figure 2 and Figure 14 for cross section views that illustrate the connections between the pinion, inner splined shaft and support shafts. To eliminate the fretting, the pinion was glued into the support shaft and the pinion splines shaft assembly lock nut preload was increased. The excessive fretting stopped, but a milder level of fretting continued to occur during tests L3737R2424, L3737R5036, L1414R1616 and L4444R5252. Inspection after run-in not performed for Tests L3737R5036 and L1414R1616 and therefore correlation coefficient analysis will not be performed since an undamaged dataset does not exist.

TABLE 11.—TESTS L2020R5050, L4040R5050 AND TEST L2121R1919 CORRELATION COEFFICIENTS

L2020R5050

	GL Damage	PL Damage	Torque (in-lb)
Torque (in-lb)	0.97	0.97	1.00
Debris (mg)	0.30	0.30	0.20
GL RMS CI	0.86	0.86	0.87
GR RMS CI	0.91	0.91	0.93
PL RMS CI	0.87	0.87	0.88
PR RMS CI	0.91	0.91	0.93
GL FM4 CI	0.63	0.63	0.64
GR FM4 CI	0.62	0.62	0.61
PL FM4 CI	-0.37	-0.37	-0.37
PR FM4 CI	0.34	0.34	0.31
GL SI1 CI	0.94	0.94	0.95
GR SI1 CI	0.92	0.92	0.95
PL SI1 CI	0.95	0.95	0.97
PR SI1 CI	0.89	0.89	0.92
GL SI3 CI	0.93	0.93	0.95
GR SI3 CI	0.94	0.94	0.96
PL SI3 CI	0.94	0.94	0.95
PR SI3 CI	0.87	0.87	0.90

L4040R5050

	GL Damage	PL Damage	Torque (in-lb)
Torque (in-lb)	0.99	0.99	1.00
Debris (mg)	0.84	0.84	0.82
GL RMS CI	0.61	0.61	0.57
GR RMS CI	0.97	0.97	0.97
PL RMS CI	0.63	0.63	0.58
PR RMS CI	0.97	0.97	0.97
GL FM4 CI	0.29	0.29	0.25
GR FM4 CI	0.68	0.68	0.69
PL FM4 CI	0.32	0.32	0.29
PR FM4 CI	-0.40	-0.40	-0.37
GL SI1 CI	-0.90	-0.90	-0.91
GR SI1 CI	0.59	0.59	0.59
PL SI1 CI	0.97	0.97	0.96
PR SI1 CI	0.82	0.82	0.83
GL SI3 CI	-0.91	-0.91	-0.92
GR SI3 CI	0.10	0.10	0.09
PL SI3 CI	0.94	0.94	0.93
PR SI3 CI	0.79	0.79	0.79

L2121R1919

	GL Damage	PL Damage	PR Damage	Torque (in-lb)
Torque (in-lb)	0.63	0.75	0.63	1.00
Debris (mg)	0.27	0.40	0.27	0.42
GL RMS CI	0.67	0.80	0.67	0.83
GR RMS CI	0.22	0.15	0.22	0.41
PL RMS CI	0.65	0.80	0.65	0.82
PR RMS CI	0.23	0.16	0.23	0.43
GL FM4 CI	-0.41	-0.47	-0.41	-0.49
GR FM4 CI	0.22	0.04	0.22	0.05
PL FM4 CI	-0.33	-0.40	-0.33	-0.44
PR FM4 CI	-0.55	-0.65	-0.55	-0.59
GL SI1 CI	-0.42	-0.63	-0.42	-0.47
GR SI1 CI	-0.26	-0.50	-0.26	-0.37
PL SI1 CI	0.34	0.30	0.34	0.19
PR SI1 CI	0.21	0.20	0.21	0.28
GL SI3 CI	-0.24	-0.39	-0.24	-0.13
GR SI3 CI	0.17	0.03	0.17	0.30
PL SI3 CI	0.21	0.29	0.21	0.27
PR SI3 CI	-0.12	-0.23	-0.12	-0.25

Figure 15.—Fretting of pinion in shaft.

During test L3737R2424, edge wear was observed on the right pinion teeth at test completion and one tooth had macropitting. In a meshing gear set, when pitting occurs on the edge or tips of the pinion teeth and causes a line of pitting on the mating gear near the lowest point of contact it is referred to as “hard line” on the gear teeth (Ref. 28). This is an undesirable failure mode because it can cause tooth fractures due to the high bending stresses in this area (Ref. 28). During test L4444R5252, edge wear was observed on the right pinion teeth and a “hard line” was observed on the right gear teeth at test completion.

Outlet oil temperatures for tests averaged 150 °F for test L3737R2424 and 120 °F for test L4444R5252 for the right and left sides. The gears were run-in at 4000 in-lb, then increased to 6000 in-lb for 1 hr before reaching 8000 in-lb torque.

The correlation coefficients for both tests are shown in Table 12. For test L3737R2424, no CIs correlated to damage. GL and PL RMS correlated to torque. For PR FM4 and GL SI1a negative correlation was observed with torque.

For test L4444R5252, only GR RMS correlated to right gear damage and PR RMS correlated to right pinion damage. All RMS values correlated to torque. PL SI1 had a positive correlation to torque, where PR SI1 had a negative correlation.

Before summarizing the results of the testing performed in the NASA Glenn Spiral Bevel Gear Fatigue Test Rig, other factors that affected CI response should be discussed. Figure 16 identifies the factors that can affect the vibration response measured by the accelerometer to the vibration signature created at the gear mesh as the pinion and gear teeth come into contact. These successive impacts generate vibration signatures. These vibration signatures at the gear mesh then transfer through the rig to the accelerometer installed on the gear housing. This accelerometer is then used to measure vibration response. Damage at the tooth contact changes these vibration signatures. A good gear condition indicator must be tuned to the specific fault vibration signature with minimal effect from other factors. Unfortunately, the effects these factors have on CI response cannot be assessed until dynamic testing is performed. Each of these parameters shown in Figure 16 affected CI response.

TABLE 12.—TESTS L3737R2424 AND L4444R5252 CORRELATION COEFFICIENTS

L3737R2424	*GL Damage*	*PR Damage*	*Torque (in-lb)*
Torque (in-lb)	-0.16	0.27	1.00
Debris (mg)	0.54	0.50	-0.24
GL RMS CI	0.23	0.26	-0.15
GR RMS CI	-0.21	0.15	0.83
PL RMS CI	0.45	0.38	-0.40
PR RMS CI	-0.17	0.18	0.80
GL FM4 CI	0.40	0.20	-0.58
GR FM4 CI	0.46	0.60	0.28
PL FM4 CI	-0.13	-0.15	0.06
PR FM4 CI	0.44	0.13	-0.75
GL SI1 CI	0.50	0.07	-0.79
GR SI1 CI	0.20	0.57	0.17
PL SI1 CI	0.16	-0.01	-0.39
PR SI1 CI	-0.35	-0.28	0.43
GL SI3 CI	0.53	0.28	-0.60
GR SI3 CI	-0.08	0.45	0.72
PL SI3 CI	0.52	0.51	-0.35
PR SI3 CI	0.08	0.46	0.72

L4444R5252	*GR Damage*	*PR Damage*	*Torque (in-lb)*
Torque (in-lb)	0.65	0.65	1.00
Debris (mg)	0.65	0.65	0.68
GL RMS CI	0.63	0.63	0.87
GR RMS CI	0.74	0.74	0.88
PL RMS CI	0.58	0.58	0.73
PR RMS CI	0.74	0.74	0.87
GL FM4 CI	-0.24	-0.24	0.01
GR FM4 CI	0.15	0.15	-0.23
PL FM4 CI	-0.13	-0.13	-0.01
PR FM4 CI	-0.38	-0.38	-0.56
GL SI1 CI	0.66	0.66	0.44
GR SI1 CI	-0.33	-0.33	-0.56
PL SI1 CI	0.67	0.67	0.87
PR SI1 CI	-0.61	-0.61	-0.77
GL SI3 CI	0.69	0.69	0.47
GR SI3 CI	0.52	0.52	0.54
PL SI3 CI	0.59	0.59	0.80
PR SI3 CI	-0.18	-0.18	-0.58

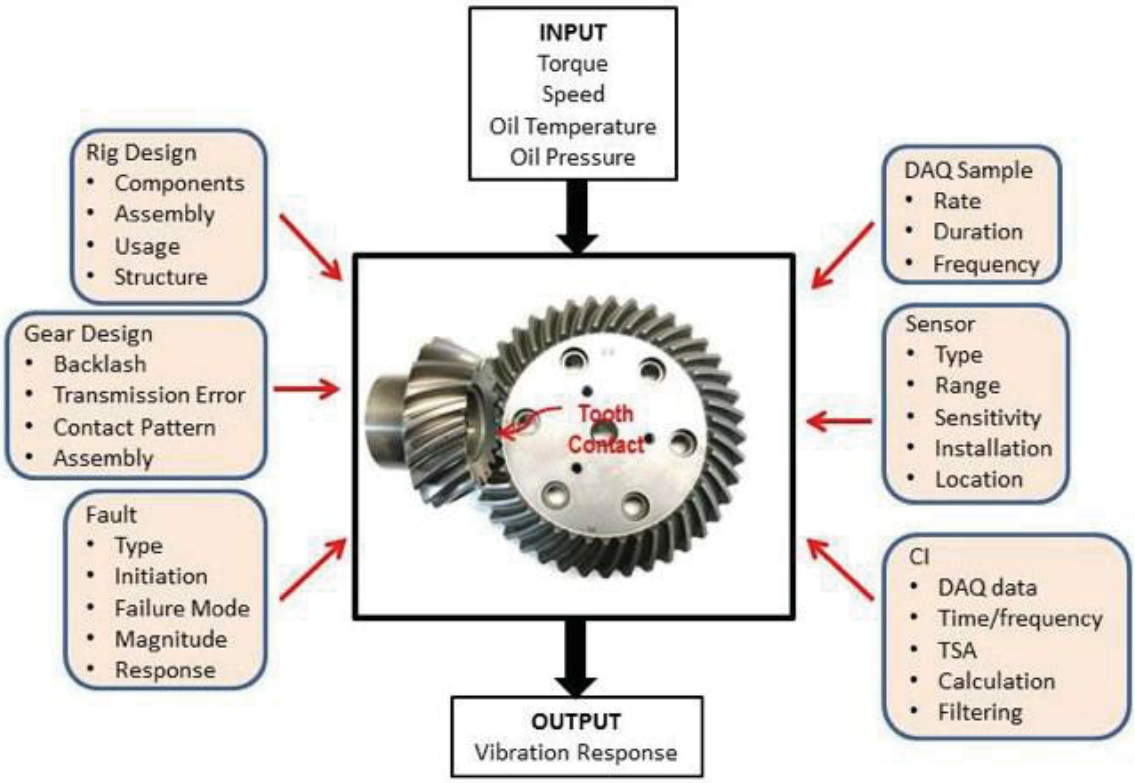

Figure 16.—Factors that affect vibration response.

In regards to the gear design, the gears were purposely designed to fail in fatigue between 100 to 200 hr at operating conditions of 3500 rpm gear speed and 8000 in-lb gear torque. Only one gear set tested lasted 100 hr before contact fatigue damage was observed on the gear teeth. Prior to superfinishing the gear sets installed on the right side of test rig, gear tooth damage occurred after 1 hr of operation at half the operating load. The surface roughness was measured on the gears and they met specifications. A cause of the failure prior to the estimated 100 hr was not determined, but it is an estimate. However, all gears are manufactured with profile and spacing errors that can vary slightly from tooth to tooth due to design tolerances.

In regards to the rig design, the four square rig operation in which the left pinion drives the gear and the right gear drives the pinion may have been the cause of the right side measured vibration always having a significantly higher amplitudes then the left. This was also observed when testing another gear design during rig checkout (Ref. 11) and with both the MDSS and MSPU systems. The numerous maintenance actions and issues in the test rig throughout testing also affected the vibration response.

The fault type (gear or pinion), mode, class, degree, magnitude, how it initiates and progresses and how it changes the signature response at the mesh all affect the measured vibration response. The fault also interacts with the rig and gear design based on the path it takes to get to the accelerometer.

DAQ Sample, Sensor and CI factors can all affect vibration response. If the CI is tuned to a specific failure mode, and the DAQ does not sample frequently enough to detect the failure mode before the fault progresses to another failure mode and component, it may not be detected. In addition, if the sensor is not located near the path of the vibration signature, it will not be detected. DAQ Sample, Sensor and CI factors will be discussed in detail in the report titled, “Investigation of Spiral Bevel Gear Condition Indicator Validation via AC–29–2C Combining Test Rig Damage Progression Data with Fielded Rotorcraft Data,” since all of the CI correlations to be discussed in this report were made using the MDSS data.

After reviewing all the factors that negatively affect the vibration response to the gear and pinion tooth damage, the challenges become obvious when implementing on a rotorcraft’s dynamic system. However, some CIs responded very well to some faults and some components. Figure 17 summarizes the performance of the CIs to specific component and faults. This table was generated from reviewing inspection Table 4, correlation coefficients Table 9 to Table 12, plots of MDSS CIs in Appendix B and CI statistical parameter tables in Appendix C for all the tests. Similar to Table 4, tests with comparable failure modes and faulted components are color coded the same. A summary of the response will be discussed:

FM4

- FM4 PL responded to macropitting on two left pinion teeth for both tests where only macropitting was observed on left pinion teeth (Tests L444R5050 and L1515R5050).
- FM4 GL responded to macropitting on two left gear teeth when macropitting was observed on two left gear teeth and one left pinion tooth at the end of the test (Tests L3030R5050 and L3535R5050). The value decreased slightly as damage progressed to the meshing pinion tooth.
- FM4 was not sensitive to torque for these tests.
- For tests where several different damage modes occurred simultaneously, it was not a good indicator of damage.
- Overall, a good indicator of macropitting on two or more gear and pinion teeth as long as damage is limited to this type of failure mode, class and degree.

SI1

- SI1 PL responded to four of the five tests with macropitting but no scuffing on one or two left pinion teeth (Tests L4545R5050, L1515R5050, L3535R5050 and L1818R1616). It did not respond to test L1515R5050.
- SI1 GL only responded to one of three tests with macropitting but no scuffing on two or more teeth (Test L3535R5050).

SI3

- SI3 PL responded to four of the five tests with macropitting but no scuffing on one to three left pinion teeth (Tests L4545R5050, L1515R5050, L3535R5050 and L1818R1616). It did not respond to test L1515R5050.
- SI3 GL only responded to one of three tests with macropitting but no scuffing on two or more teeth (Test L3535R5050).
- It makes sense that SI3 performs comparable to SI3 since SI3 is SI1 with an additional two sidebands averaged.
- SI3 PL responded to one test with macropitting on ten left pinion teeth, scuffing on left gear and pinion teeth and edge wear on right pinion teeth (Test L2121R1919).

RMS

- RMS GR and PR values measured by the accelerometer installed on the right side of the test rig were higher than the left side of the test rig for every test except L2020R5050.
- RMS PL responded to the three tests with scuffing (Tests L2020R5050, L4040R5050 and L2121R1919).
- RMS GL responded to two of the three tests with scuffing (Tests L2020R5050 and L4040R5050).
- RMS PL responded to one test with pinion macropitting (L4545R5050) and one test with pinion ad gear macropitting (L3535R5050).
- RMS GR and PR responded to the test with right pinion and gear edge and root wear (L4444R5252). During this test, edge wear on the pinion dug into the mating gear.
- RMS GR and PR were sensitive to torque for the majority of tests performed.
- RMS GR and PR were sensitive to transients in temperatures and torques.

Based on the review of the four CIs for the four components during the tests performed, FM4, SI1 and SI3 can be used to detect macro pitting on two more gear or pinion teeth. Once damage progresses to other components within the system, the CI sensitivity reduces. It is important that the data acquisition system can detect the damage before it transitions to another failure mode or other components.

RMS sensitivity to torque and other system and operational conditions limit its reliability for systems that are not maintained at steady state. Many helicopter HUMS system only acquire data within a fixed band of quasi steady state conditions. More studies are required to determine if RMS is not sensitive to the changes within this band.

Test	GL	GR	PL	PR	RMS	FM4	SI1	SI3
L4545R5050					PLV	PLV	PLV	PLV
L3030R5050						GLV	PLV	PLV
L1515R5050						PLV		
L2020R5050					GLV & PLV			
L4040R5050					GLV & PLV			
L3535R5050					GLV & PLV	GLV	GLV & PLV	GLV & PLV
L1818R1616							PLV	PLV
L2121R1919					PLV			PLV
L1616R1919								
L3737R2424								
L3737R5036								
L1414R1616								
L4444R5252					GRV & PRV			

Figure 17.—Summary of CI Response.

RMS was sensitive to the scuffing failure mode. This is a challenging failure mode since the damage is distributed across all the gear and pinion teeth, smearing the signatures typically used for gear health. New methods may be required to reliably detect this type of fault.

The response of all the CIs was affected by a fretting issue that was present for many of the tests. Similar to scuffing, fretting also causes unusual wear patterns distributed across the all the gear and pinion teeth. New methods may be required to detect this type of fault.

12.0 Summary

Tests were performed on 19 spiral bevel gear sets in the NASA Glenn Spiral Bevel Gear Fatigue Test Rig to simulate the fielded failures of spiral bevel gears installed in a helicopter to support validation and demonstration of rotorcraft Health and Usage Monitoring Systems (HUMS) for maintenance credits. Gear sets were tested until damage initiated and progressed while gear health monitoring data and operational parameters were measured and tooth damage progression documented using photographs. The "naturally occurring" accelerated failure modes were generated to simulate fielded failure modes. Gear tooth damage modes and magnitude were summarized for each test within inspection intervals. Similar damage modes from different gear tests were clustered for analysis. Gear condition indicator response was correlated to damage mode and operational parameters. A reliable gear condition indicator must be tuned to the specific fault with minimal effect from other factors such as gear and system design, system maintenance, sensing system and data acquisitions methods.

Results of rig testing found condition indicators FM4, SI1 and SI3 can be used to detect macro pitting on two more gear or pinion teeth as long it is detected before damage progresses to other components within the system or another failure mode is generated. The sensitivity of condition indicator RMS to system design and operational conditions limit its reliability for systems that are not maintained at steady state. Failure modes due to scuffing or fretting are challenging to detect using current gear diagnostic tools since the damage is distributed across all the gear and pinion teeth, smearing the impacting signatures typically used to differentiate between a healthy and damaged tooth contact. New methods may be required to detect these types of fault conditions.

Results of the rig CI performance presented in this report will be compared to the helicopter performance in the second report titled, "Investigation of Spiral Bevel Gear Condition Indicator Validation via AC–29–2C Using Fielded Rotorcraft HUMS Data," by reprocessing the helicopter HUMS data with the same analysis techniques applied to spiral bevel rig test data. Results from analysis of the rig and helicopter data will be correlated and observations, findings and lessons learned using sub-scale rig failure progression tests to validate helicopter gear condition indicators will be discussed in a third report titled, "Investigation of Spiral Bevel Gear Condition Indicator Validation Via AC–29–2C Combining Test Rig Damage Progression Data with Fielded Rotorcraft Data."

Appendix A.—Representative Photos of Gear and Pinion Teeth Damage

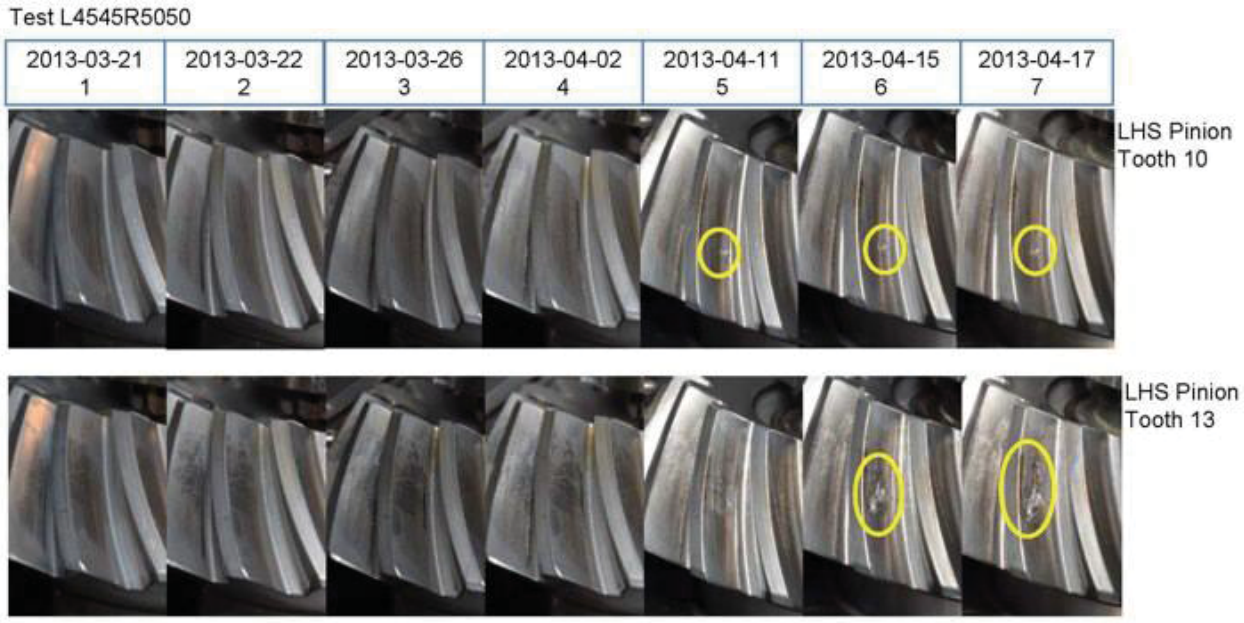

Figure A.1.1.—Test L4545R5050 pinion damage modes.

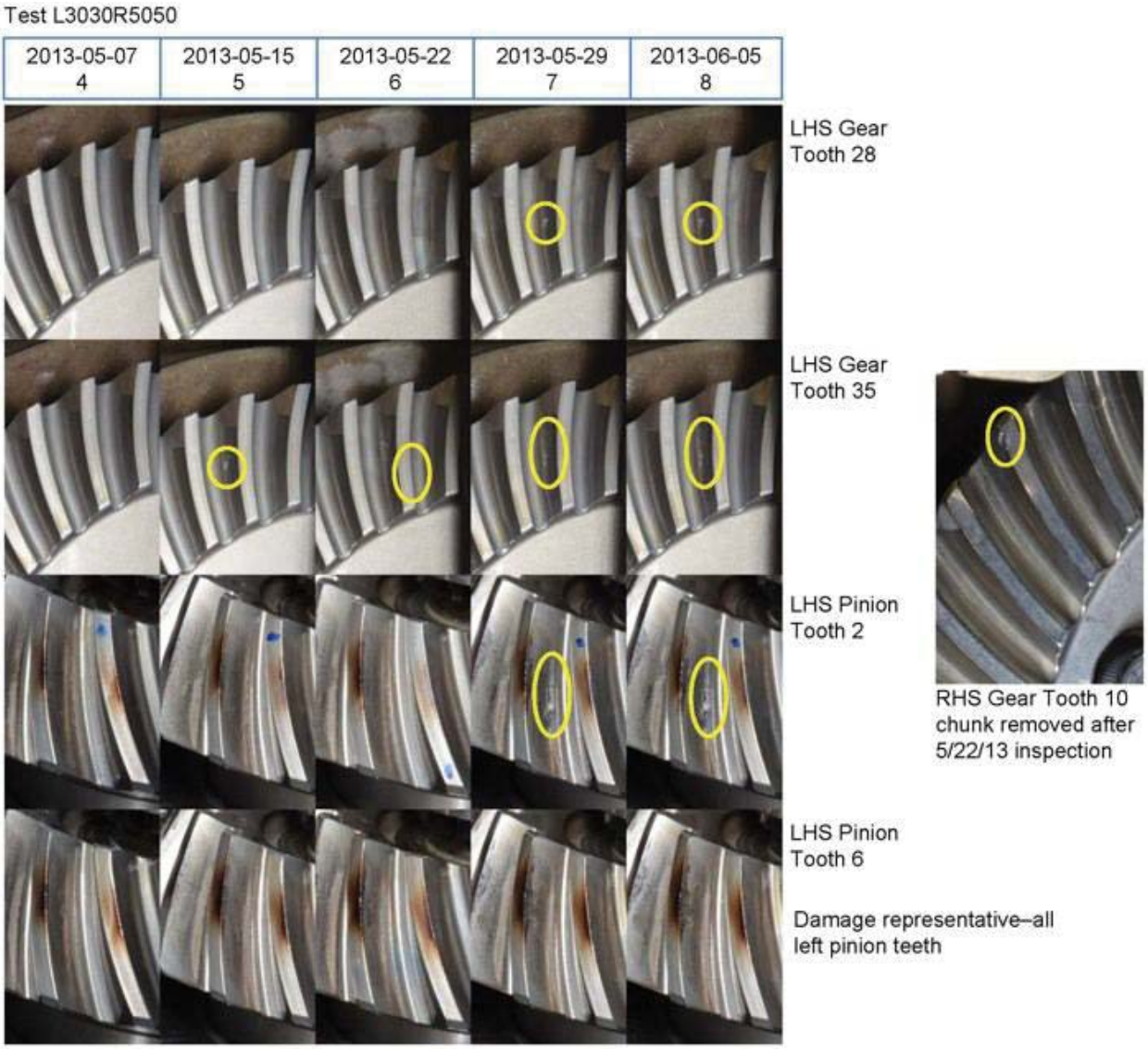

Figure A.1.2.—Test L3030R5050 pinion and gear damage modes.

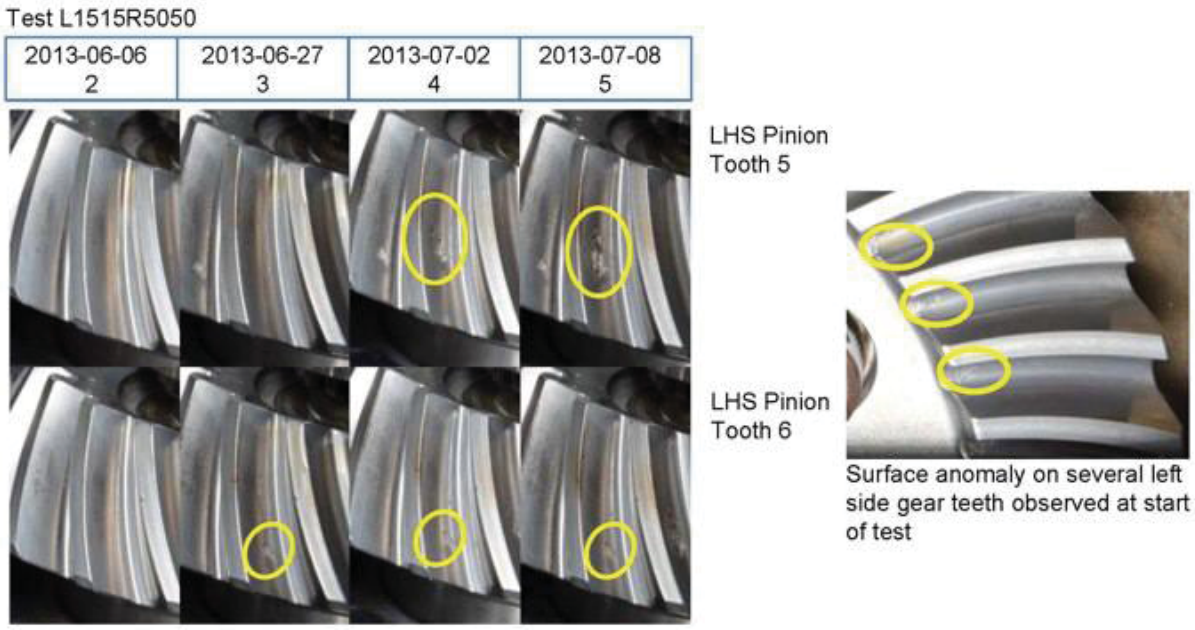

Figure A.1.3.—Test L1515R5050 pinion and gear damage modes.

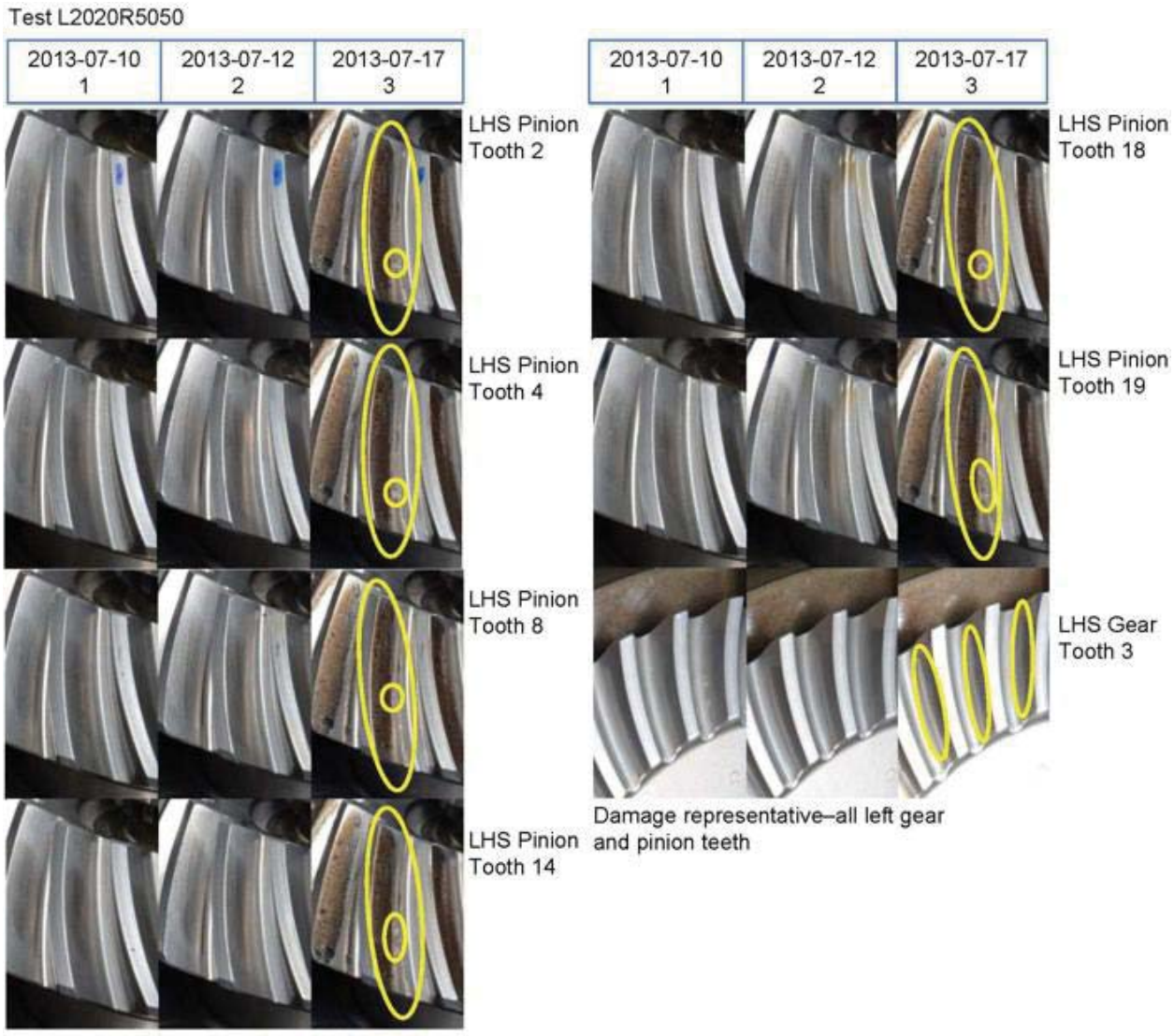

Figure A.1.4.—Test L2020R5050 pinion and gear damage modes.

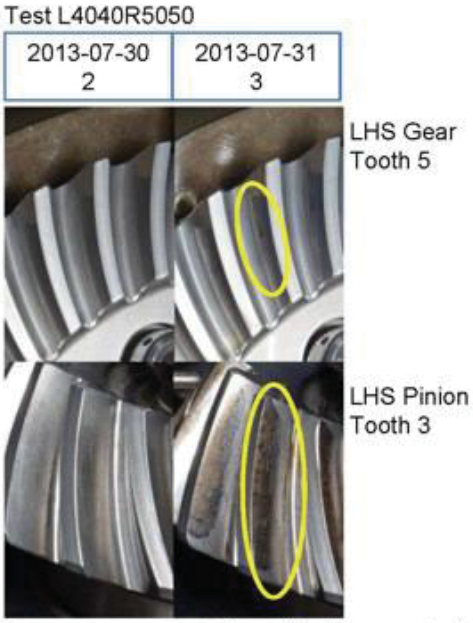

Figure A.1.5.—Test L4040R5050 pinion and gear damage modes.

Figure A.1.6.—Test L3535R5050 pinion and gear damage modes.

Figure A.1.7.—Test L1818R1616 pinion and gear damage modes.

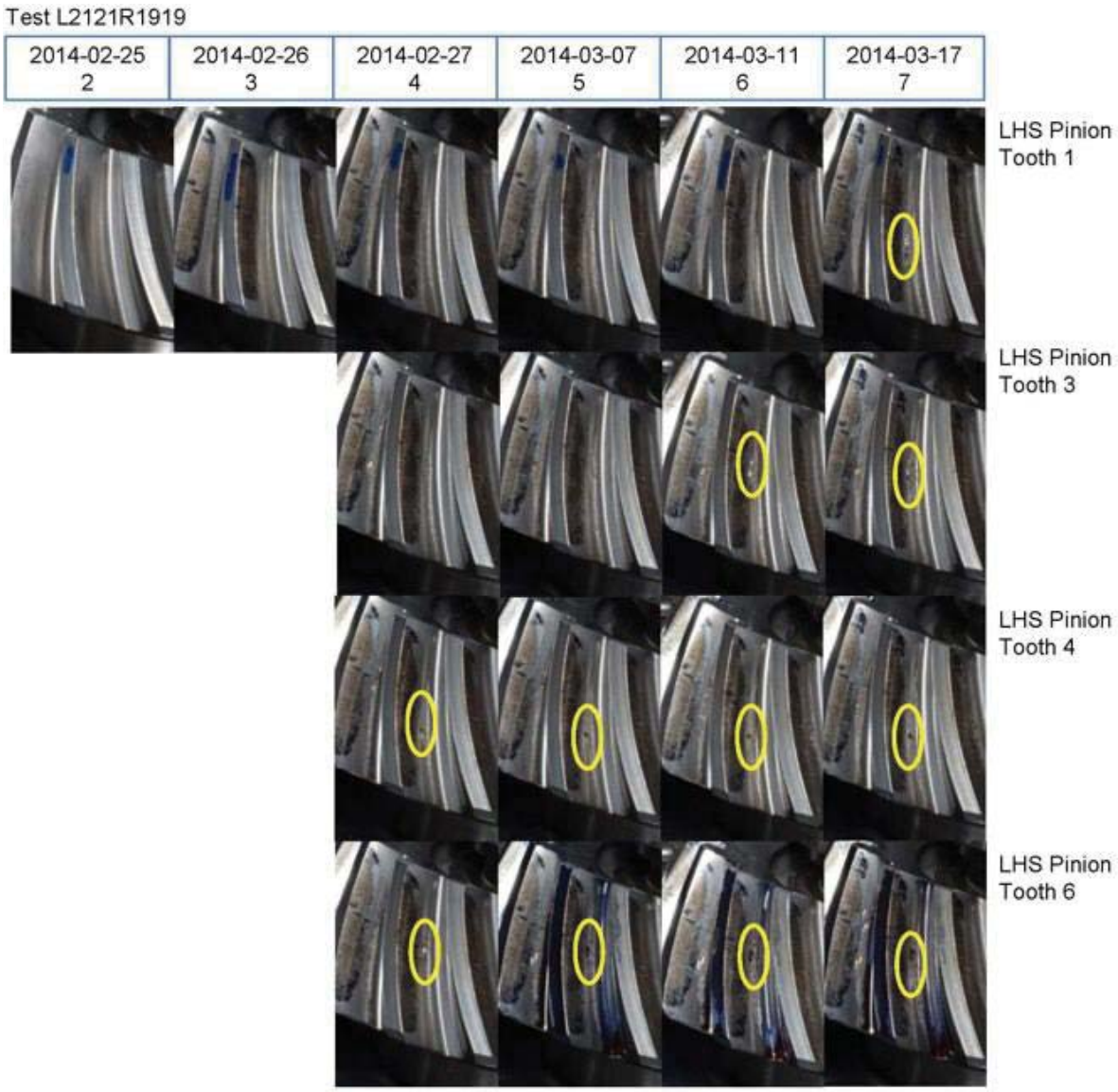

Figure A.1.8.—Test L2121R1919 pinion damage modes.

Figure A.1.9.—Test L2121R1919 pinion damage modes.

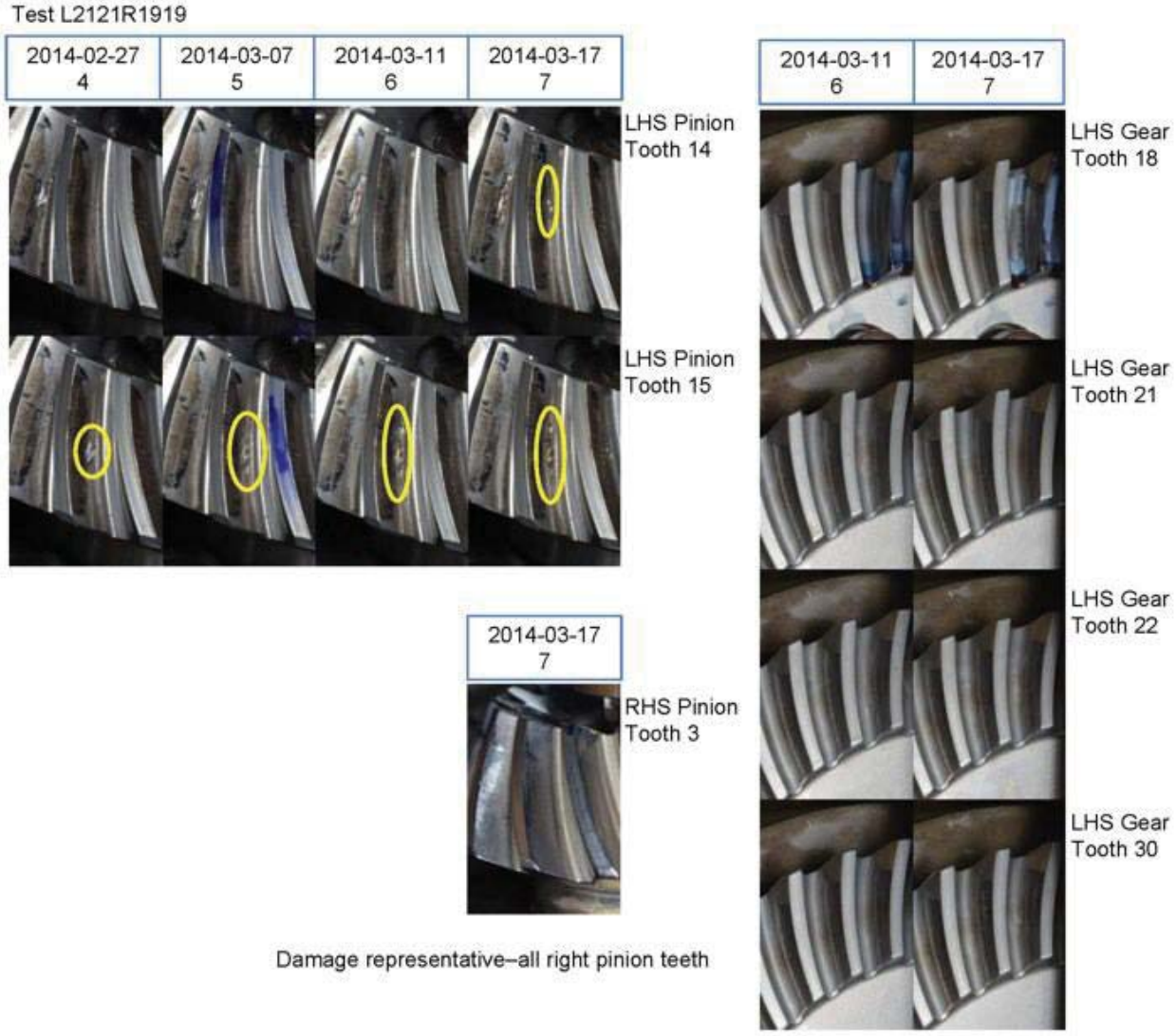

Figure A.1.10.—Test L2121R1919 pinion damage modes.

Figure A.1.11.—Test L1616R1919 pinion damage modes.

Figure A.1.12.—Test L3737R2424 damage modes.

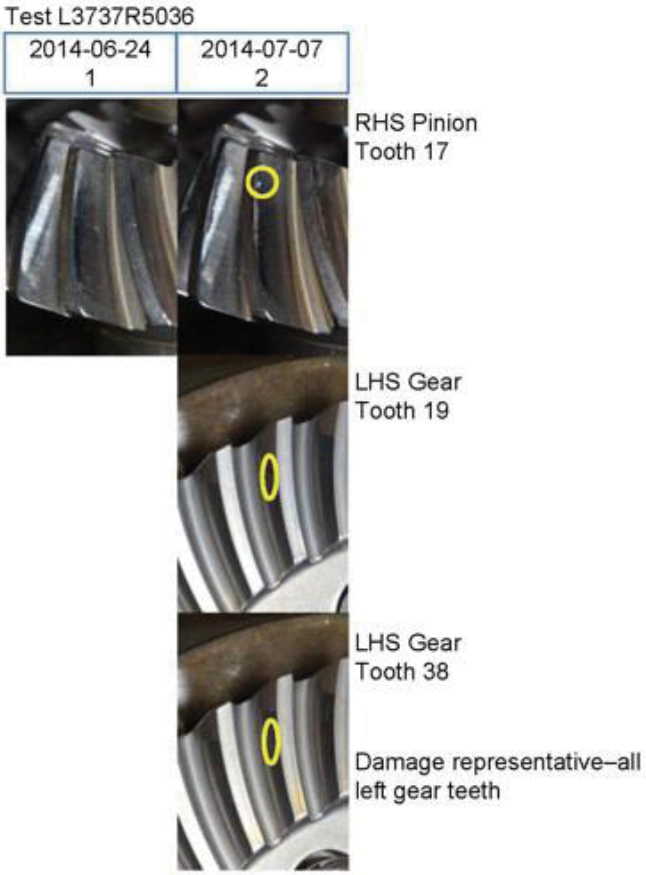

Figure A.1.13.—Test L3737R5036 damage modes.

Figure A.1.14.—Test L1414R1616 damage modes.

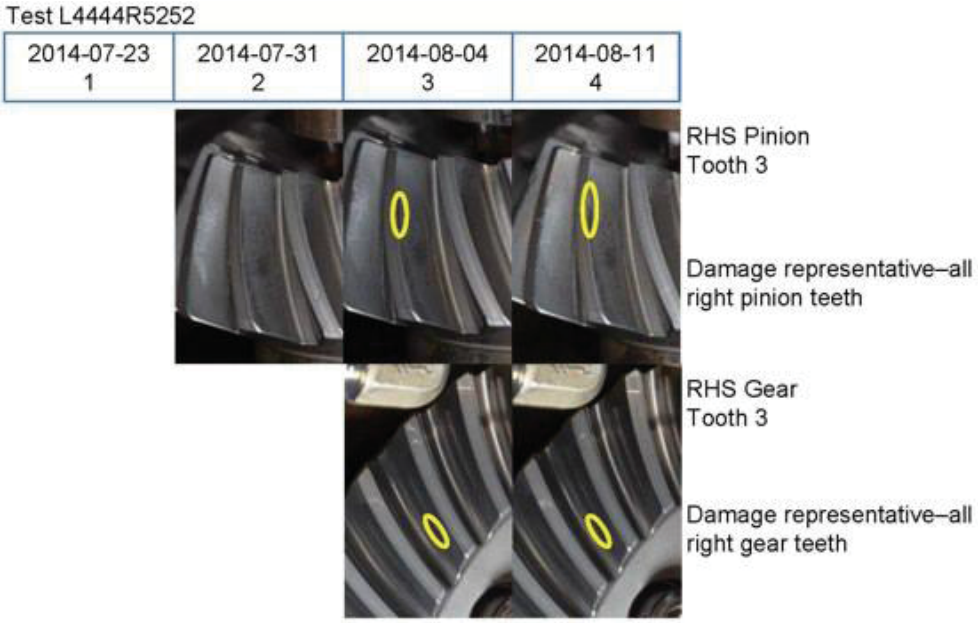

Figure A.1.15.—Test L4444R5252 damage modes.

Appendix B.—Plots of MDSS Condition Indicators and Operational Data

B.1 Test L4545R5050

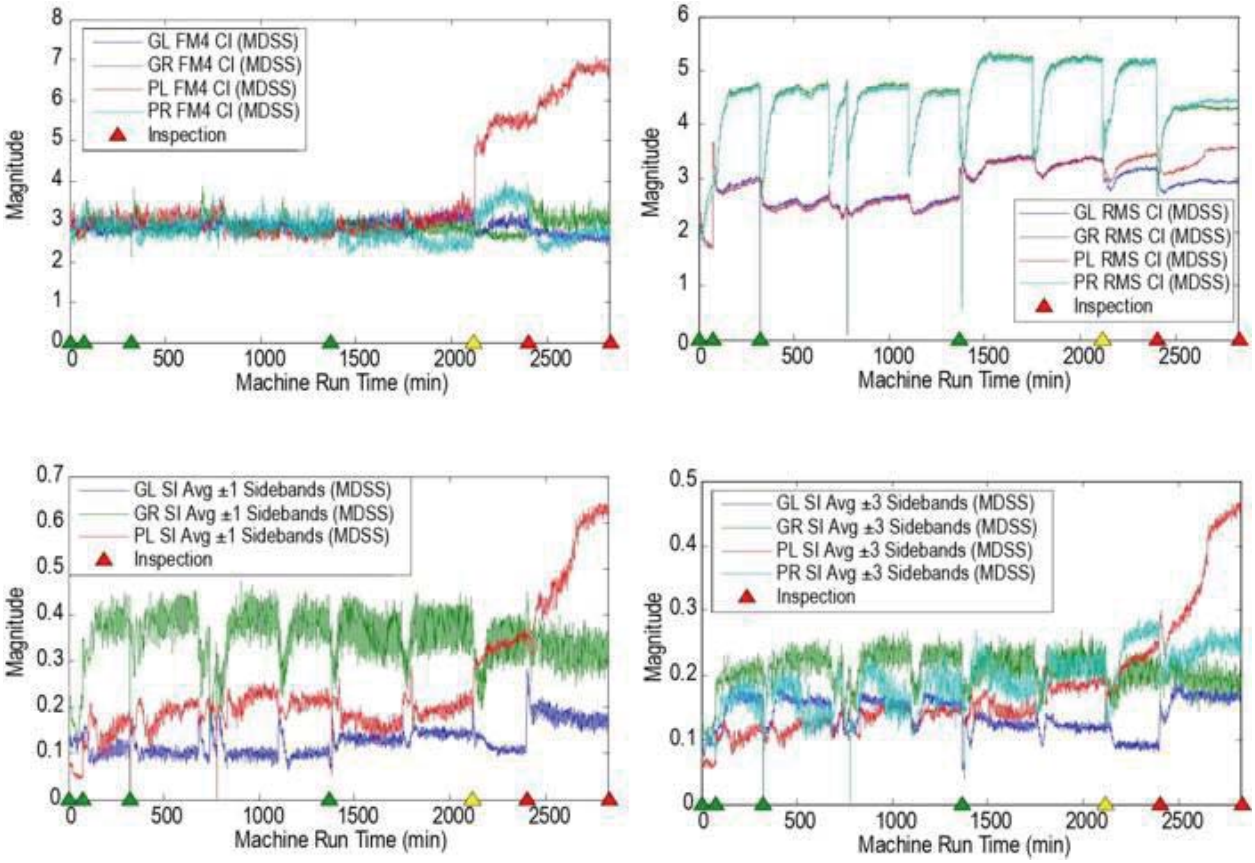

Figure B.1.1.—Test L4545R5050 Plots of FM4, RMS, SI1 and SI3.

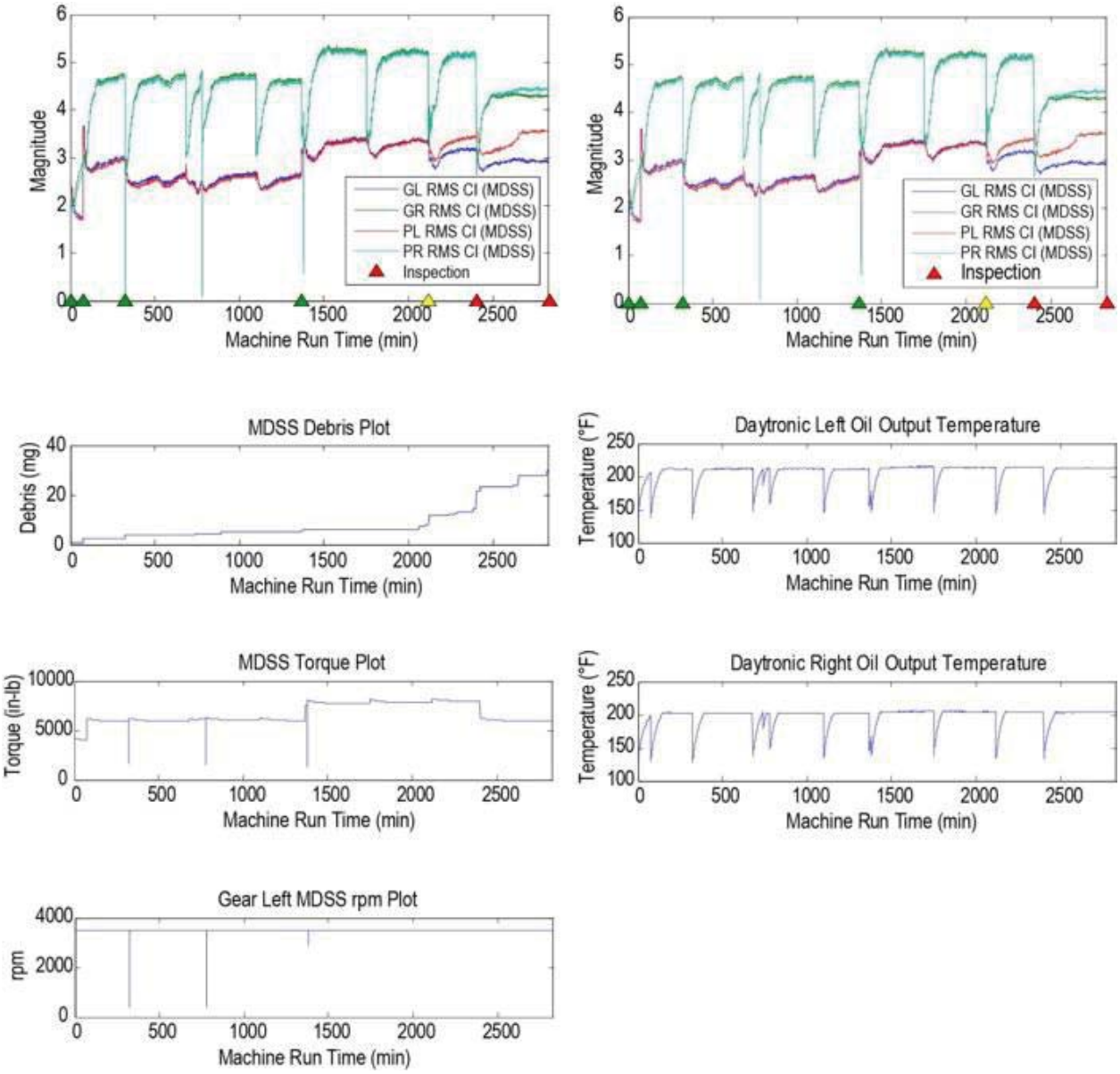

Figure B.1.2.—Test L4545R5050 Plots of RMS and Operational Parameters.

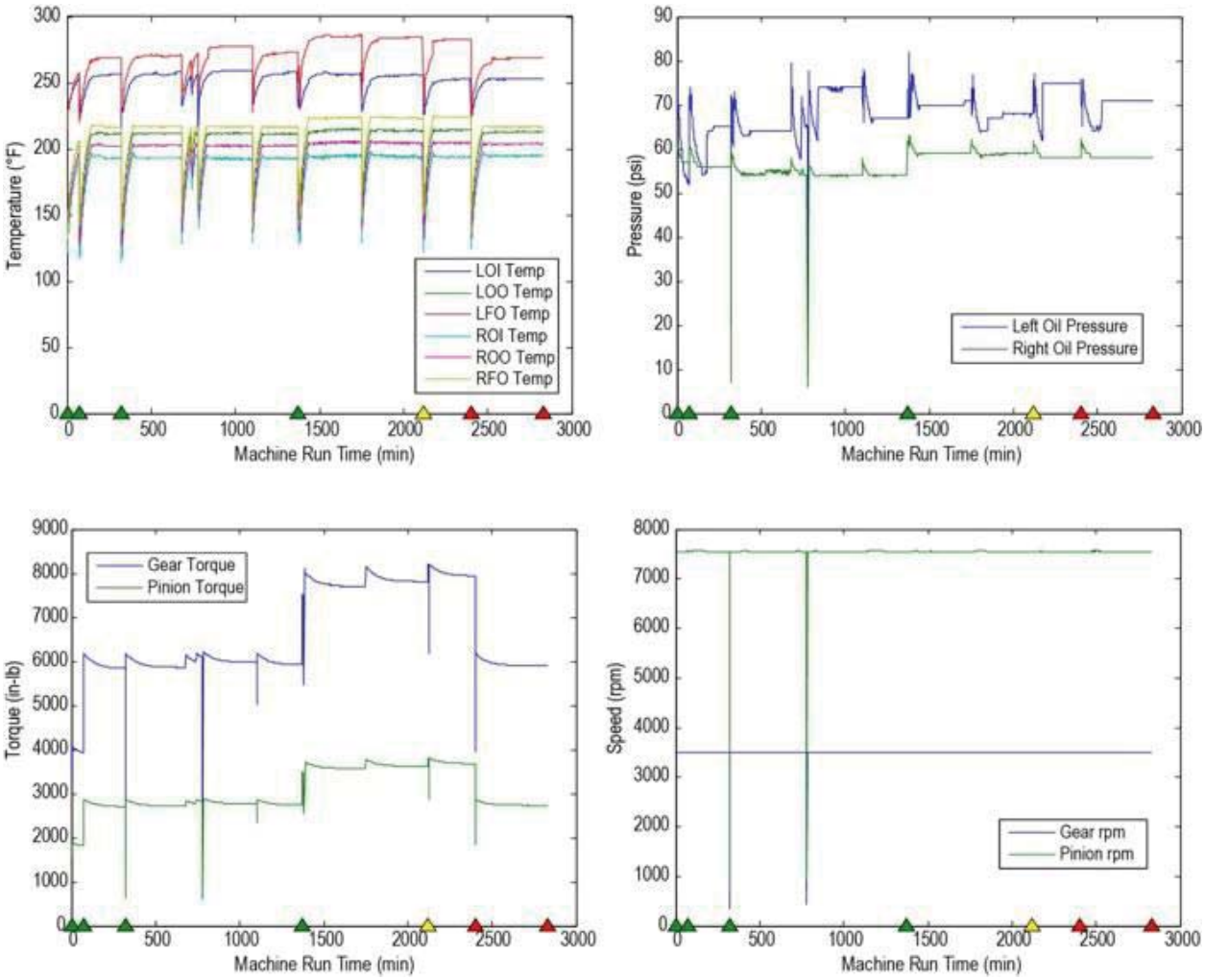

Figure B.1.3.—Test L4545R5050 Plots of Operational Parameters.

B.2 Test L3030R5050

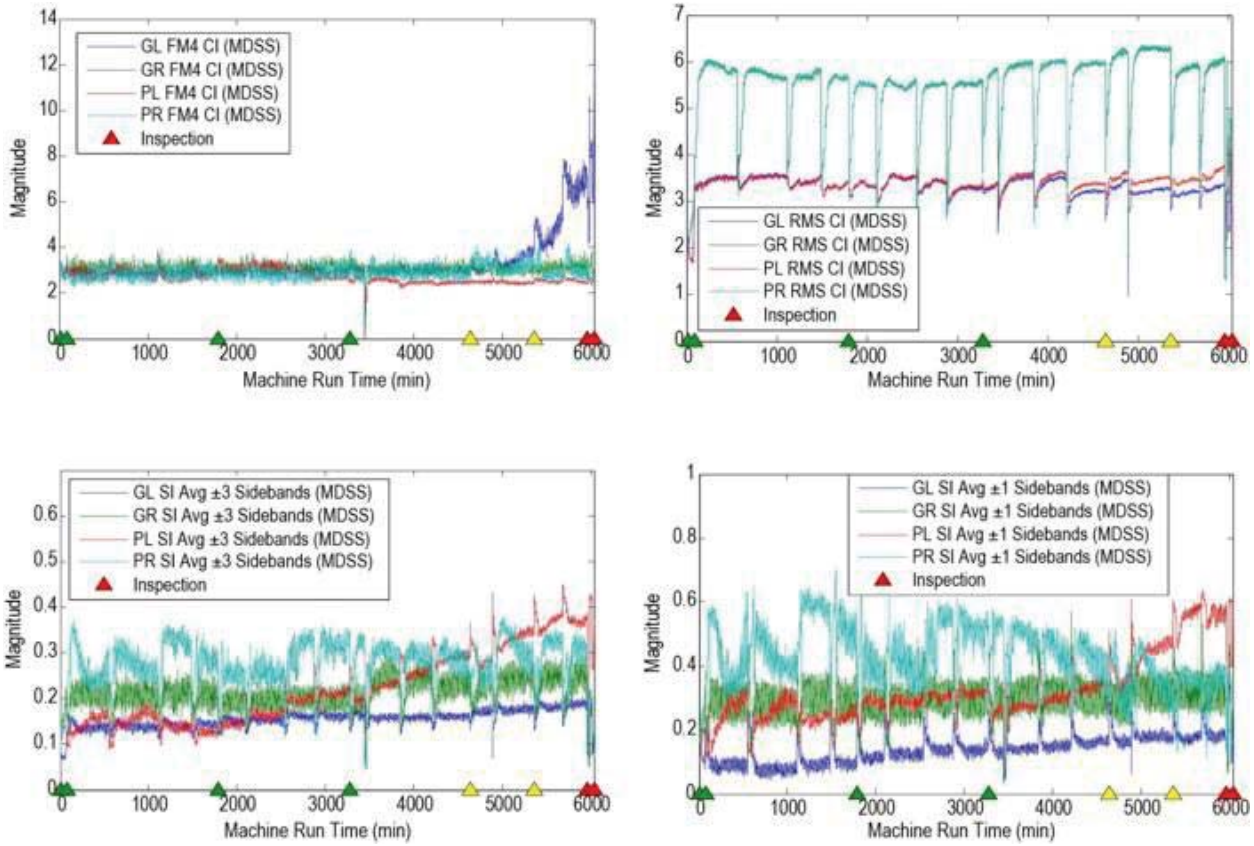

Figure B.2.1.—Test L3030R5050 Plots of FM4, RMS, SI1 and SI3.

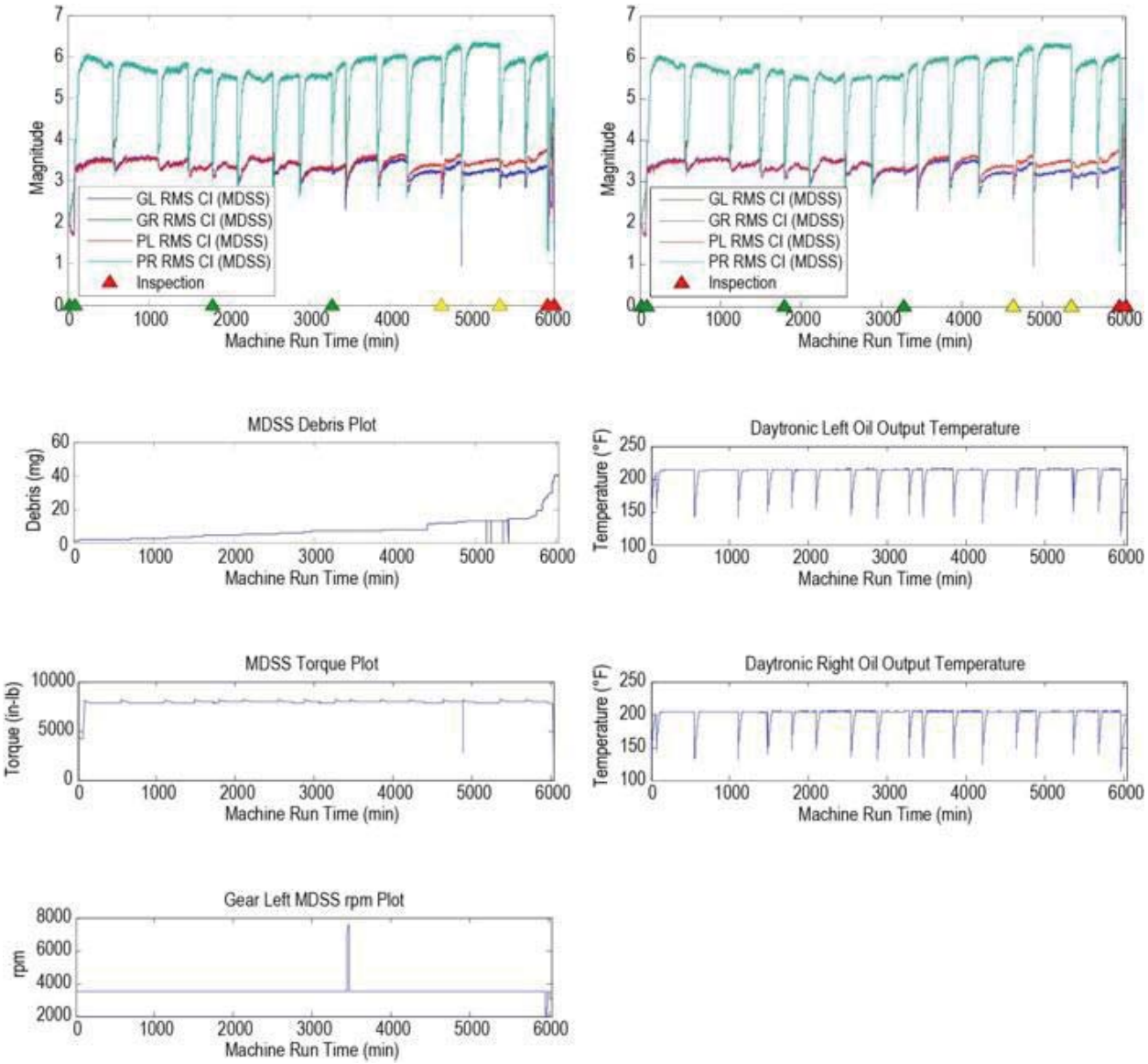

Figure B.2.2.—Test L3030R5050 Plots of RMS and Operational Parameters.

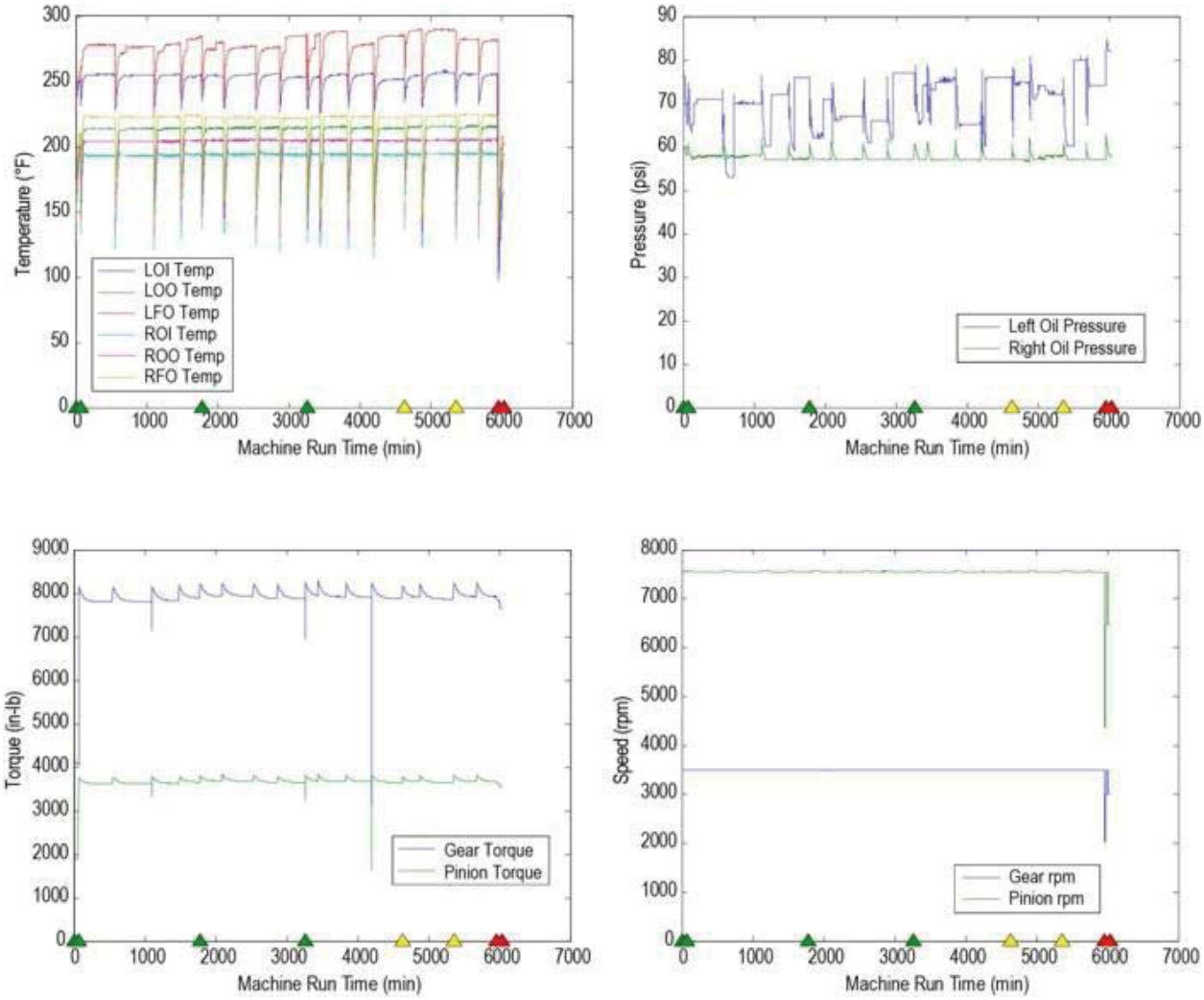

Figure B.2.3.—Test L3030R5050 Plots of Operational Parameters.

B.3 Test L1515R5050

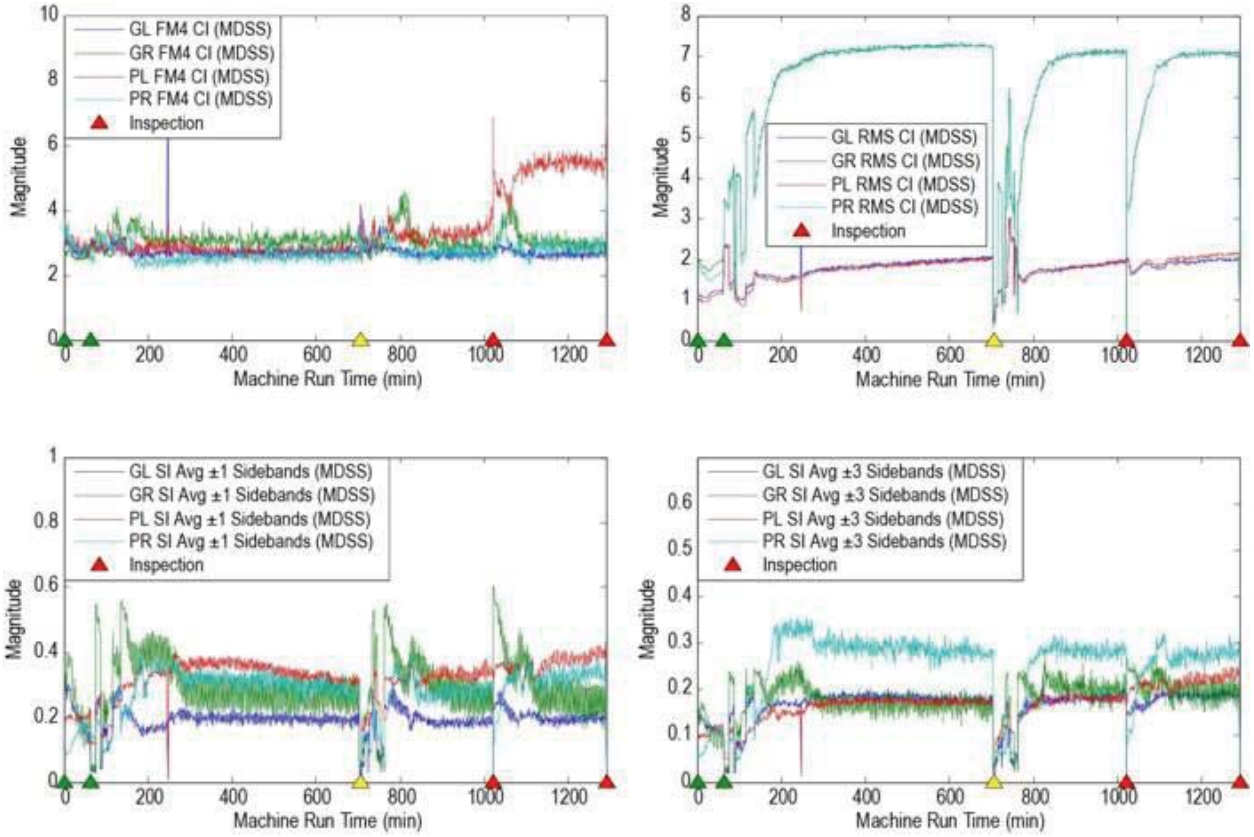

Figure B.3.1.—Test L1515R5050 Plots of FM4, RMS, SI1 and SI3.

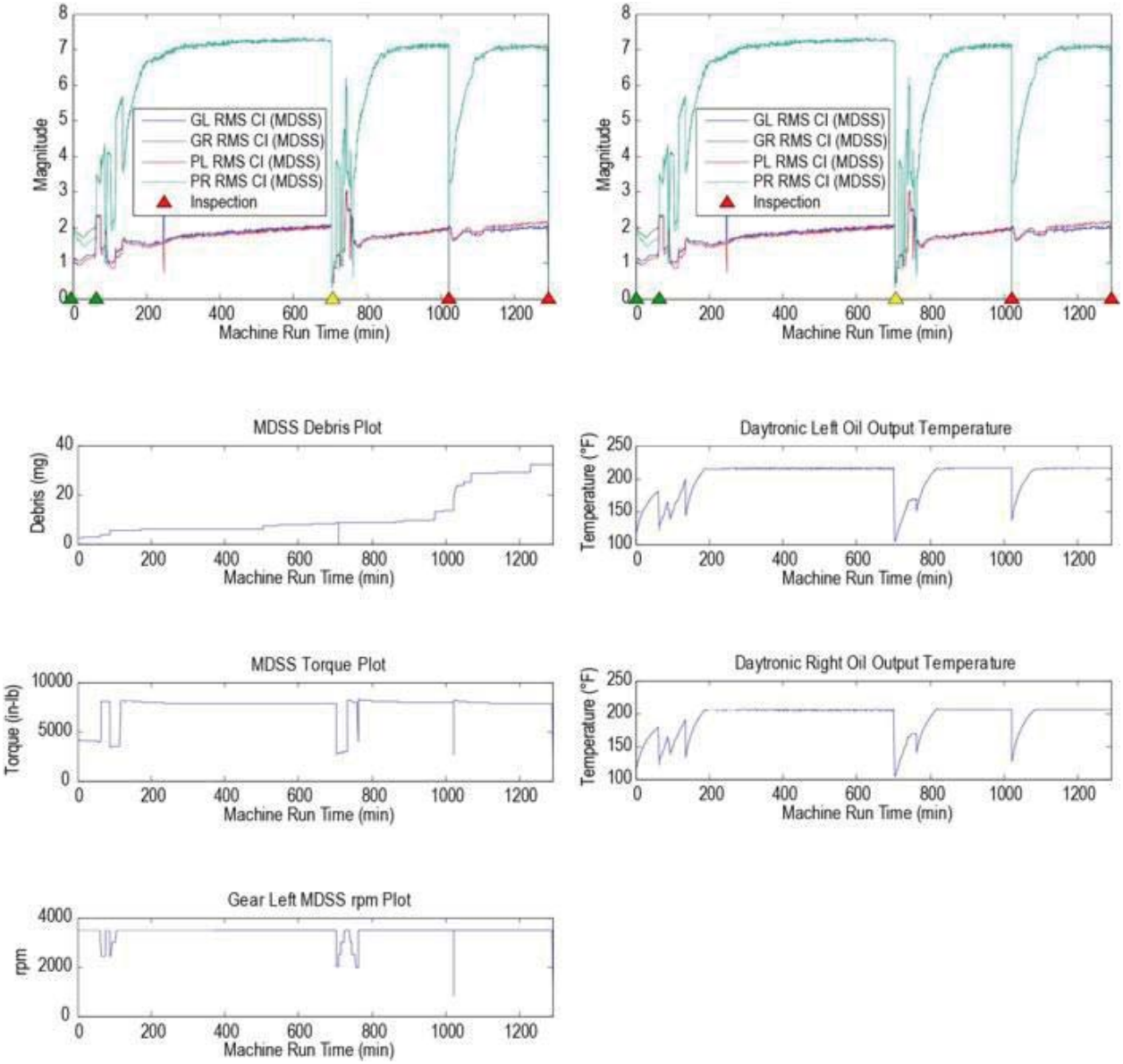

Figure B.3.2.—Test L1515R5050 Plots of RMS and Operational Parameters.

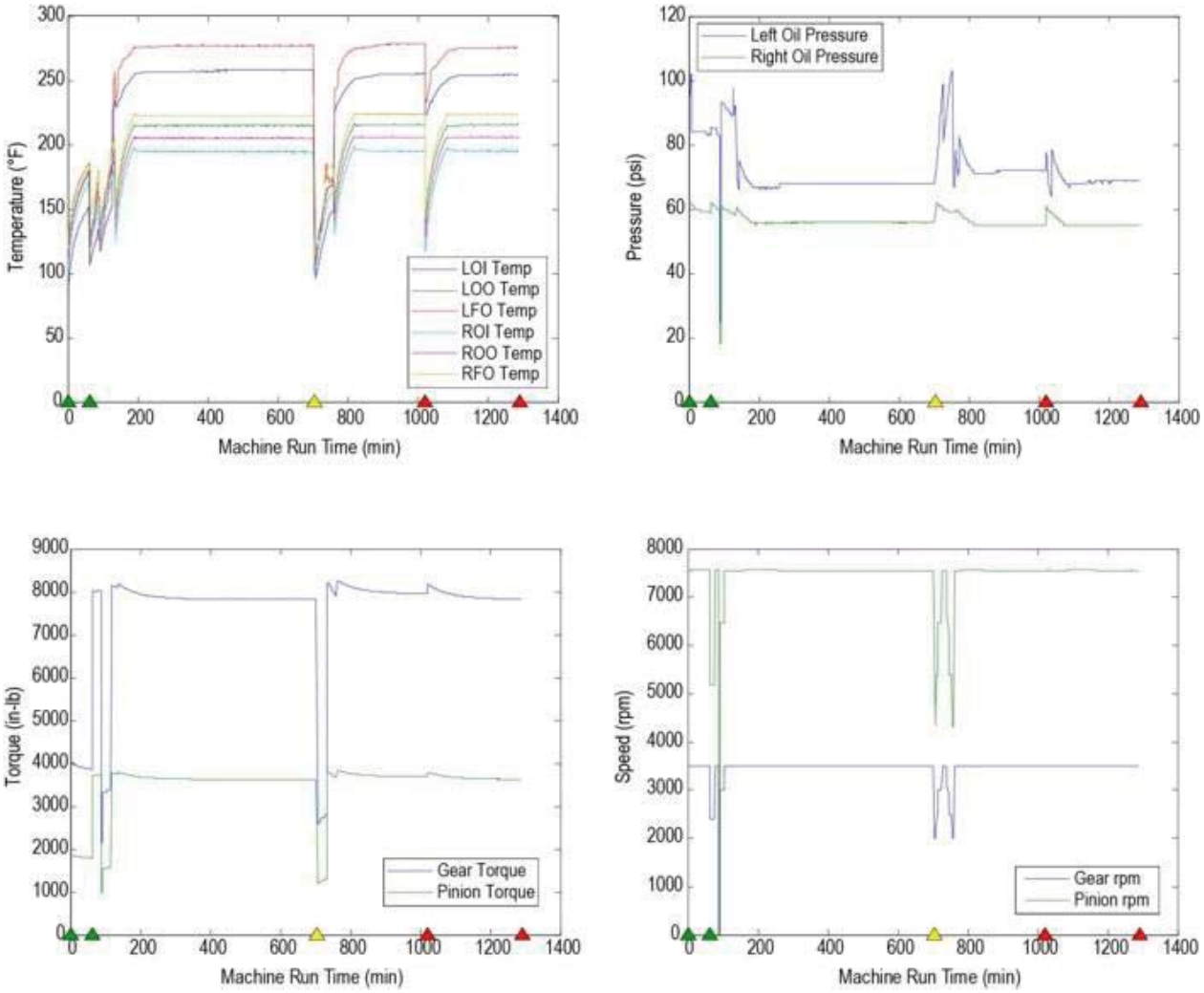

Figure B.3.3.—Test L1515R5050 Plots of Operational Parameters.

B.4 Test L2020R5050

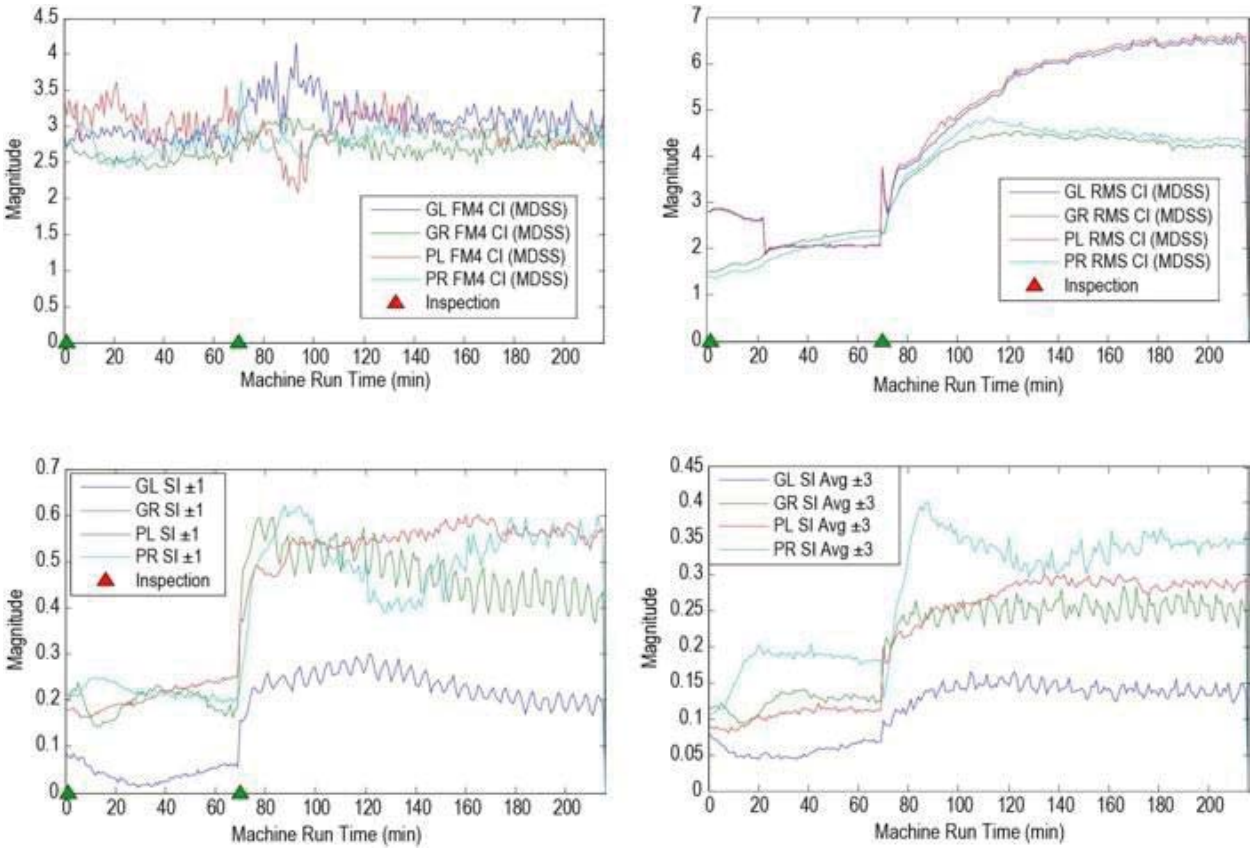

Figure B.4.1.—Test L2020R5050 Plots of FM4, RMS, SI1 and SI3.

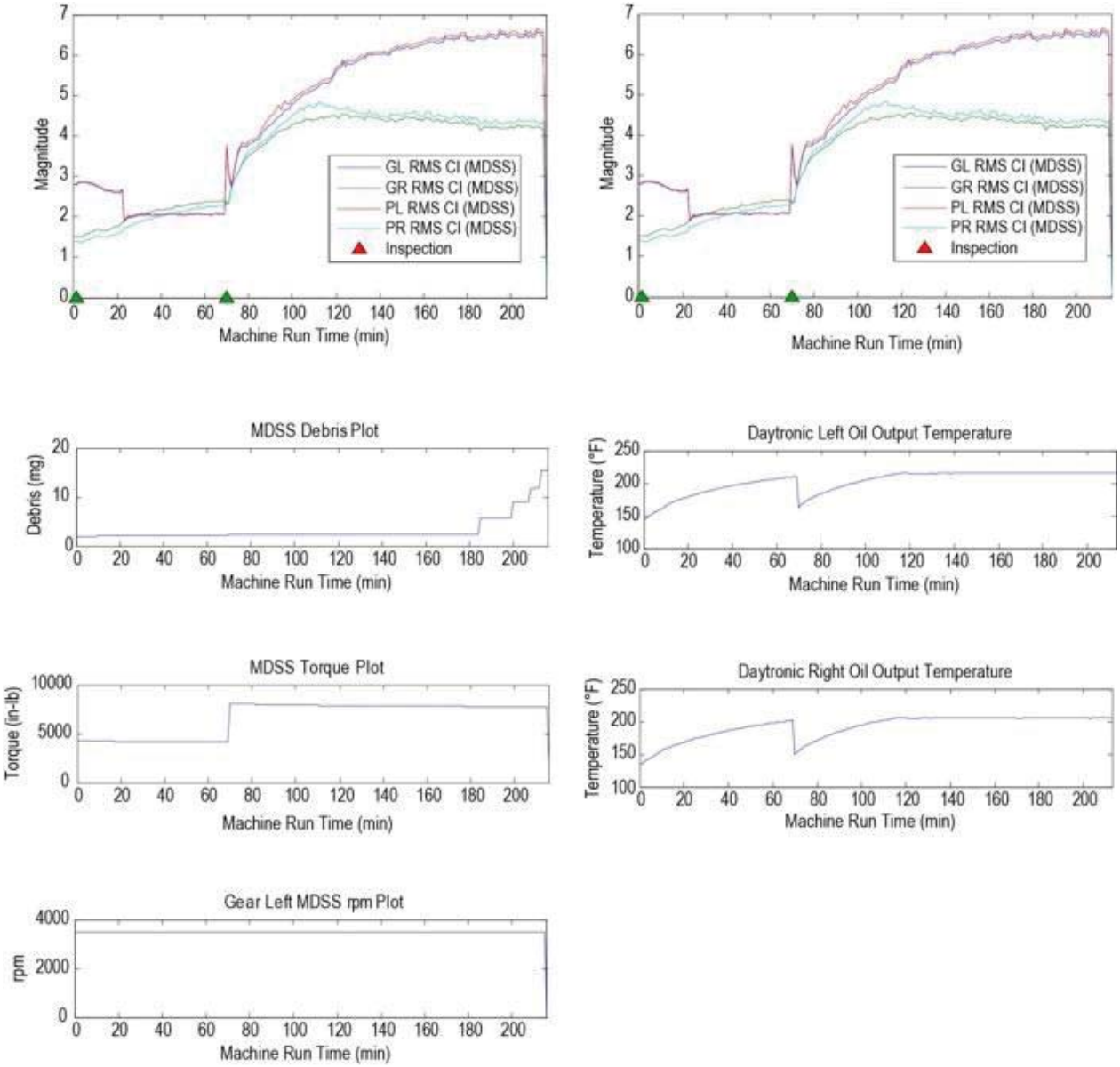

Figure B.4.2.—Test L2020R5050 Plots of RMS and Operational Parameters.

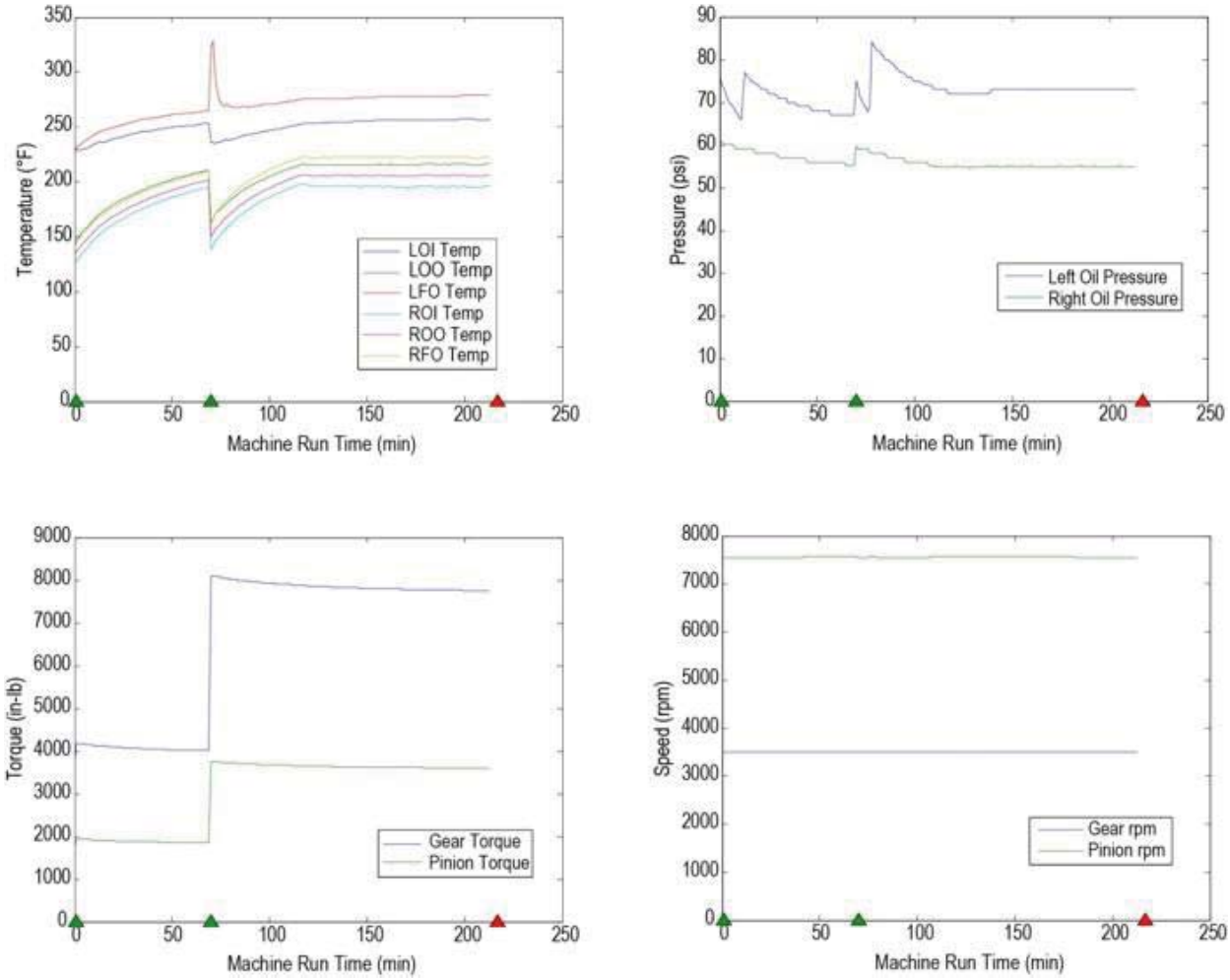

Figure B.4.3.—Test L2020R5050 Plots of Operational Parameters.

B.5 Test L4040R5050

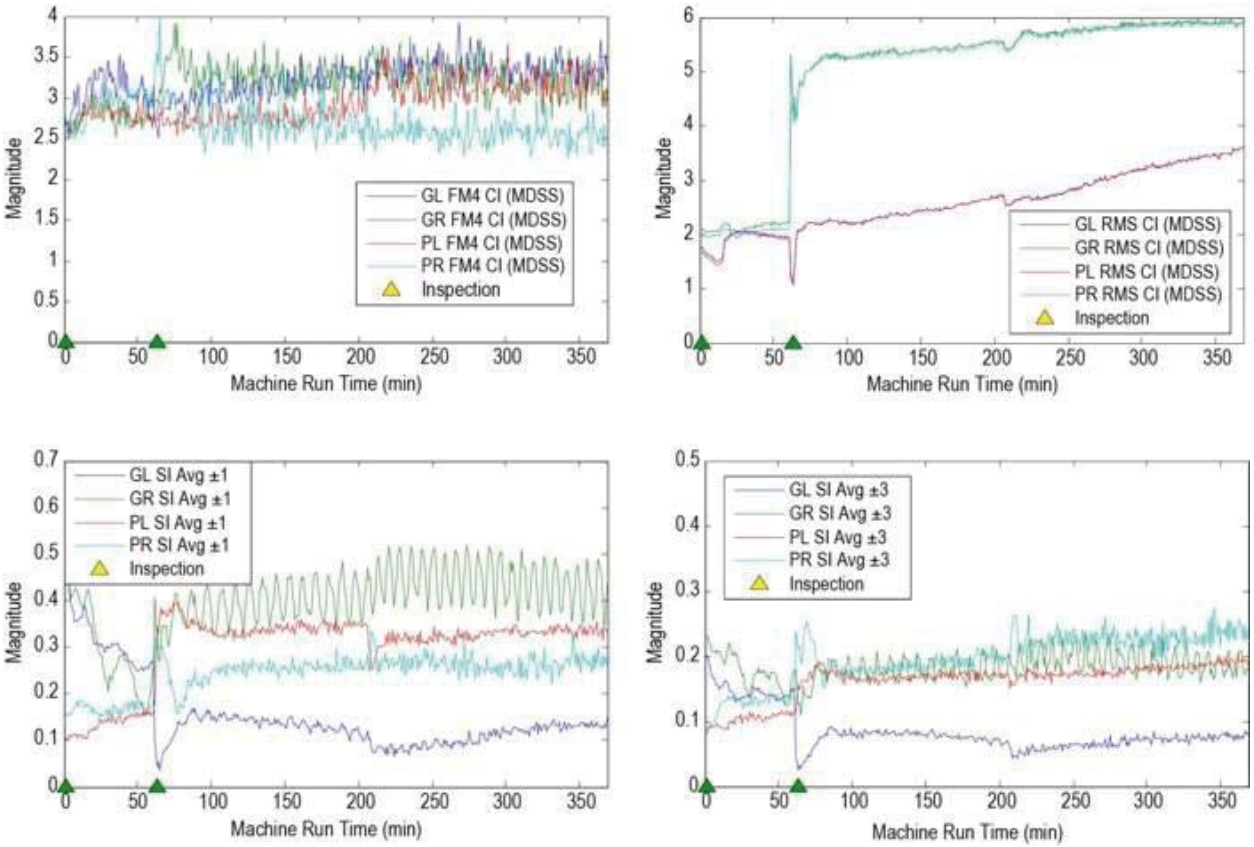

Figure B.5.1.—Test L4040R5050 Plots of FM4, RMS, SI1 and SI3.

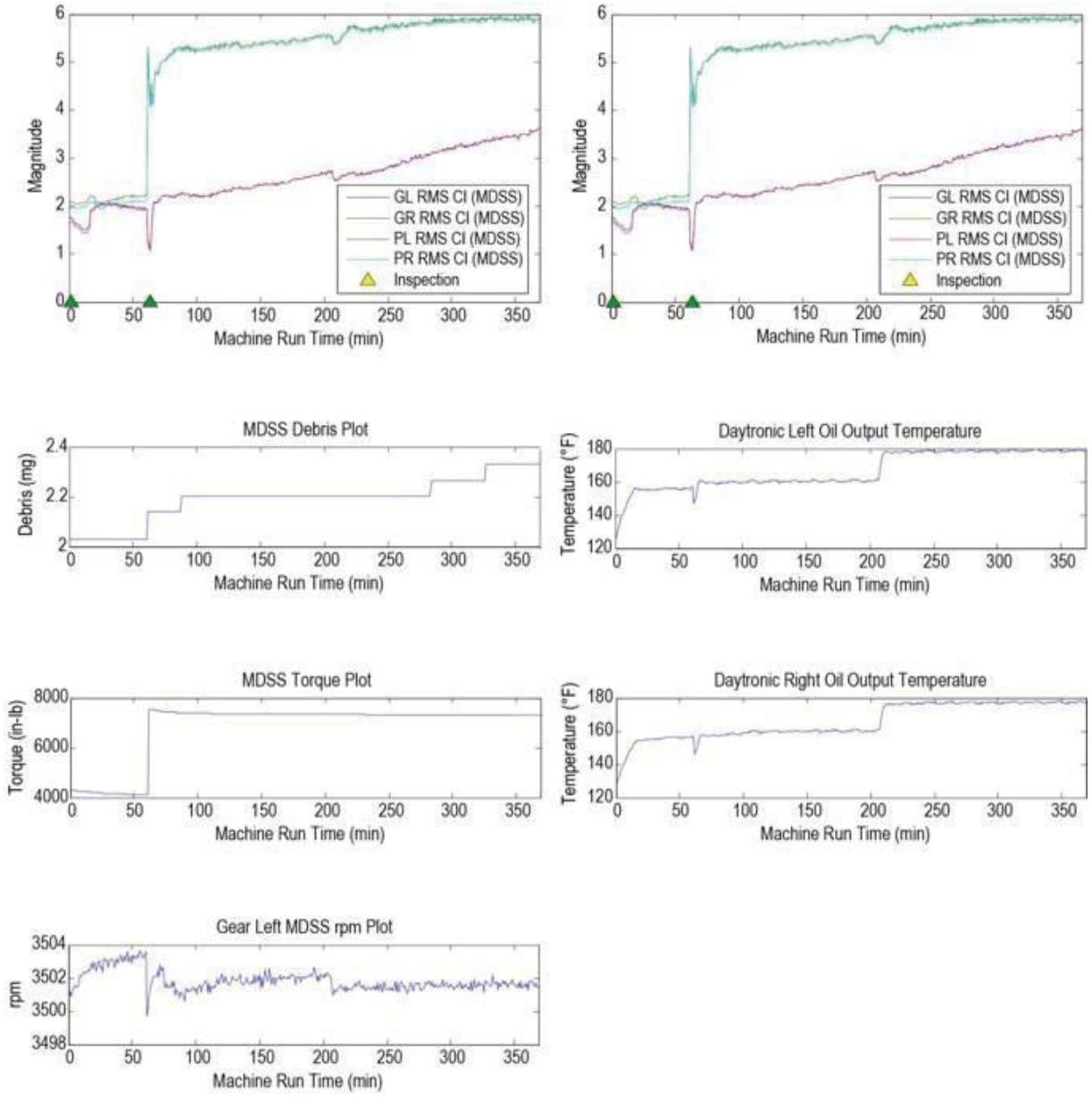

Figure B.5.2.—Test L4040R5050 Plots of RMS and Operational Parameters.

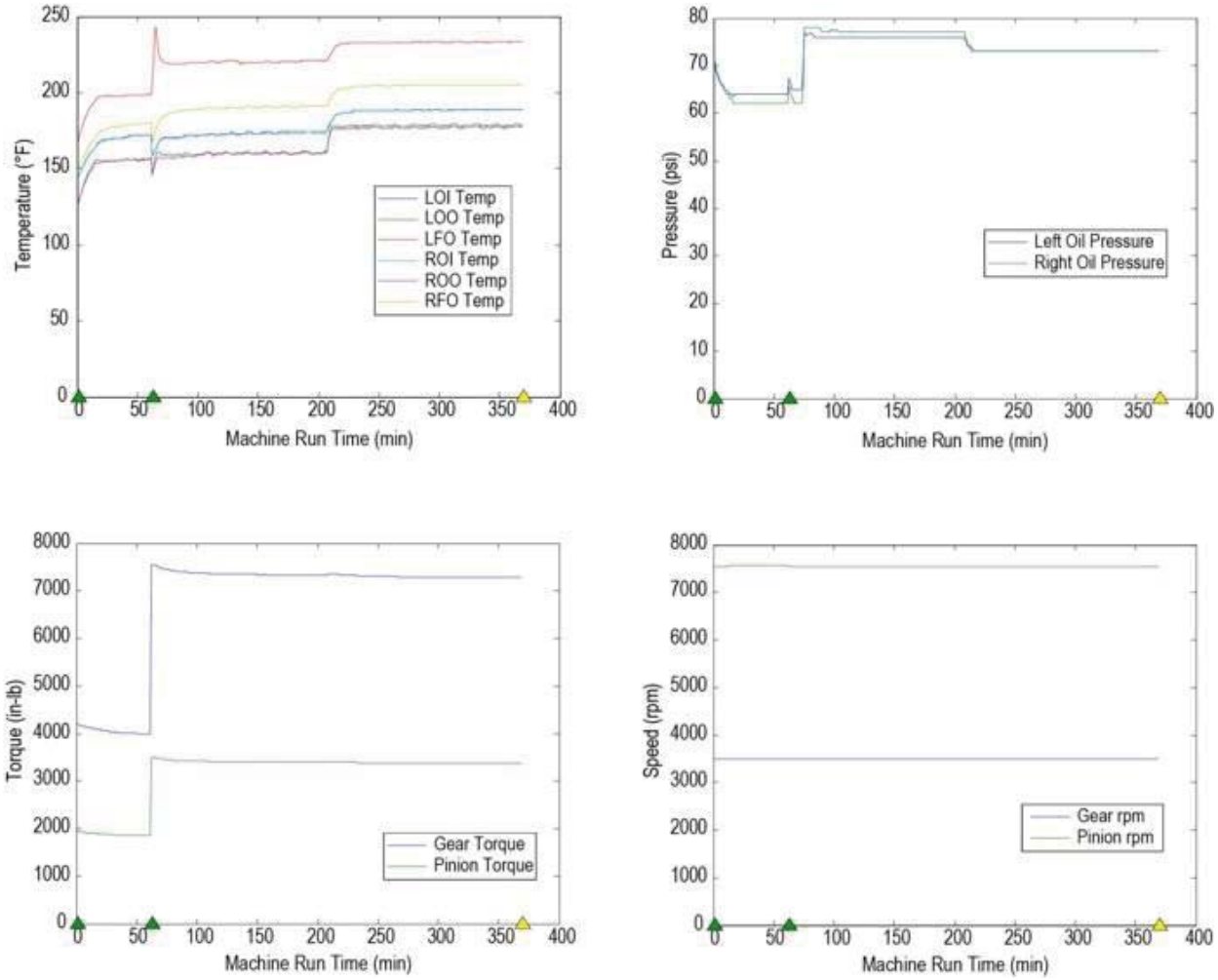

Figure B.5.3.—Test L4040R5050 Plots of Operational Parameters.

B.6 Test L3535R5050

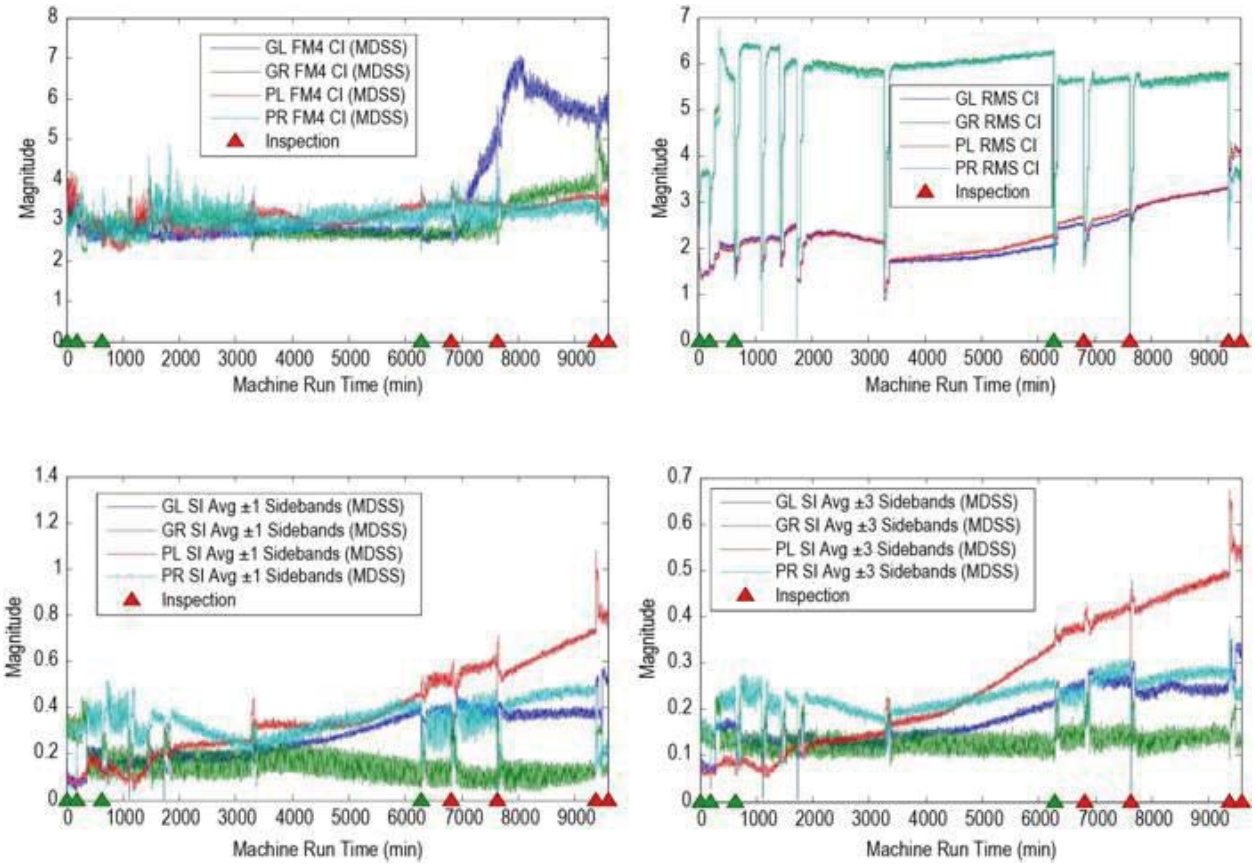

Figure B.6.1.—Test L3535R5050 Plots of FM4, RMS, SI1 and SI3.

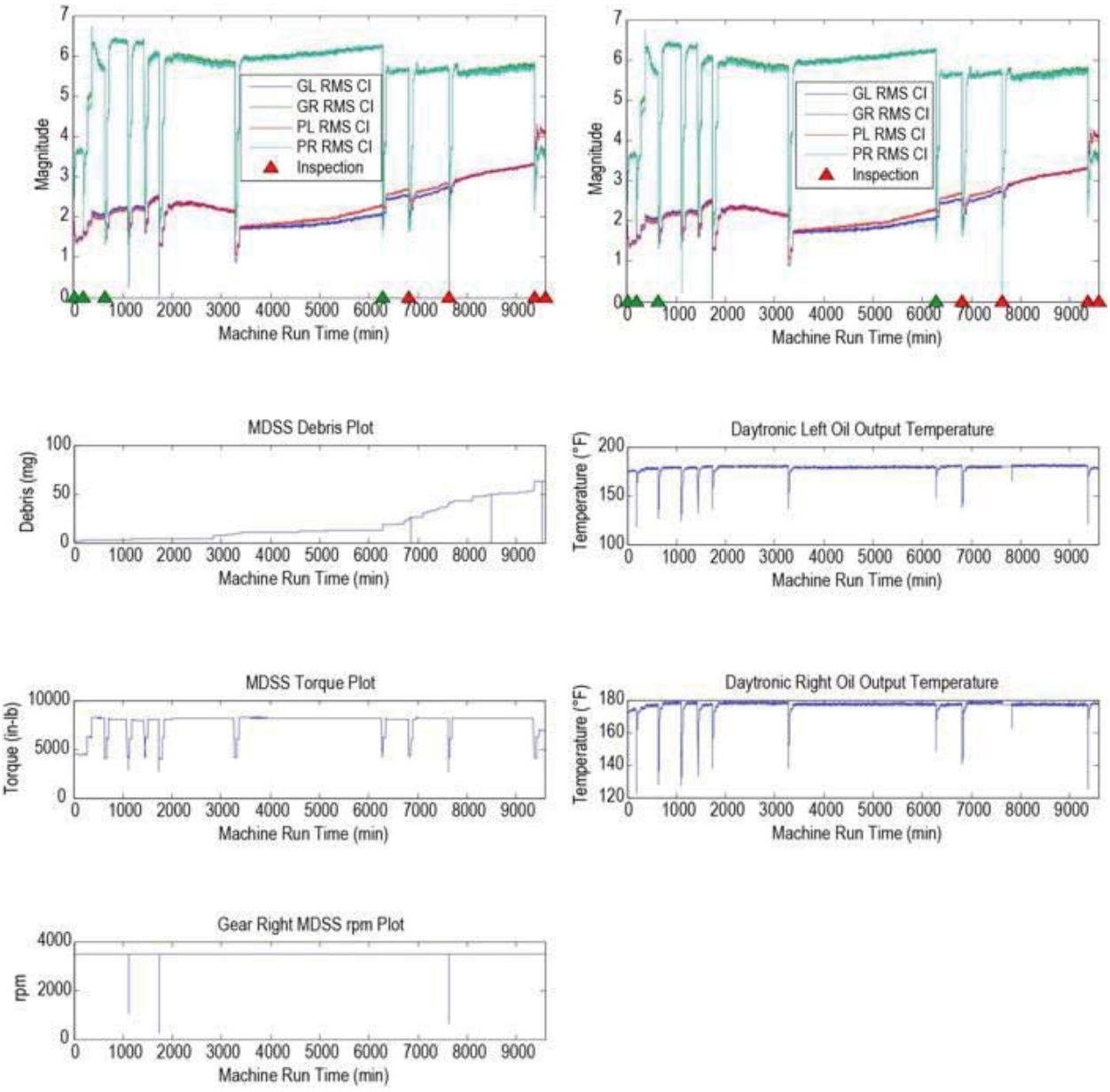

Figure B.6.2.—Test L3535R5050 Plots of RMS and Operational Parameters.

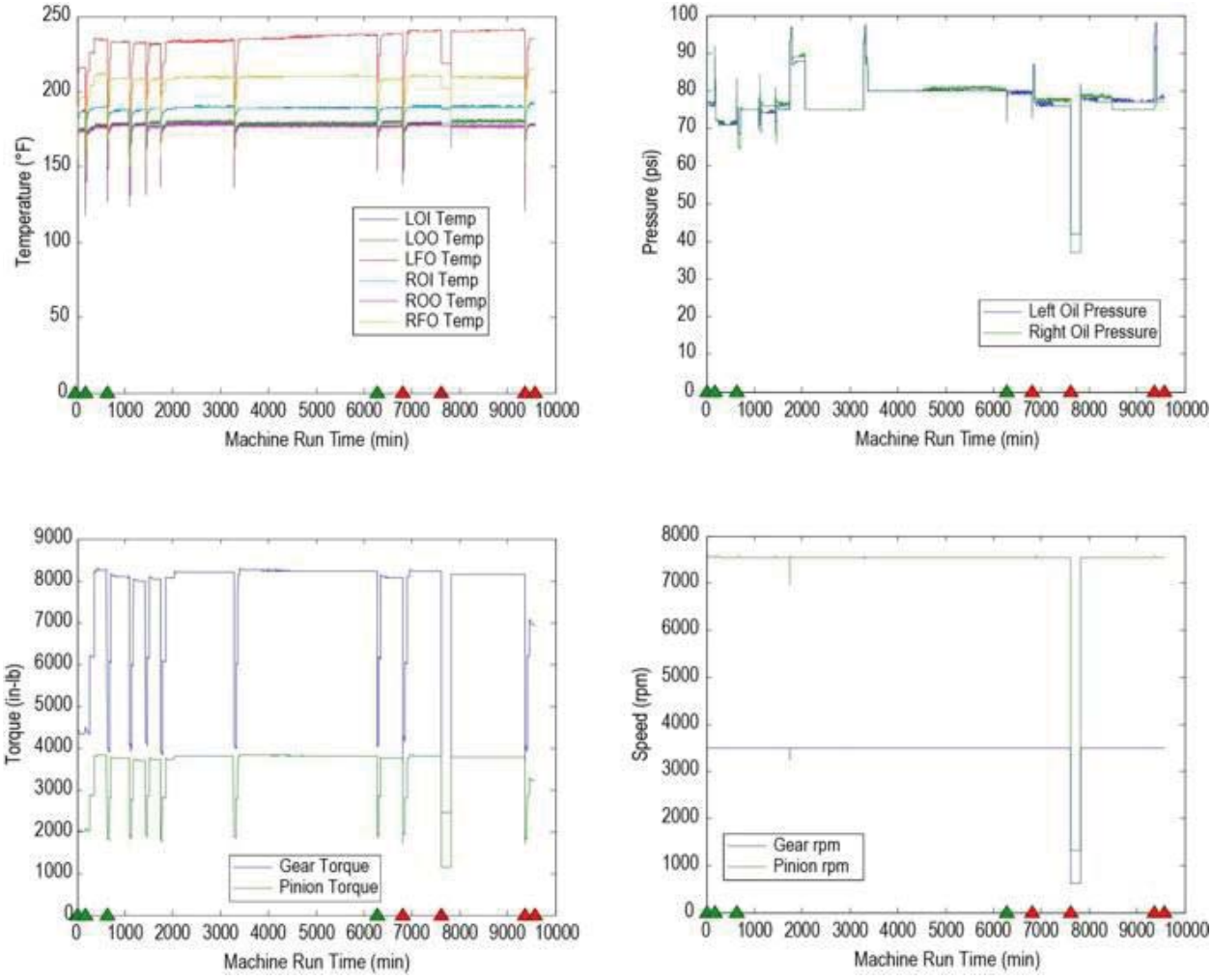

Figure B.6.3.—Test L3535R5050 Plots of Operational Parameters.

B.7 Test L1818R1616

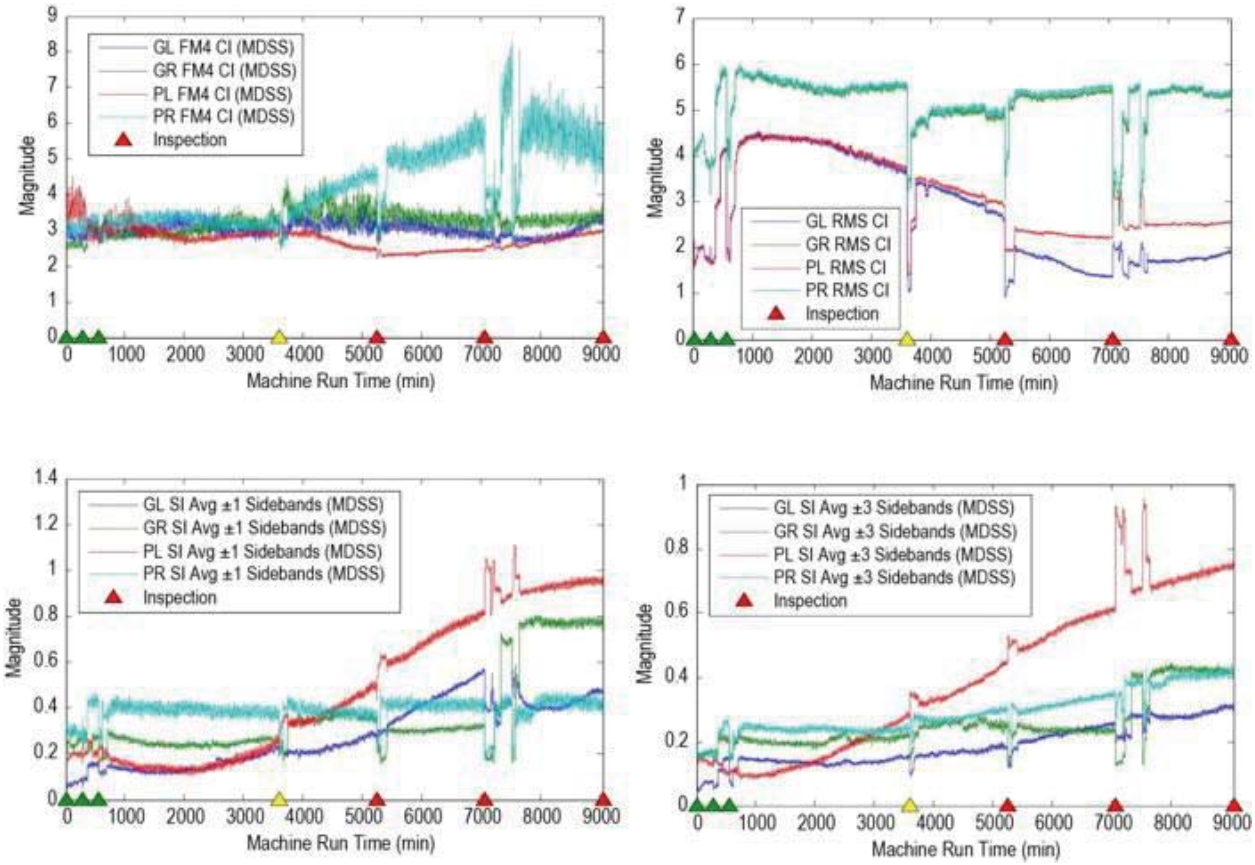

Figure B.7.1.—Test L1818R1616 Plots of FM4, RMS, SI1 and SI3.

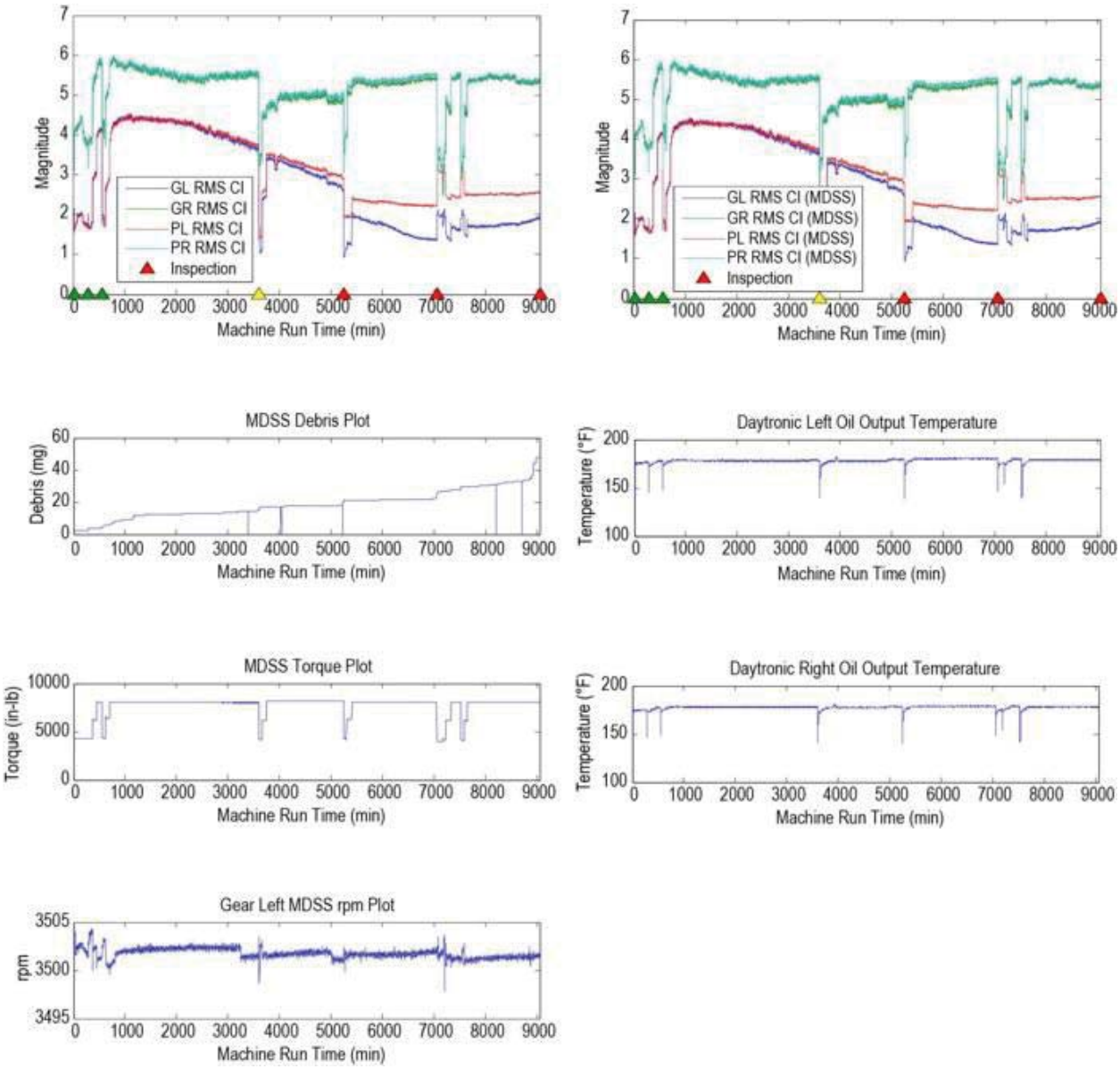

Figure B.7.2.—Test L1818R1616 Plots of RMS and Operational Parameters.

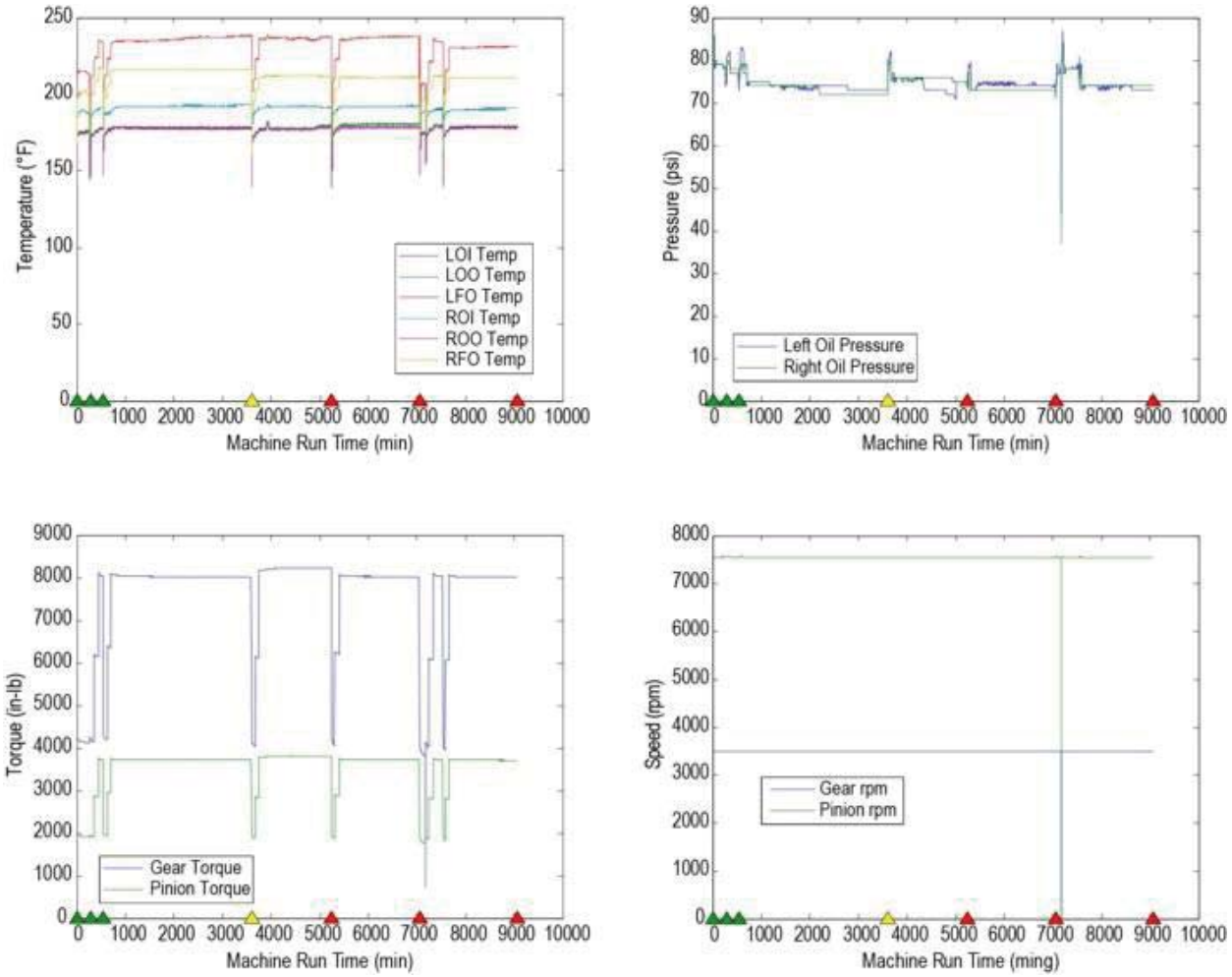

Figure B.7.3.—Test L1818R1616 Plots of Operational Parameters.

B.8 Test L2121R1919

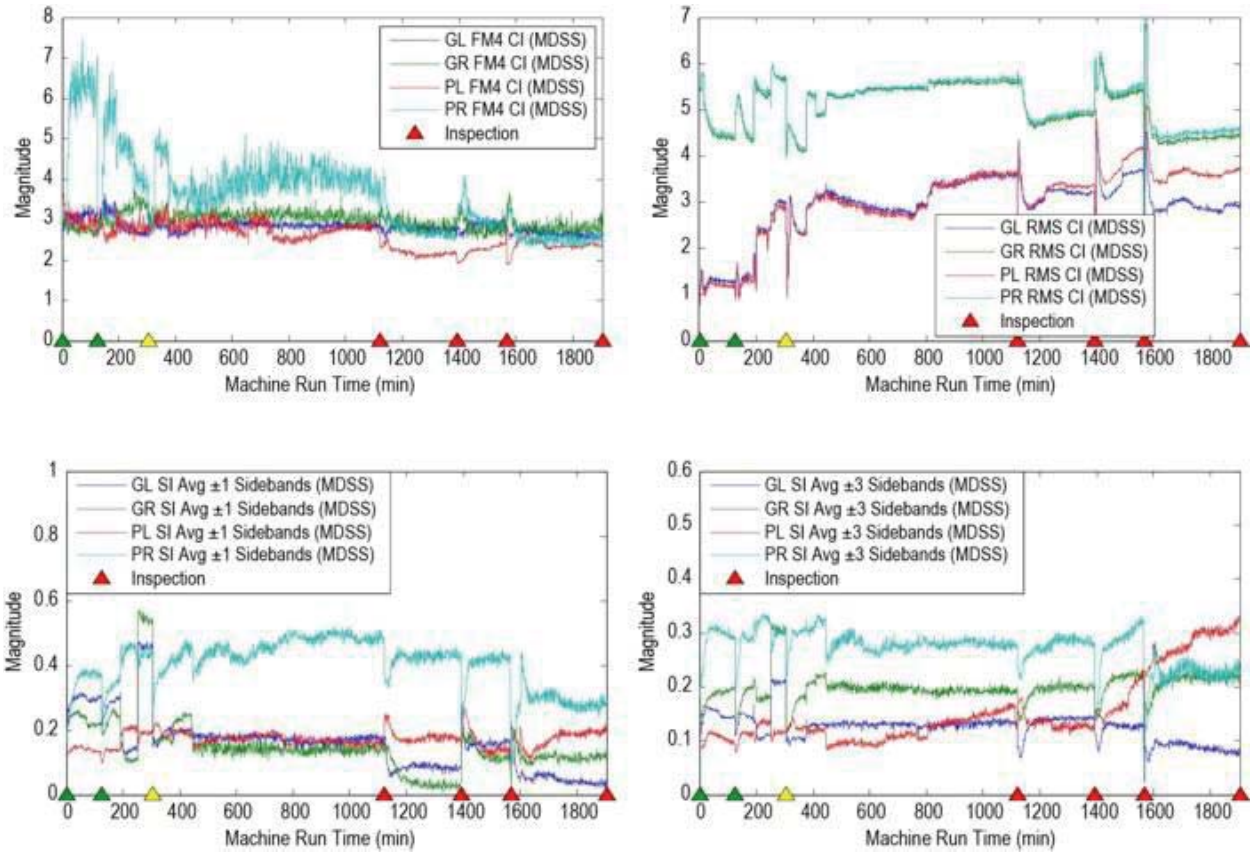

Figure B.8.1.—Test L2121R1919 Plots of FM4, RMS, SI1 and SI3.

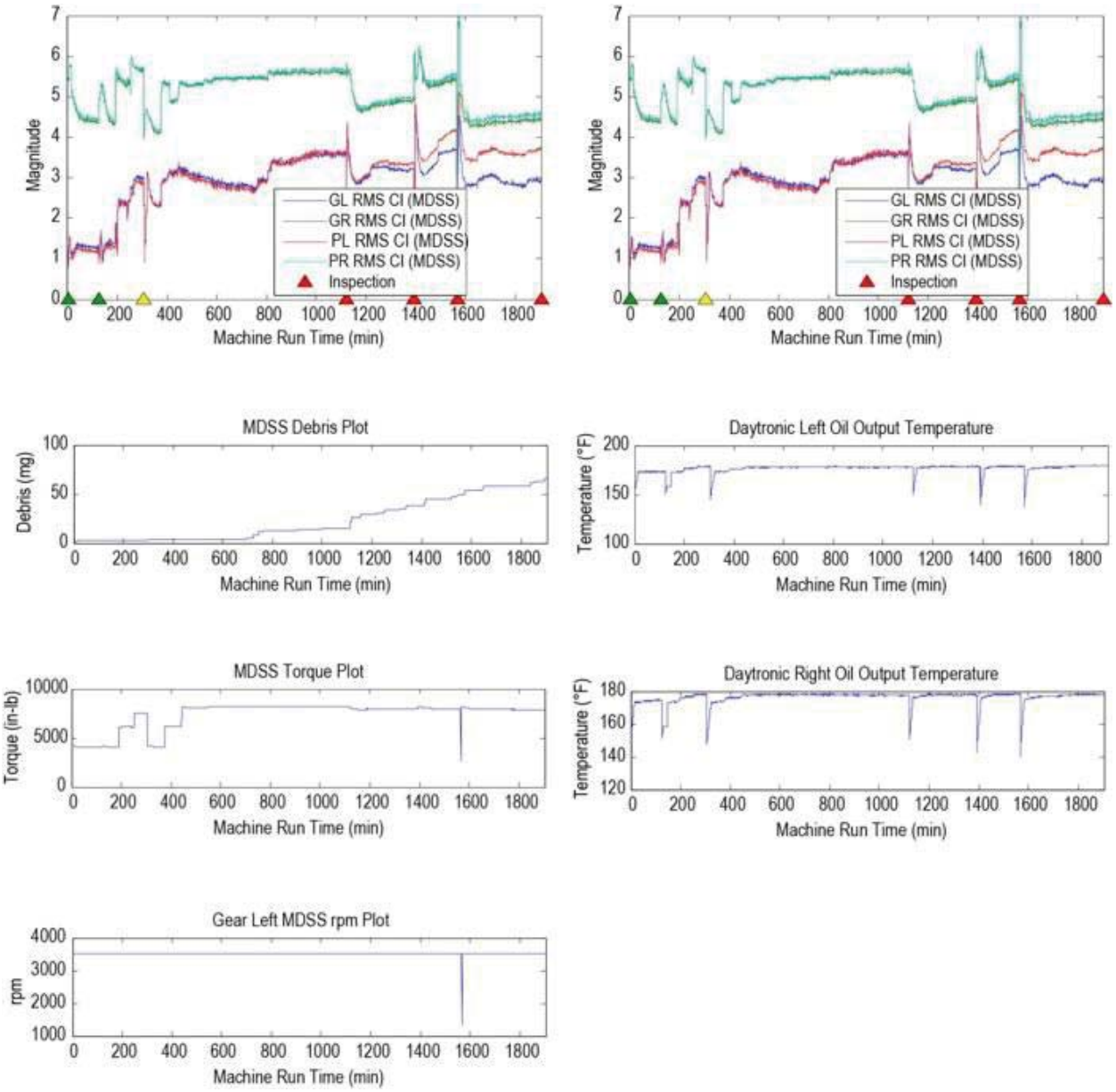

Figure B.8.2.—Test L2121R1919 Plots of RMS and Operational Parameters.

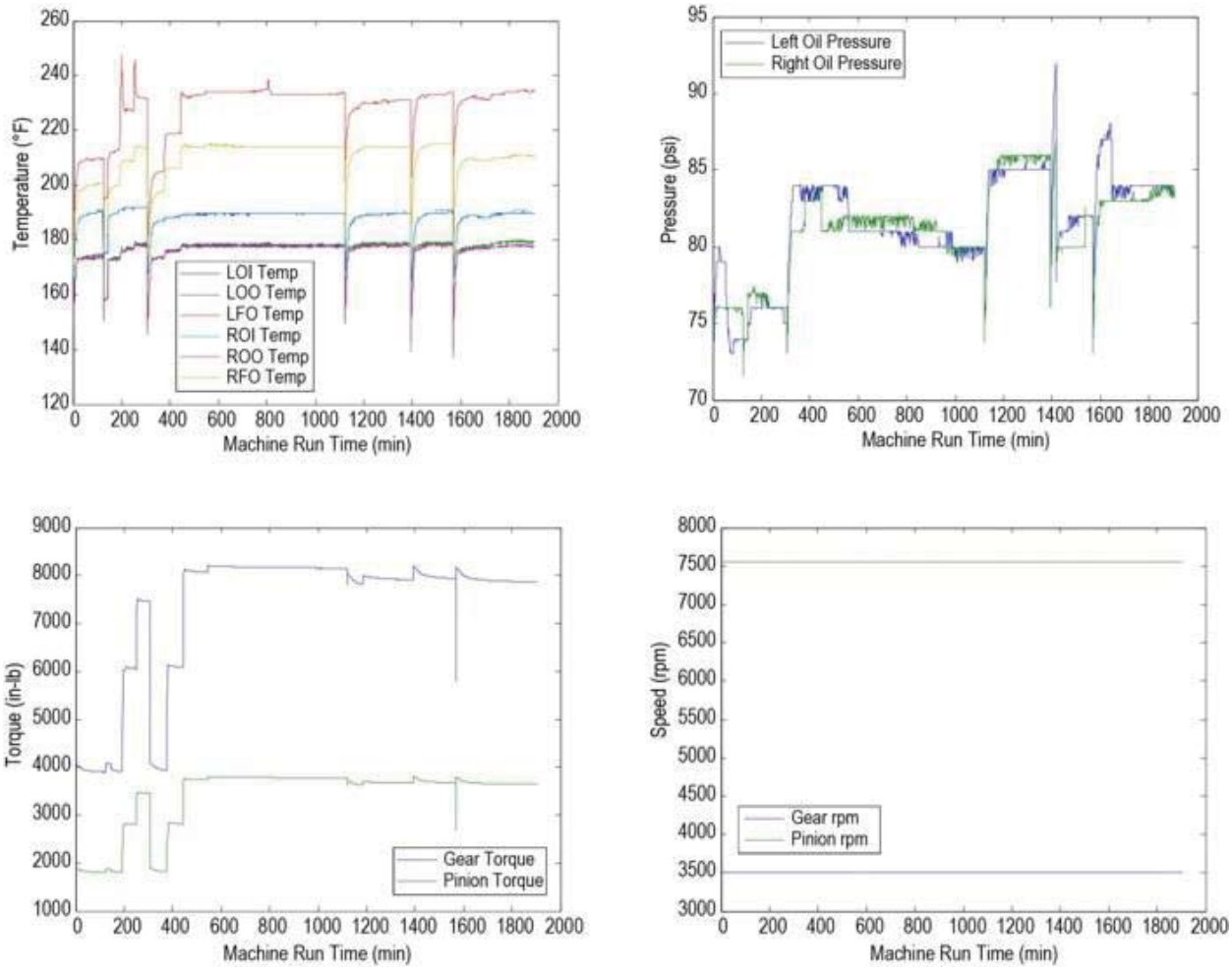

Figure B.8.3.—Test L2121R1919 Plots of Operational Parameters.

B.9 Test L1616R1919

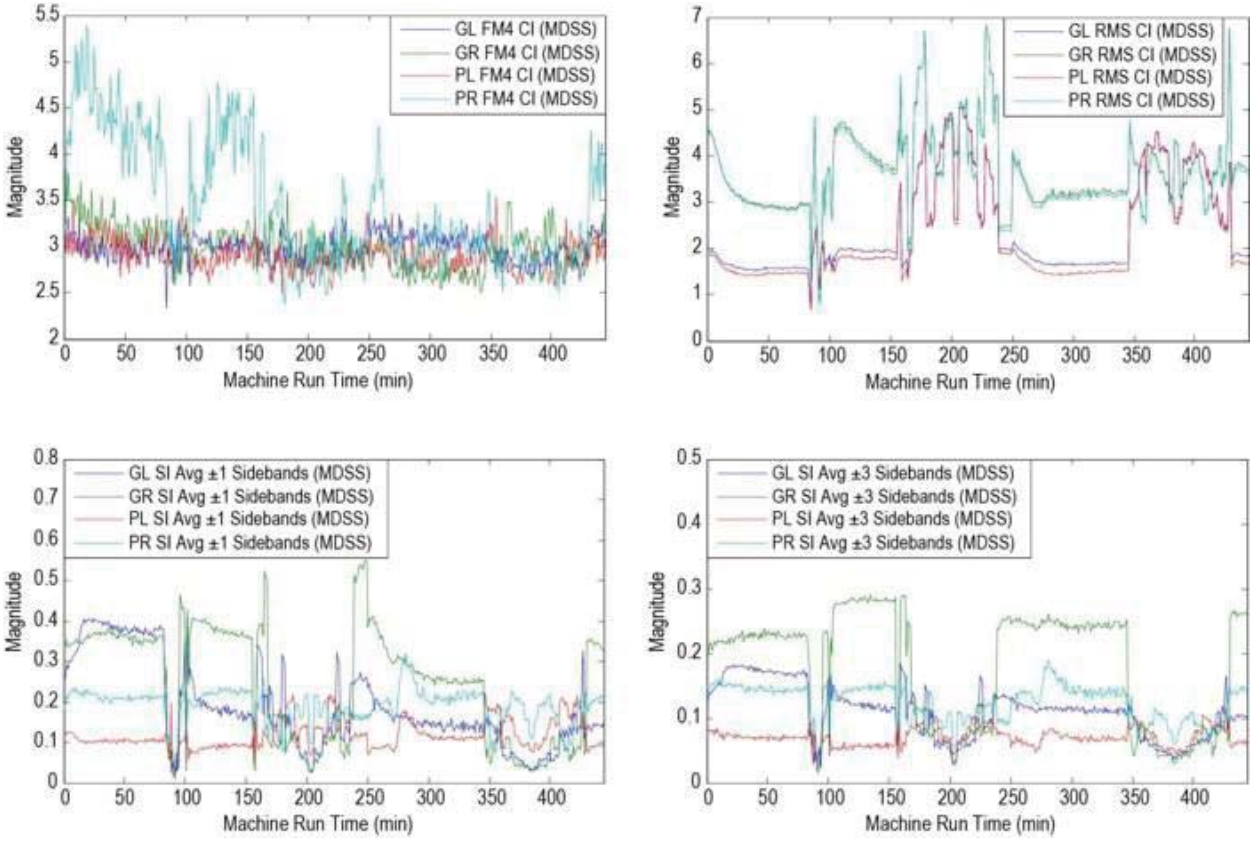

Figure B.9.1.—Test L1616R1919 Plots of FM4, RMS, SI1 and SI3.

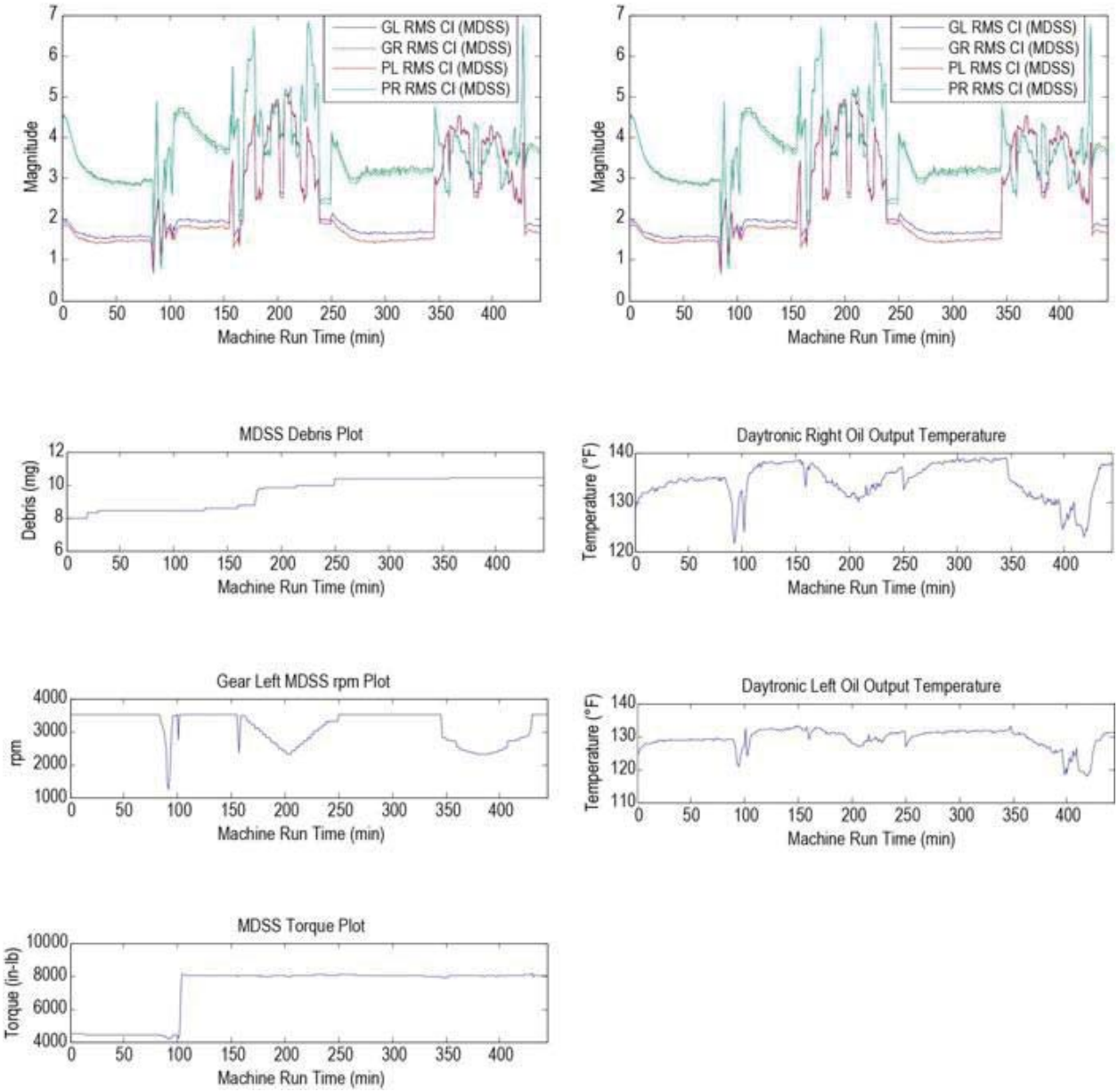

Figure B.9.2.—Test L1616R1919 Plots of RMS and Operational Parameters.

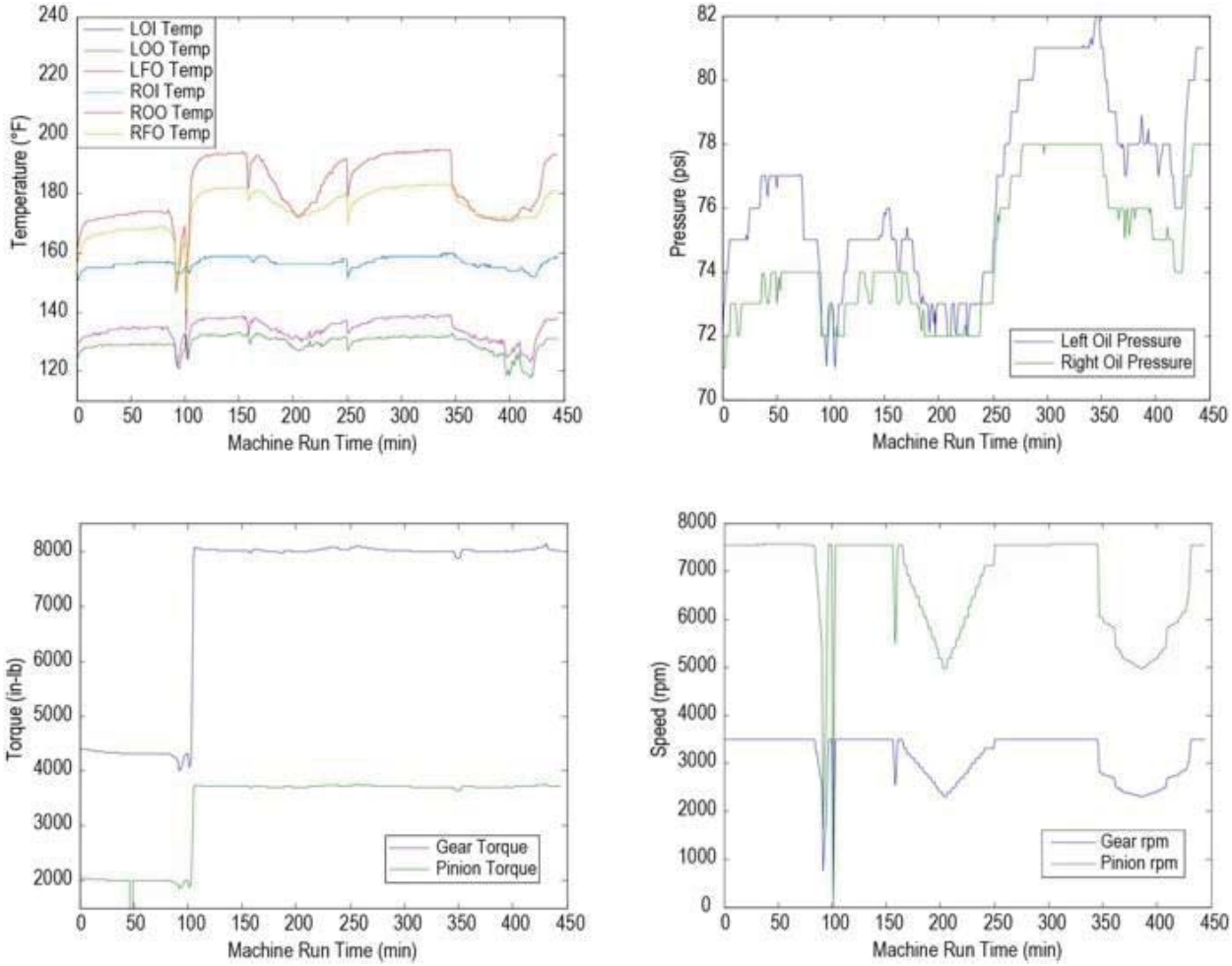

Figure B.9.3.—Test L1616R1919 Plots of Operational Parameters.

B.10 Test L3737R2424

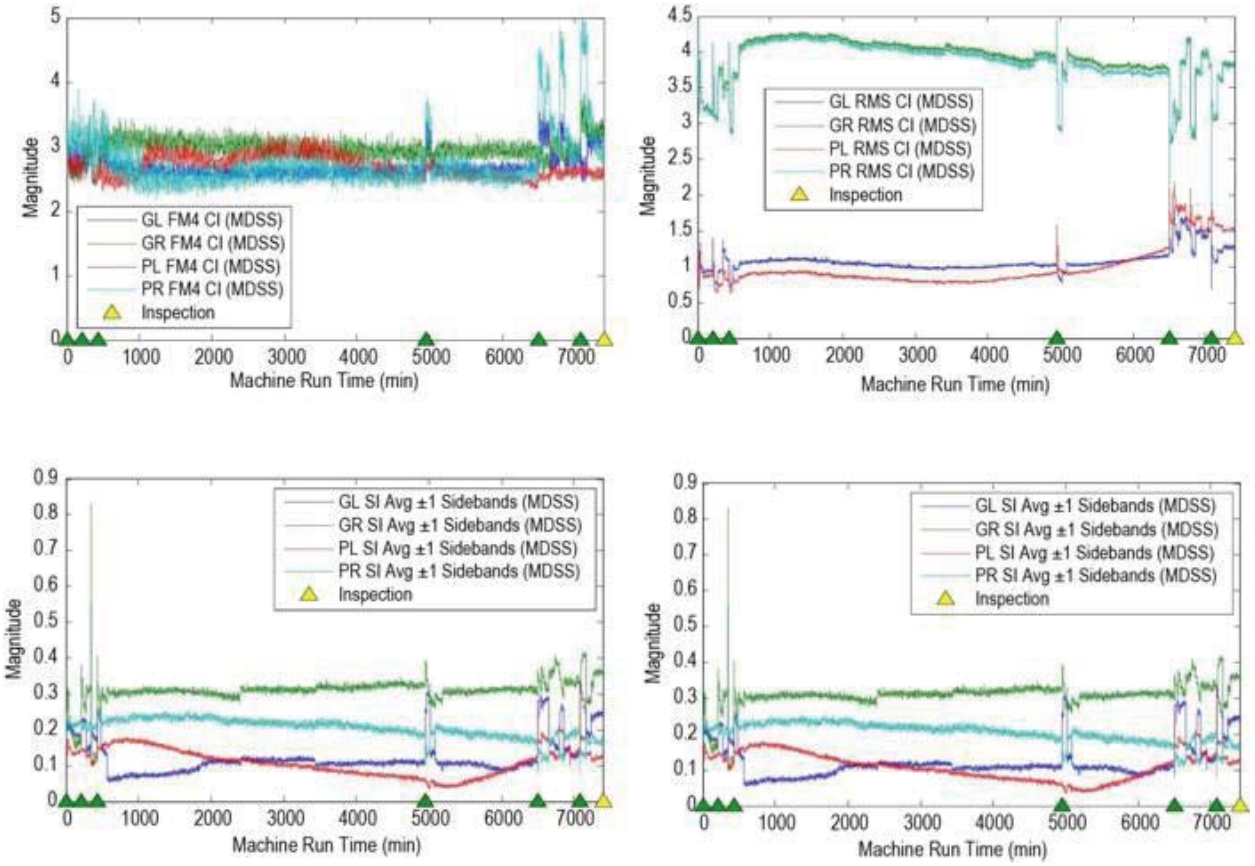

Figure B.10.1.—Test L3737R2424 Plots of FM4, RMS, SI1 and SI3.

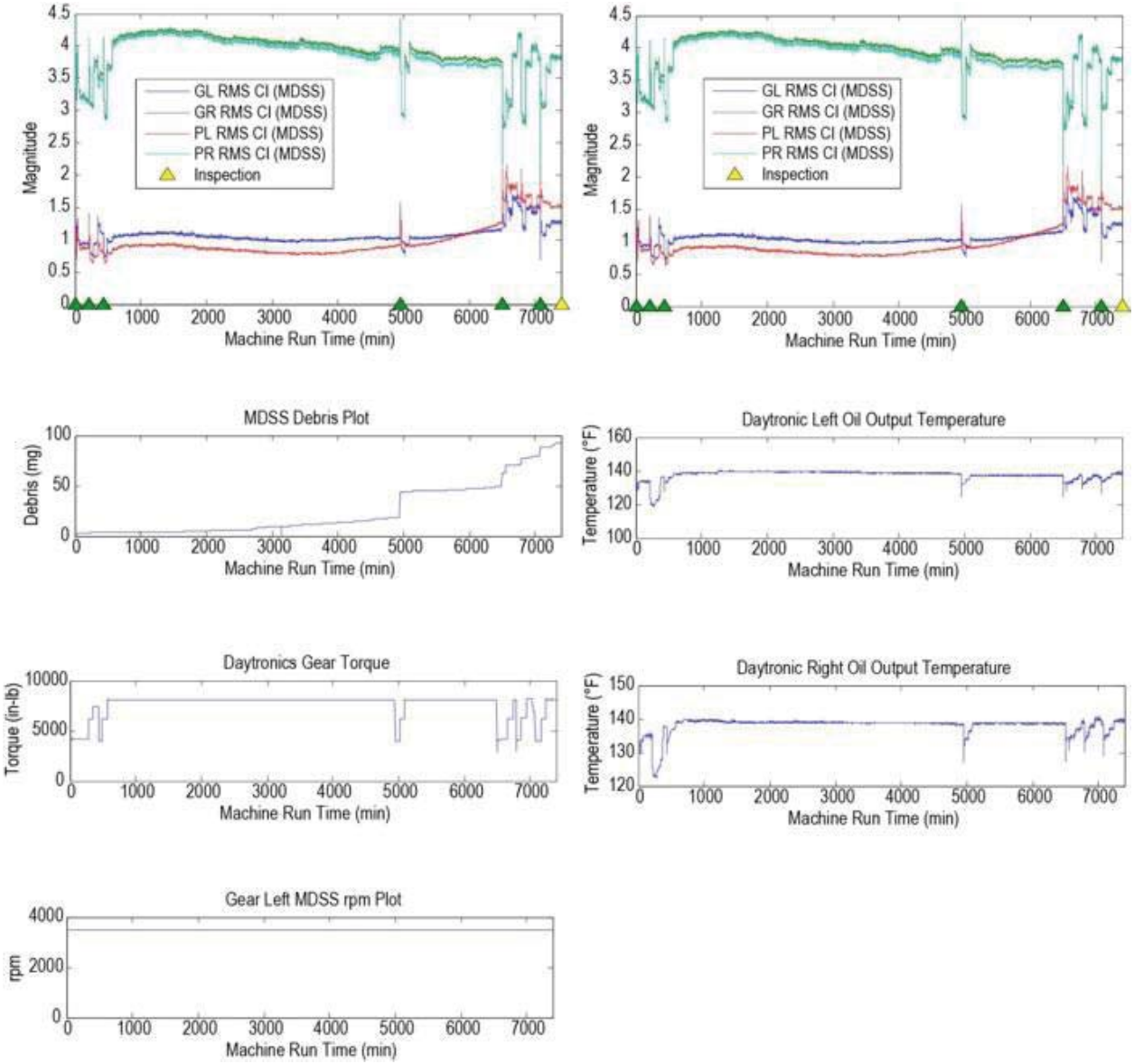

Figure B.10.2.—Test L3737R2424 Plots of RMS and Operational Parameters.

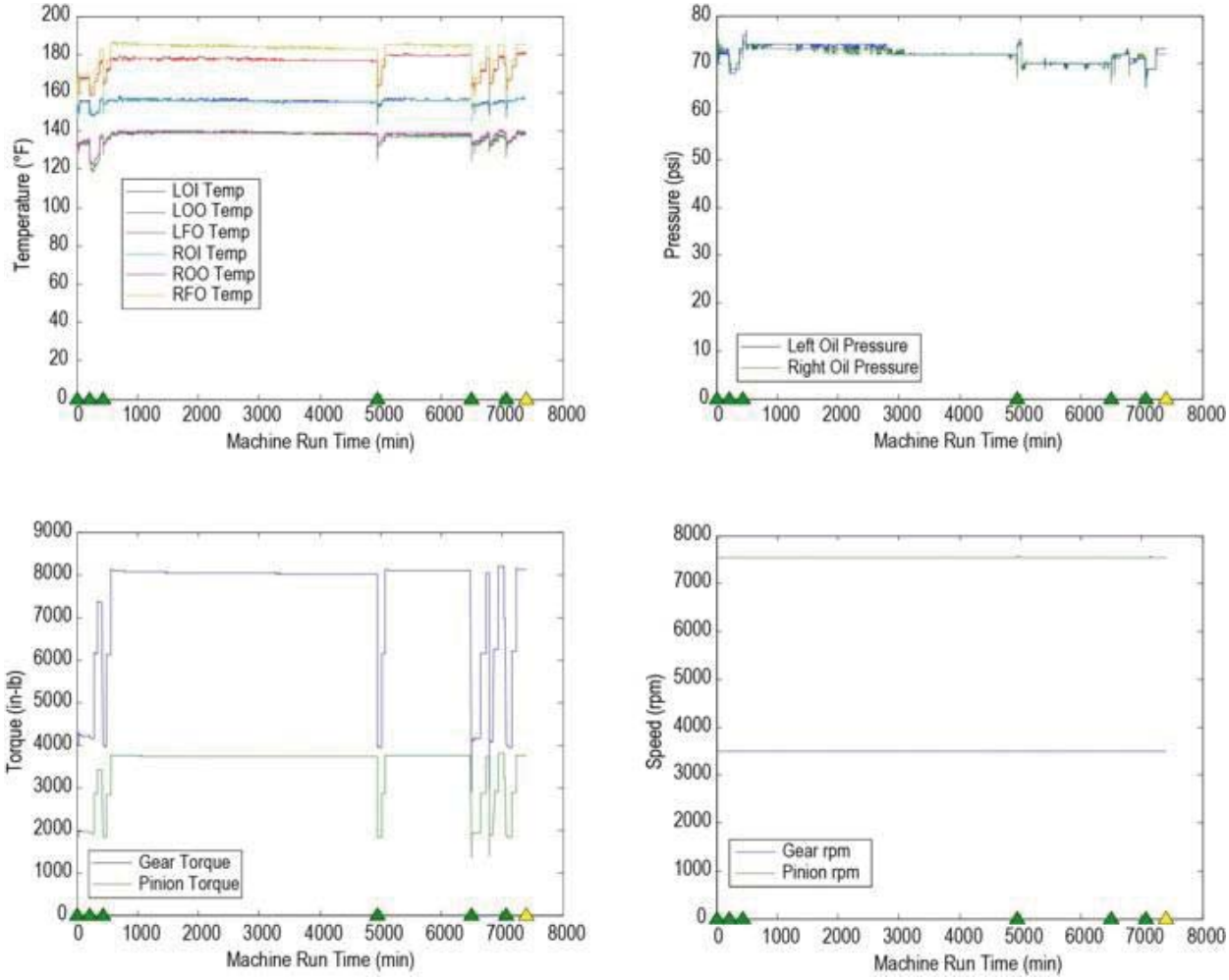

Figure B.10.3.—Test L3737R2424 Plots of Operational Parameters.

B.11 Test L3737R5036

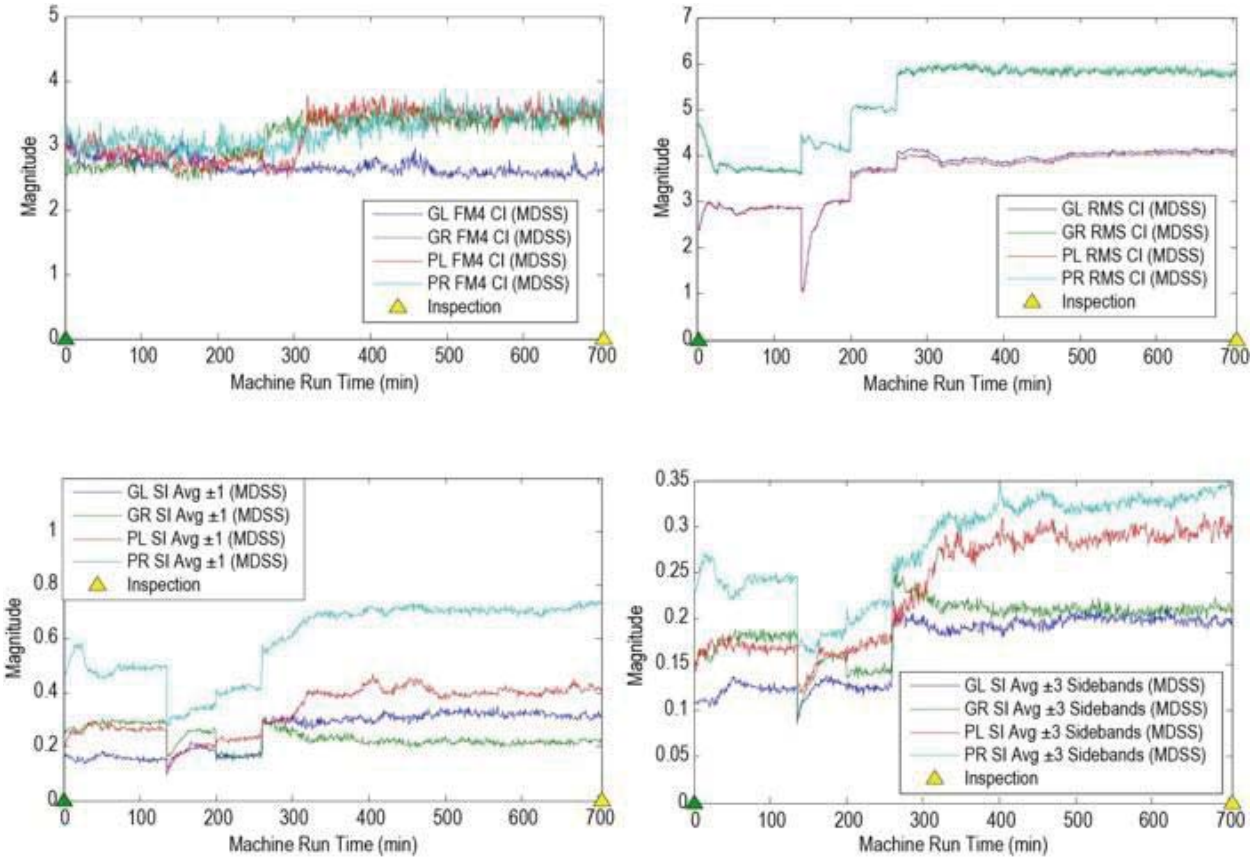

Figure B.11.1.—Test L3737R5036 Plots of FM4, RMS, SI1 and SI3.

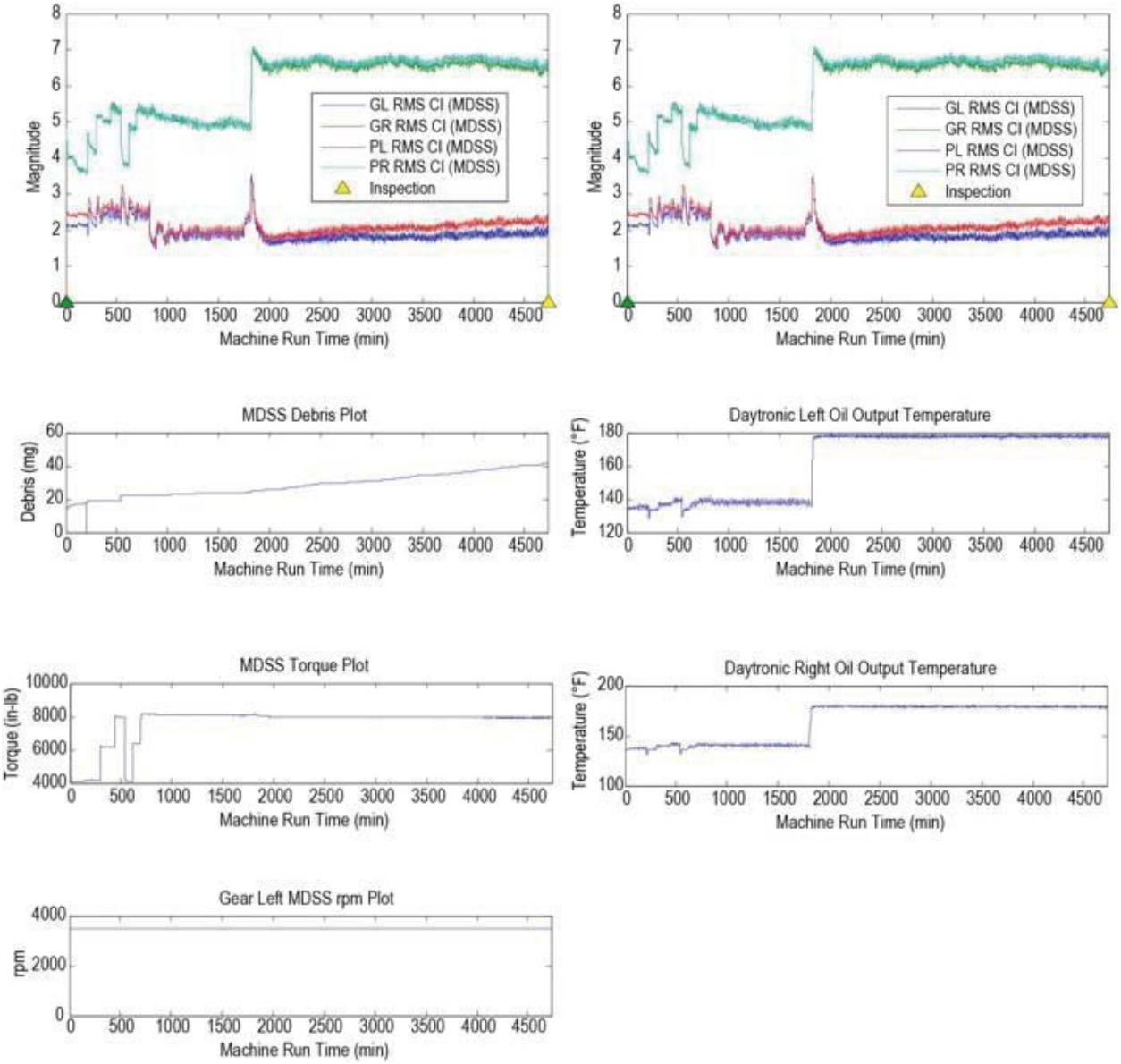

Figure B.11.2.—Test L3737R5036 Plots of RMS and Operational Parameters.

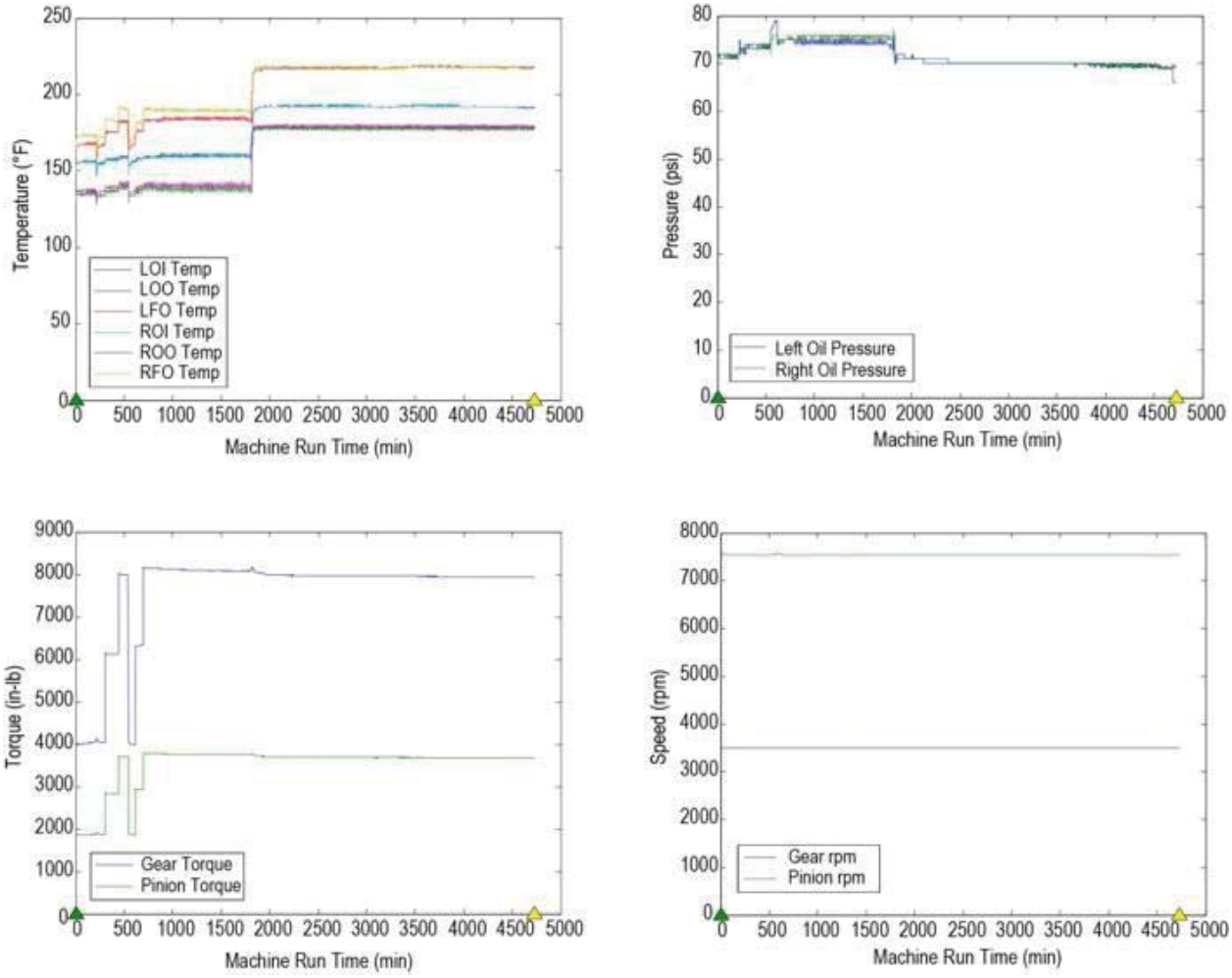

Figure B.11.3.—Test L3737R5036 Plots of Operational Parameters.

B.12 Test L1414R1616

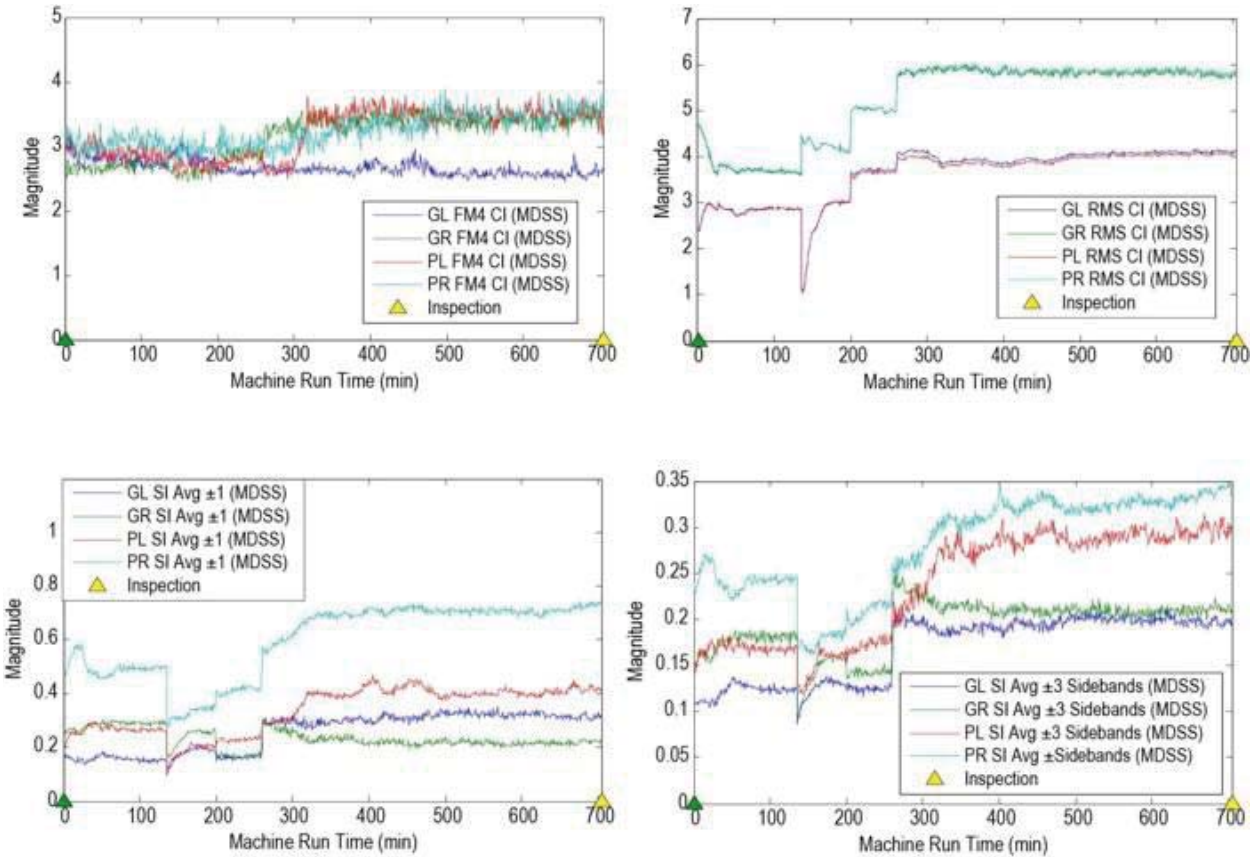

Figure B.12.1.—Test L1414R1616 Plots of FM4, RMS, SI1 and SI3.

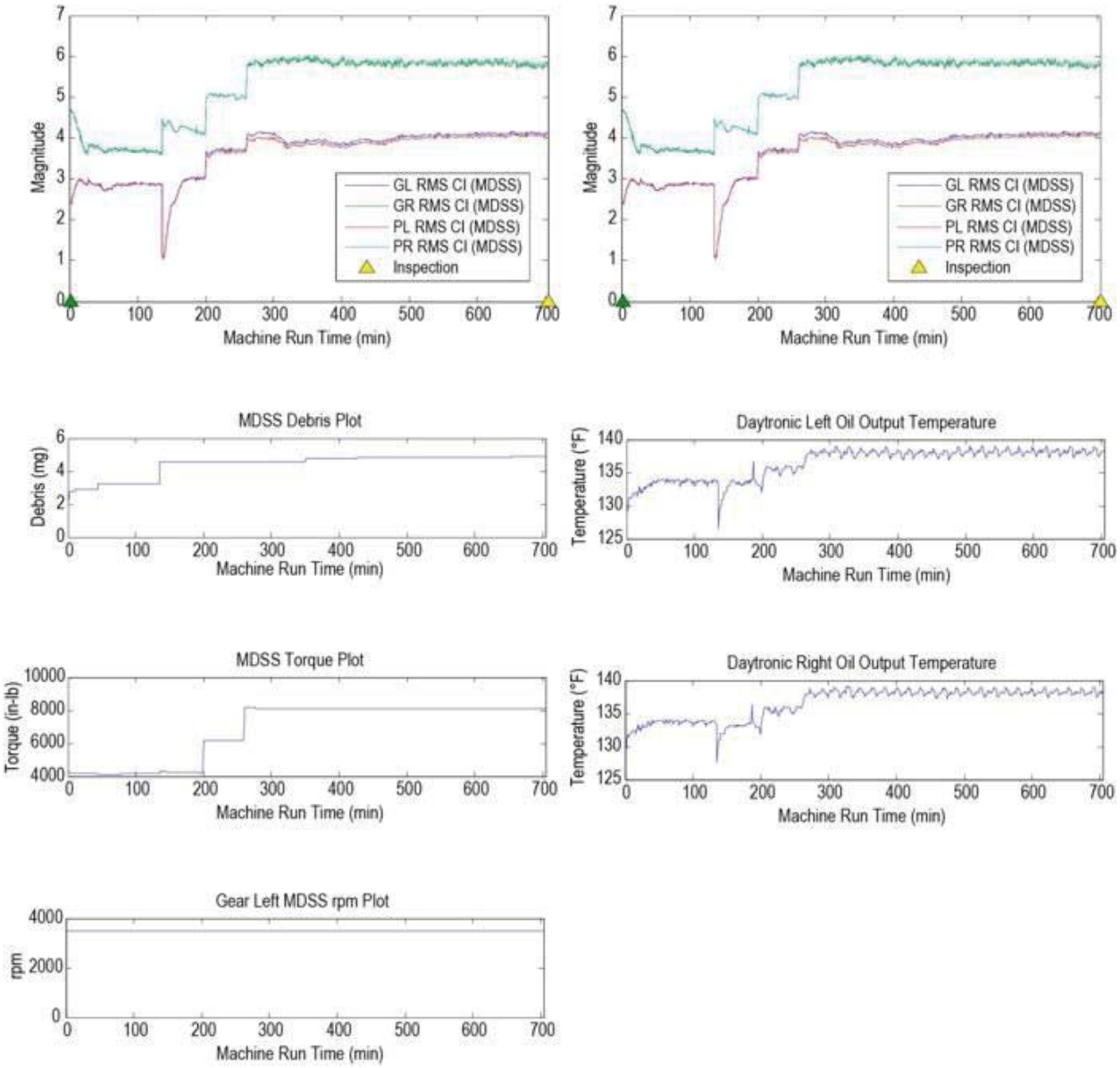

Figure B.12.2.—Test L1414R1616 Plots of RMS and Operational Parameters.

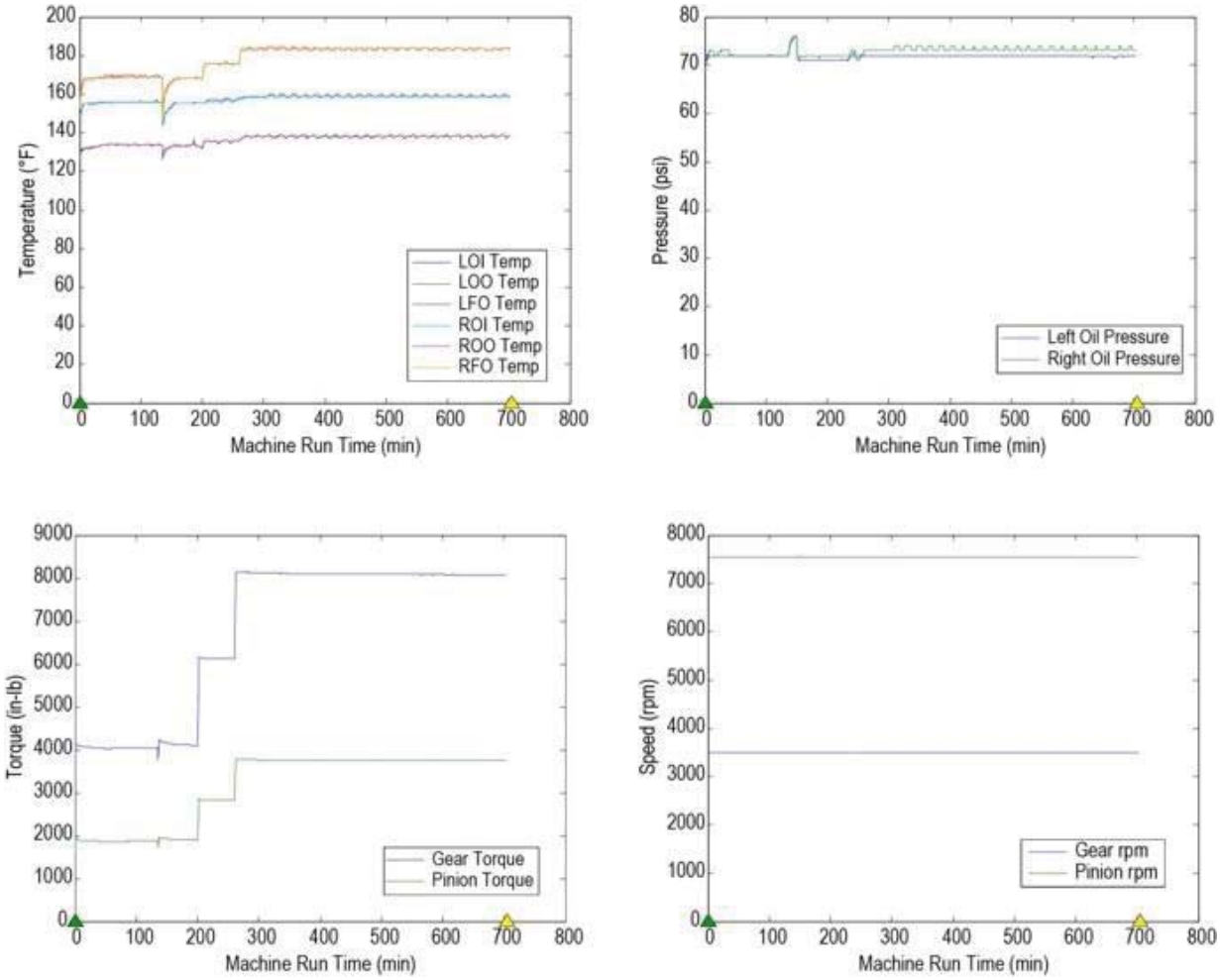

Figure B.12.3.—Test L1414R1616 Plots of Operational Parameters.

B.13 Test L4444R5252

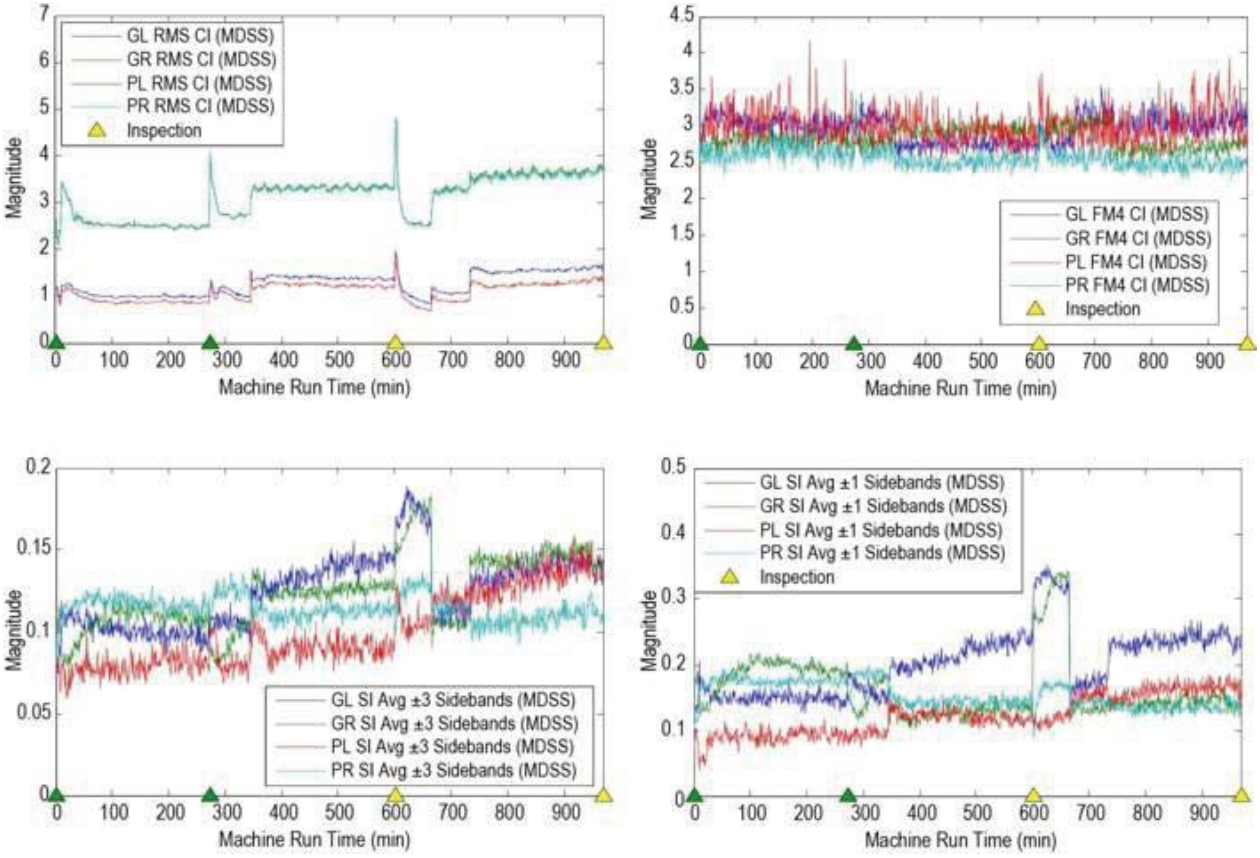

Figure B.13.1.—Test L4444R5252 Plots of FM4, RMS, SI1 and SI3.

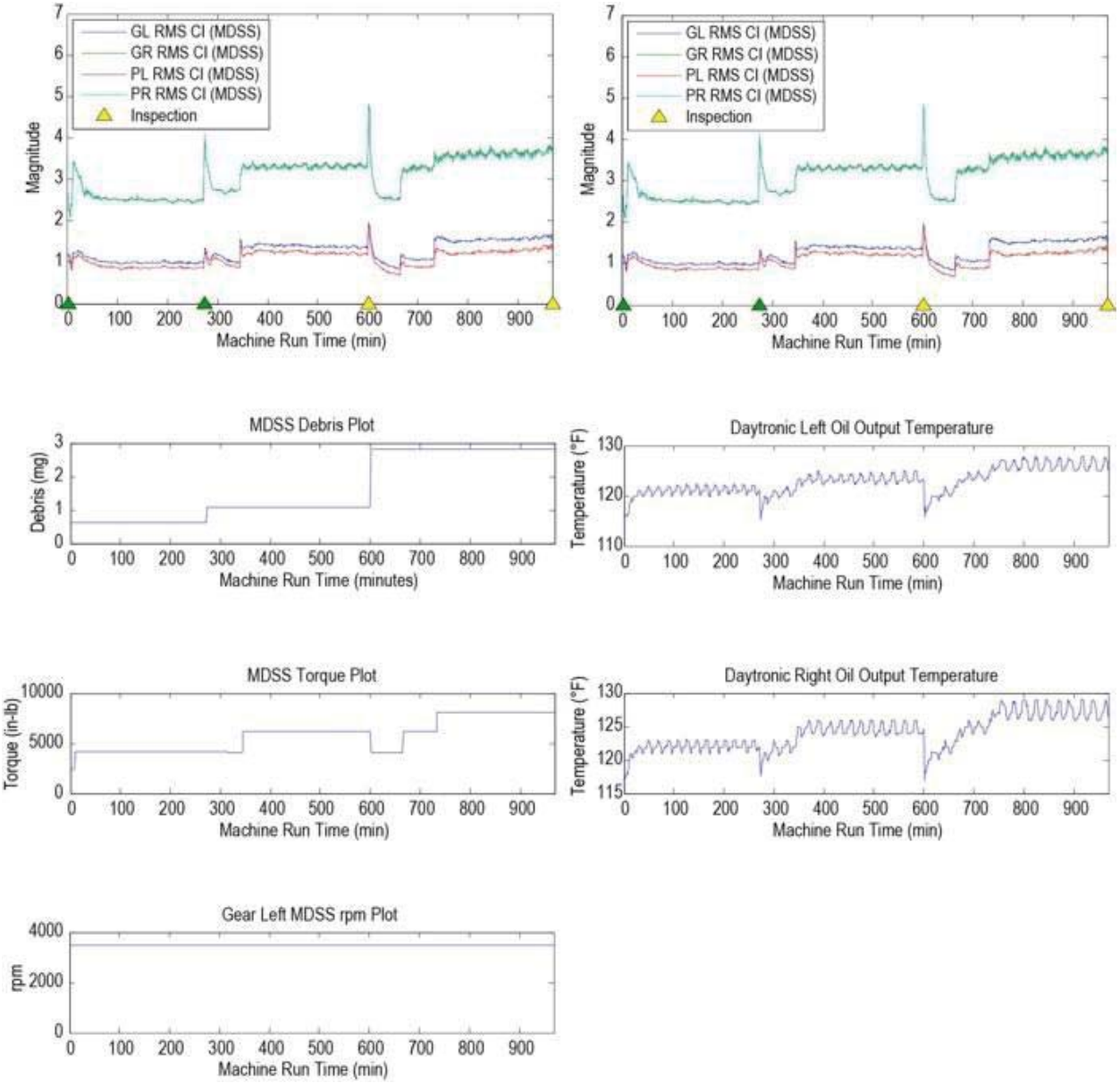

Figure B.13.2.—Test L4444R5252 Plots of RMS and Operational Parameters.

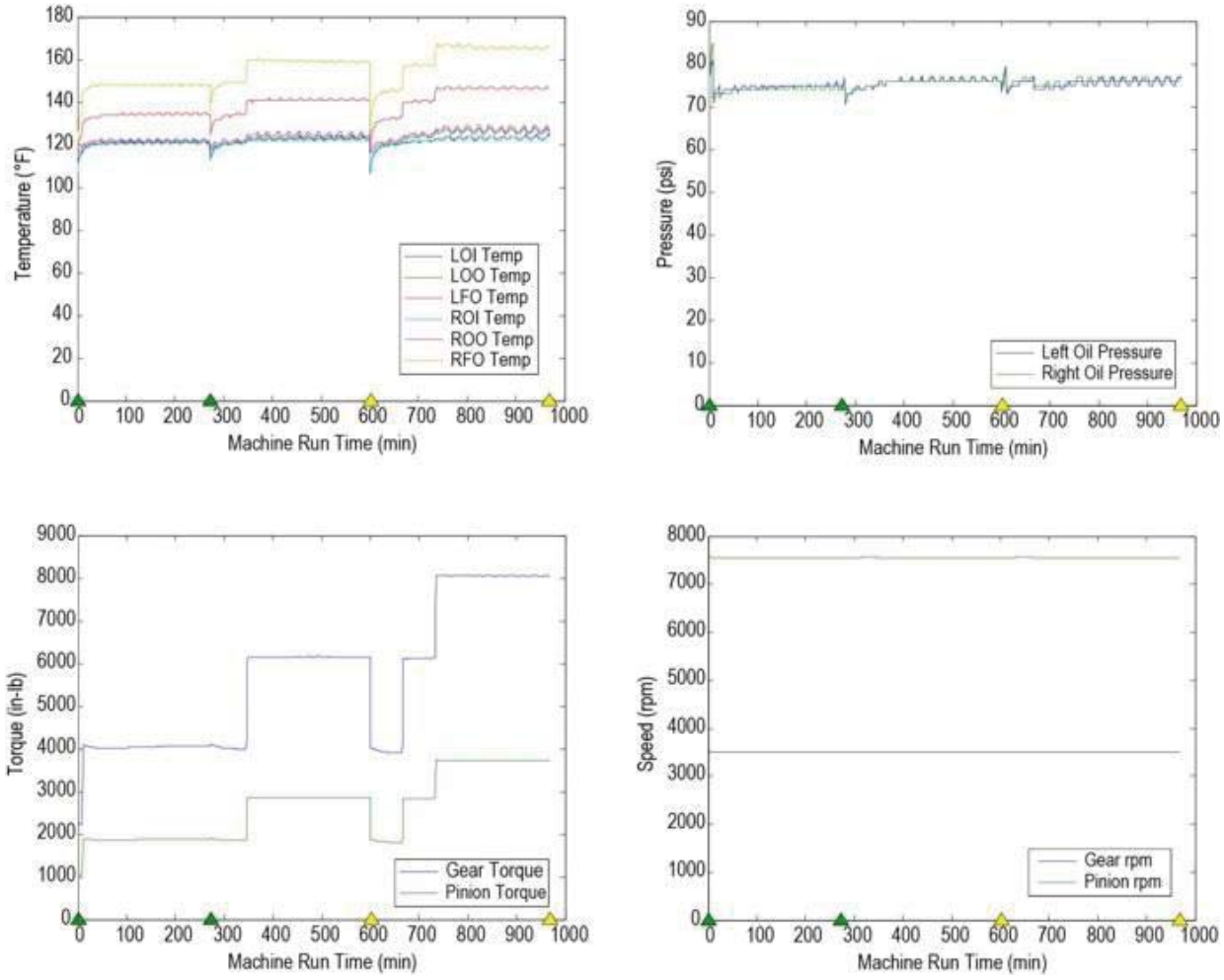

Figure B.13.3.—Test L4444R5252 Plots of Operational Parameters.

Appendix C.—Condition Indicator Inspection Statistical Parameters

TABLE C.1.1.—TEST L4545R5050

L4545R5050								
MDSS RMS	Mean	STDEV	Mean	STDEV	Mean	STDEV	Mean	STDEV
Inspection	GL	GL	GR	GR	PL	PL	PR	PR
1 - 76	1.93	0.21	2.46	0.27	1.88	0.22	2.29	0.26
76 - 324	2.90	0.24	4.34	0.60	2.84	0.24	4.29	0.61
324 - 1370	2.53	0.14	4.42	0.48	2.48	0.15	4.36	0.48
1370 - 2120	3.26	0.16	4.97	0.55	3.24	0.16	4.92	0.57
2120 - 2403	3.08	0.13	4.85	0.51	3.28	0.15	4.83	0.52
2403 - 2833	2.91	0.07	4.19	0.30	3.35	0.19	4.28	0.31
MDSS FM4	Mean	STDEV	Mean	STDEV	Mean	STDEV	Mean	STDEV
Inspection	GL	GL	GR	GR	PL	PL	PR	PR
1 - 76	2.84	0.11	2.64	0.09	2.90	0.16	2.85	0.22
76 - 324	2.79	0.09	2.91	0.20	2.98	0.16	2.90	0.19
324 - 1370	2.88	0.09	2.89	0.22	2.88	0.22	2.87	0.21
1370 - 2120	2.98	0.15	2.84	0.13	2.95	0.22	2.57	0.22
2120 - 2403	2.91	0.13	2.67	0.10	**5.29**	0.40	3.47	0.23
2403 - 2833	2.65	0.10	3.07	0.20	**6.37**	0.46	2.62	0.19
MDSS ±1 SI	Mean	STDEV	Mean	STDEV	Mean	STDEV	Mean	STDEV
Inspection	GL	GL	GR	GR	PL	PL	PR	PR
1 - 76	0.13	0.01	0.18	0.03	0.06	0.01	0.10	0.03
76 - 324	0.11	0.02	0.37	0.04	0.15	0.03	0.20	0.05
324 - 1370	0.11	0.02	0.36	0.06	0.20	0.03	0.18	0.05
1370 - 2120	0.14	0.01	0.36	0.04	0.19	0.03	0.16	0.03
2120 - 2403	0.12	0.02	0.33	0.05	0.33	0.03	0.30	0.06
2403 - 2833	0.18	0.02	0.33	0.03	**0.51**	0.10	0.22	0.04
MDSS ±3 SI	Mean	STDEV	Mean	STDEV	Mean	STDEV	Mean	STDEV
Inspection	GL	GL	GR	GR	PL	PL	PR	PR
1 - 76	0.09	0.01	0.12	0.01	0.06	0.00	0.10	0.01
76 - 324	0.15	0.02	0.20	0.02	0.11	0.01	0.16	0.02
324 - 1370	0.15	0.02	0.22	0.03	0.13	0.02	0.16	0.03
1370 - 2120	0.12	0.01	0.21	0.02	0.16	0.02	0.20	0.03
2120 - 2403	0.10	0.01	0.20	0.02	0.22	0.03	0.24	0.04
2403 - 2833	0.16	0.01	0.20	0.02	**0.36**	0.08	0.24	0.02

Operational Parameters

	Mean	STDEV	Mean	STDEV	Mean	STDEV
Inspection	Torque	Torque	LOO	LOO	ROO	ROO
1 - 76	4115	45	166	27	142	40
76 - 324	5961	317	201	20	189	27
324 - 1370	6037	215	198	24	185	33
1370 - 2120	7801	271	199	29	187	34
2120 - 2403	7995	127	196	25	179	37
2403 - 2833	6011	64	207	15	198	16

TABLE C.1.2.—TEST L1515R5050

L1515R5050								
MDSS RMS	Mean	STDEV	Mean	STDEV	Mean	STDEV	Mean	STDEV
Inspection (min)	GL	GL	GR	GR	PL	PL	PR	PR
1 - 63	1.15	0.07	1.86	0.09	1.06	0.08	1.63	0.11
63 - 705	1.79	0.28	6.58	1.26	1.73	0.27	6.57	1.30
705 - 1022	1.75	0.36	5.92	1.83	1.71	0.37	5.89	1.87
1022 - 1291	1.89	0.17	6.48	1.12	1.98	0.19	6.47	1.14
MDSS FM4	Mean	STDEV	Mean	STDEV	Mean	STDEV	Mean	STDEV
Inspection (min)	GL	GL	GR	GR	PL	PL	PR	PR
1 - 63	2.84	0.21	2.59	0.09	2.92	0.19	2.92	0.27
63 - 705	2.74	0.36	3.10	0.23	2.80	0.16	2.61	0.23
705 - 1022	2.72	0.20	3.09	0.40	3.26	0.32	2.75	0.23
1022 - 1291	2.67	0.12	3.10	0.32	5.27	0.40	2.87	0.27
MDSS ±1 SI	Mean	STDEV	Mean	STDEV	Mean	STDEV	Mean	STDEV
Inspection (min)	GL	GL	GR	GR	PL	PL	PR	PR
1 - 63	0.22	0.06	0.25	0.08	0.20	0.01	0.14	0.03
63 - 705	0.19	0.04	0.30	0.09	0.32	0.06	0.29	0.06
705 - 1022	0.18	0.05	0.30	0.11	0.30	0.06	0.26	0.07
1022 - 1291	0.20	0.03	0.31	0.09	0.36	0.04	0.31	0.05
MDSS ±3 SI	Mean	STDEV	Mean	STDEV	Mean	STDEV	Mean	STDEV
Inspection (min)	GL	GL	GR	GR	PL	PL	PR	PR
1 - 63	0.12	0.01	0.12	0.03	0.11	0.01	0.09	0.02
63 - 705	0.17	0.03	0.18	0.04	0.16	0.03	0.27	0.07
705 - 1022	0.16	0.04	0.18	0.05	0.16	0.04	0.23	0.09
1022 - 1291	0.18	0.02	0.20	0.03	0.21	0.02	0.26	0.05

Operational Parameters

	Mean	STDEV	Mean	STDEV	Mean	STDEV
Inspection	torque	torque	LOO	LOO	ROO	ROO
1 - 63	4053	51	155	23	154	23
63 - 705	7666	928	202	28	194	25
705 - 1022	7505	1547	194	35	186	32
1022 - 1291	7858	462	208	17	198	19

TABLE C.1.3.—TEST L3030R5050

L3030R5050								
MDSS RMS	Mean	STDEV	Mean	STDEV	Mean	STDEV	Mean	STDEV
Inspection (min)	GL	GL	GR	GR	PL	PL	PR	PR
1 - 70	1.85	0.15	2.45	0.23	1.81	0.15	2.35	0.23
70 - 1784	3.44	0.12	5.53	0.58	3.42	0.12	5.53	0.59
1784 - 3270	3.33	0.14	5.25	0.63	3.36	0.13	5.25	0.64
3270 - 4633	3.30	0.18	5.64	0.66	3.41	0.16	5.65	0.66
4633 - 5359	3.22	0.17	5.97	0.64	3.45	0.13	6.00	0.63
5359 - 5962	3.20	0.10	5.64	0.58	3.50	0.11	5.67	0.57
5962 - 6037	3.03	0.98	4.01	1.31	3.41	0.90	4.05	1.32
MDSS FM4	Mean	STDEV	Mean	STDEV	Mean	STDEV	Mean	STDEV
Inspection (min)	GL	GL	GR	GR	PL	PL	PR	PR
1 - 70	2.91	0.15	2.78	0.14	2.98	0.13	2.86	0.20
70 - 1784	2.90	0.10	3.07	0.18	2.82	0.20	2.81	0.24
1784 - 3270	2.94	0.10	3.09	0.17	2.99	0.23	2.84	0.21
3270 - 4633	2.97	0.24	3.01	0.27	2.50	0.16	2.90	0.24
4633 - 5359	3.32	0.27	3.09	0.17	2.48	0.06	3.20	0.25
5359 - 5962	5.60	1.18	3.12	0.18	2.55	0.08	3.00	0.33
5962 - 6037	7.20	1.79	3.06	0.26	2.56	0.11	2.73	0.33
MDSS +1 SI	Mean	STDEV	Mean	STDEV	Mean	STDEV	Mean	STDEV
Inspection (min)	GL	GL	GR	GR	PL	PL	PR	PR
1 - 70	0.12	0.02	0.20	0.05	0.16	0.04	0.24	0.04
70 - 1784	0.10	0.04	0.29	0.05	0.24	0.05	0.48	0.09
1784 - 3270	0.14	0.03	0.29	0.05	0.29	0.03	0.45	0.08
3270 - 4633	0.15	0.03	0.31	0.06	0.30	0.05	0.44	0.08
4633 - 5359	0.18	0.03	0.32	0.05	0.42	0.05	0.37	0.06
5359 - 5962	0.18	0.02	0.33	0.05	0.56	0.03	0.34	0.05
5962 - 6037	0.18	0.08	0.25	0.11	0.42	0.14	0.24	0.10
MDSS ± 3 SI	Mean	STDEV	Mean	STDEV	Mean	STDEV	Mean	STDEV
Inspection (min)	GL	GL	GR	GR	PL	PL	PR	PR
1 - 70	0.07	0.00	0.15	0.03	0.13	0.01	0.13	0.01
70 - 1784	0.14	0.01	0.21	0.02	0.14	0.02	0.28	0.04
1784 - 3270	0.15	0.01	0.19	0.02	0.18	0.03	0.27	0.05
3270 - 4633	0.16	0.01	0.22	0.03	0.25	0.04	0.28	0.04
4633 - 5359	0.17	0.01	0.23	0.03	0.32	0.03	0.29	0.04
5359 - 5962	0.18	0.01	0.24	0.03	0.37	0.02	0.29	0.04
5962 - 6037	0.12	0.04	0.13	0.05	0.28	0.10	0.15	0.05

Operational Parameters

	Mean	STDEV	Mean	STDEV	Mean	STDEV
Inspection (min)	torque	torque	LOO	LOO	ROO	ROO
1 - 70	4228	39	188	19	176	21
70 - 1784	7867	124	204	23	191	32
1784 - 3270	7956	80	205	21	194	29
3270 - 4633	7956	83	206	19	193	30
4633 - 5359	7916	207	211	13	200	16
5359 - 5962	7976	82	207	18	192	30
5962 - 6037	7711	590	148	37	148	36

TABLE C.1.4.—TEST L3535R5050

L3535R5050								
MDSS RMS	Mean	STDEV	Mean	STDEV	Mean	STDEV	Mean	STDEV
Inspection (min)	GL	GL	GR	GR	PL	PL	PR	PR
1 - 178	1.51	0.12	3.53	0.26	1.46	0.12	3.48	0.27
178 - 636	1.96	0.17	5.18	1.16	1.88	0.16	5.09	1.19
636 - 6276	1.99	0.27	5.83	0.84	2.03	0.24	5.78	0.89
6276 - 6818	2.42	0.18	5.27	0.93	2.56	0.14	5.26	1.00
6818 - 7617	2.54	0.18	5.35	0.92	2.67	0.15	5.33	0.96
7617 - 9358	3.08	0.19	5.56	0.60	3.10	0.16	5.49	0.63
9358 - 9578	4.02	0.19	3.44	0.43	4.07	0.14	3.37	0.44
MDSS FM4	Mean	STDEV	Mean	STDEV	Mean	STDEV	Mean	STDEV
Inspection (min)	GL	GL	GR	GR	PL	PL	PR	PR
1 - 178	3.10	0.22	3.07	0.22	3.47	0.29	2.95	0.18
178 - 636	2.69	0.15	2.79	0.34	2.90	0.23	2.87	0.27
636 - 6276	2.72	0.10	2.79	0.21	2.98	0.24	3.01	0.23
6276 - 6818	2.62	0.11	2.65	0.10	3.37	0.09	3.24	0.14
6818 - 7617	3.76	0.81	2.77	0.15	3.43	0.09	3.21	0.24
7617 - 9358	6.00	0.41	3.61	0.29	3.42	0.11	3.27	0.12
9358 - 9578	5.54	0.29	4.23	0.49	3.42	0.20	3.06	0.17
MDSS ± 1 SI	Mean	STDEV	Mean	STDEV	Mean	STDEV	Mean	STDEV
Inspection (min)	GL	GL	GR	GR	PL	PL	PR	PR
1 - 178	0.09	0.02	0.31	0.03	0.09	0.01	0.30	0.03
178 - 636	0.15	0.06	0.23	0.10	0.13	0.04	0.33	0.06
636 - 6276	0.23	0.07	0.16	0.05	0.28	0.09	0.32	0.06
6276 - 6818	0.38	0.03	0.13	0.06	0.51	0.03	0.32	0.06
6818 - 7617	0.39	0.03	0.12	0.06	0.56	0.04	0.36	0.07
7617 - 9358	0.37	0.02	0.12	0.05	0.63	0.06	0.44	0.06
9358 - 9578	0.49	0.07	0.20	0.08	0.85	0.09	0.21	0.04
MDSS ± 3 SI	Mean	STDEV	Mean	STDEV	Mean	STDEV	Mean	STDEV
Inspection (min)	GL	GL	GR	GR	PL	PL	PR	PR
1 - 178	0.08	0.01	0.14	0.01	0.07	0.01	0.16	0.01
178 - 636	0.15	0.04	0.15	0.03	0.08	0.01	0.19	0.04
636 - 6276	0.15	0.03	0.12	0.02	0.18	0.07	0.21	0.03
6276 - 6818	0.24	0.02	0.15	0.02	0.37	0.01	0.22	0.02
6818 - 7617	0.26	0.02	0.15	0.02	0.40	0.02	0.27	0.03
7617 - 9358	0.24	0.01	0.14	0.02	0.46	0.03	0.27	0.02
9358 - 9578	0.31	0.03	0.15	0.03	0.57	0.05	0.26	0.04

Operational Parameters

	Mean	STDEV	Mean	STDEV	Mean	STDEV
Inspection (min)	**torque**	torque	LOO	LOO	ROO	ROO
1 - 178	4474	51	171	11	170	10
178 - 636	7056	1507	172	15	172	13
636 - 6276	7937	860	176	12	175	10
6276 - 6818	7690	968	173	19	171	16
6818 - 7617	7880	988	177	8	176	8
7617 - 9358	7996	642	180	1	177	1
9358 - 9578	6122	1155	171	17	171	16

TABLE C.1.5.—TEST L1818R1616

L1818R1616								
MDSS RMS	Mean	STDEV	Mean	STDEV	Mean	STDEV	Mean	STDEV
Inspection (min)	GL	GL	GR	GR	PL	PL	PR	PR
1 - 277	1.87	0.13	4.09	0.26	1.83	0.13	4.05	0.27
277 - 546	2.98	0.99	4.99	0.86	2.95	0.98	5.00	0.92
546 - 3603	4.07	0.49	5.48	0.30	4.09	0.49	5.52	0.31
3603 - 5249	2.97	0.45	4.81	0.33	3.14	0.40	4.88	0.34
5249 - 7065	1.60	0.23	5.25	0.31	2.26	0.11	5.34	0.31
7065 - 9062	1.75	0.14	5.08	0.70	2.57	0.20	5.14	0.65
MDSS FM4	Mean	STDEV	Mean	STDEV	Mean	STDEV	Mean	STDEV
Inspection (min)	GL	GL	GR	GR	PL	PL	PR	PR
1 - 277	2.89	0.11	2.62	0.07	3.58	0.27	3.07	0.11
277 - 546	2.97	0.14	2.89	0.28	3.05	0.26	3.12	0.18
546 - 3603	3.06	0.15	3.04	0.19	2.92	0.17	3.24	0.14
3603 - 5249	3.18	0.17	3.54	0.32	2.74	0.19	3.98	0.48
5249 - 7065	3.05	0.14	3.33	0.16	2.38	0.06	5.07	0.59
7065 - 9062	2.90	0.19	3.29	0.15	2.72	0.15	5.39	0.98
MDSS ±1 SI	Mean	STDEV	Mean	STDEV	Mean	STDEV	Mean	STDEV
Inspection (min)	GL	GL	GR	GR	PL	PL	PR	PR
1 - 277	0.07	0.01	0.24	0.02	0.19	0.01	0.30	0.02
277 - 546	0.13	0.03	0.25	0.03	0.21	0.03	0.38	0.07
546 - 3603	0.15	0.03	0.25	0.02	0.16	0.03	0.39	0.03
3603 - 5249	0.23	0.03	0.34	0.04	0.39	0.06	0.38	0.03
5249 - 7065	0.43	0.08	0.30	0.03	0.70	0.07	0.41	0.04
7065 - 9062	0.42	0.04	0.67	0.19	0.94	0.04	0.39	0.07
MDSS ±3 SI	Mean	STDEV	Mean	STDEV	Mean	STDEV	Mean	STDEV
Inspection (min)	GL	GL	GR	GR	PL	PL	PR	PR
1 - 277	0.07	0.01	0.16	0.01	0.14	0.01	0.16	0.01
277 - 546	0.11	0.04	0.19	0.03	0.12	0.02	0.21	0.04
546 - 3603	0.14	0.01	0.20	0.01	0.16	0.06	0.23	0.02
3603 - 5249	0.17	0.02	0.25	0.02	0.37	0.04	0.28	0.02
5249 - 7065	0.22	0.03	0.23	0.02	0.55	0.04	0.32	0.02
7065 - 9062	0.27	0.03	0.38	0.09	0.73	0.07	0.39	0.03

Operational Parameters

MDSS RMS	Mean	STDEV	Mean	STDEV	Mean	STDEV
Inspection (min)	**torque**	torque	LOO	LOO	ROO	ROO
1 - 277	4271	39	173	8	172	8
277 - 546	6248	1586	170	16	170	13
546 - 3603	7871	637	177	7	177	6
3603 - 5249	7941	880	177	4	177	4
5249 - 7065	7786	793	180	4	178	4
7065 - 9062	7409	1319	174	14	174	12

TABLE C.1.6.—TEST L2020R5050

L2020R5050								
MDSS RMS	Mean	STDEV	Mean	STDEV	Mean	STDEV	Mean	STDEV
Inspection (min)	GL	GL	GR	GR	PL	PL	PR	PR
1 - 70	2.29	0.33	2.03	0.30	2.27	0.33	1.88	0.31
70 - 217	5.56	1.11	4.16	0.55	5.64	1.11	4.29	0.59
MDSS FM4	Mean	STDEV	Mean	STDEV	Mean	STDEV	Mean	STDEV
Inspection (min)	GL	GL	GR	GR	PL	PL	PR	PR
1 - 70	2.85	0.09	2.56	0.08	3.10	0.22	2.75	0.22
70 - 217	3.19	0.23	2.77	0.14	2.91	0.24	2.88	0.13
MDSS ±1 SI	Mean	STDEV	Mean	STDEV	Mean	STDEV	Mean	STDEV
Inspection (min)	GL	GL	GR	GR	PL	PL	PR	PR
1 - 70	0.04	0.02	0.20	0.03	0.21	0.03	0.22	0.02
70 - 217	0.23	0.04	0.47	0.07	0.54	0.06	0.50	0.09
MDSS ± 3 SI	Mean	STDEV	Mean	STDEV	Mean	STDEV	Mean	STDEV
Inspection (min)	GL	GL	GR	GR	PL	PL	PR	PR
1 - 70	0.06	0.01	0.12	0.01	0.10	0.01	0.18	0.03
70 - 217	0.14	0.02	0.25	0.03	0.27	0.04	0.33	0.05

Operational Parameters

MDSS RMS	Mean	STDEV	Mean	STDEV	Mean	STDEV
Inspection (min)	torque	torque	LOO	LOO	ROO	ROO
1 - 70	4185	50	175	23	150	39
70 - 217	7781	576	184	33	162	43

TABLE C.1.7.—TEST L4040R5050

L4040R5050								
MDSS RMS	Mean	STDEV	Mean	STDEV	Mean	STDEV	Mean	STDEV
Inspection (min)	GL	GL	GR	GR	PL	PL	PR	PR
1 - 63	1.89	0.20	2.18	0.41	1.85	0.22	2.08	0.41
63 - 370	2.74	0.46	5.58	0.31	2.74	0.46	5.54	0.31
MDSS FM4	Mean	STDEV	Mean	STDEV	Mean	STDEV	Mean	STDEV
Inspection (min)	GL	GL	GR	GR	PL	PL	PR	PR
1 - 63	3.07	0.22	2.77	0.12	2.78	0.11	2.90	0.20
63 - 370	3.24	0.21	3.24	0.20	2.98	0.25	2.65	0.23
MDSS ± 1 SI	Mean	STDEV	Mean	STDEV	Mean	STDEV	Mean	STDEV
Inspection (min)	GL	GL	GR	GR	PL	PL	PR	PR
1 - 63	0.31	0.06	0.30	0.09	0.14	0.02	0.17	0.02
63 - 370	0.12	0.03	0.42	0.05	0.33	0.02	0.26	0.02
MDSS ± 3 SI	Mean	STDEV	Mean	STDEV	Mean	STDEV	Mean	STDEV
Inspection (min)	GL	GL	GR	GR	PL	PL	PR	PR
1 - 63	0.15	0.02	0.18	0.03	0.10	0.01	0.13	0.02
63 - 370	0.07	0.01	0.18	0.02	0.17	0.01	0.21	0.02

Operational Parameters

	Mean	STDEV	Mean	STDEV	Mean	STDEV
Inspection (min)	torque	torque	LOO	LOO	ROO	ROO
1 - 63	4232	429	141	20	139	25
63 - 370	7345	49	169	10	168	10

TABLE C.1.8.—TEST L2121R1919

L2121R1919

MDSS RMS	Mean	STDEV	Mean	STDEV	Mean	STDEV	Mean	STDEV
Inspection (min)	GL	GL	GR	GR	PL	PL	PR	PR
1 - 127	1.28	0.10	4.65	0.41	1.19	0.11	4.72	0.39
127 - 307	2.14	0.68	5.21	0.49	2.05	0.67	5.26	0.48
307 - 1122	3.12	0.38	5.35	0.37	3.07	0.40	5.39	0.37
1122 - 1393	3.16	0.20	4.87	0.23	3.27	0.21	4.94	0.22
1393 - 1568	3.44	0.42	5.40	0.40	3.81	0.43	5.49	0.40
1568 - 1905	2.95	0.28	4.45	0.42	3.64	0.28	4.58	0.44
MDSS FM4	Mean	STDEV	Mean	STDEV	Mean	STDEV	Mean	STDEV
Inspection (min)	GL	GL	GR	GR	PL	PL	PR	PR
1 - 127	3.06	0.15	2.79	0.13	2.98	0.19	5.70	1.27
127 - 307	2.92	0.26	3.17	0.24	2.78	0.17	4.56	0.87
307 - 1122	2.85	0.09	3.10	0.13	2.78	0.19	3.94	0.42
1122 - 1393	2.77	0.07	2.84	0.17	2.19	0.10	2.81	0.30
1393 - 1568	2.86	0.11	2.82	0.20	2.24	0.16	3.08	0.29
1568 - 1905	2.66	0.08	2.82	0.18	2.36	0.14	2.56	0.21
MDSS ± 1 SI	Mean	STDEV	Mean	STDEV	Mean	STDEV	Mean	STDEV
Inspection (min)	GL	GL	GR	GR	PL	PL	PR	PR
1 - 127	0.29	0.02	0.23	0.02	0.14	0.01	0.34	0.06
127 - 307	0.28	0.13	0.28	0.17	0.17	0.03	0.39	0.07
307 - 1122	0.18	0.01	0.15	0.03	0.17	0.02	0.45	0.04
1122 - 1393	0.09	0.02	0.05	0.04	0.18	0.02	0.42	0.03
1393 - 1568	0.16	0.02	0.13	0.03	0.16	0.04	0.40	0.05
1568 - 1905	0.05	0.03	0.12	0.02	0.17	0.03	0.28	0.05
MDSS ± 3 SI	Mean	STDEV	Mean	STDEV	Mean	STDEV	Mean	STDEV
Inspection (min)	GL	GL	GR	GR	PL	PL	PR	PR
1 - 127	0.15	0.01	0.18	0.02	0.10	0.01	0.29	0.03
127 - 307	0.15	0.04	0.22	0.06	0.12	0.01	0.30	0.03
307 - 1122	0.13	0.01	0.19	0.02	0.12	0.02	0.28	0.02
1122 - 1393	0.13	0.02	0.19	0.02	0.13	0.01	0.27	0.02
1393 - 1568	0.12	0.01	0.21	0.03	0.17	0.03	0.28	0.05
1568 - 1905	0.09	0.01	0.21	0.02	0.28	0.03	0.22	0.02

Operational Parameters

MDSS RMS	Mean	STDEV	Mean	STDEV	Mean	STDEV
Inspection (min)	torque	torque	LOO	LOO	ROO	ROO
1 - 127	4050	48	163	16	164	15
127 - 307	5760	1417	163	23	165	19
307 - 1122	7641	1217	164	24	160	30
1122 - 1393	7934	44	167	23	169	18
1393 - 1568	7969	415	173	13	170	14
1568 - 1905	7905	298	176	8	175	8

TABLE C.1.9.—TEST L1616R1919

L1616R1919

MDSS RMS	Mean	STDEV	Mean	STDEV	Mean	STDEV	Mean	STDEV
Inspection(min)	GL	GL	GR	GR	PL	PL	PR	PR
1 - 445	2.42	1.02	3.66	0.86	2.32	1.07	3.62	0.87
MDSS FM4	Mean	STDEV	Mean	STDEV	Mean	STDEV	Mean	STDEV
Inspection(min)	GL	GL	GR	GR	PL	PL	PR	PR
1 - 445	2.98	0.15	2.99	0.23	2.90	0.16	3.42	0.68
MDSS +1 SI	Mean	STDEV	Mean	STDEV	Mean	STDEV	Mean	STDEV
Inspection(min)	GL	GL	GR	GR	PL	PL	PR	PR
1 - 445	0.19	0.11	0.25	0.14	0.12	0.04	0.19	0.04
MDSS +3 SI	Mean	STDEV	Mean	STDEV	Mean	STDEV	Mean	STDEV
Inspection(min)	GL	GL	GR	GR	PL	PL	PR	PR
1 - 445	0.11	0.04	0.18	0.09	0.07	0.01	0.12	0.03

Operational Parameters

Inspection(min)	Mean	STDEV	Mean	STDEV	Mean	STDEV
Minutes	torque	torque	LOO	LOO	ROO	ROO
1 - 445	7187	1525	128	5	132	5

TABLE C.1.10.—TEST L3737R2424

L3737R2424

MDSS RMS	Mean	STDEV	Mean	STDEV	Mean	STDEV	Mean	STDEV
Inspection (min)	GL	GL	GR	GR	PL	PL	PR	PR
1 - 214	0.98	0.10	3.32	0.25	0.91	0.10	3.30	0.24
214 - 427	1.00	0.17	3.50	0.28	0.80	0.12	3.43	0.27
427 - 4945	1.03	0.05	4.07	0.17	0.85	0.05	4.01	0.17
4945 - 6493	1.07	0.07	3.79	0.18	1.05	0.12	3.71	0.17
6493 - 7072	1.46	0.14	3.52	0.50	1.70	0.14	3.54	0.47
7072 - 7394	1.23	0.11	3.60	0.32	1.57	0.11	3.61	0.29
MDSS FM4	Mean	STDEV	Mean	STDEV	Mean	STDEV	Mean	STDEV
Inspection (min)	GL	GL	GR	GR	PL	PL	PR	PR
1 - 214	2.77	0.13	2.68	0.15	2.73	0.11	3.12	0.17
214 - 427	2.68	0.15	2.76	0.15	2.77	0.18	2.98	0.22
427 - 4945	2.62	0.07	2.99	0.12	2.75	0.16	2.59	0.16
4945 - 6493	2.67	0.11	2.93	0.08	2.55	0.09	2.61	0.18
6493 - 7072	2.94	0.22	2.91	0.13	2.58	0.06	3.43	0.56
7072 - 7394	2.97	0.21	3.28	0.14	2.59	0.06	3.54	0.69
MDSS +1SI	Mean	STDEV	Mean	STDEV	Mean	STDEV	Mean	STDEV
Minutes	GL	GL	GR	GR	PL	PL	PR	PR
1 - 214	0.20	0.01	0.21	0.06	0.14	0.01	0.22	0.01
214 - 427	0.19	0.05	0.24	0.11	0.13	0.02	0.21	0.01
427 - 4945	0.10	0.02	0.31	0.01	0.11	0.03	0.22	0.01
4945 - 6493	0.11	0.04	0.31	0.01	0.07	0.03	0.18	0.02
6493 - 7072	0.19	0.06	0.34	0.03	0.15	0.03	0.16	0.03
7072 - 7394	0.24	0.04	0.34	0.05	0.14	0.03	0.16	0.02
MDSS +3 SI	Mean	STDEV	Mean	STDEV	Mean	STDEV	Mean	STDEV
Inspection (min)	GL	GL	GR	GR	PL	PL	PR	PR
1 - 214	0.11	0.01	0.15	0.01	0.07	0.01	0.14	0.01
214 - 427	0.10	0.02	0.16	0.04	0.08	0.01	0.15	0.01
427 - 4945	0.09	0.01	0.22	0.01	0.10	0.01	0.18	0.01
4945 - 6493	0.11	0.01	0.23	0.01	0.14	0.03	0.18	0.01
6493 - 7072	0.13	0.02	0.20	0.03	0.26	0.04	0.17	0.02
7072 - 7394	0.15	0.02	0.21	0.02	0.27	0.04	0.18	0.01

Operational Parameters

	Mean	STDEV	Mean	STDEV	Mean	STDEV	Mean	STDEV
Inspection (min)	torque	torque	G	G	LOO	LOO	ROO	ROO
1 - 214		63	3654	240	106	17	106	17
214 - 427		390	4888	1624	118	17	119	18
427 - 4945		119	7933	596	139	1	139	1
4945 - 6493		218	7600	1386	137	3	138	2
6493 - 7072		463	5658	1738	134	3	136	4
7072 - 7394	6608	1732	6407	1838	136	3	137	3

TABLE C.1.11.—TEST L3737R5036

L3737R5036

MDSS RMS	Mean	STDEV	Mean	STDEV	Mean	STDEV	Mean	STDEV
Inspection(min)	GL	GL	GR	GR	PL	PL	PR	PR
1 - 4730	1.93	0.26	5.90	0.91	2.14	0.27	5.98	0.96
MDSS FM4	Mean	STDEV	Mean	STDEV	Mean	STDEV	Mean	STDEV
Inspection(min)	GL	GL	GR	GR	PL	PL	PR	PR
1 - 4730	2.92	0.12	2.94	0.11	3.22	0.39	2.98	0.27
MDSS +1 SI	Mean	STDEV	Mean	STDEV	Mean	STDEV	Mean	STDEV
Inspection(min)	GL	GL	GR	GR	PL	PL	PR	PR
1 - 4730	0.33	0.05	0.43	0.08	0.29	0.08	0.26	0.04
MDSS +3 SI	Mean	STDEV	Mean	STDEV	Mean	STDEV	Mean	STDEV
Inspection(min)	GL	GL	GR	GR	PL	PL	PR	PR
1 - 4730	0.22	0.02	0.21	0.04	0.37	0.02	0.25	0.05

Operational Parameters

	Mean	STDEV	Mean	STDEV	Mean	STDEV
Inspection(min)	torque	torque	LOO	LOO	ROO	ROO
1 - 4730	7603	1093	161	20	163	20

TABLE C.1.12.—TEST L1414R1616

L1616R1414

MDSS RMS	Mean	STDEV	Mean	STDEV	Mean	STDEV	Mean	STDEV
Inspection	GL	GL	GR	GR	PL	PL	PR	PR
1 - 705	3.64	0.59	5.22	0.86	3.59	0.57	5.25	0.87
MDSS FM4	Mean	STDEV	Mean	STDEV	Mean	STDEV	Mean	STDEV
Inspection	GL	GL	GR	GR	PL	PL	PR	PR
1 - 705	2.67	0.12	3.14	0.35	3.19	0.36	3.23	0.25
MDSS ± 1 SI	Mean	STDEV	Mean	STDEV	Mean	STDEV	Mean	STDEV
Inspection	GL	GL	GR	GR	PL	PL	PR	PR
1 - 705	0.26	0.07	0.23	0.04	0.34	0.09	0.60	0.14
MDSS ± 3 SI	Mean	STDEV	Mean	STDEV	Mean	STDEV	Mean	STDEV
Inspection	GL	GL	GR	GR	PL	PL	PR	PR
1 - 705	0.17	0.04	0.19	0.03	0.24	0.06	0.28	0.05

Operational Parameters

	Mean	STDEV	Mean	STDEV	Mean	STDEV
Inspection	torque	torque	LOO	LOO	ROO	ROO
1 - 705	6815	1744	135	5	136	3

TABLE C.1.13.—TEST L4444R5252

L4444R5252

MDSS RMS	Mean	STDEV	Mean	STDEV	Mean	STDEV	Mean	STDEV
Inspection	GL	GL	GR	GR	PL	PL	PR	PR
1 - 273	1.03	0.08	2.57	0.19	0.91	0.09	2.55	0.19
273 - 602	1.33	0.14	3.22	0.26	1.18	0.12	3.19	0.25
602 - 970	1.39	0.26	3.42	0.40	1.14	0.22	3.37	0.39
MDSS FM4	Mean	STDEV	Mean	STDEV	Mean	STDEV	Mean	STDEV
Inspection	GL	GL	GR	GR	PL	PL	PR	PR
1 - 273	3.03	0.12	2.81	0.08	3.03	0.24	2.64	0.12
273 - 602	2.83	0.17	2.90	0.11	2.92	0.20	2.54	0.14
602 - 970	3.03	0.17	2.80	0.17	3.01	0.26	2.51	0.12
MDSS ± 1 SI	Mean	STDEV	Mean	STDEV	Mean	STDEV	Mean	STDEV
Inspection	GL	GL	GR	GR	PL	PL	PR	PR
1 - 273	0.15	0.01	0.19	0.02	0.09	0.01	0.17	0.01
273 - 602	0.20	0.03	0.13	0.02	0.12	0.01	0.15	0.02
602 - 970	0.24	0.05	0.17	0.07	0.15	0.02	0.14	0.01
MDSS ± 3 SI	Mean	STDEV	Mean	STDEV	Mean	STDEV	Mean	STDEV
Inspection	GL	GL	GR	GR	PL	PL	PR	PR
1 - 273	0.10	0.01	0.11	0.01	0.08	0.01	0.12	0.01
273 - 602	0.13	0.01	0.12	0.01	0.09	0.01	0.11	0.01
602 - 970	0.14	0.02	0.14	0.02	0.13	0.01	0.11	0.01

Operational Parameters

	Mean	STDEV	Mean	STDEV	Mean	STDEV
Inspection	torque	torque	LOO	LOO	ROO	ROO
1 - 273	4091	317	116	11	117	10
273 - 602	5733	871	120	8	121	8
602 - 970	7003	1545	121	10	123	9

Appendix D.—Clustering of Condition Indicators and Damage Modes Between Inspections

D.1 L4545R5050 and L1515R4545

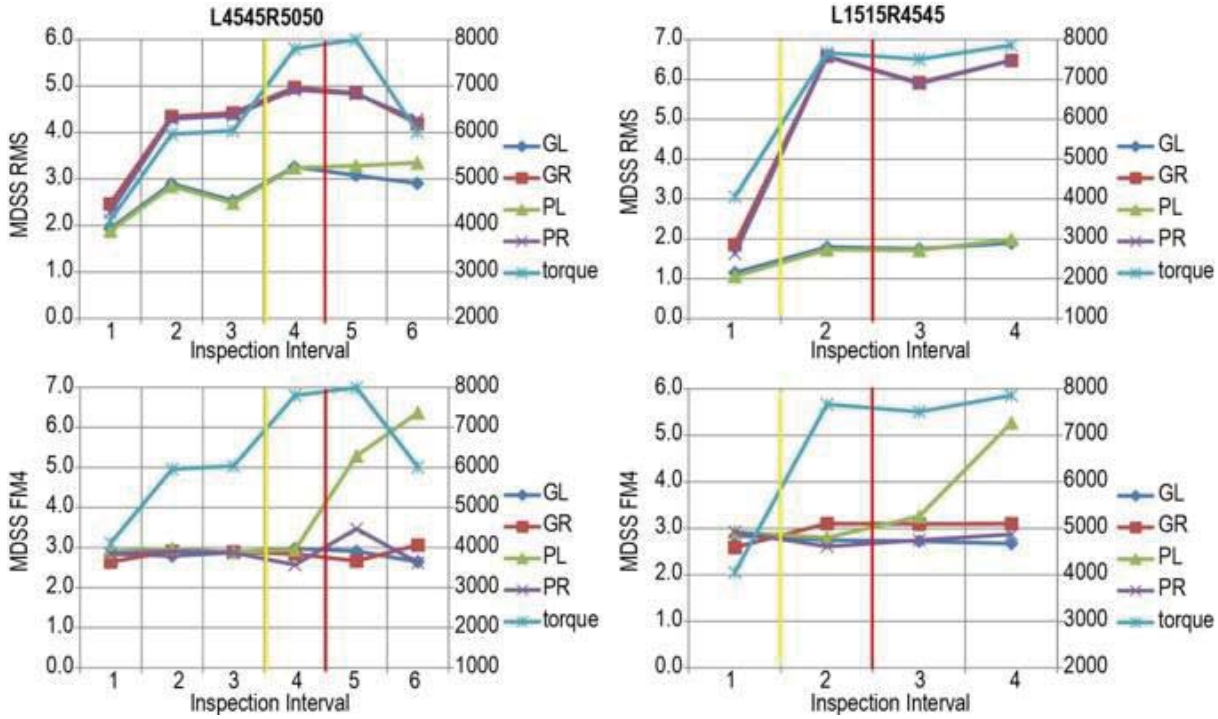

Figure D.1.1.—Compare RMS and FM4 to damage modes between inspection intervals L4545R5050 and L1515R4545—2 teeth left pinion macro pitting.

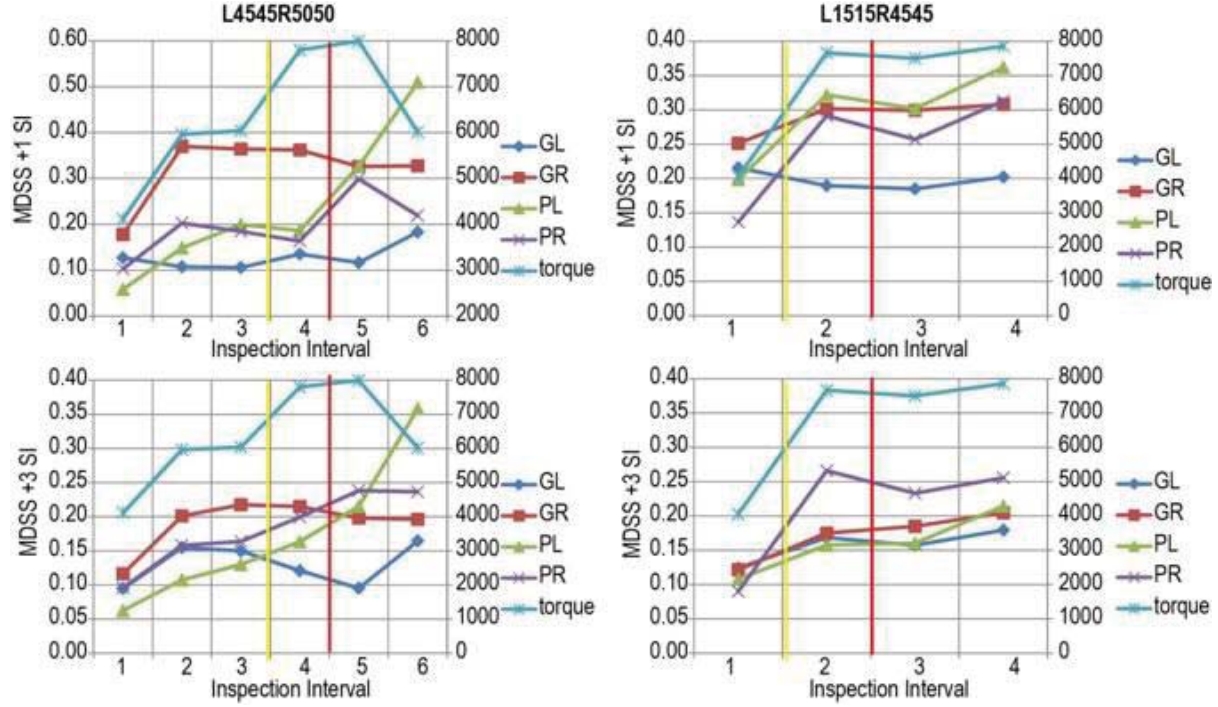

Figure D.1.2.—Compare SI1 and SI3 to damage modes between inspection intervals L4545R5050 and L1515R4545—2 teeth left pinion macro pitting.

D.2 L3030R5050, L3535R5050, and L1818R1616

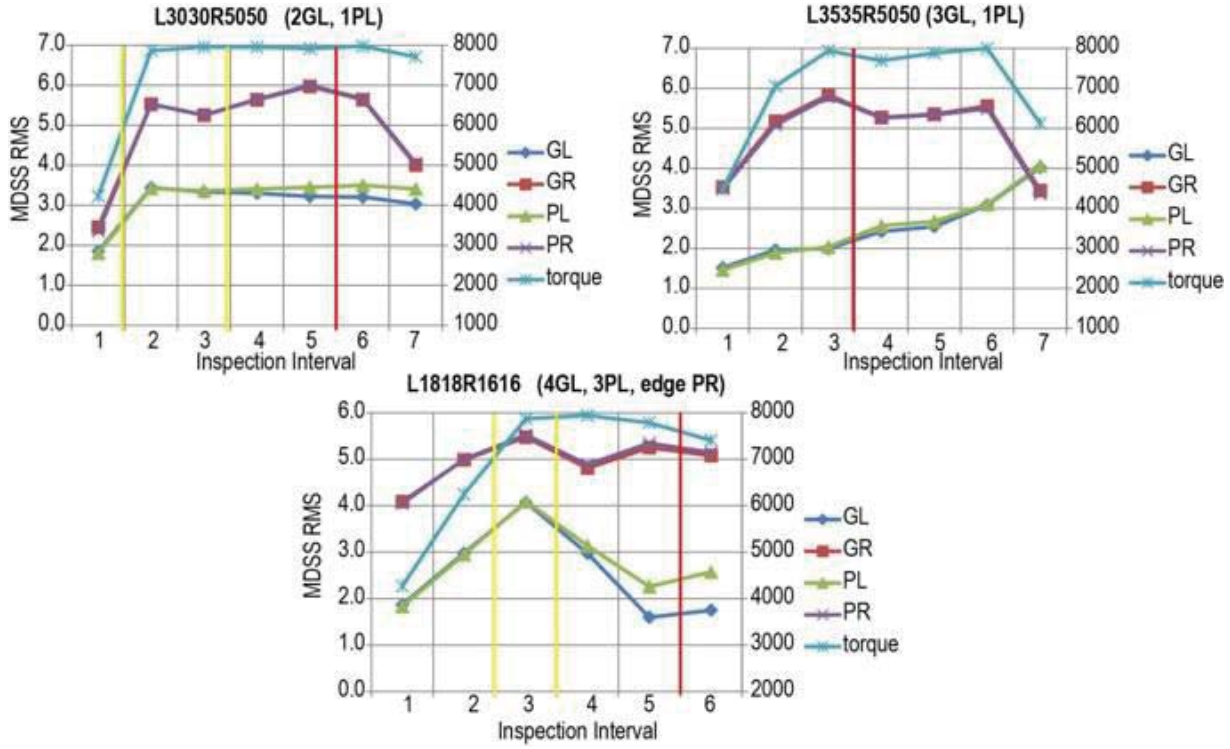

Figure D.2.1.—Compare RMS to damage modes left gear teeth macro pitting L3030R5050 (2GL, 1PL); L3535R5050 (3GL, 1PL); L1818R1616 (4GL, 3PL, edge PR).

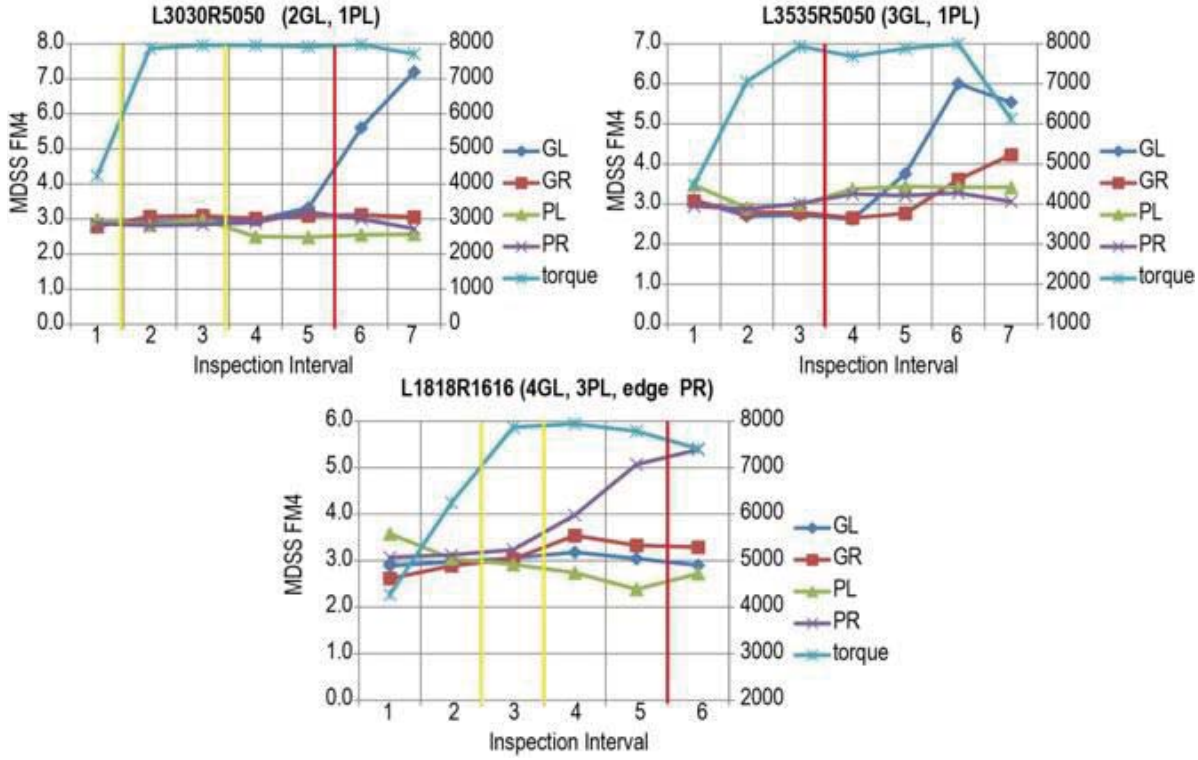

Figure D.2.2.—Compare FM4 to damage modes left gear teeth macro pittingL3030R5050 (2GL, 1PL); L3535R5050 (3GL, 1PL); L1818R1616 (4GL, 3PL, edge PR).

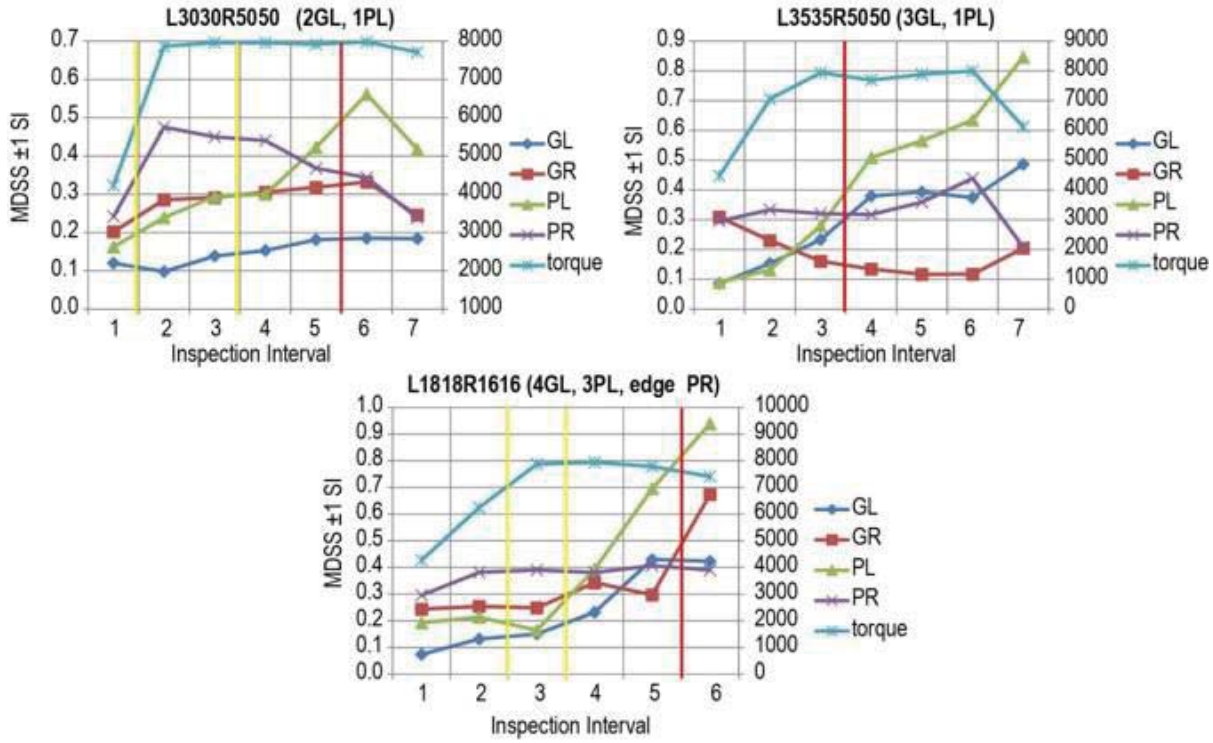

Figure D.2.3.—Compare SI1 to damage modes left gear teeth macro pittingL3030R5050 (2GL, 1PL); L3535R5050 (3GL, 1PL); L1818R1616 (4GL, 3PL, edge PR).

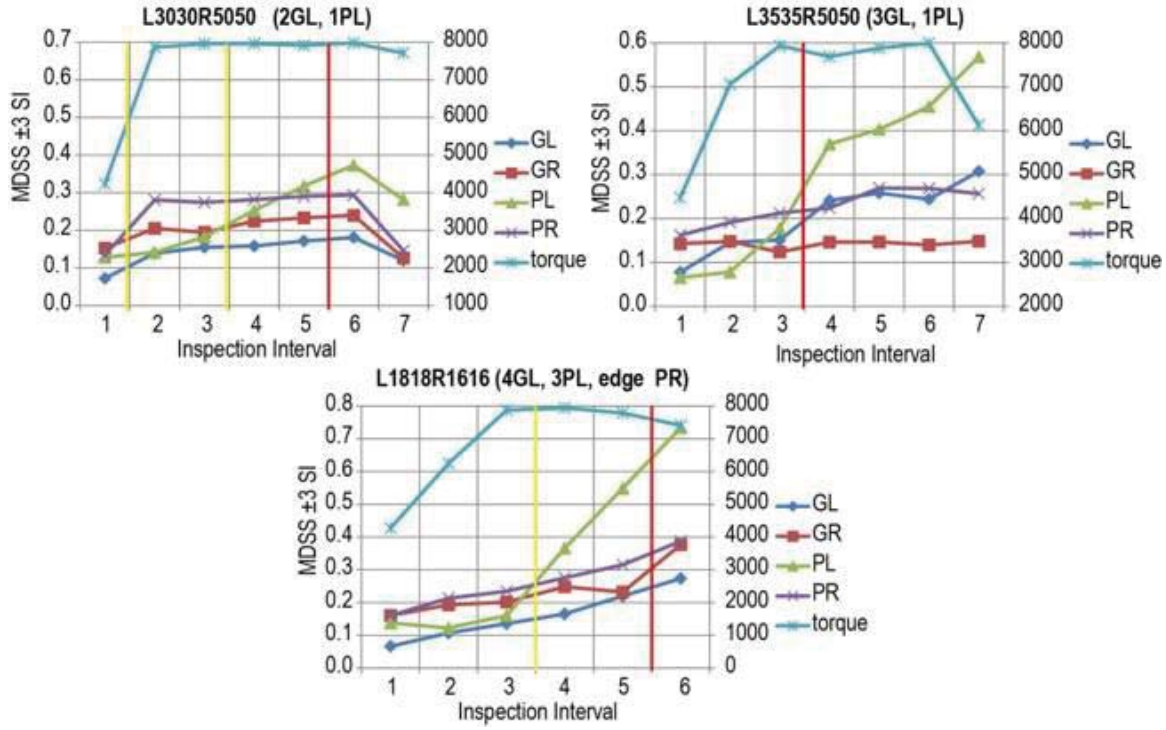

Figure D.2.4.—Compare SI3 to damage modes left gear teeth macro pitting L3030R5050 (2GL, 1PL); L3535R5050 (3GL, 1PL); L1818R1616 (4GL, 3PL, edge PR).

D.3 L2020R5050 and L2121R1919

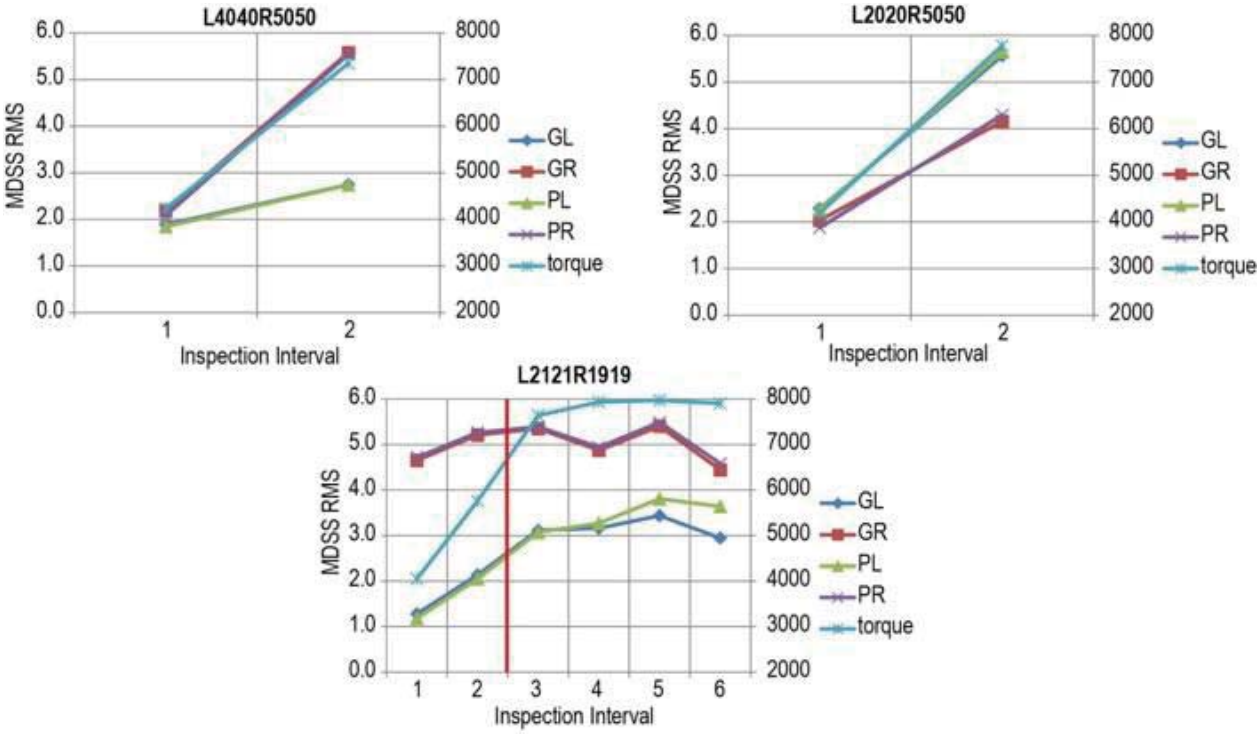

Figure D.3.1.—Compare RMS to damage modes left pinion/gear scuffing.

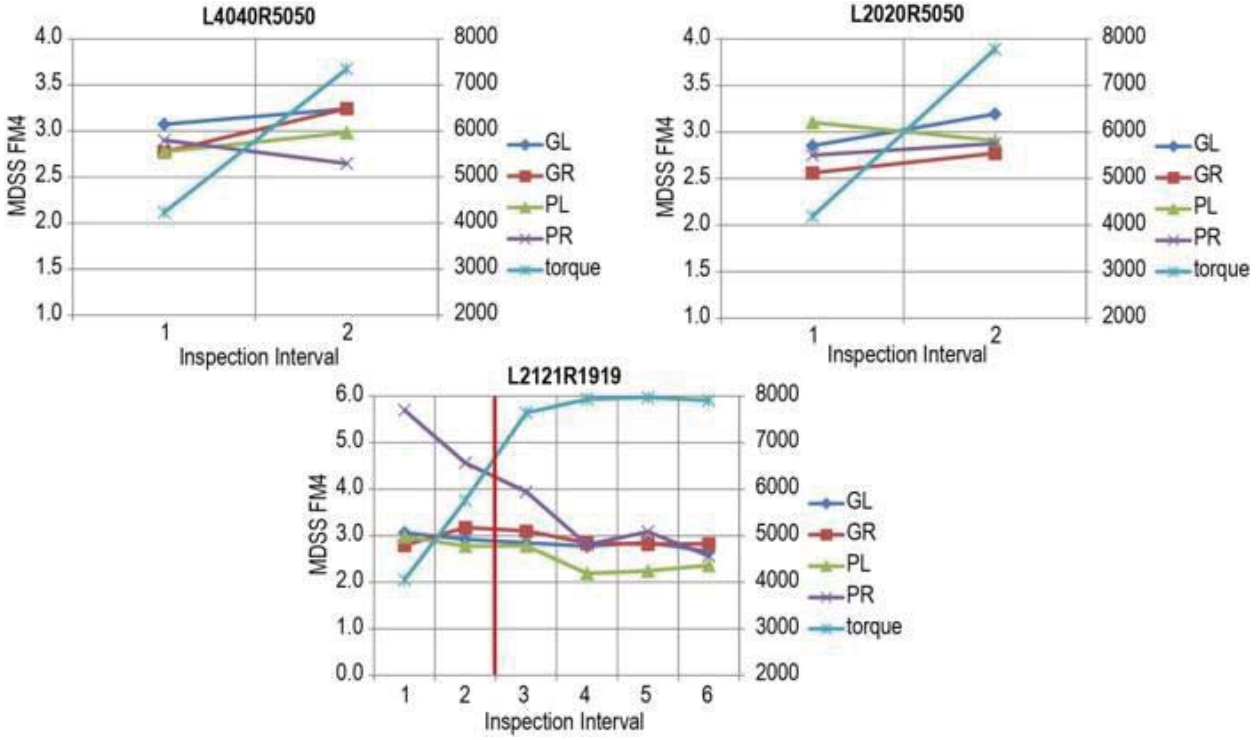

Figure D.3.2.—Compare FM4 to damage modes left pinion/gear scuffing.

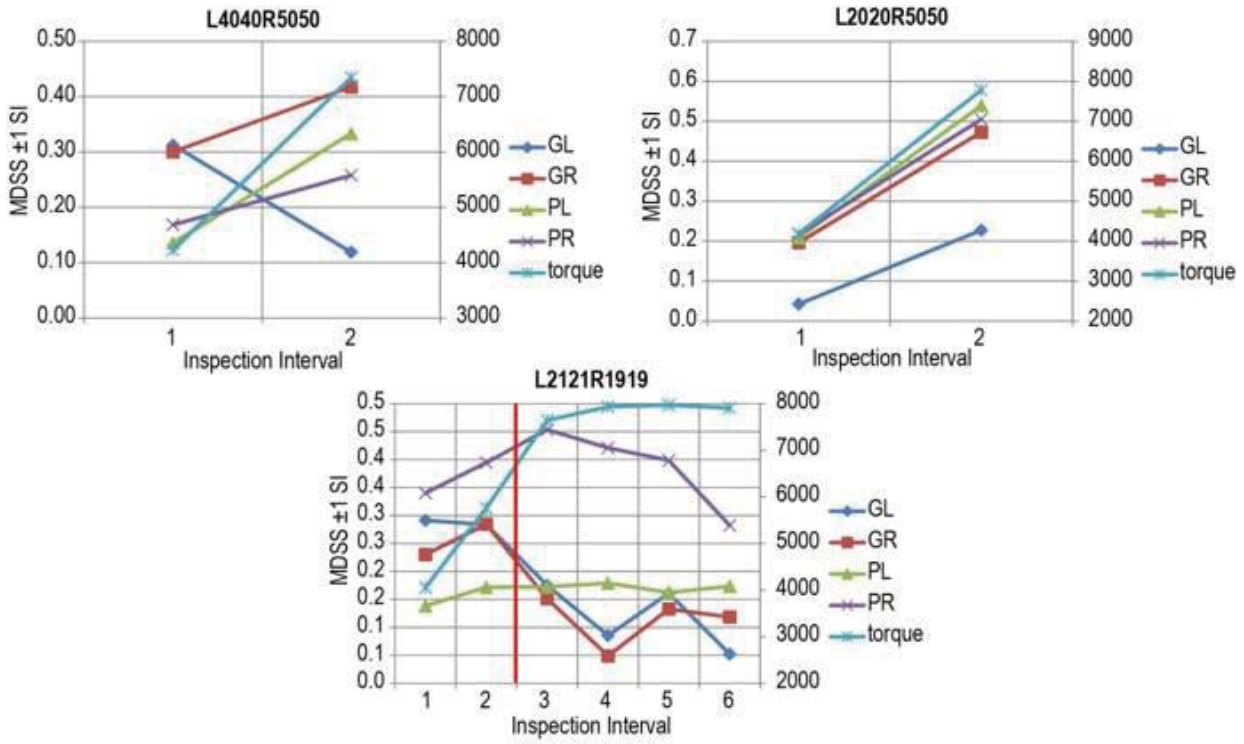

Figure D.3.3.—Compare SI1 to damage modes left pinion/gear scuffing.

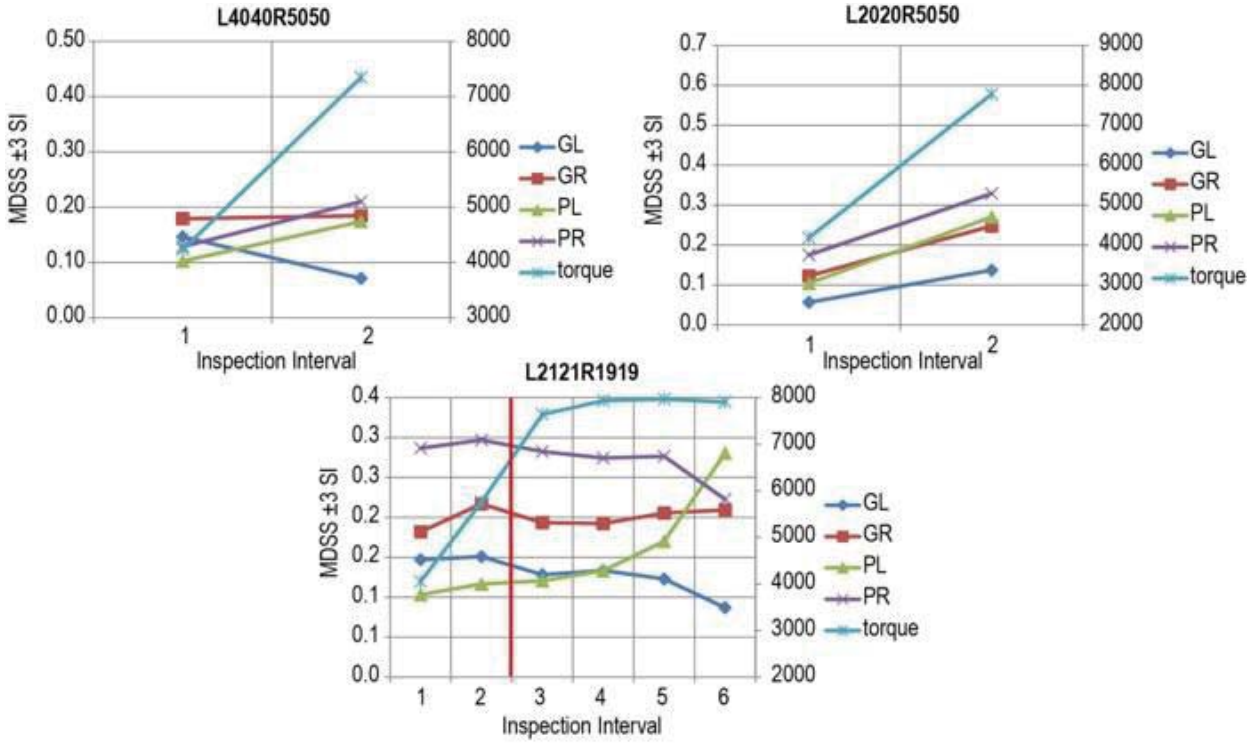

Figure D.3.4.—Compare SI1 to damage modes left pinion/gear scuffing.

Appendix E.—Correlation of MDSS CI Data to MSPU CI Data

E.1 L4545R5050

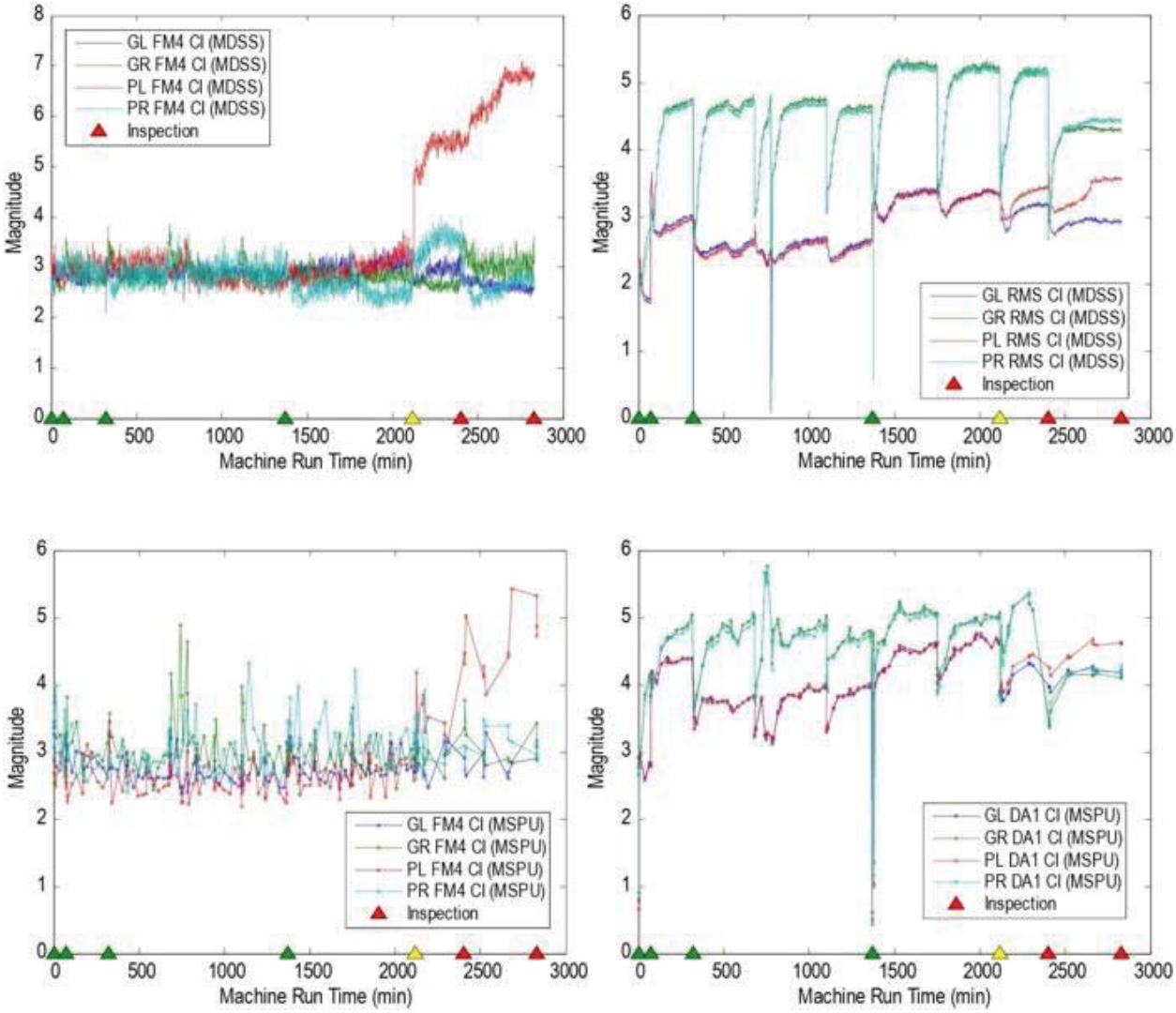

Figure E.1.1.—Compare Test L4545R5050 FM4 and RMS/DA1 for MDSS and MSPU.

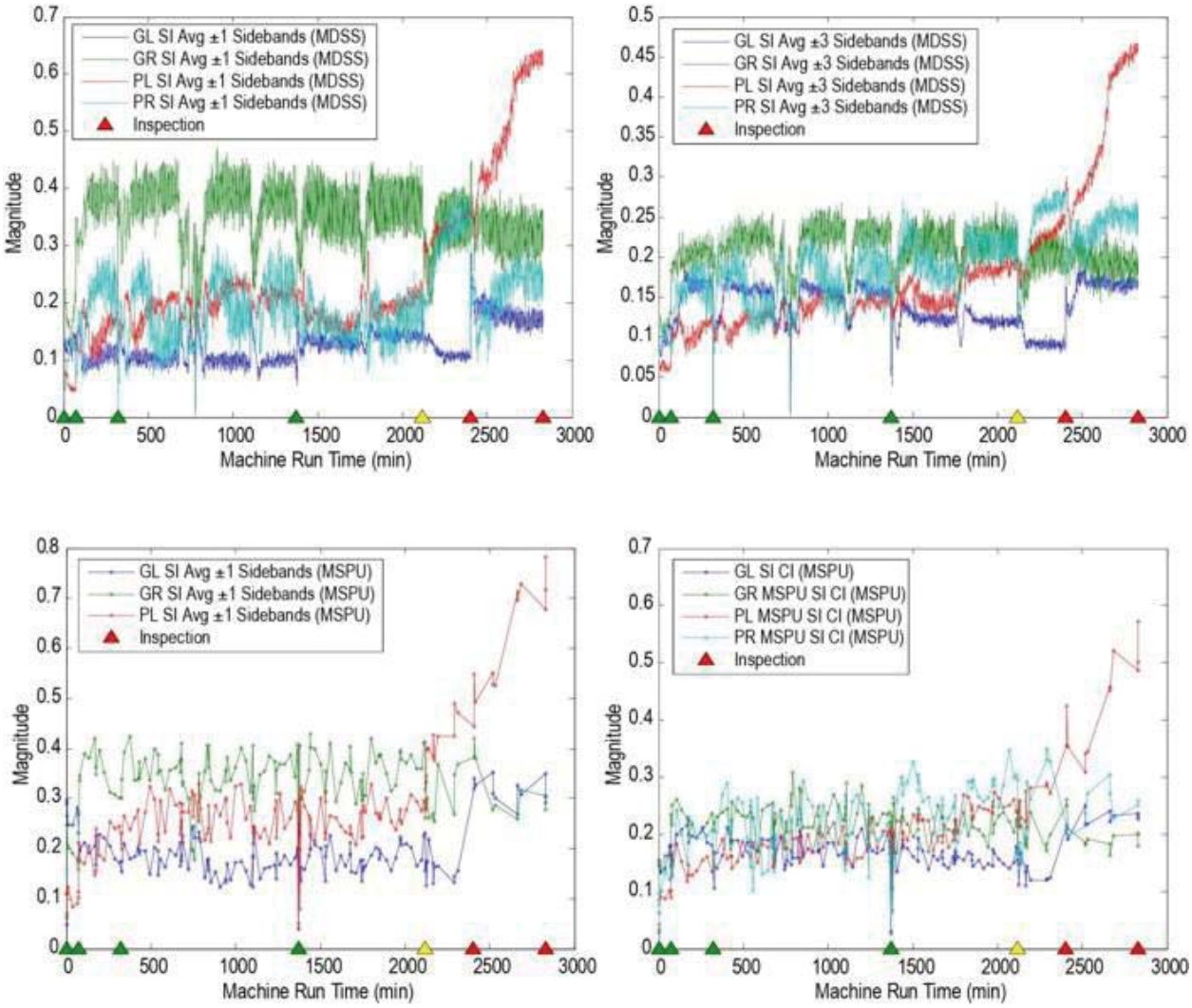

Figure E.1.2.—Compare Test L4545R5050 SI1 and SI3 for MDSS and MSPU.

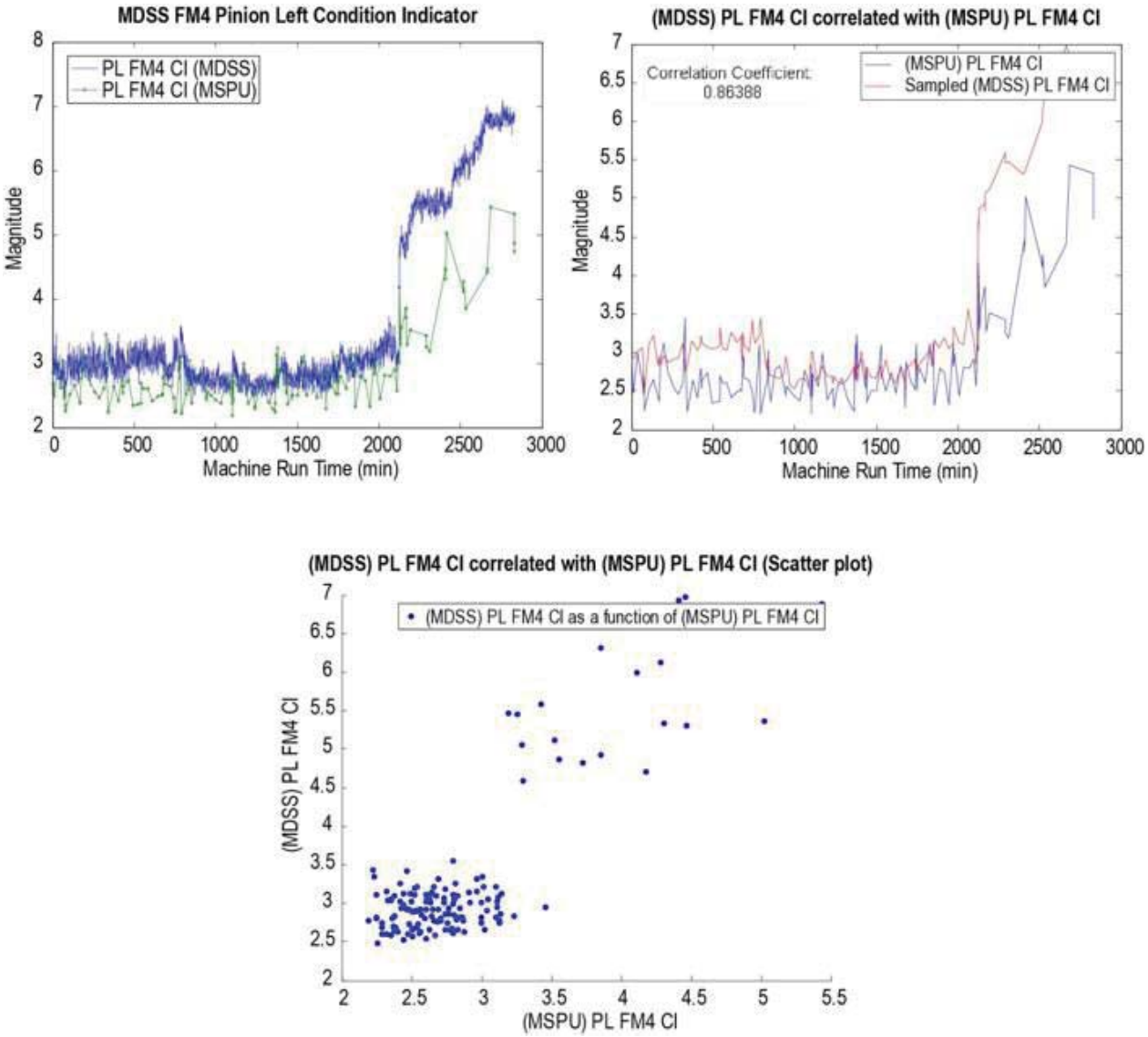

Figure E.1.3.—Compare Test L4545R5050 FM4 Nearest Time Correlation Methods.

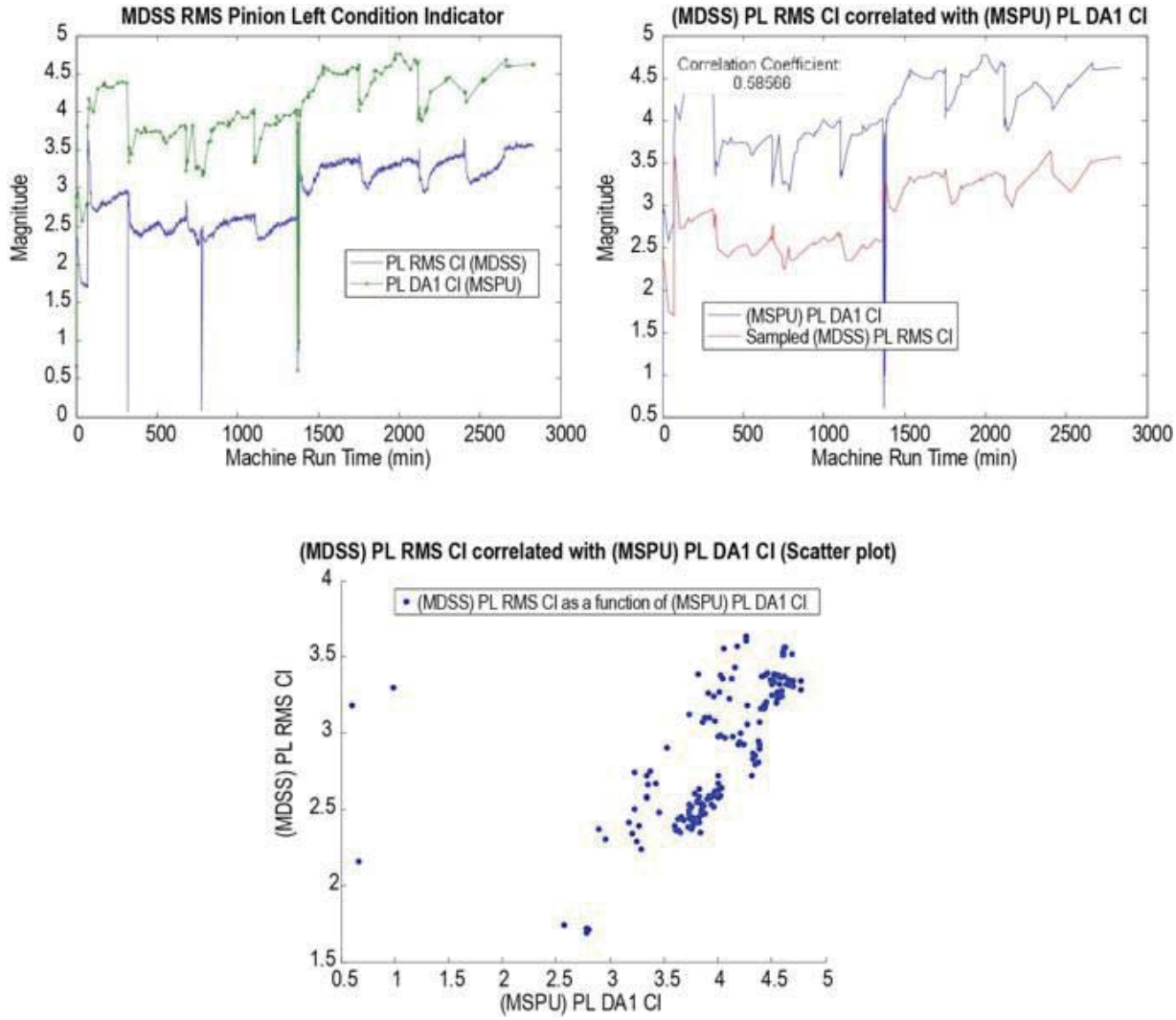

Figure E.1.4.—Compare Test L4545R5050 RMS/DA1 Nearest Time Correlation Methods.

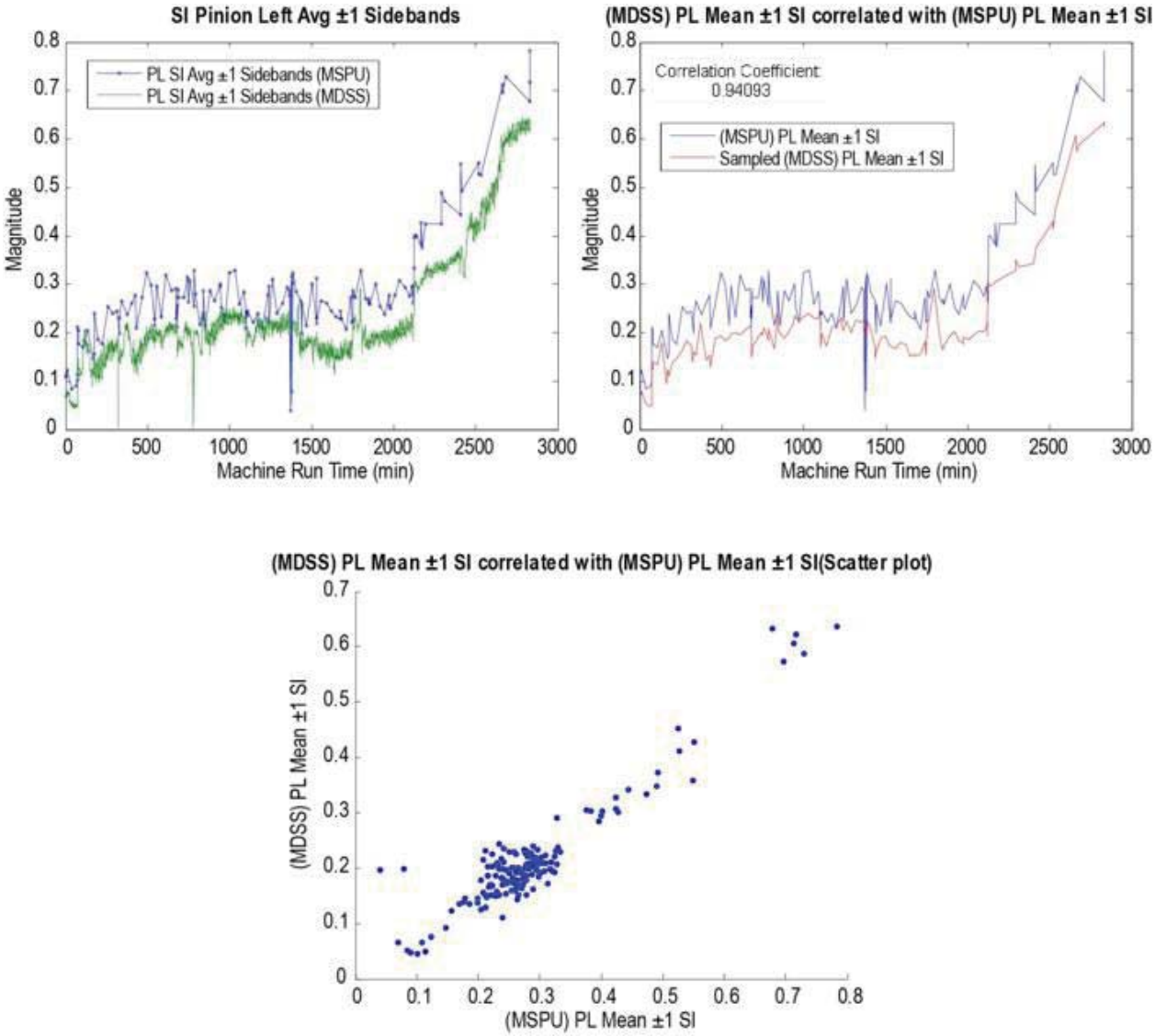

Figure E.1.5.—Compare Test L4545R5050 SI1 Nearest Time Correlation Methods.

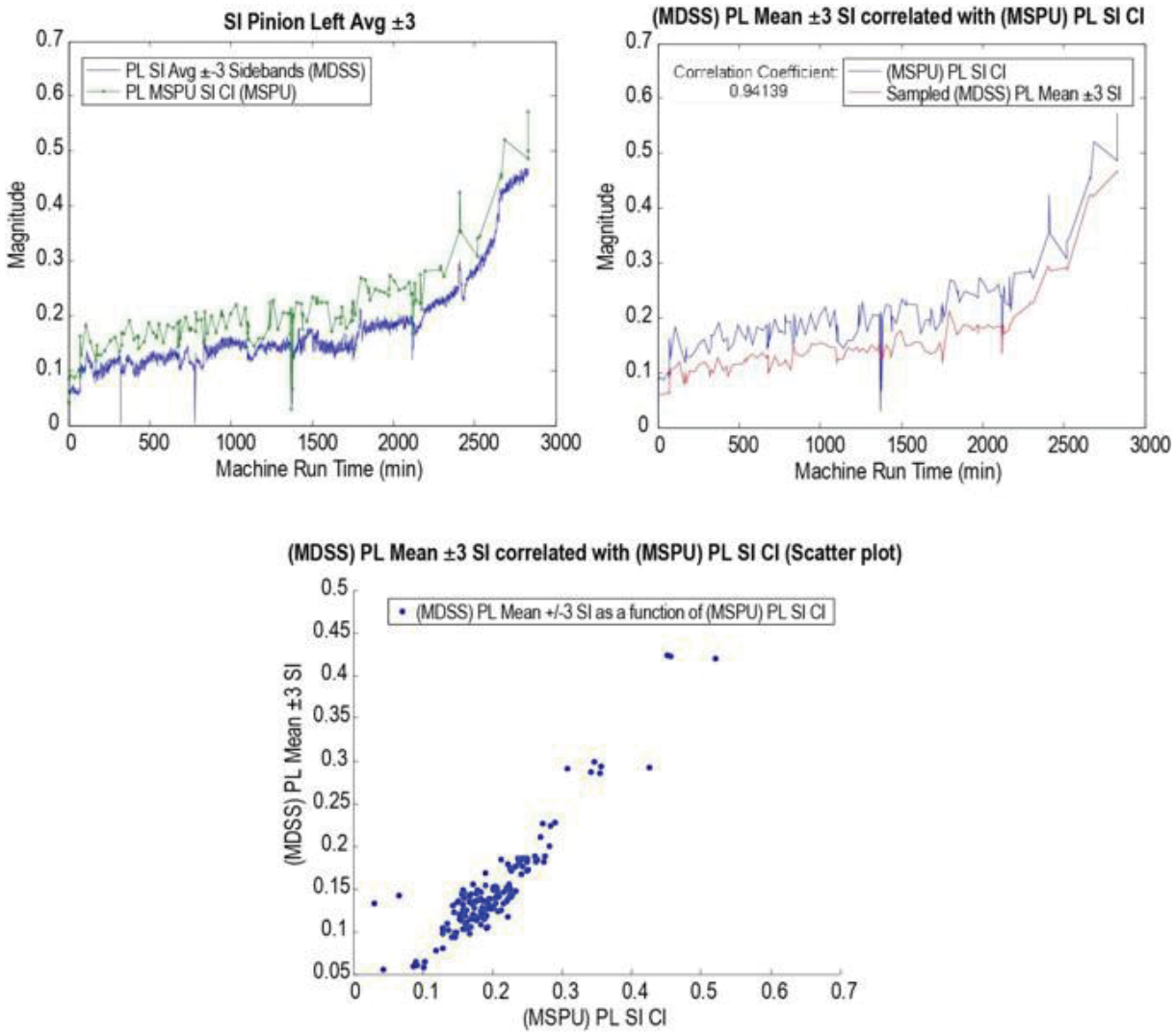

Figure E.1.6.—Compare Test L4545R5050 SI3 and SI Nearest Time Correlation Methods.

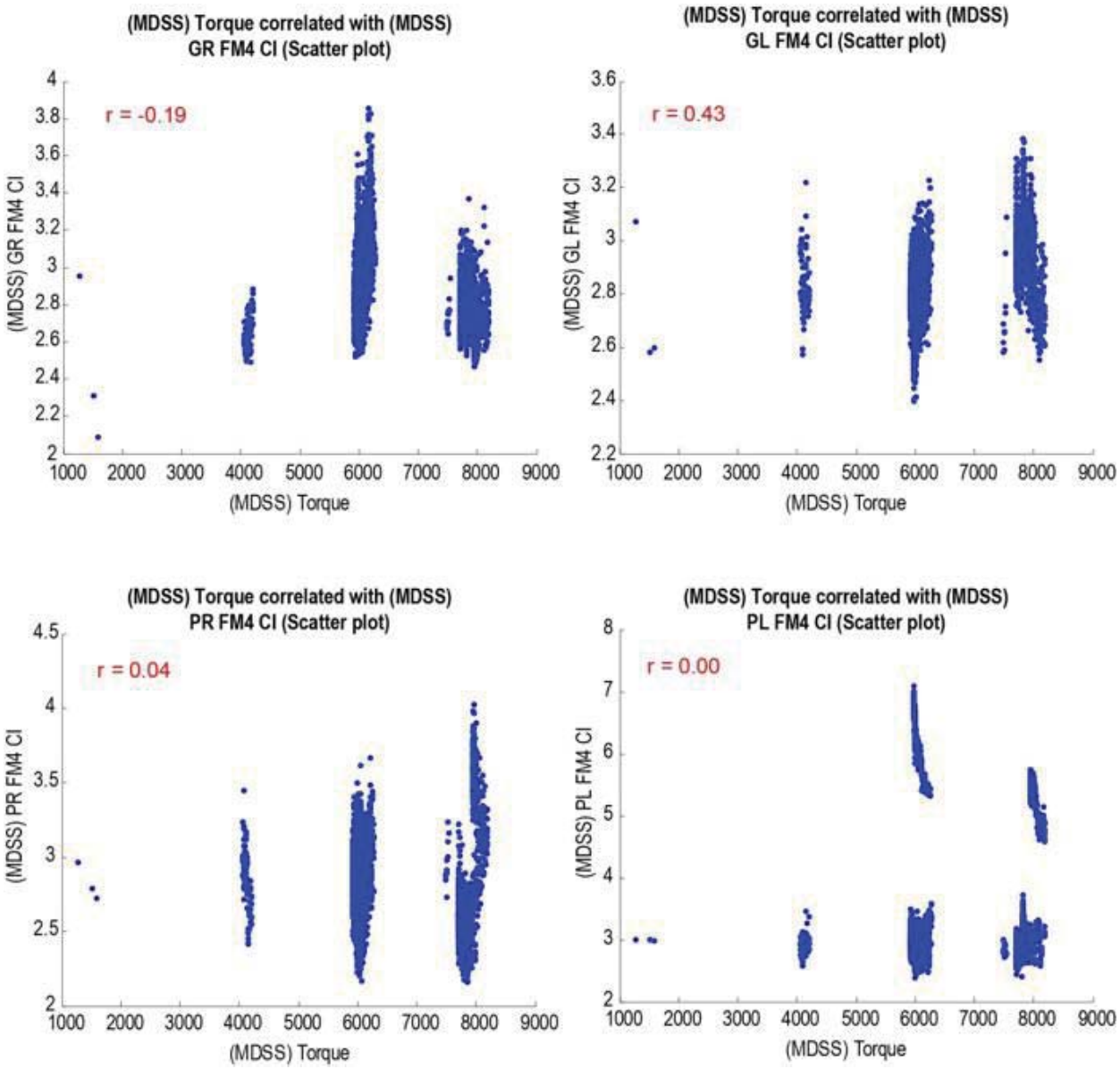

Figure E.1.7.—Compare Test L4545R5050 MDSS FM4 to Torque.

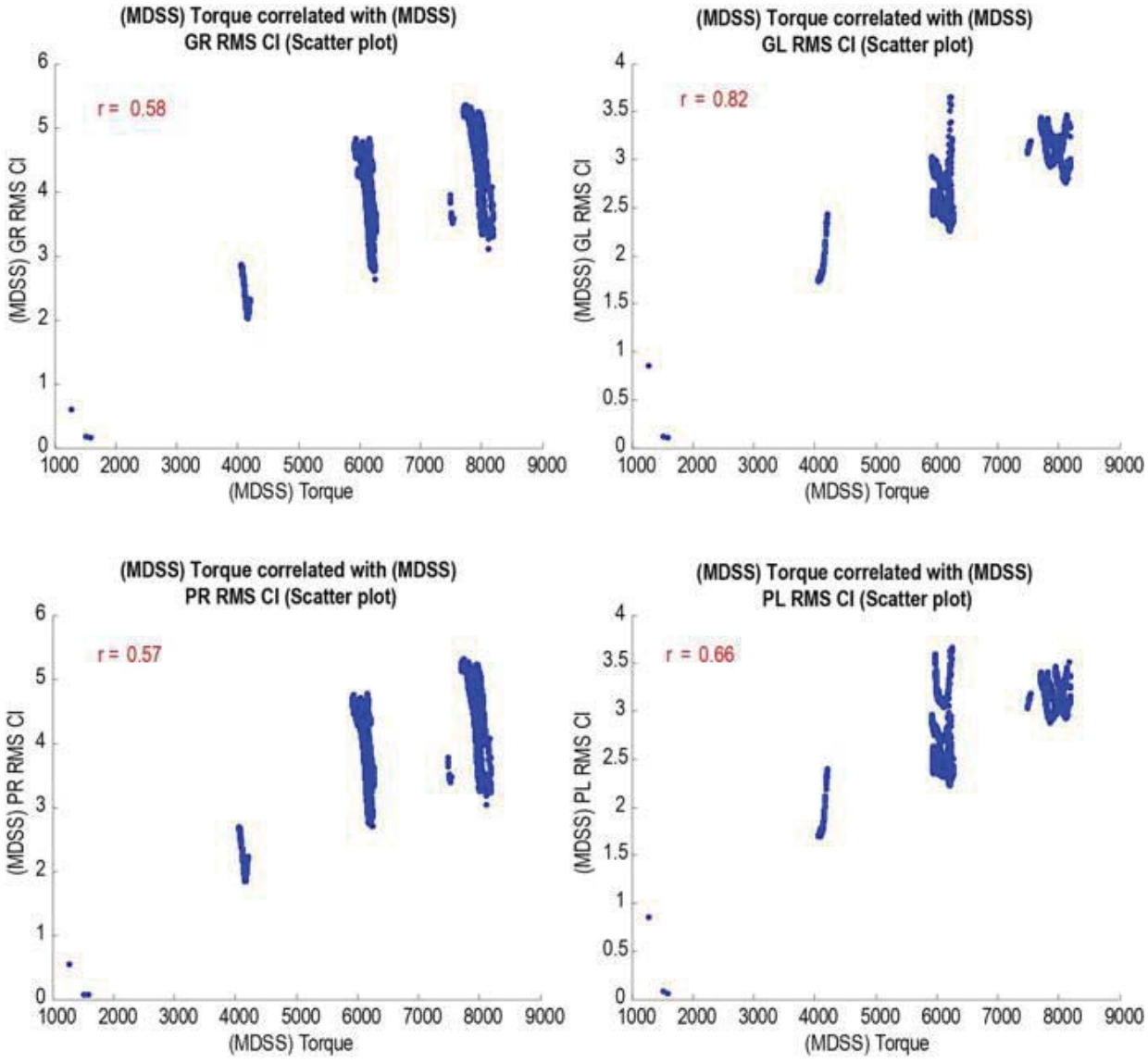

Figure E.1.8.—Compare Test L4545R5050 MDSS RMS to Torque.

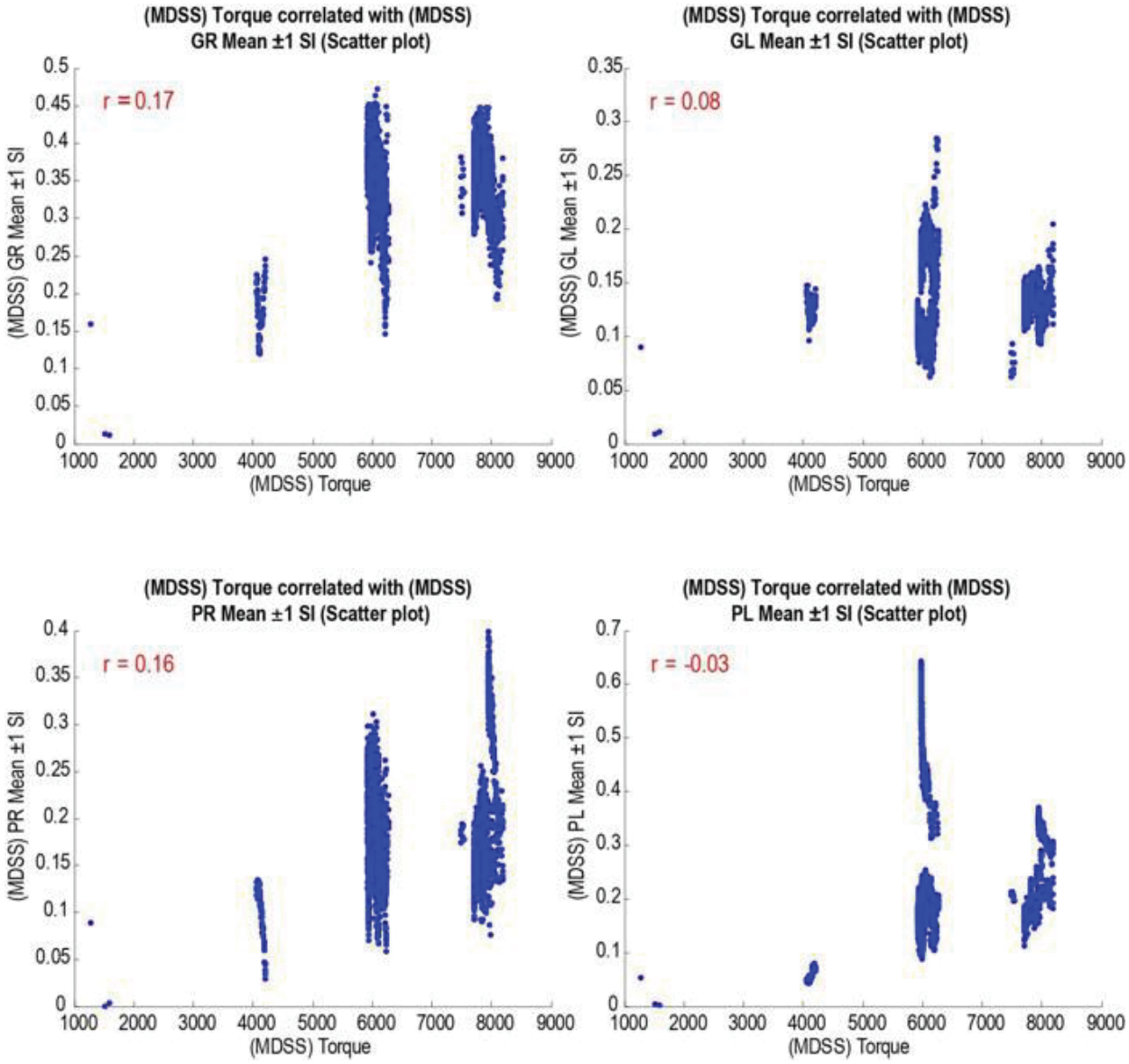

Figure E.1.9.—Compare Test L4545R5050 MDSS SI1 to Torque.

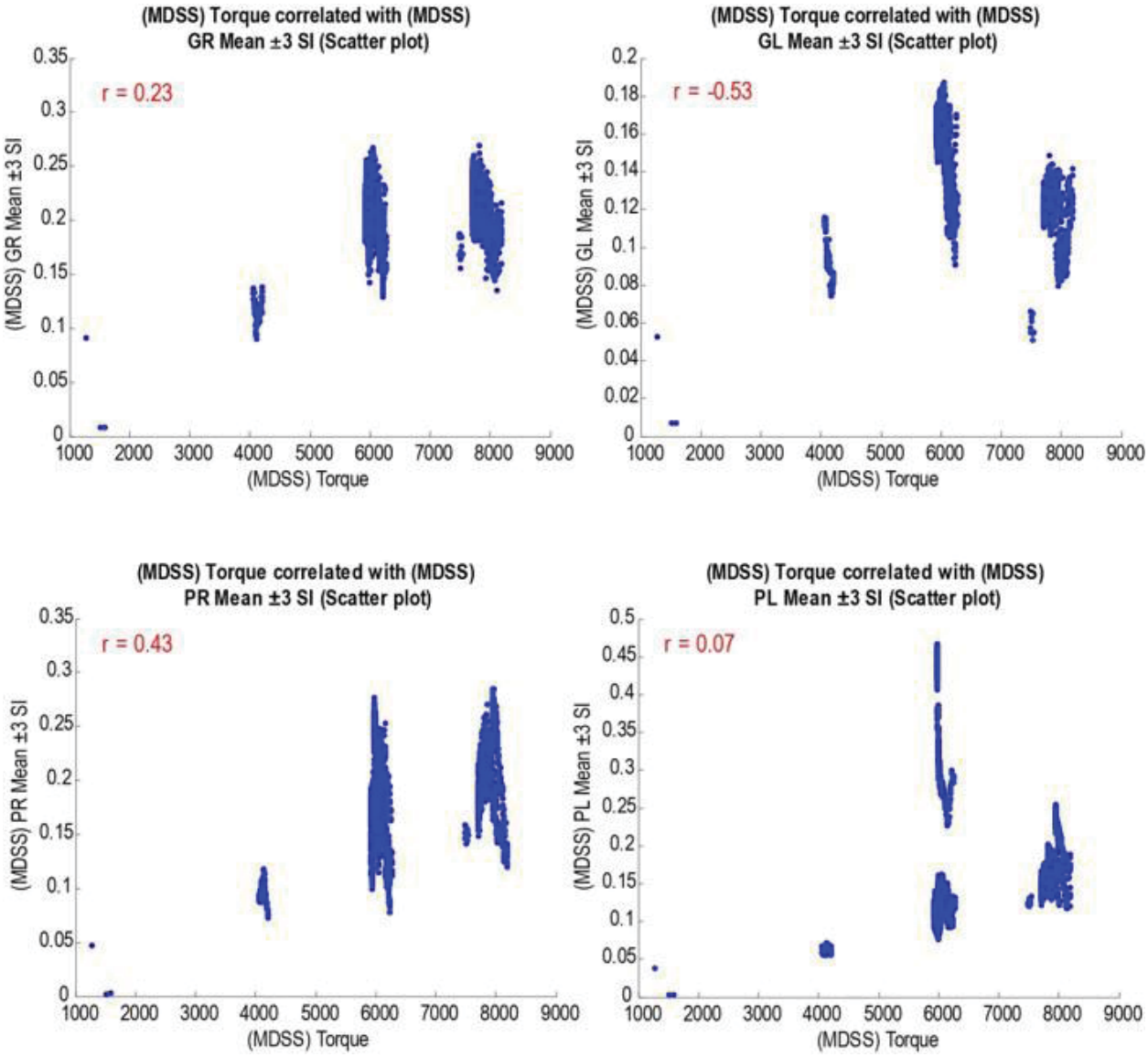

Figure E.1.10.—Compare Test L4545R5050 MDSS SI3 to Torque.

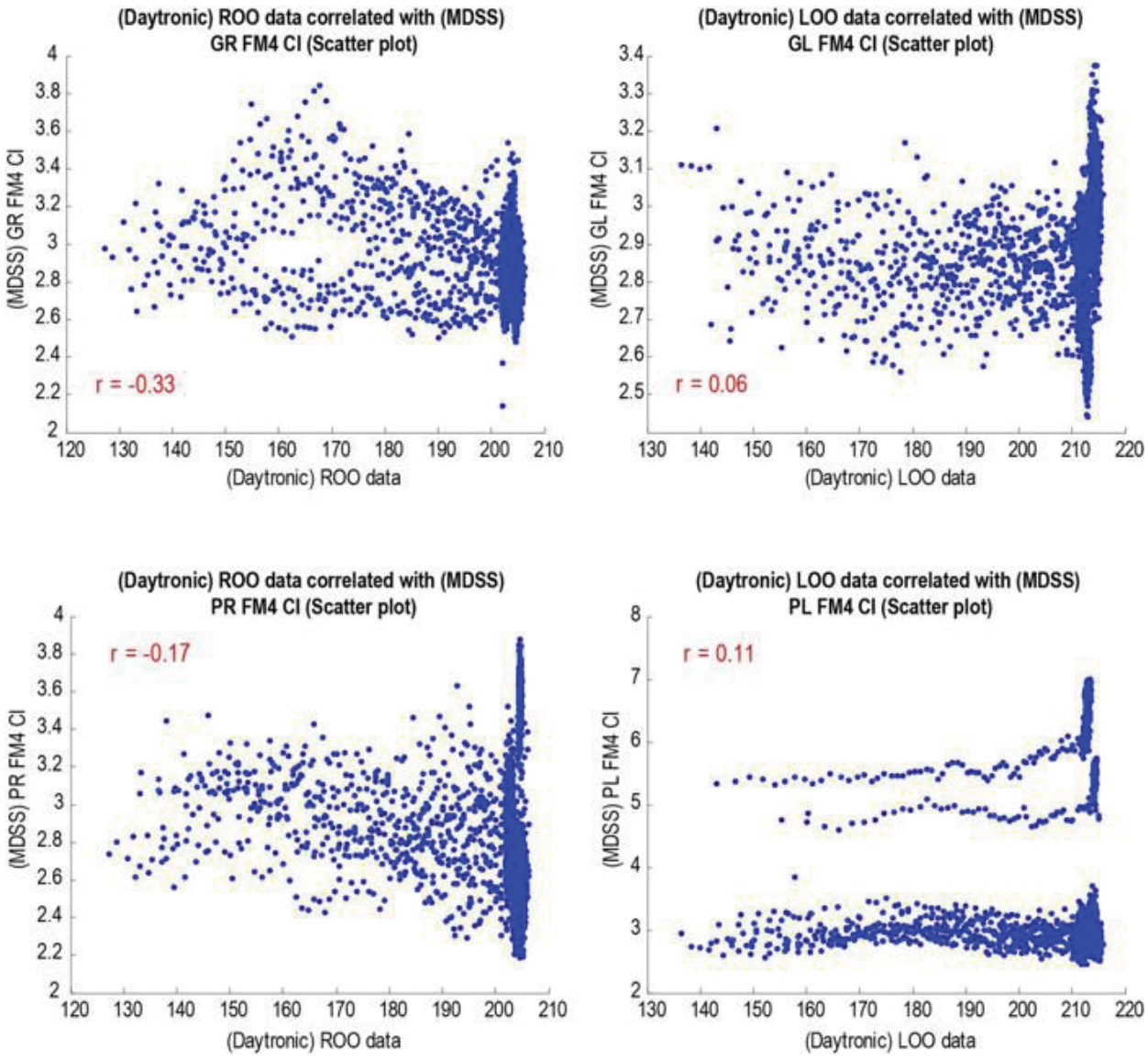

Figure E.1.11.—Compare Test L4545R5050 Outlet Oil Temperatures to FM4.

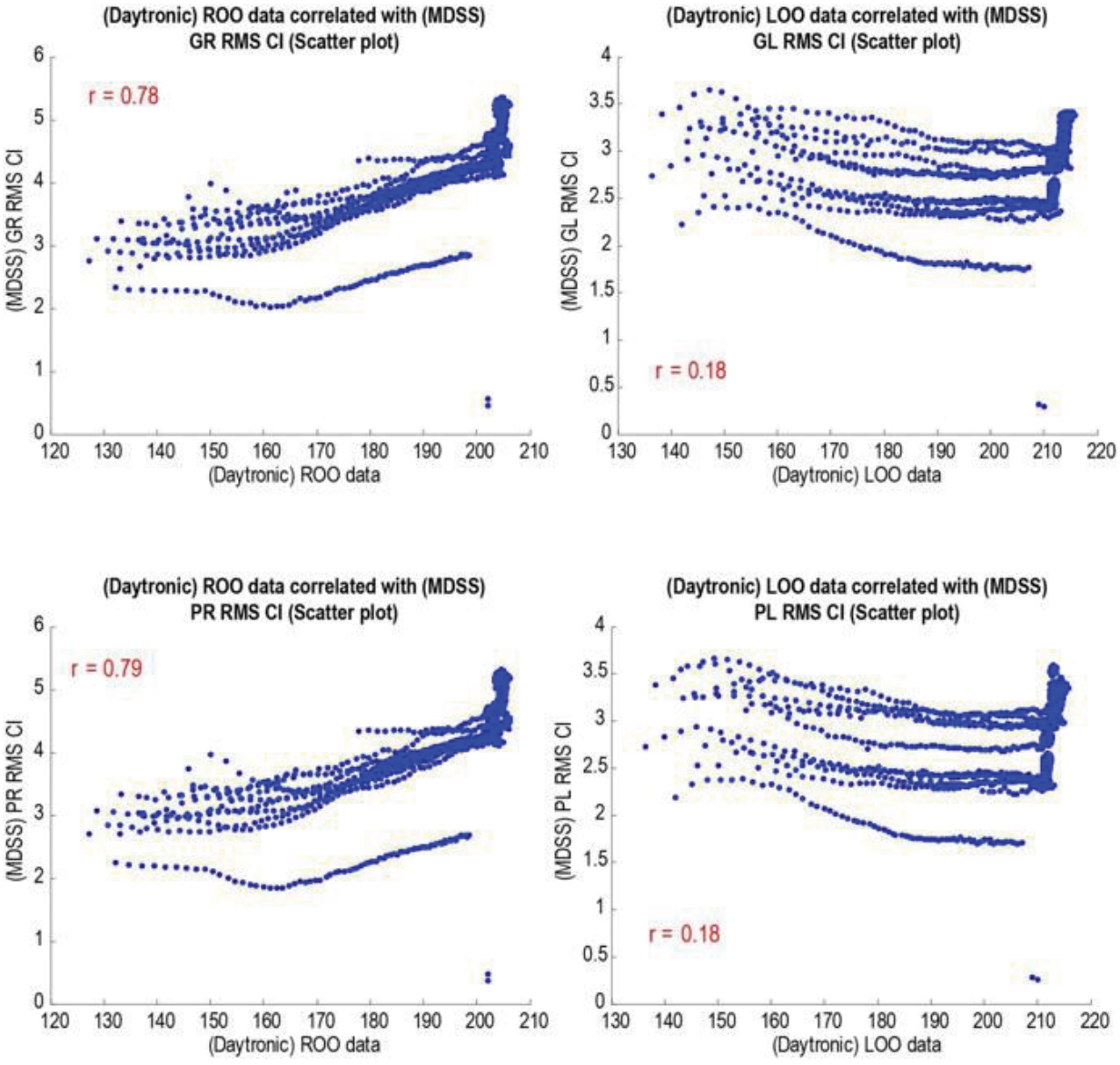

Figure E.1.12.—Compare Test L4545R5050 Outlet Oil Temperatures to RMS.

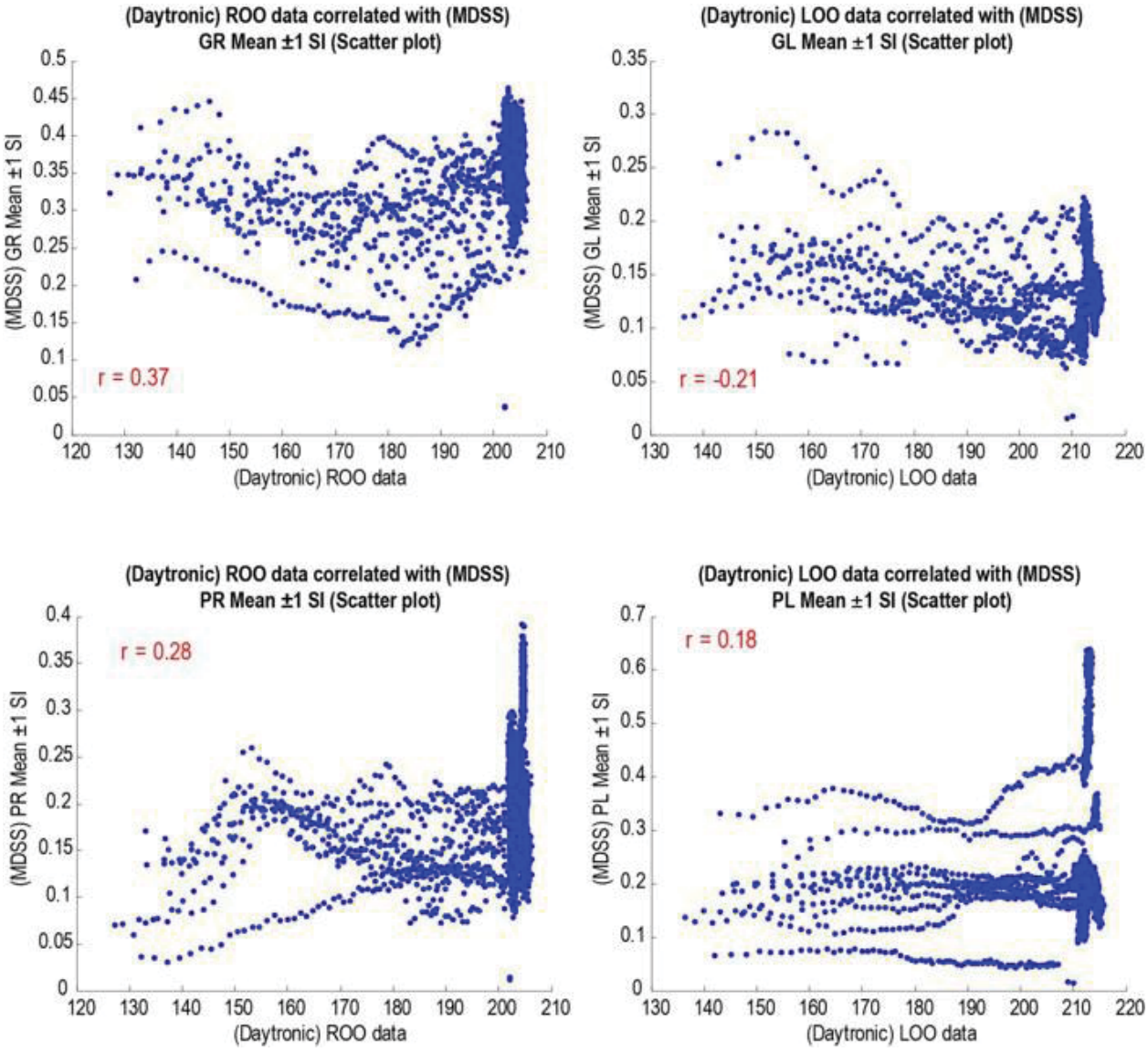

Figure E.1.13.—Compare Test L4545R5050 Outlet Oil Temperatures to SI1.

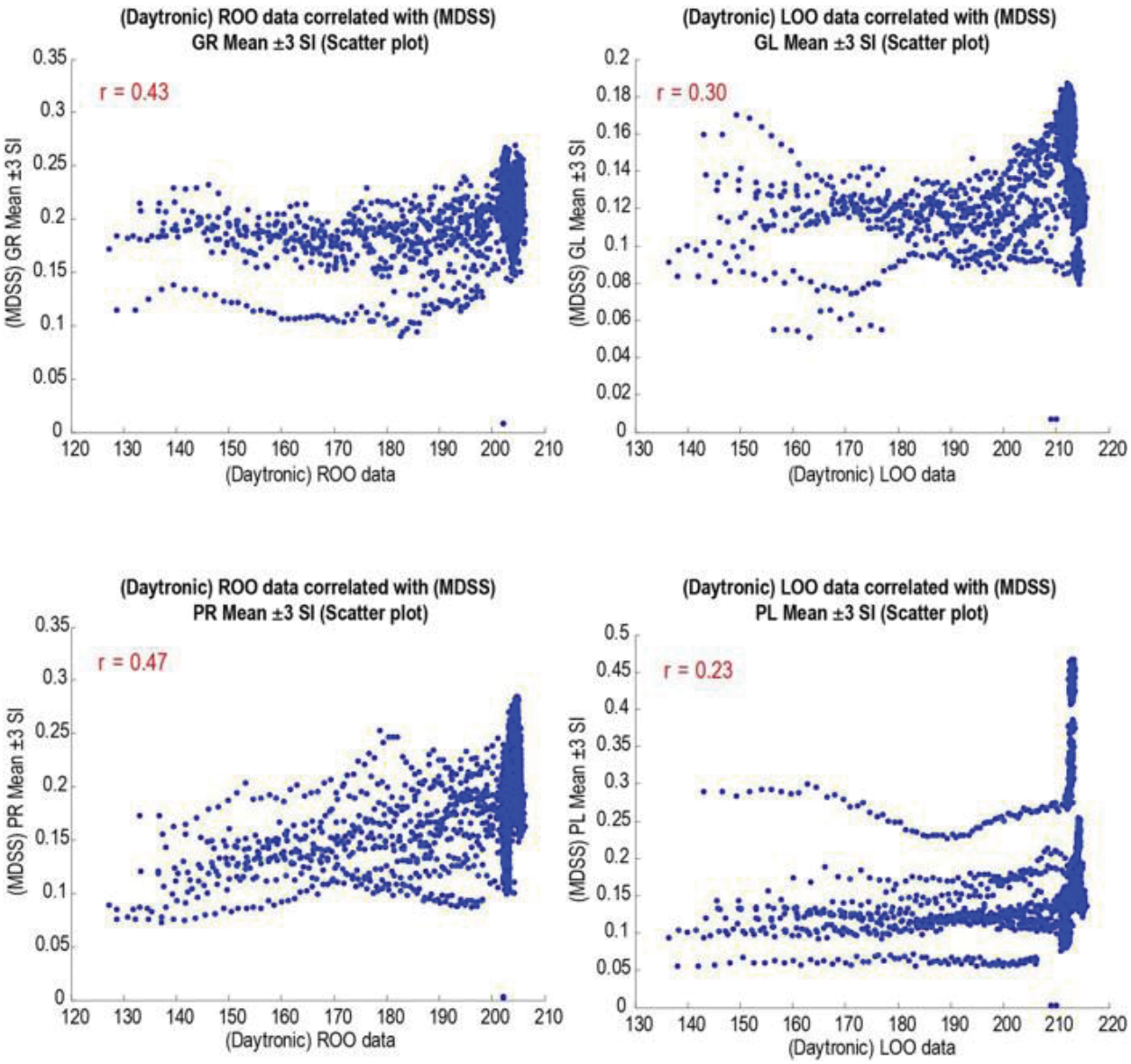

Figure E.1.14.—Compare Test L4545R5050 Outlet Oil Temperatures to SI3.

E.2 L3030R5050

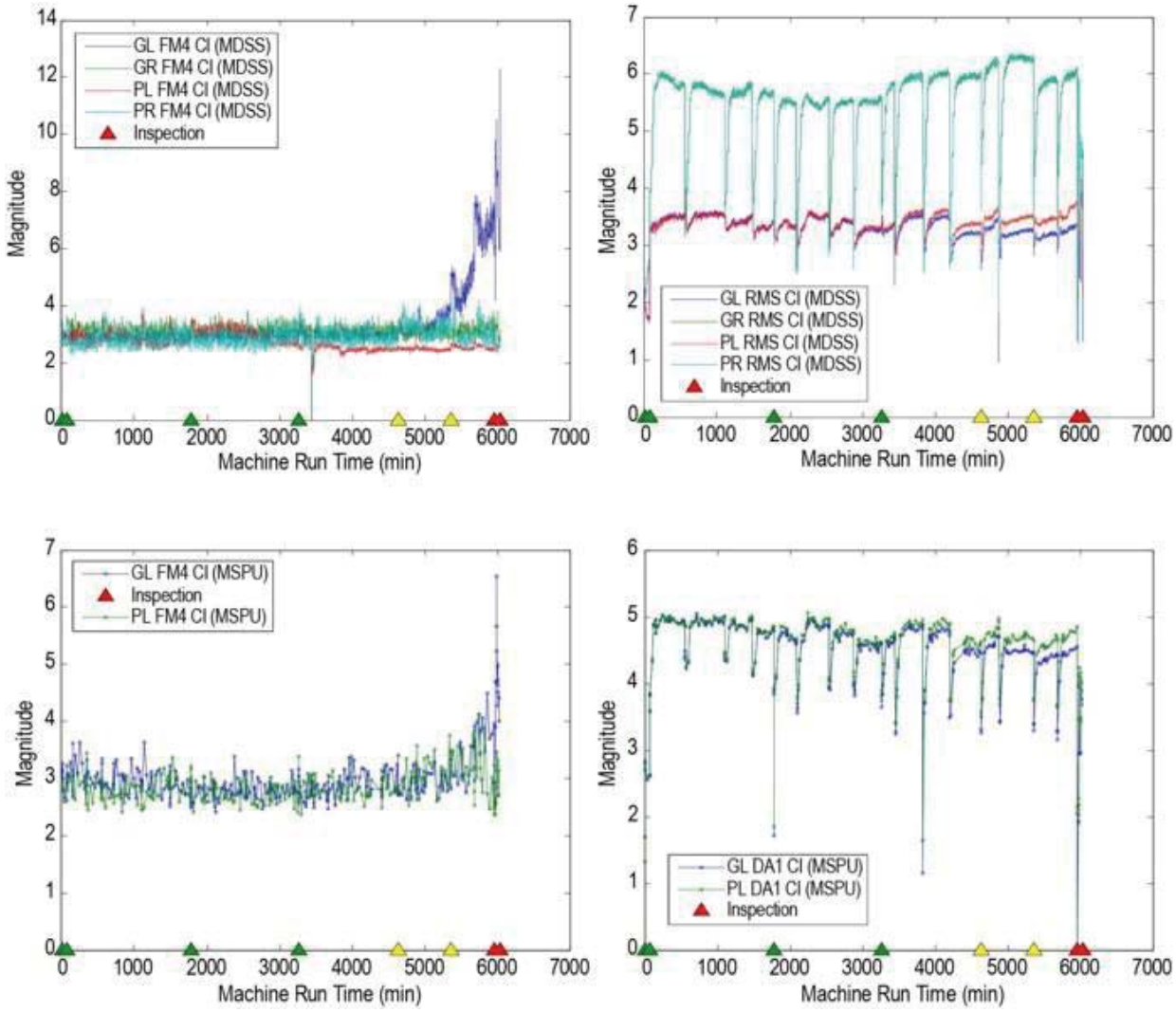

Figure E.2.1.—Compare Test L3030R5050 FM4 and RMS/DA1 for MDSS and MSPU.

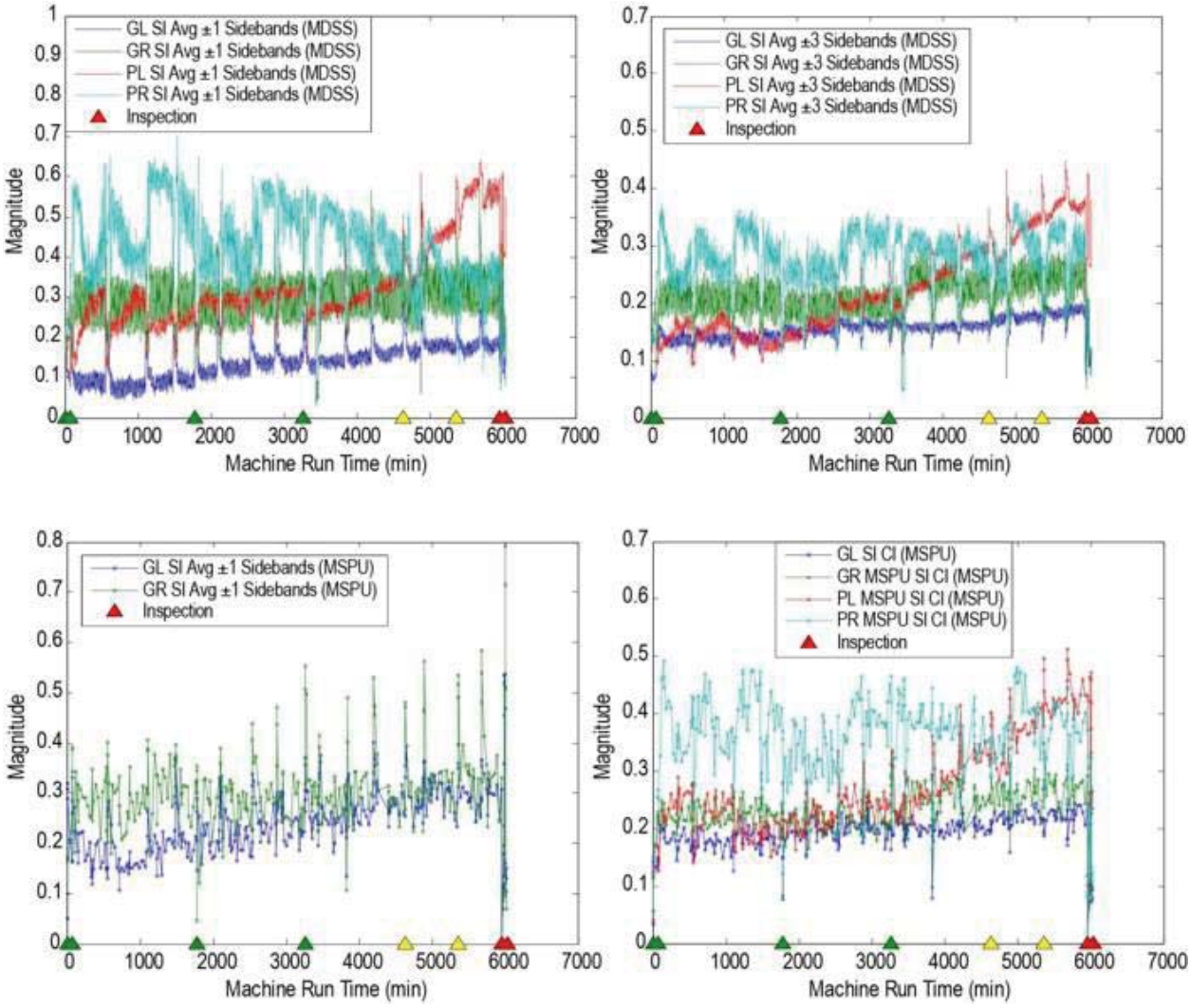

Figure E.2.2.—Compare Test L3030R5050 SI1 and SI3 for MDSS and MSPU.

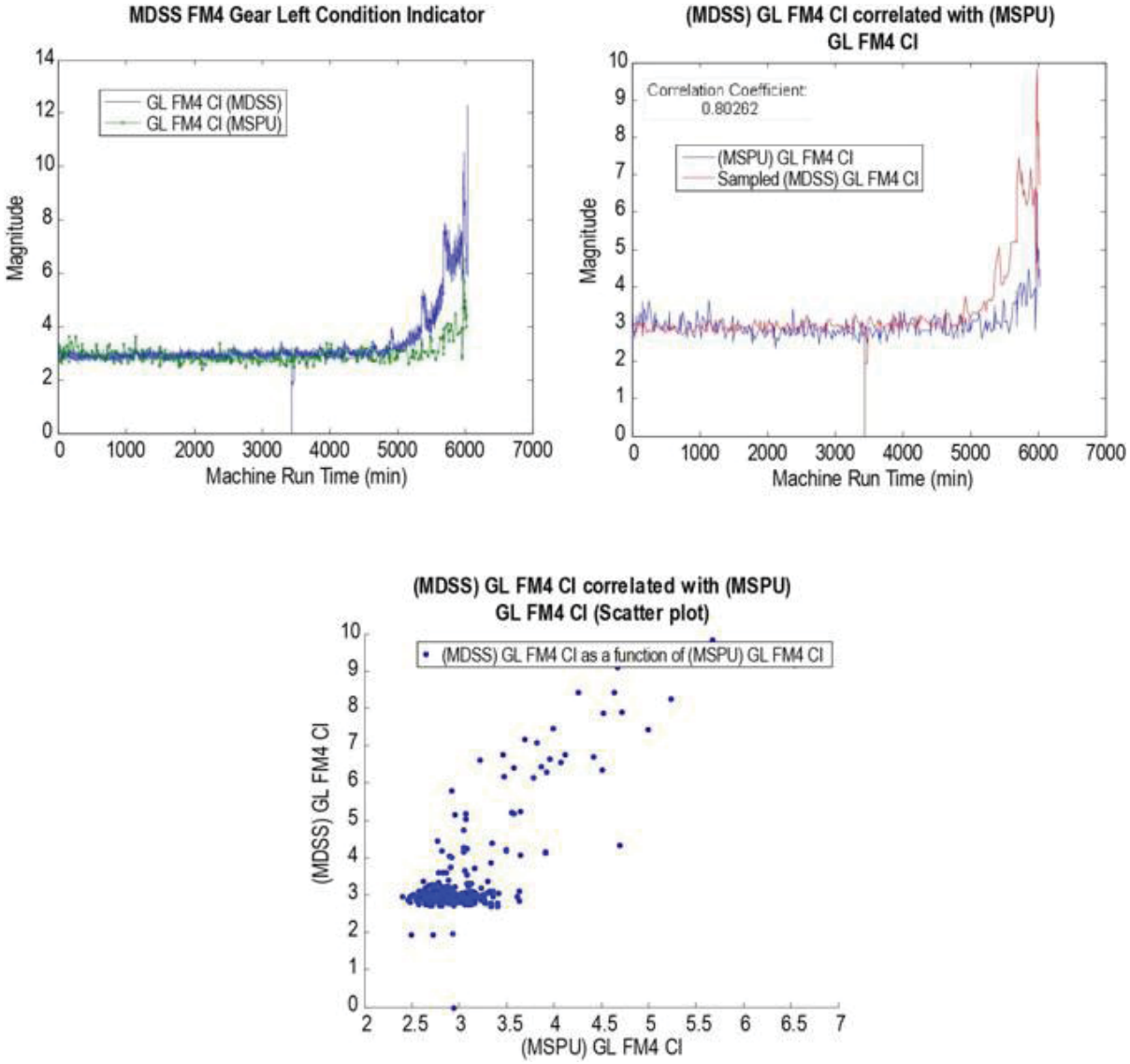

Figure E.2.3.—Compare Test L3030R5050 FM4 Nearest Time Correlation Methods.

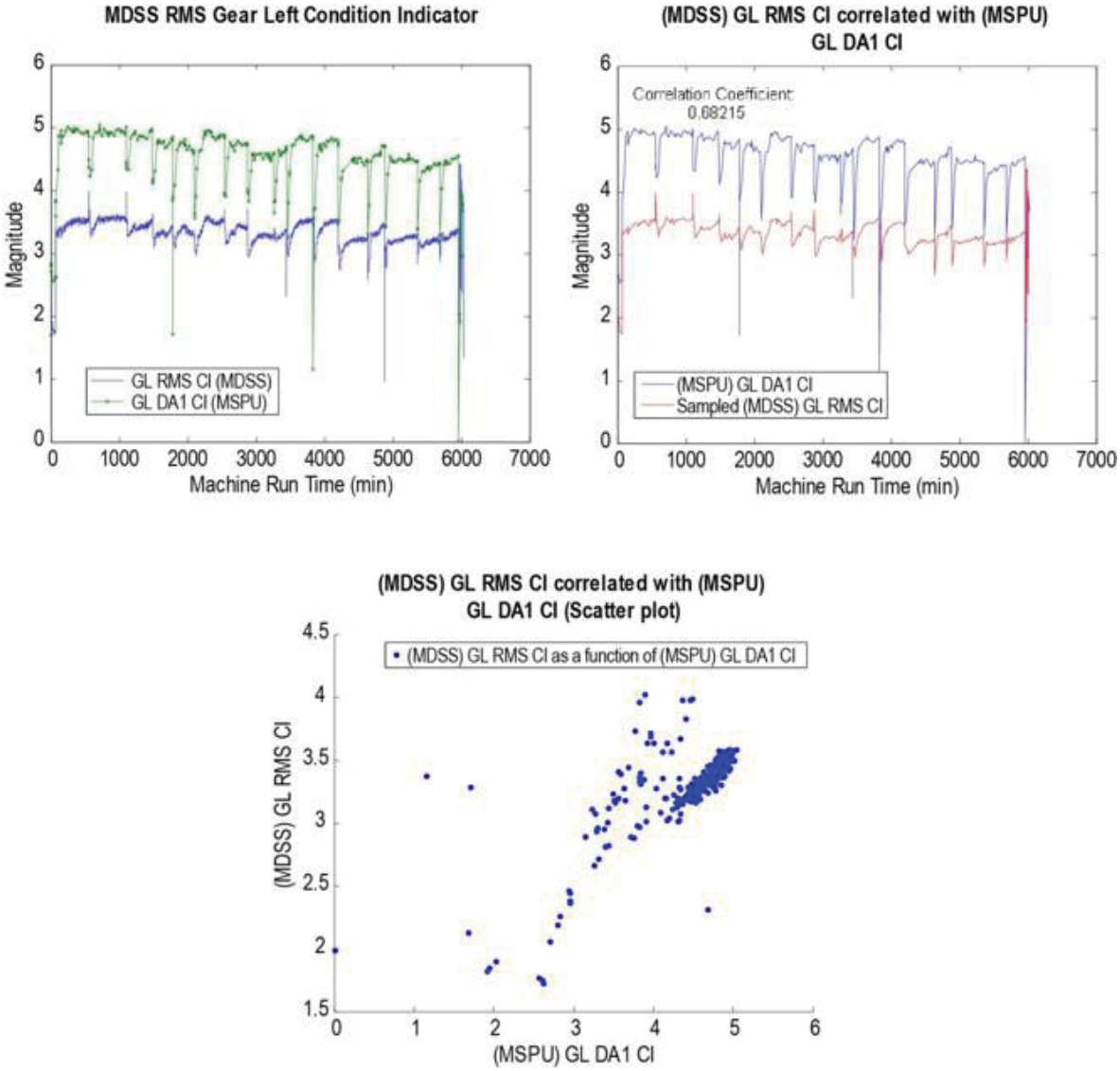

Figure E.2.4.—Compare Test L3030R5050 RMS Nearest Time Correlation Methods.

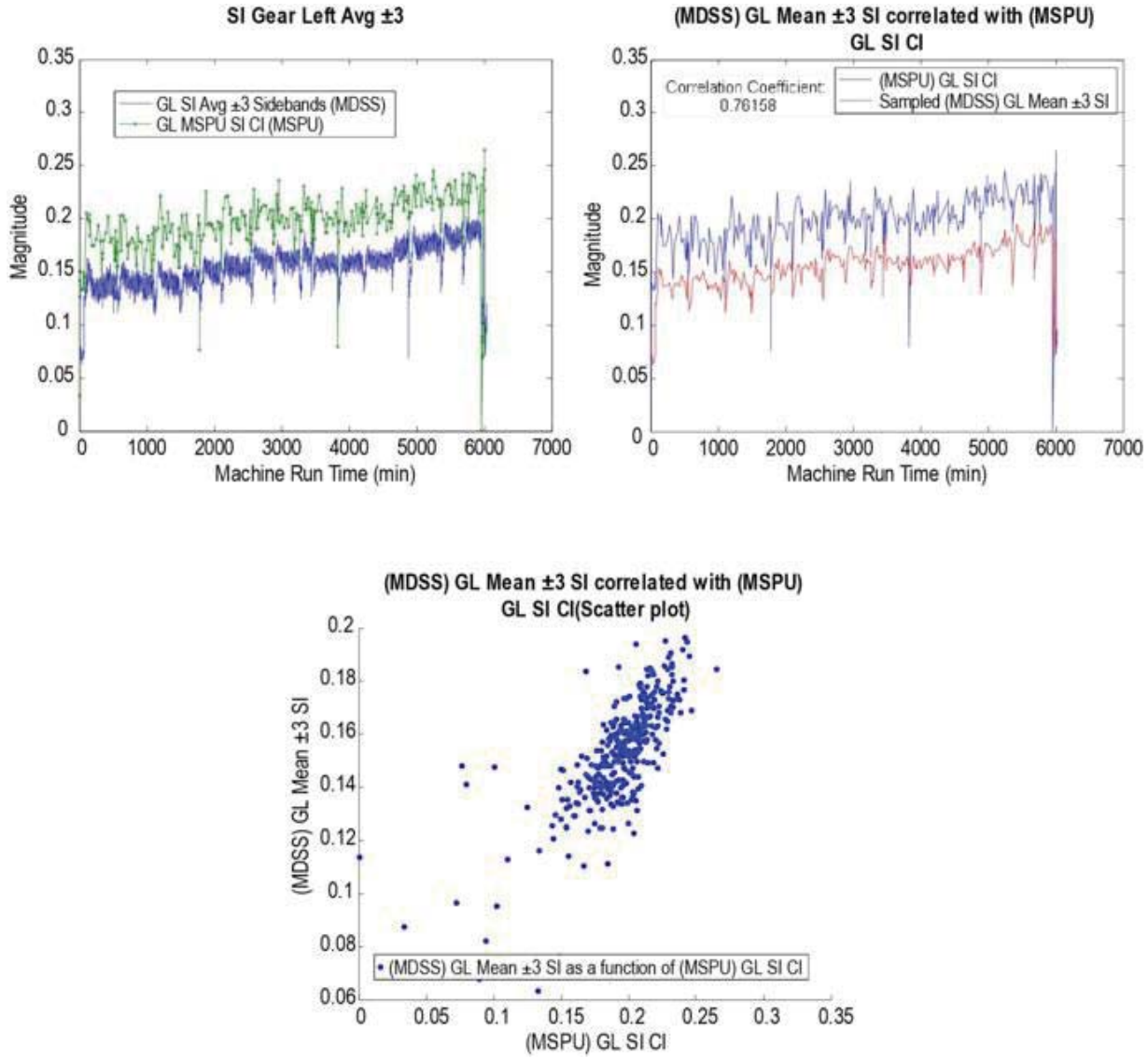

Figure E.2.5.—Compare Test L3030R5050 SI3 and SI Nearest Time Correlation Methods.

E.3 L2020R5050

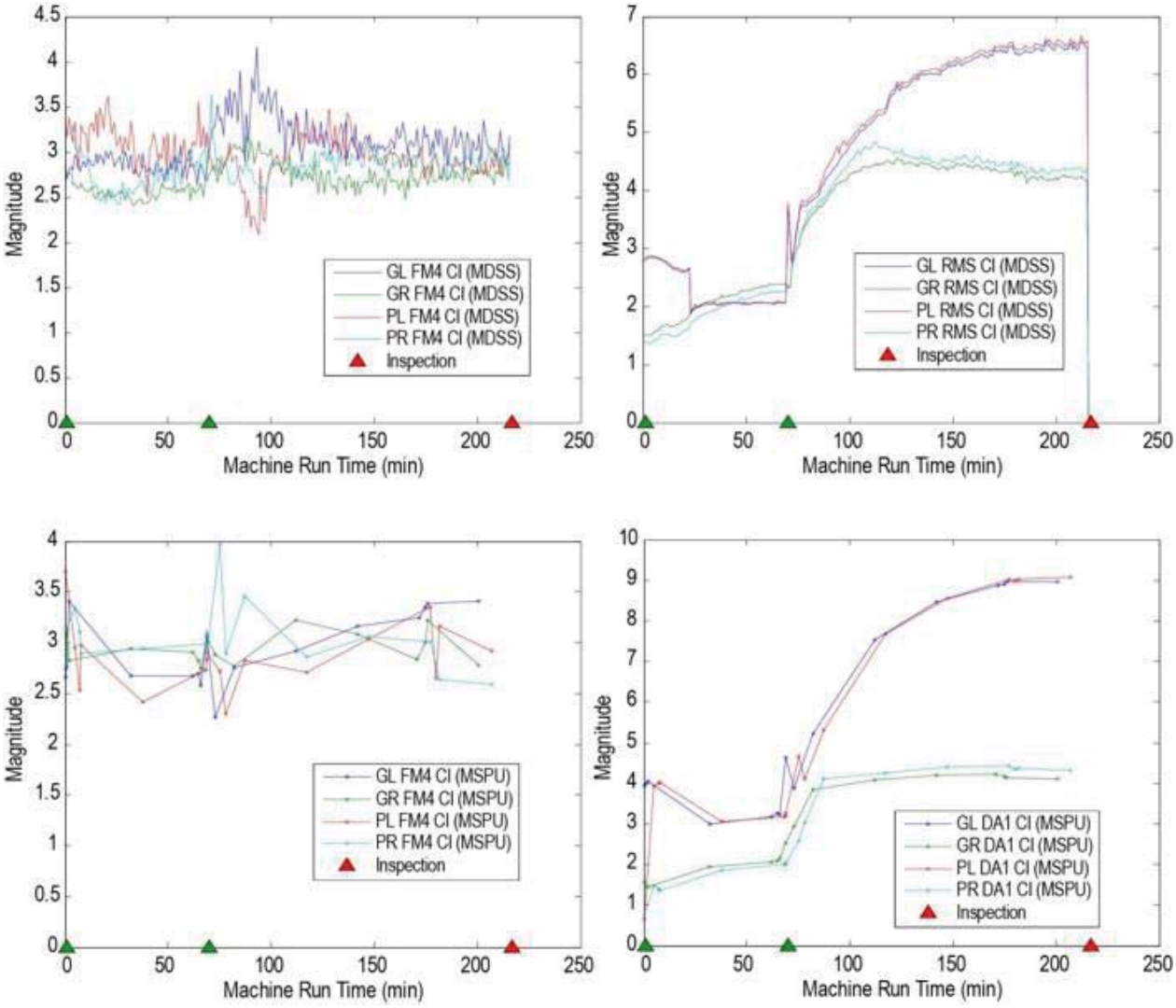

Figure E.3.1.—Compare Test L2020R5050 FM4 and RMS/DA1 for MDSS and MSPU.

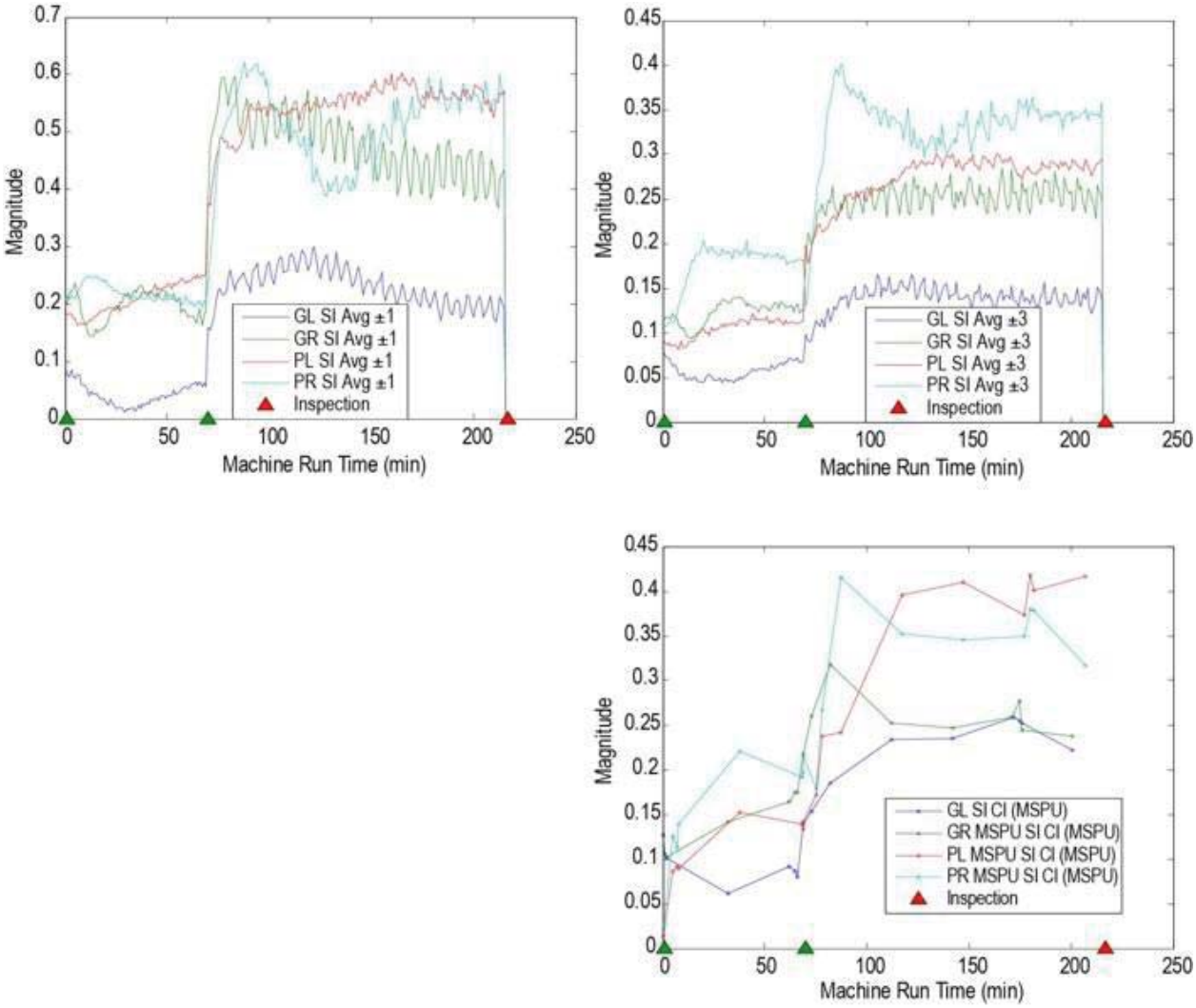

Figure E.3.2.—Compare Test L2020R5050 FM4 and RMS/DA1 for MDSS and MSPU.

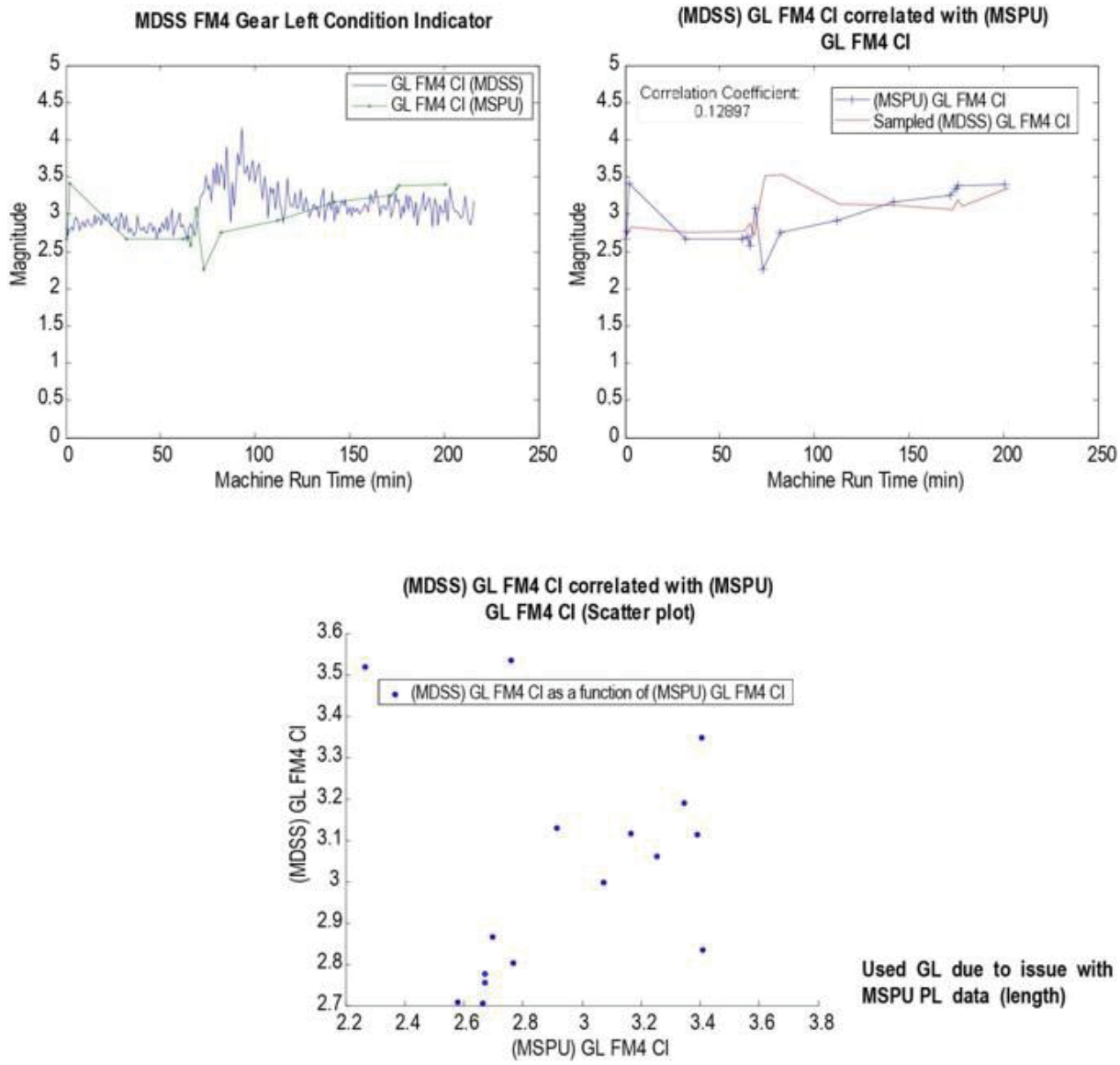

Figure E.3.3.—Compare Test L2020R5050 FM4 Nearest Time Correlation Methods.

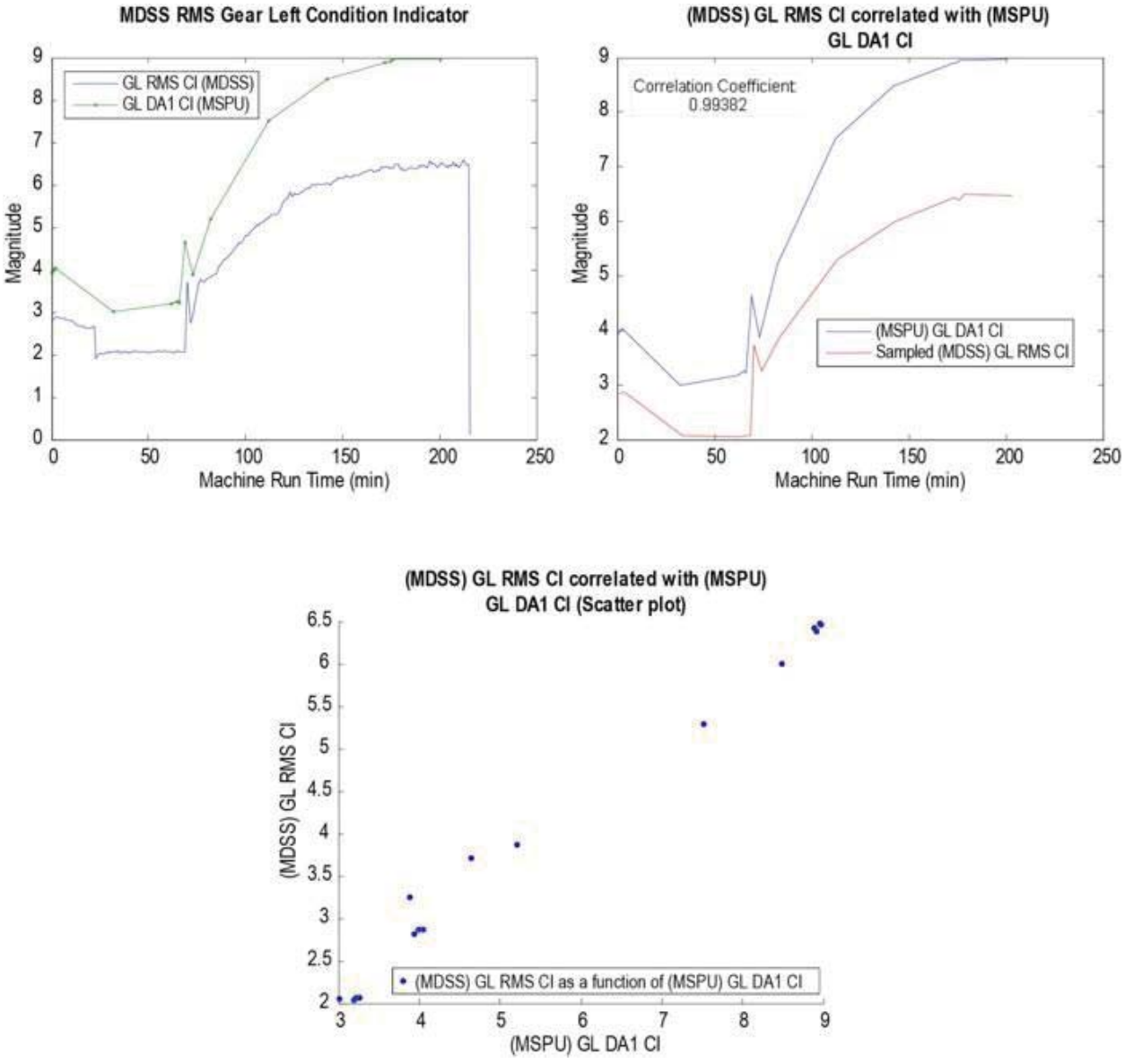

Figure E.3.4.—Compare Test L2020R5050 RMS Nearest Time Correlation Methods.

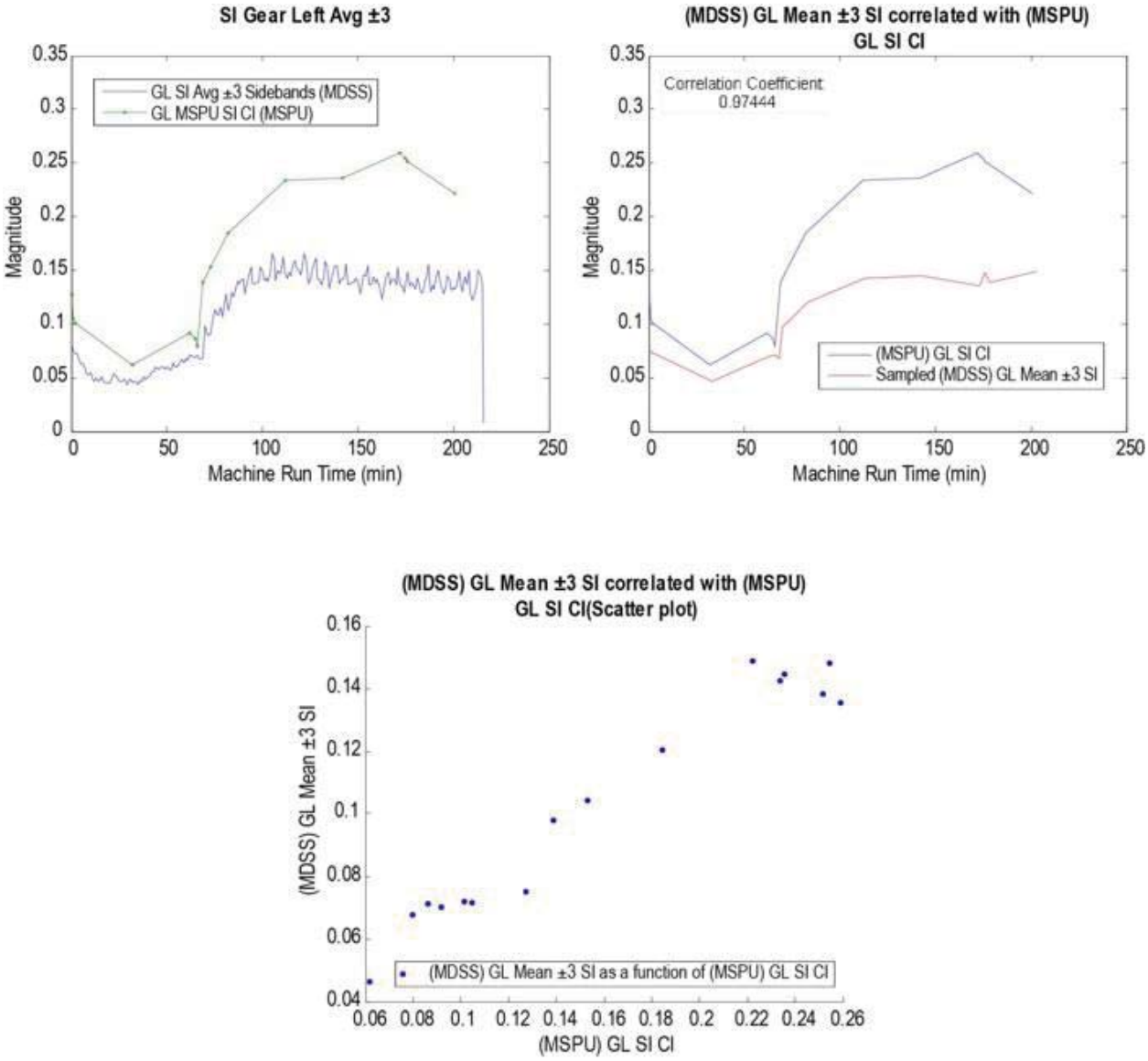

Figure E.3.5.—Compare Test L2020R5050 SI3 Nearest Time Correlation Methods.

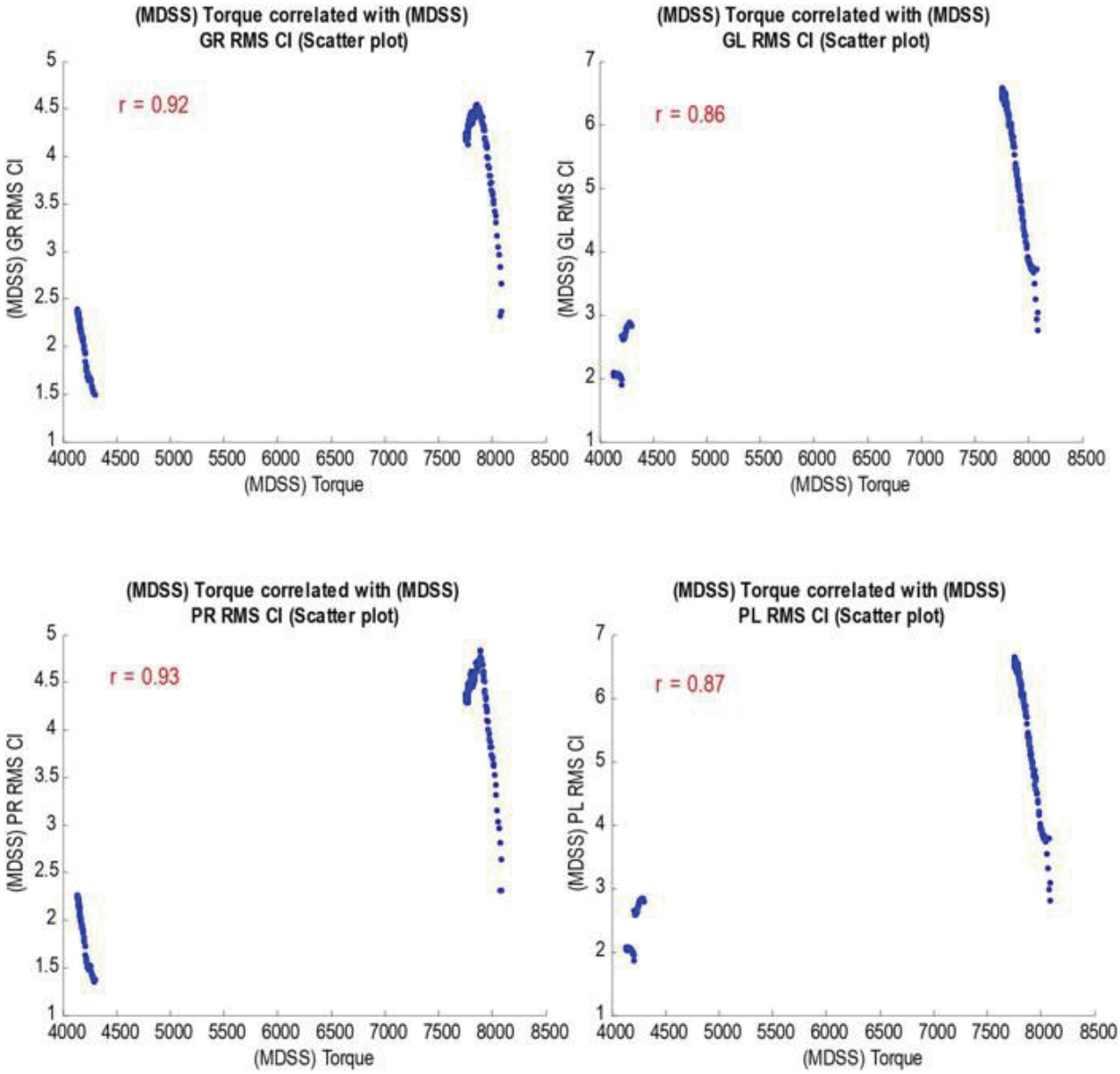

Figure E.3.6.—Compare Test L2020R5050 MDSS RMS to Torque.

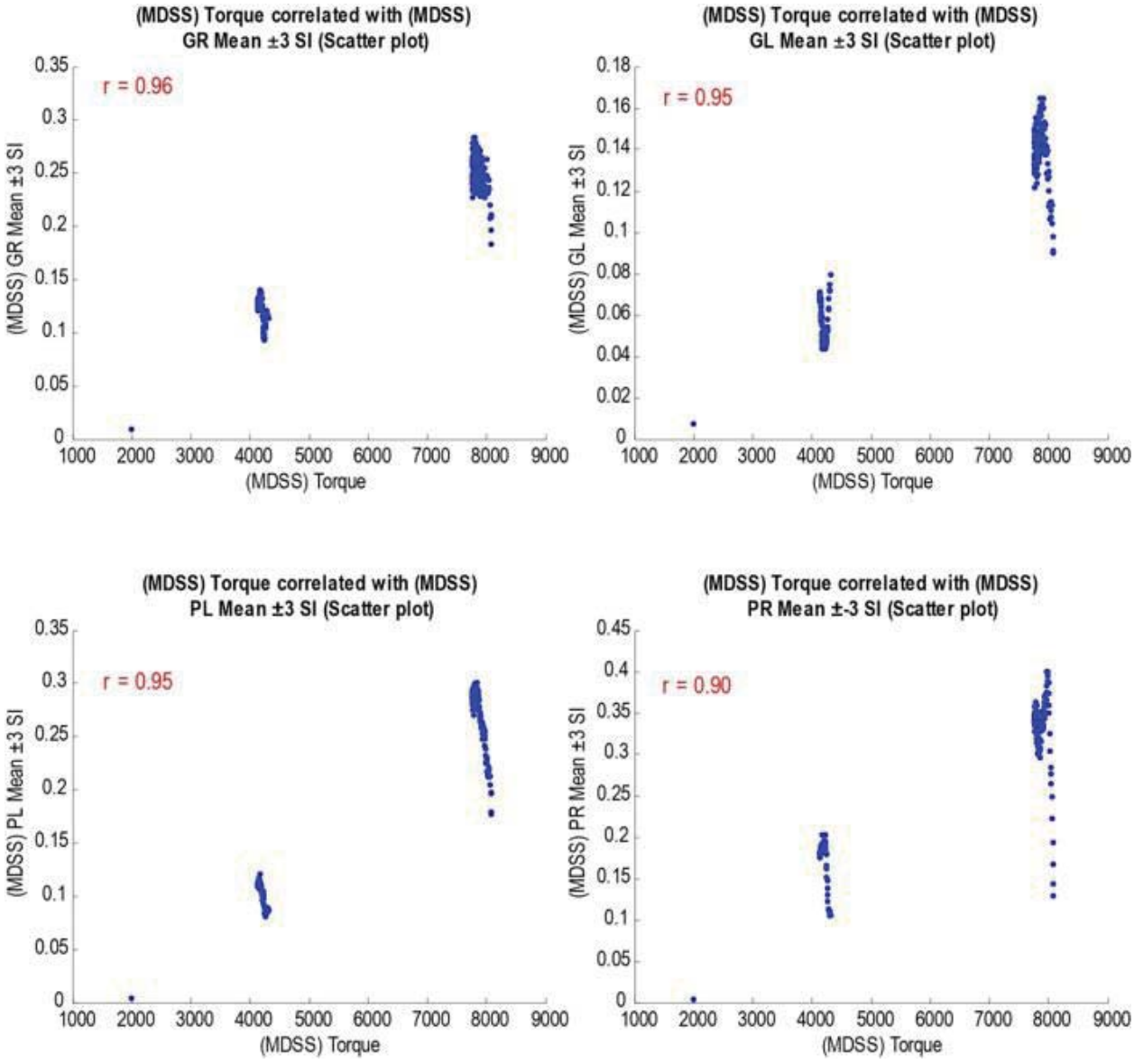

Figure E.3.7.—Compare Test L2020R5050 MDSS SI3 to Torque.

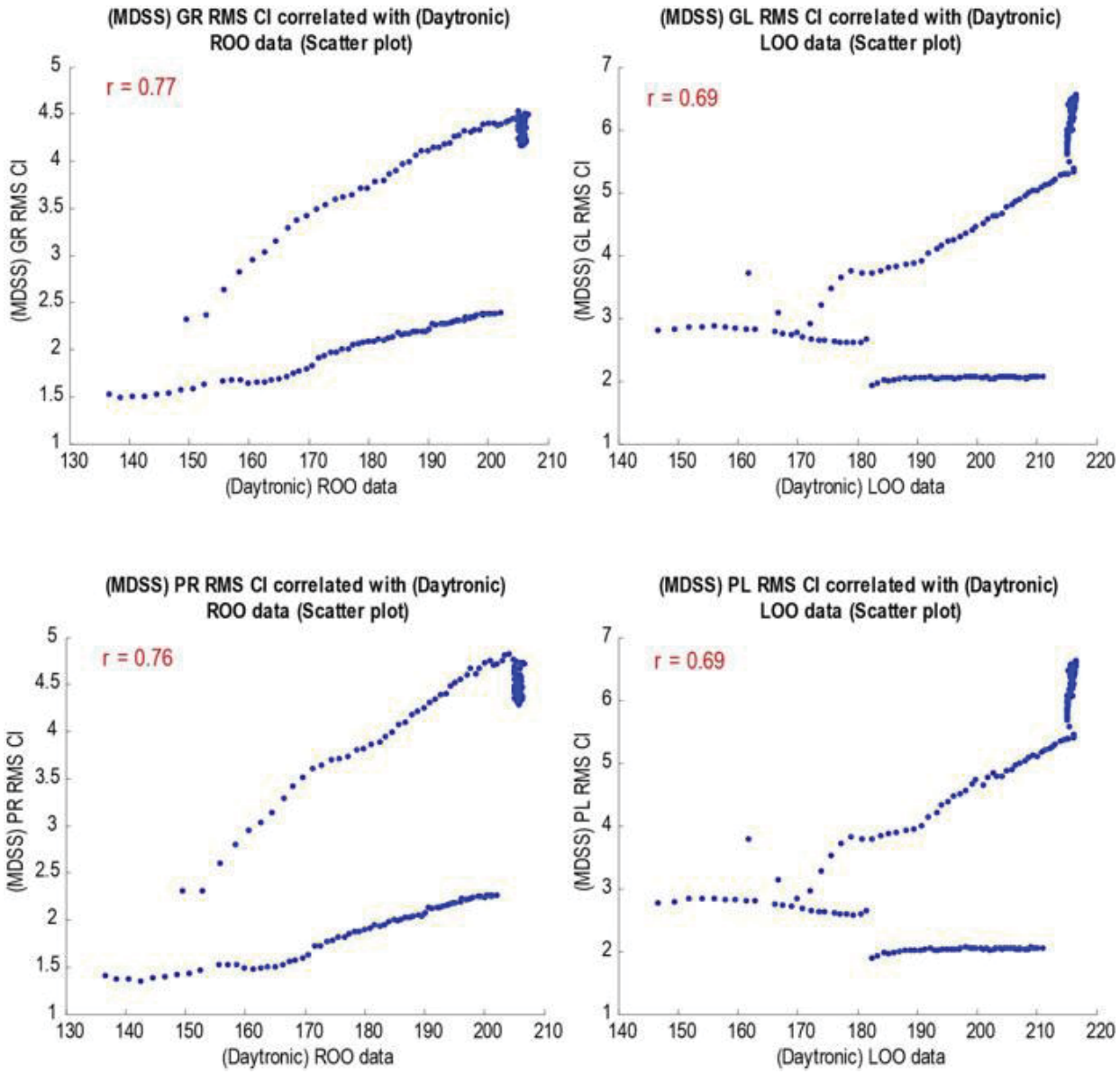

Figure E.3.8.—Compare Test L2020R5050 Outlet Oil Temperatures to RMS.

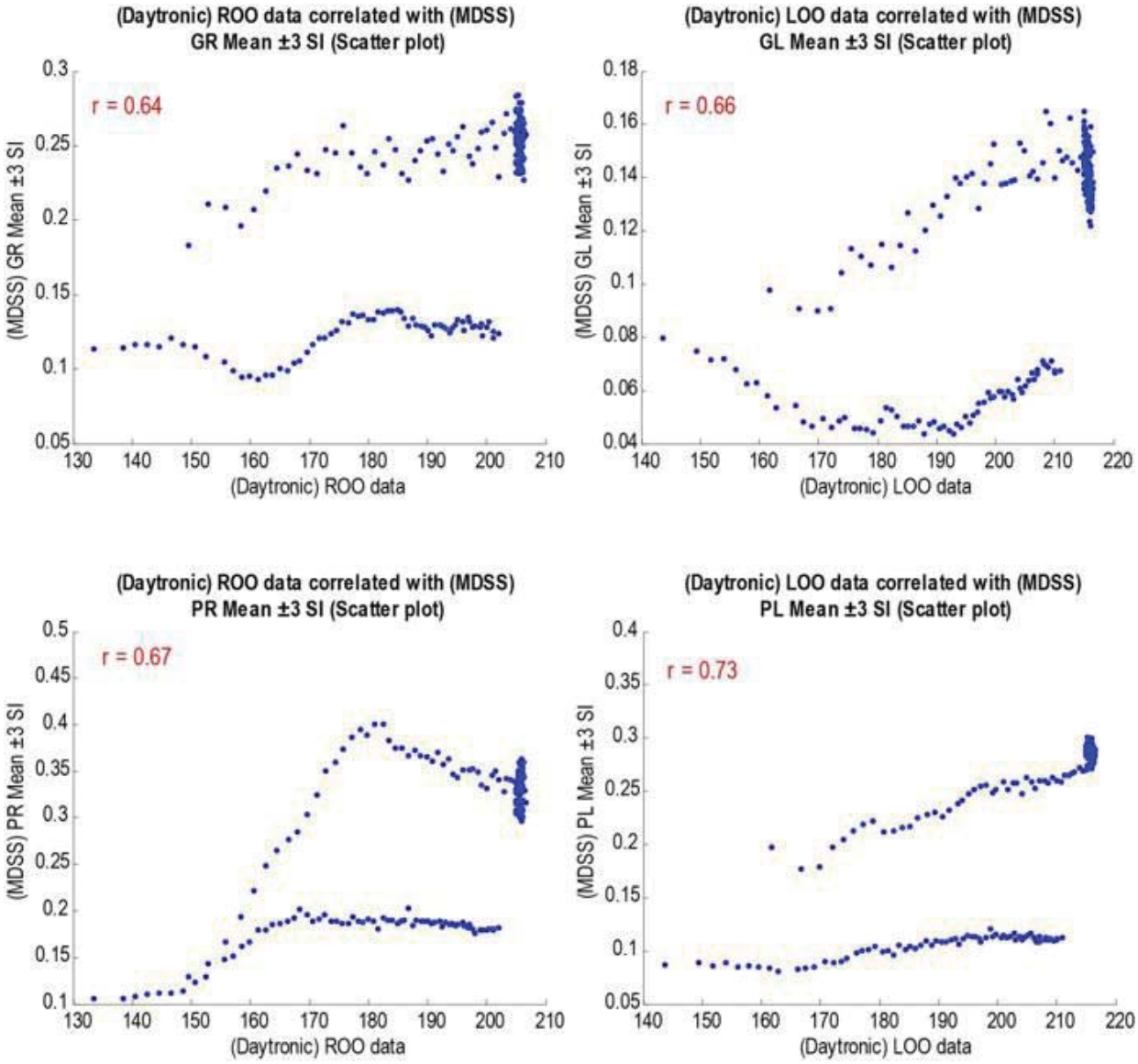

Figure E.3.9.—Compare Test L2020R5050 Outlet Oil Temperatures to SI3.

E.4 L3535R5050

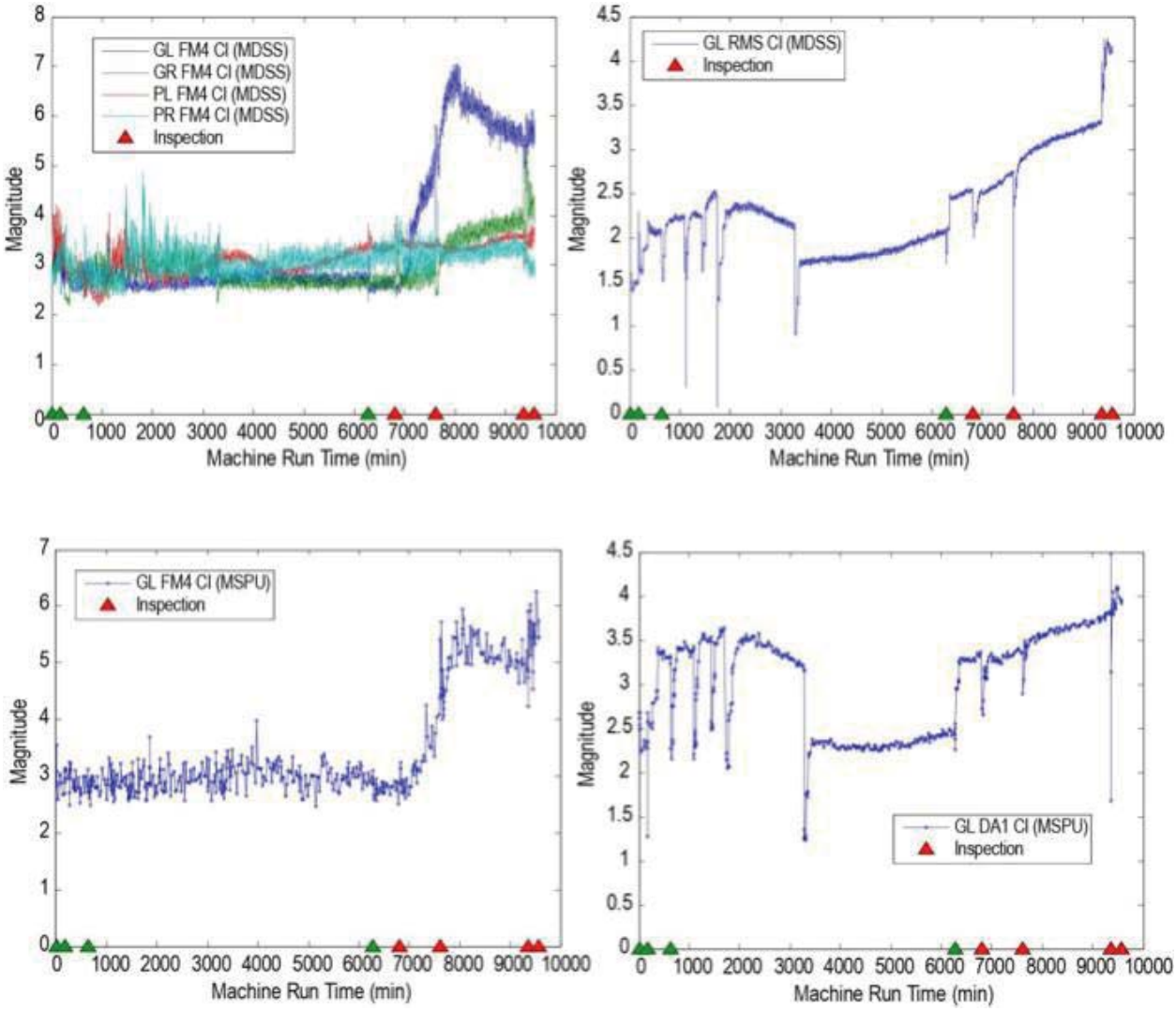

Figure E.4.1.—Compare Test L3535R5050 FM4 and RMS/DA1 for MDSS and MSPU.

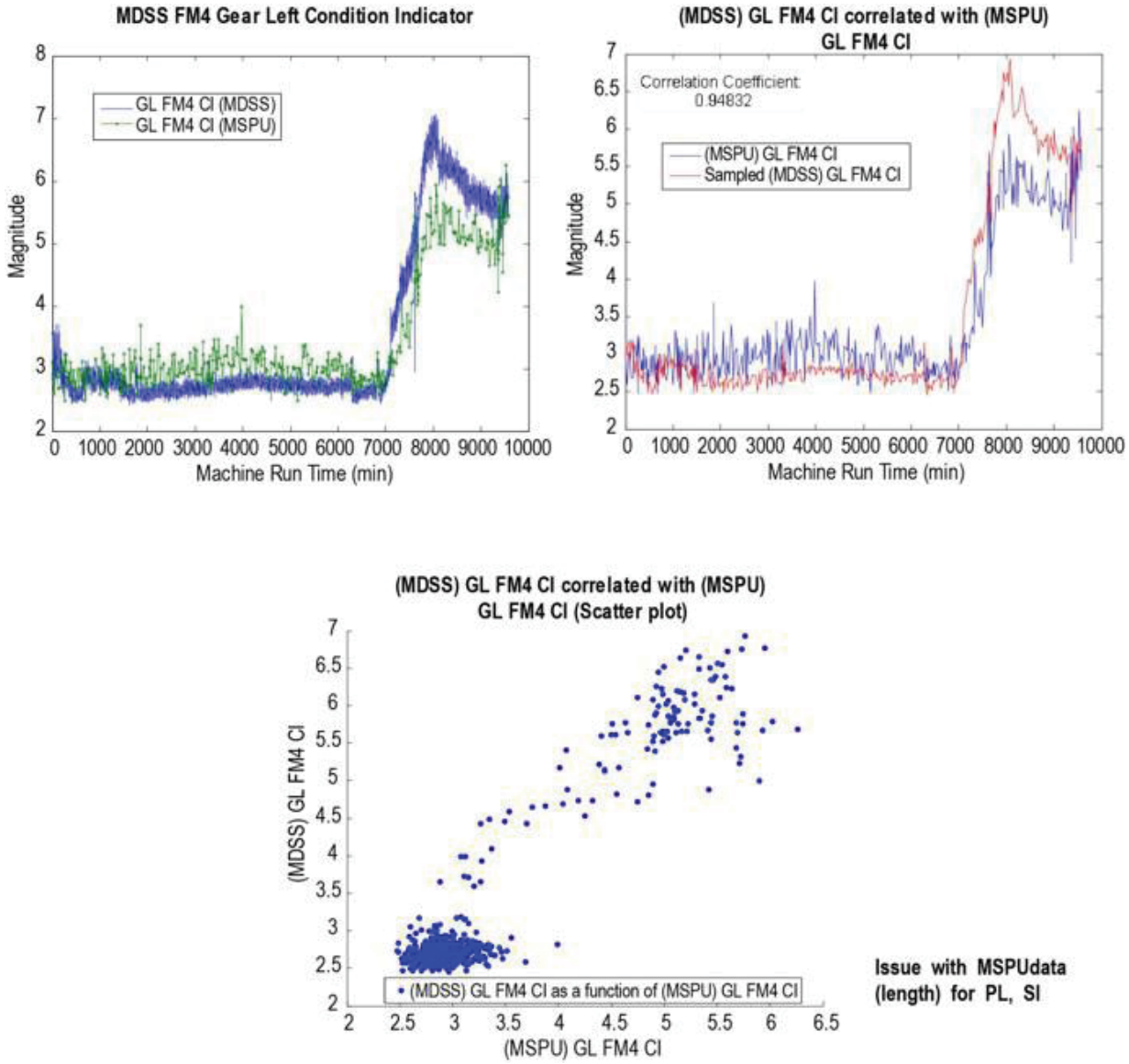

Figure E.4.2.—Compare Test L3535R5050 FM4 Nearest Time Correlation Methods.

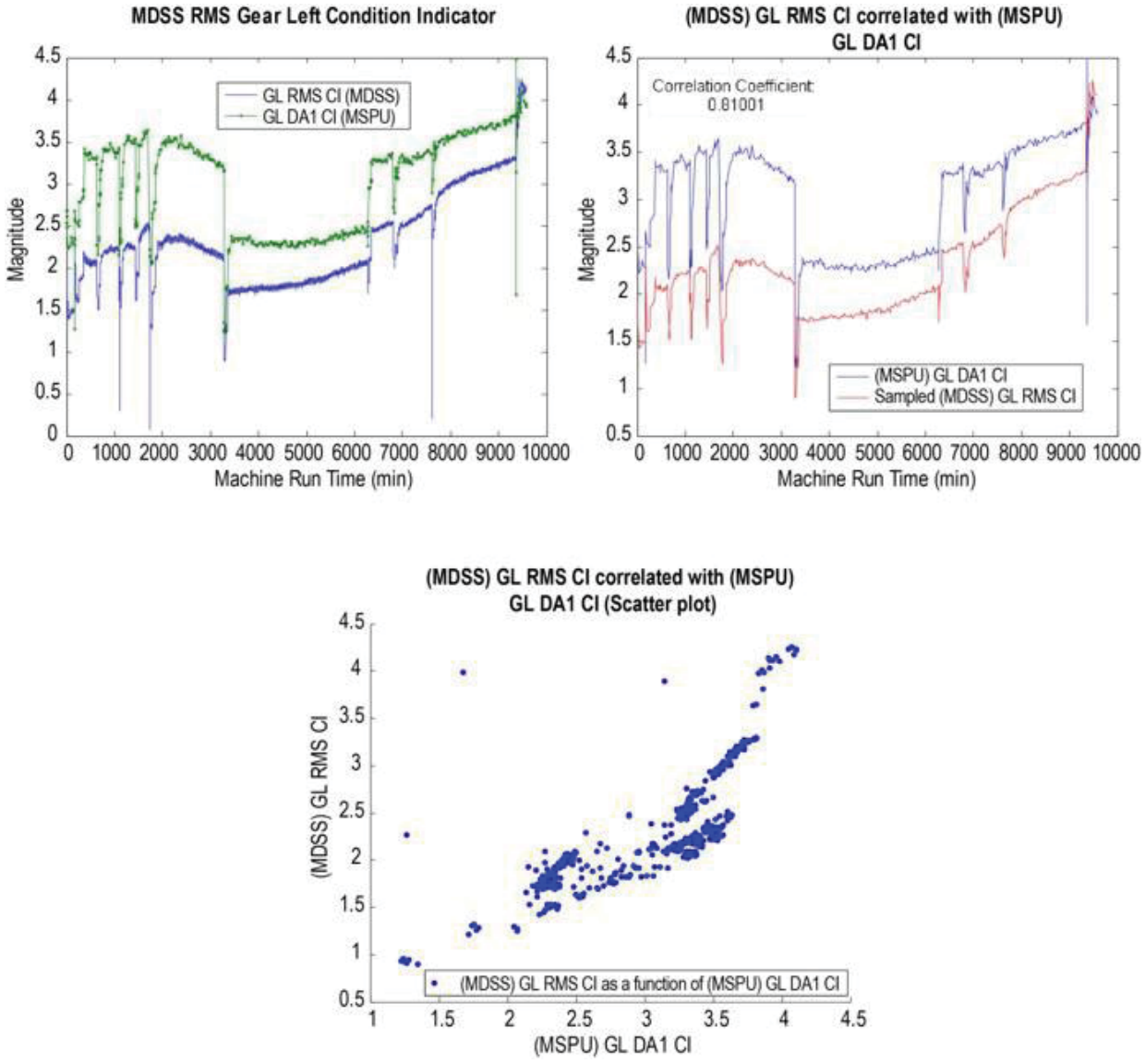

Figure E.4.3.—Compare Test L3535R5050 FM4 Nearest Time Correlation Methods.

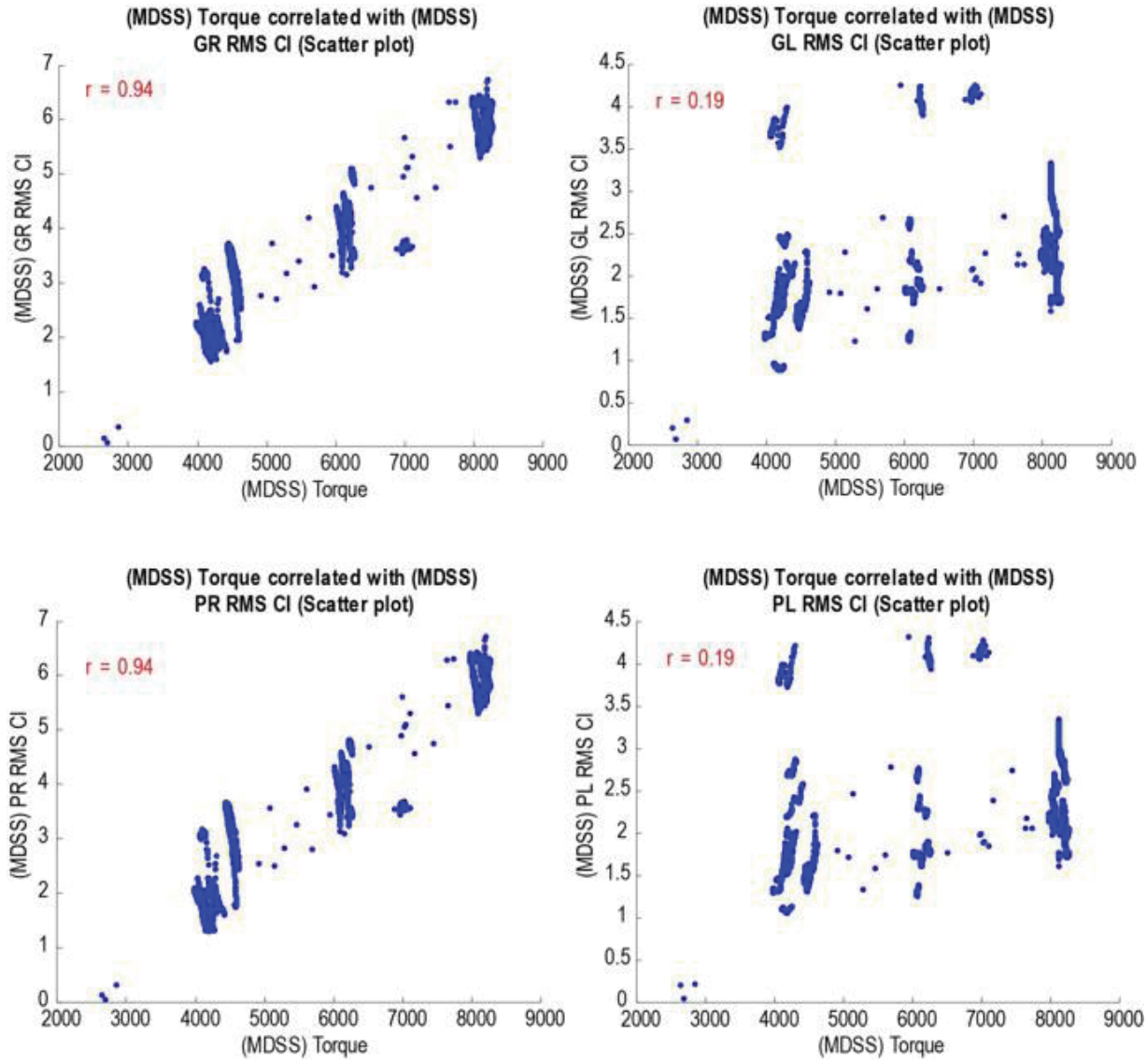

Figure E.4.4.—Compare Test L35355050 MDSS RMS to Torque.

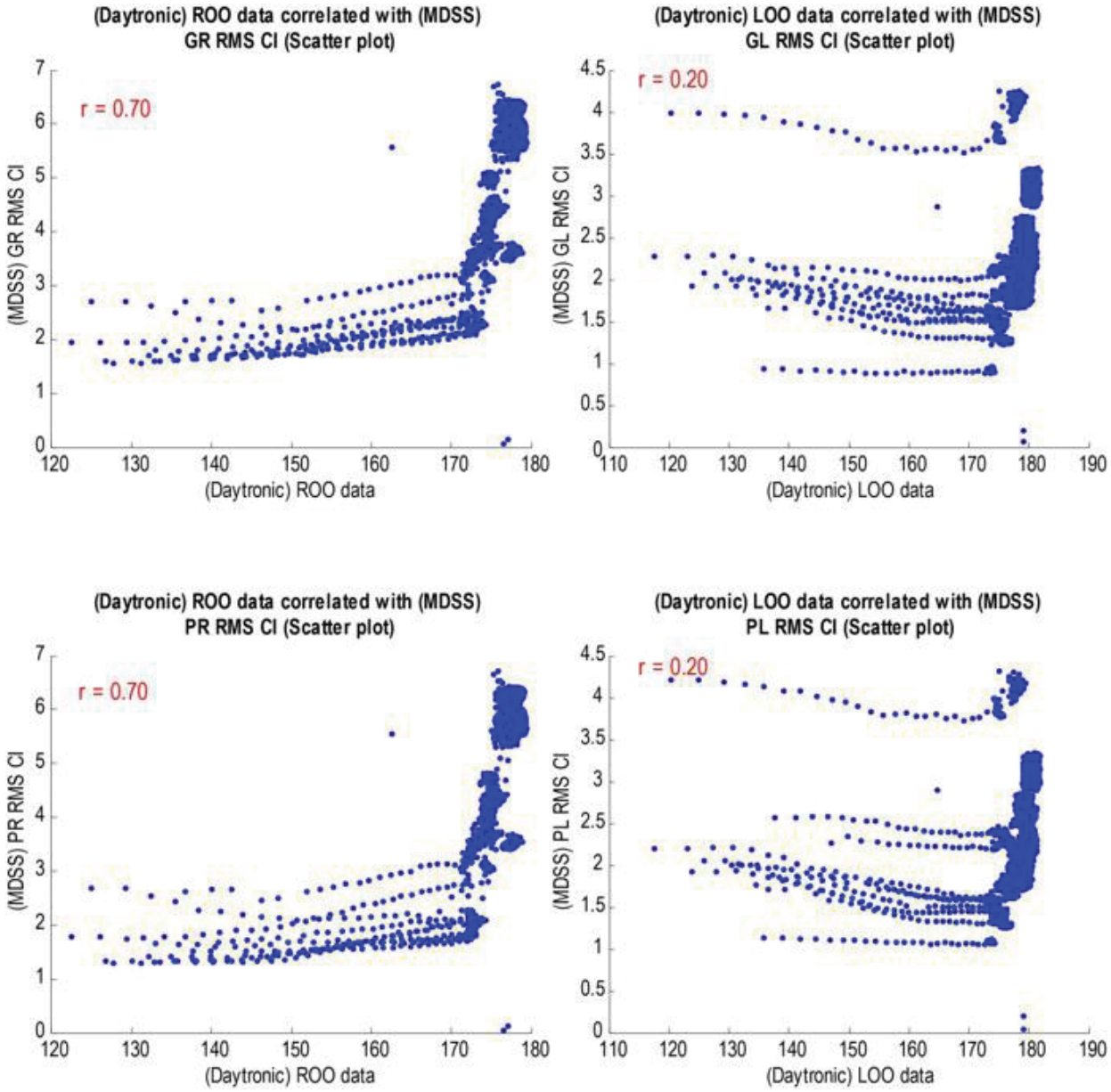

Figure E.4.5.—Compare Test L35355050 Outlet Oil Temperatures to RMS.

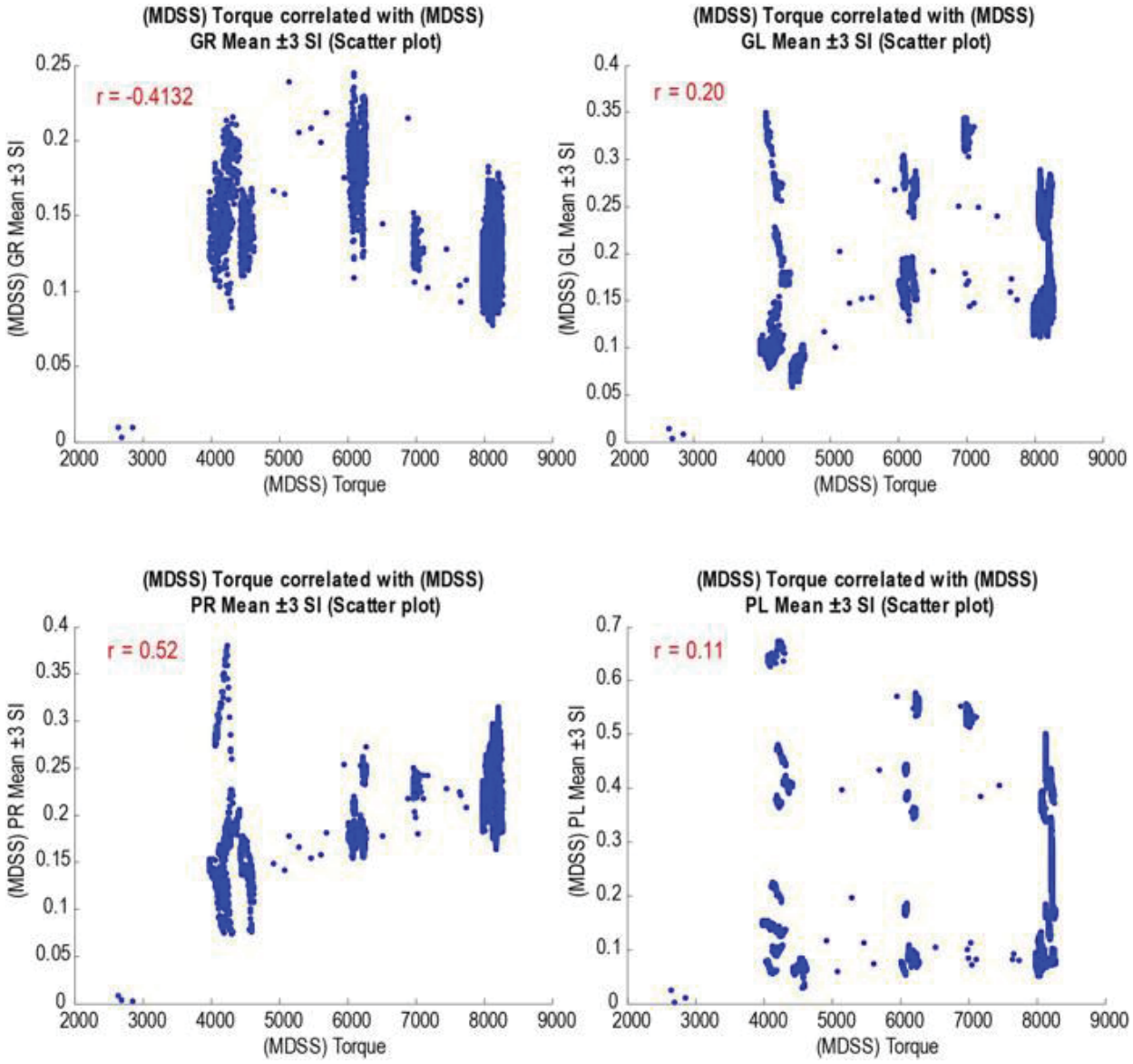

Figure E.4.6.—Compare Test L35355050 MDSS SI3 to Torque.

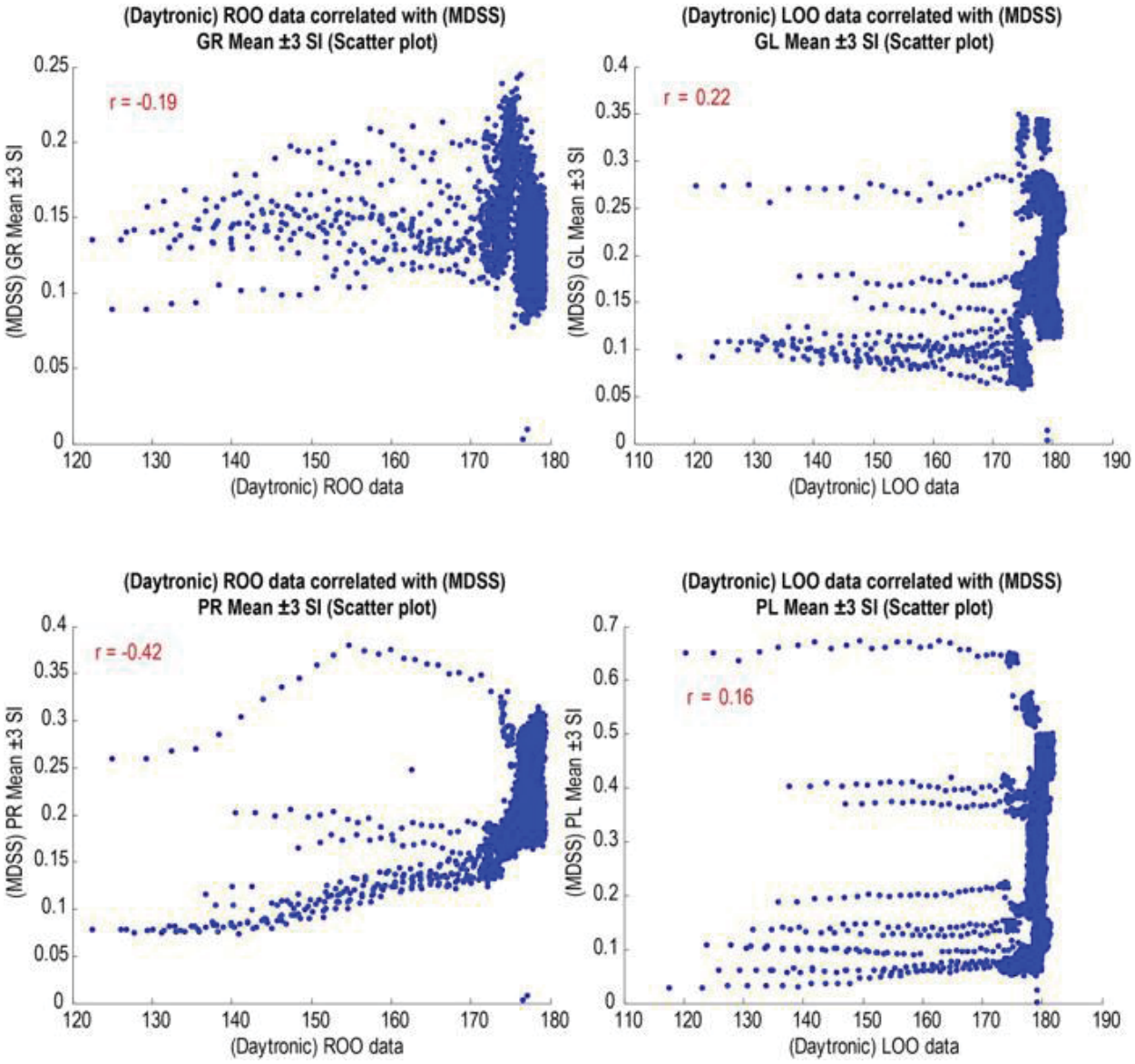

Figure E.4.7.—Compare Test L35355050 Outlet Oil Temperatures to SI3.

E.5 L1818R1616

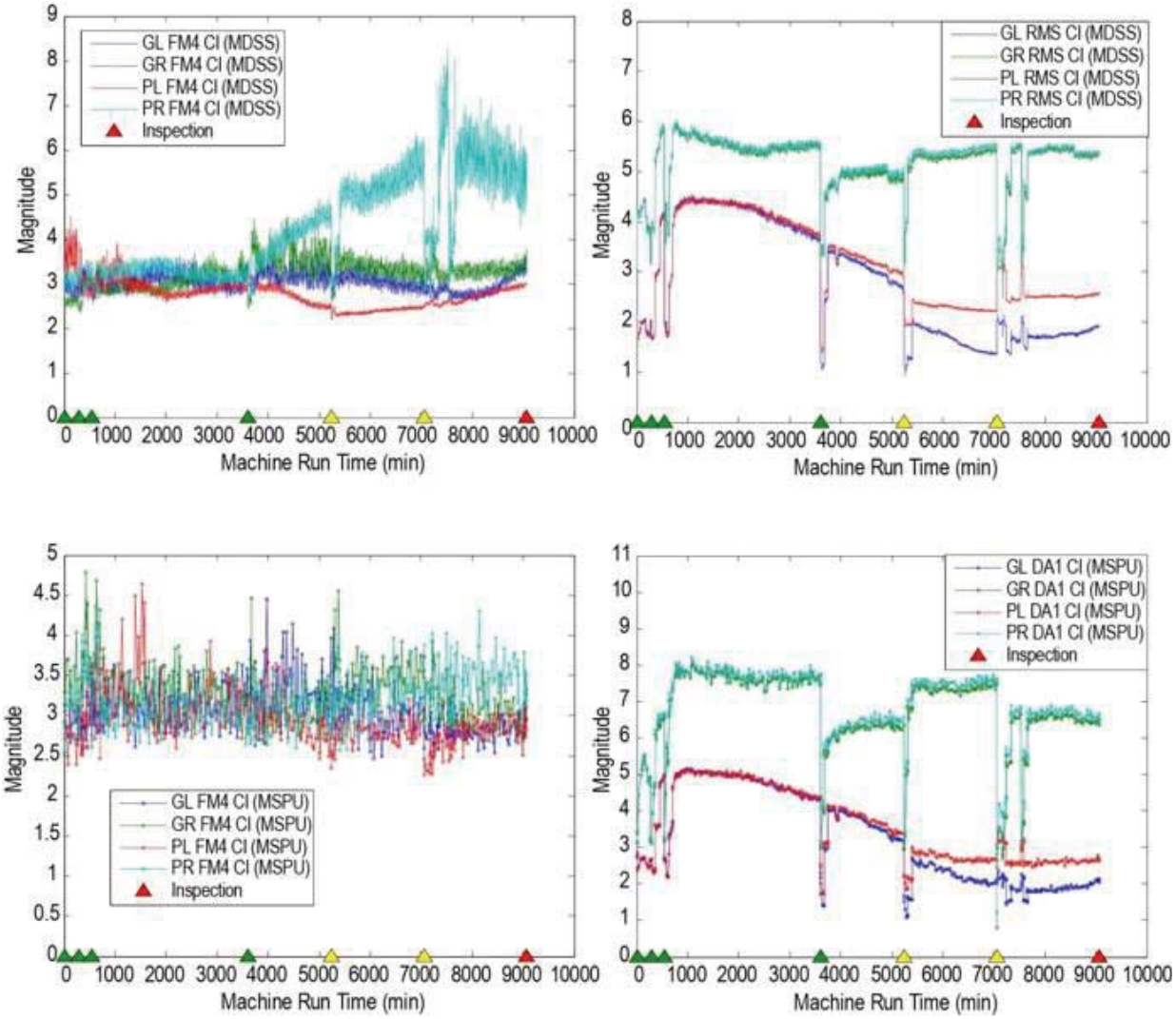

Figure E.5.1.—Compare Test L1818R1616 FM4 and RMS/DA1 for MDSS and MSPU.

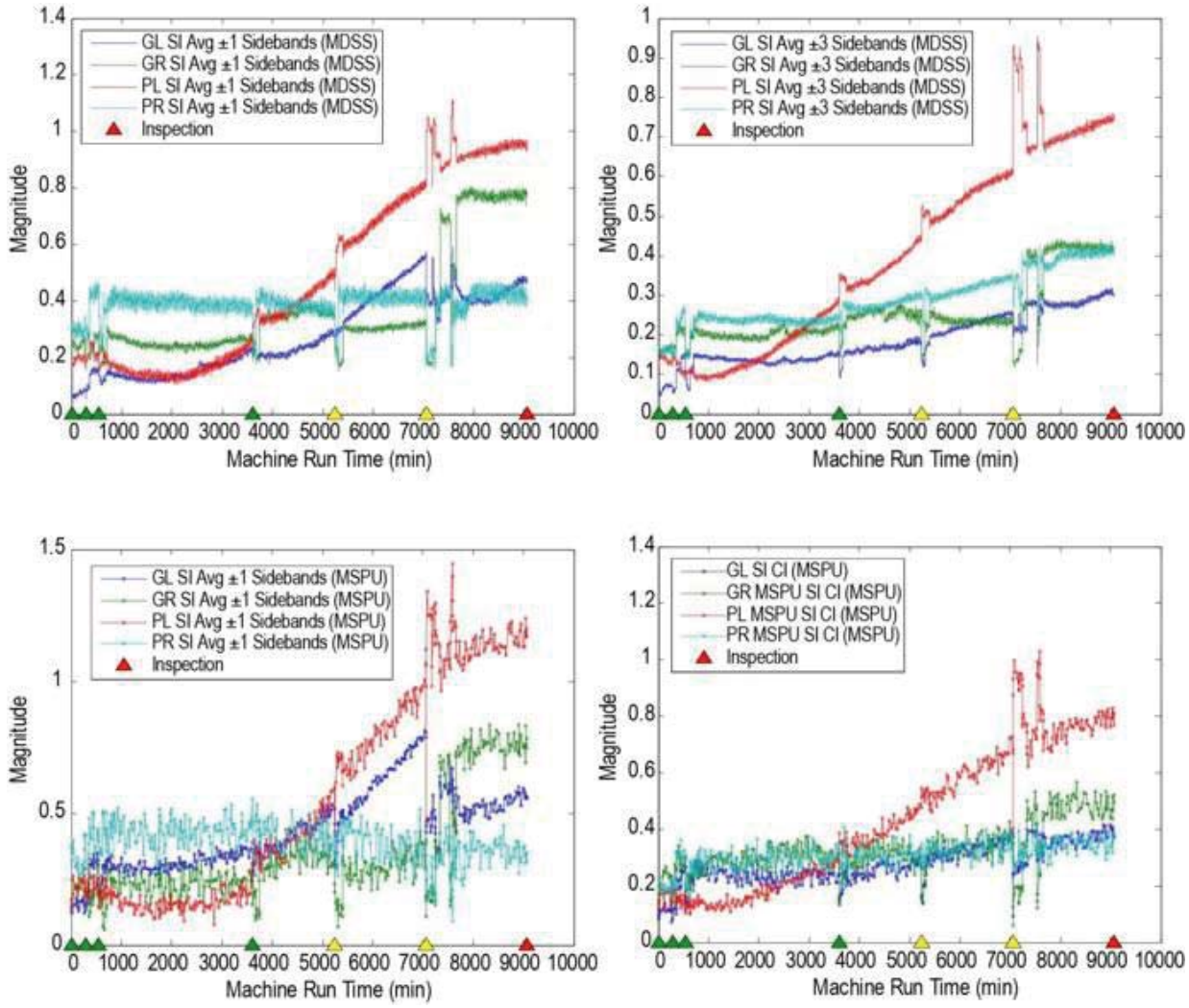

Figure E.5.2.—Compare Test L1818R1616 SI1and SI3 for MDSS and MSPU.

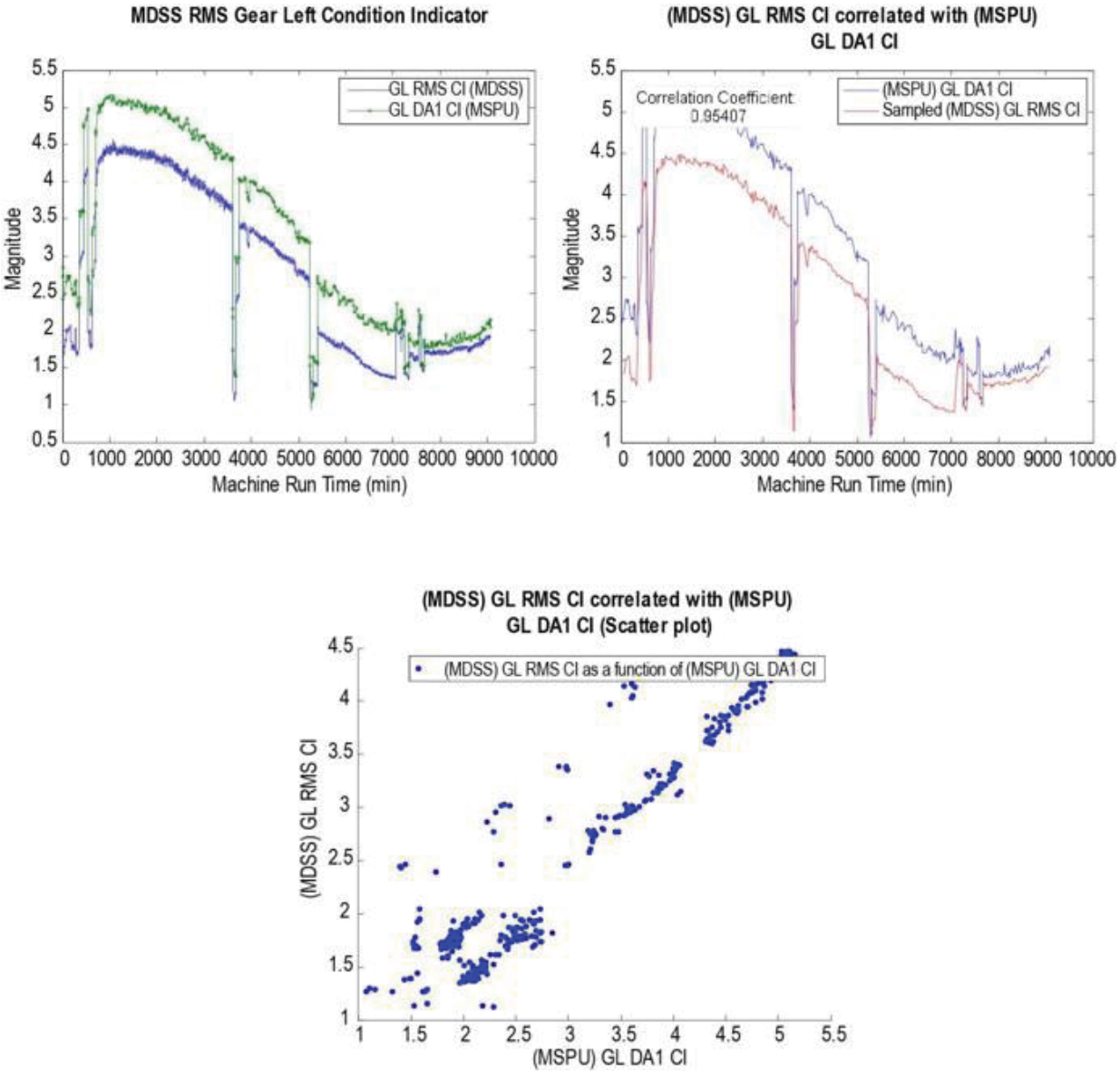

Figure E.5.3.—Compare Test L1818R1616 GL RMS/DA1 Nearest Time Correlation Methods.

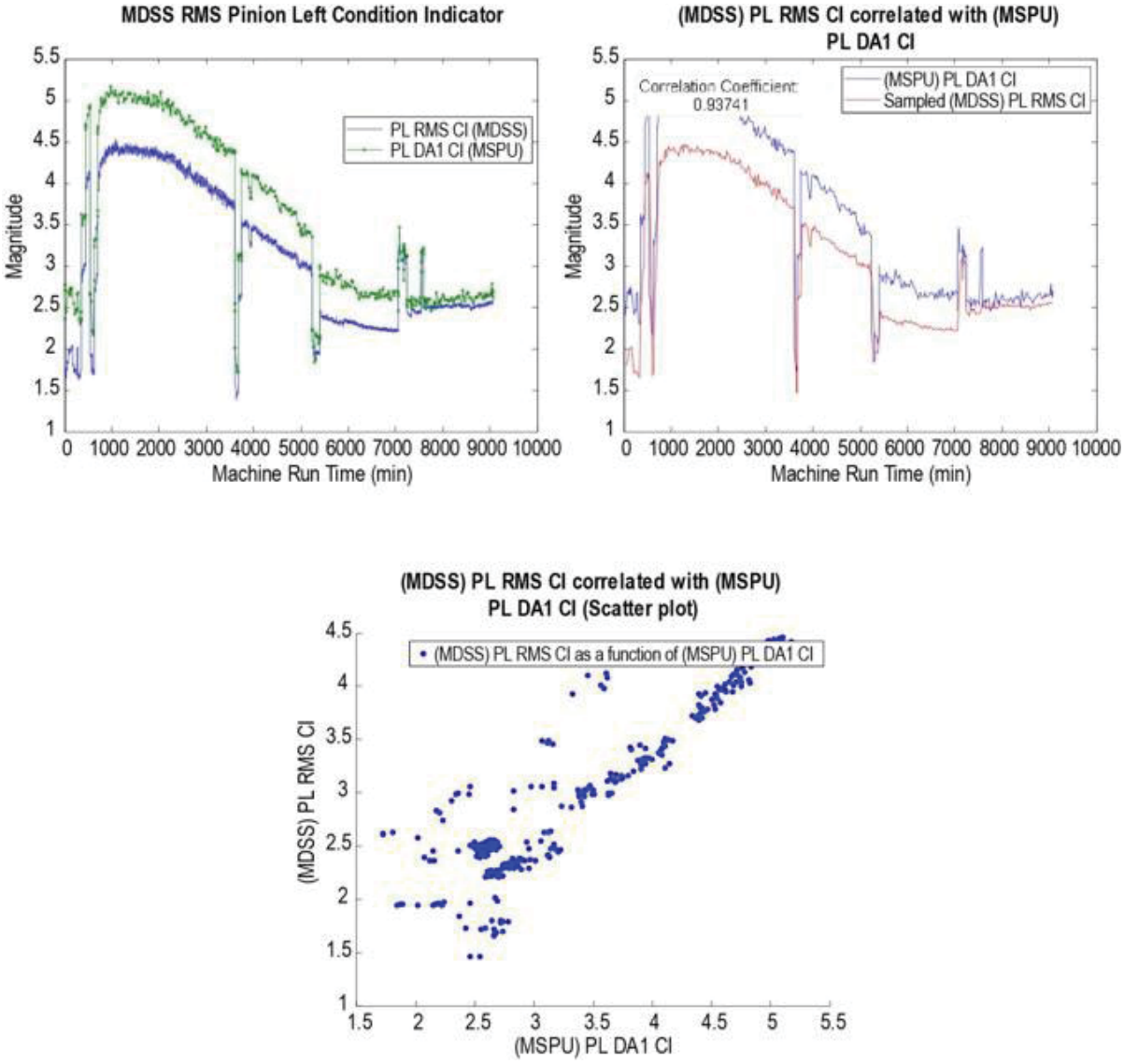

Figure E.5.4.—Compare Test L1818R1616 PL RMS/DA1 Nearest Time Correlation Methods.

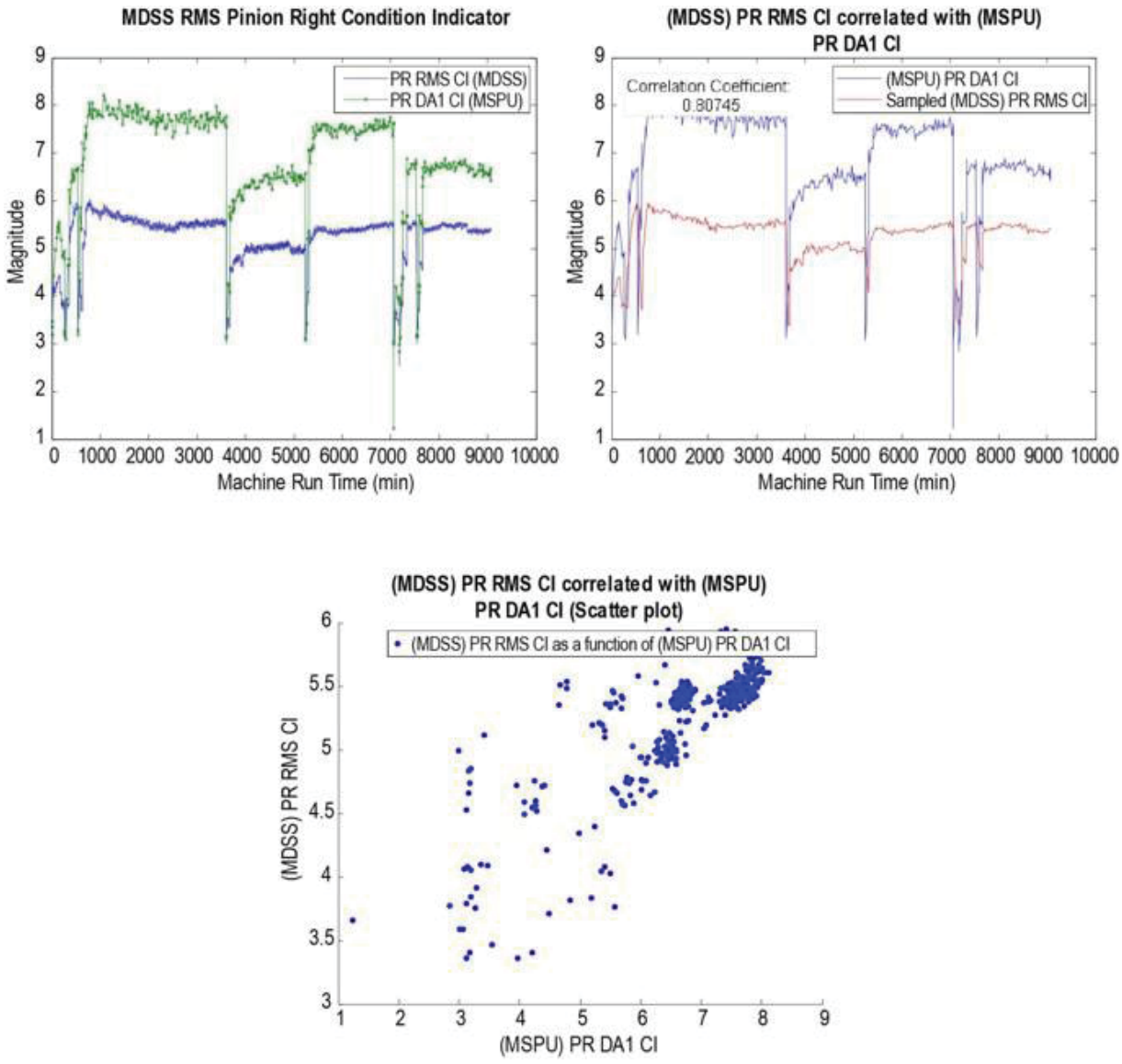

Figure E.5.5.—Compare Test L1818R1616 PR RMS/DA1 Nearest Time Correlation Methods.

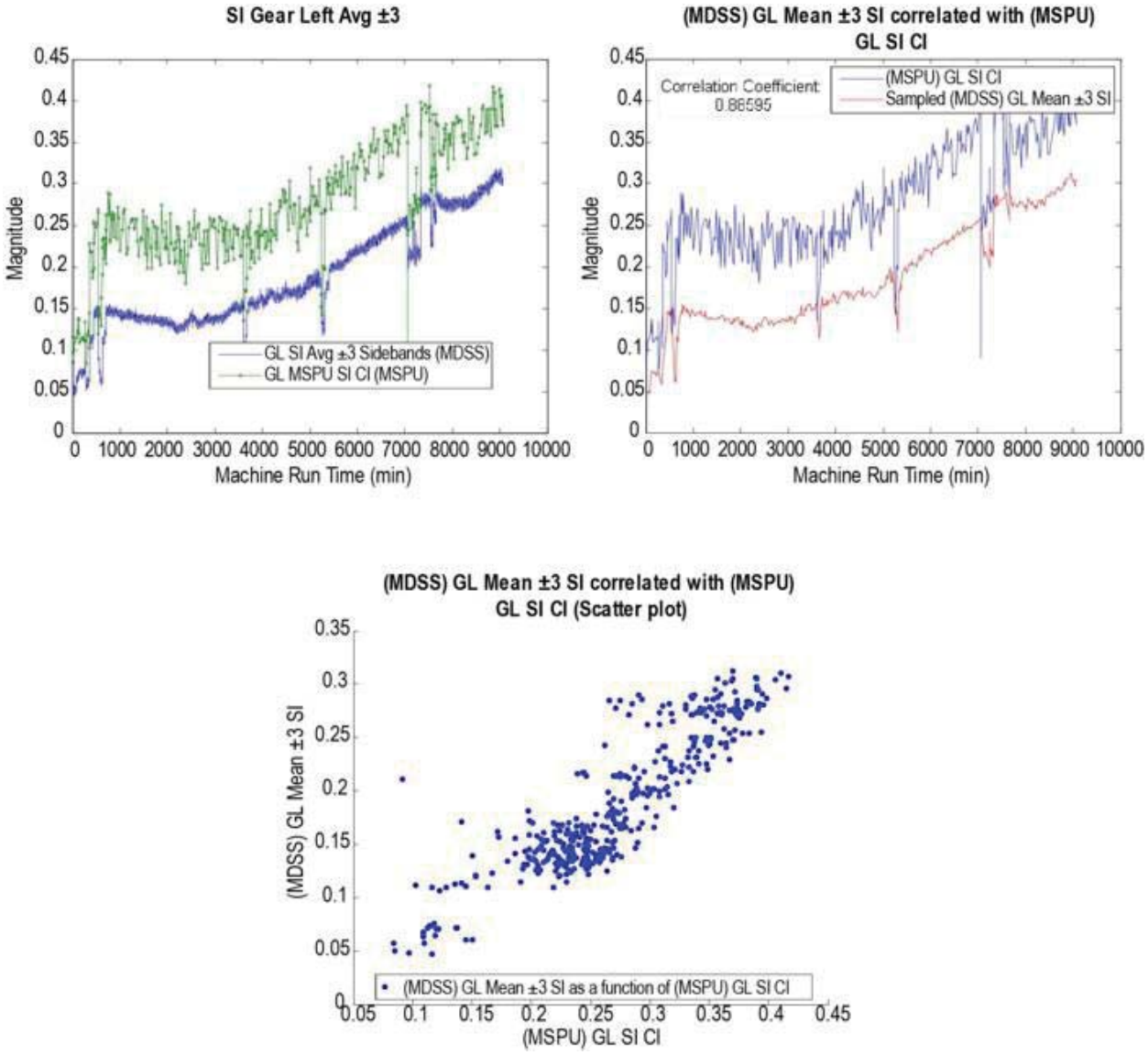

Figure E.5.6.—Compare Test L1818R1616 GL SI3 and SI Nearest Time Correlation Methods.

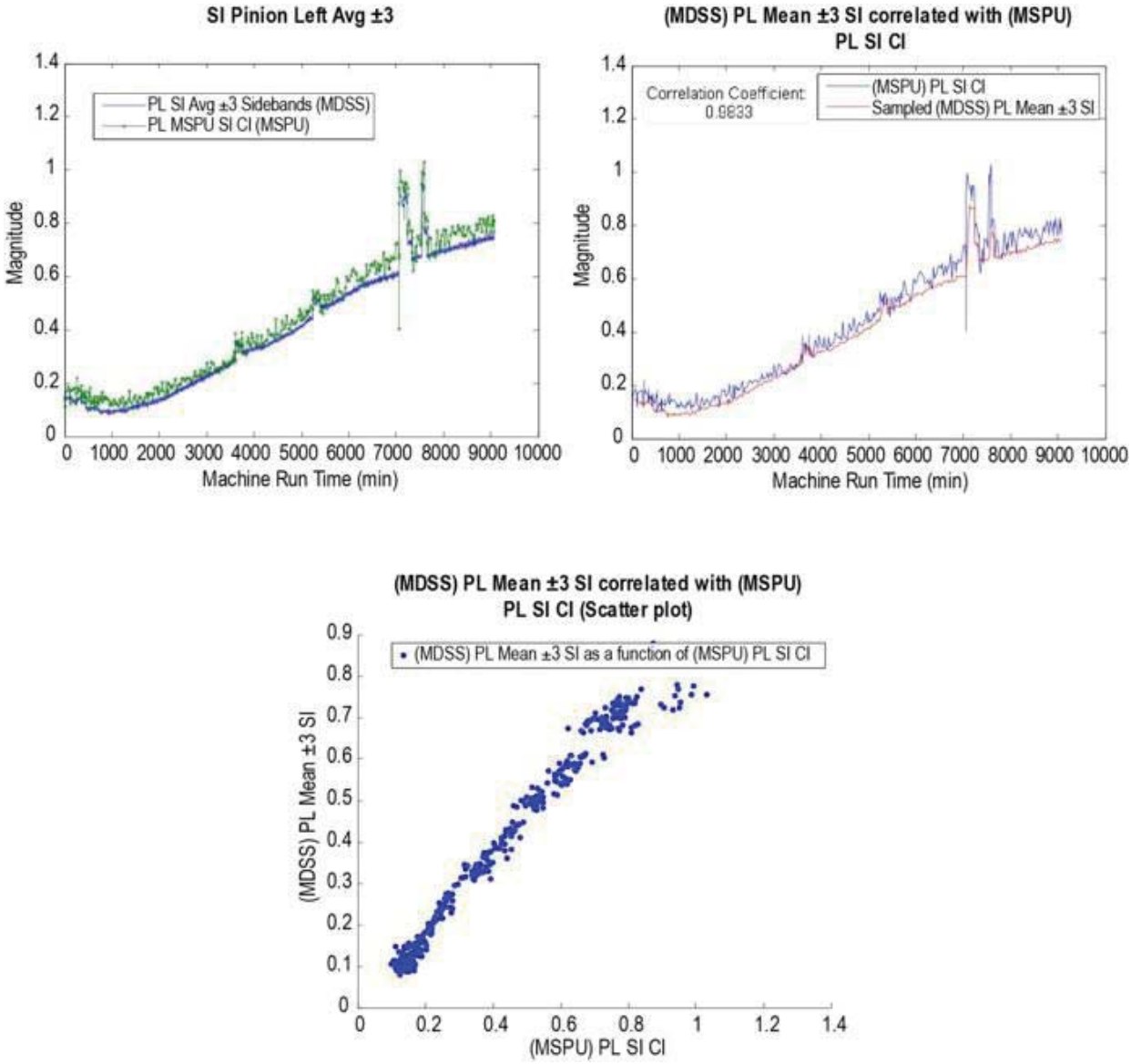

Figure E.5.7.—Compare Test L1818R1616 PL SI3 and SI Nearest Time Correlation Methods.

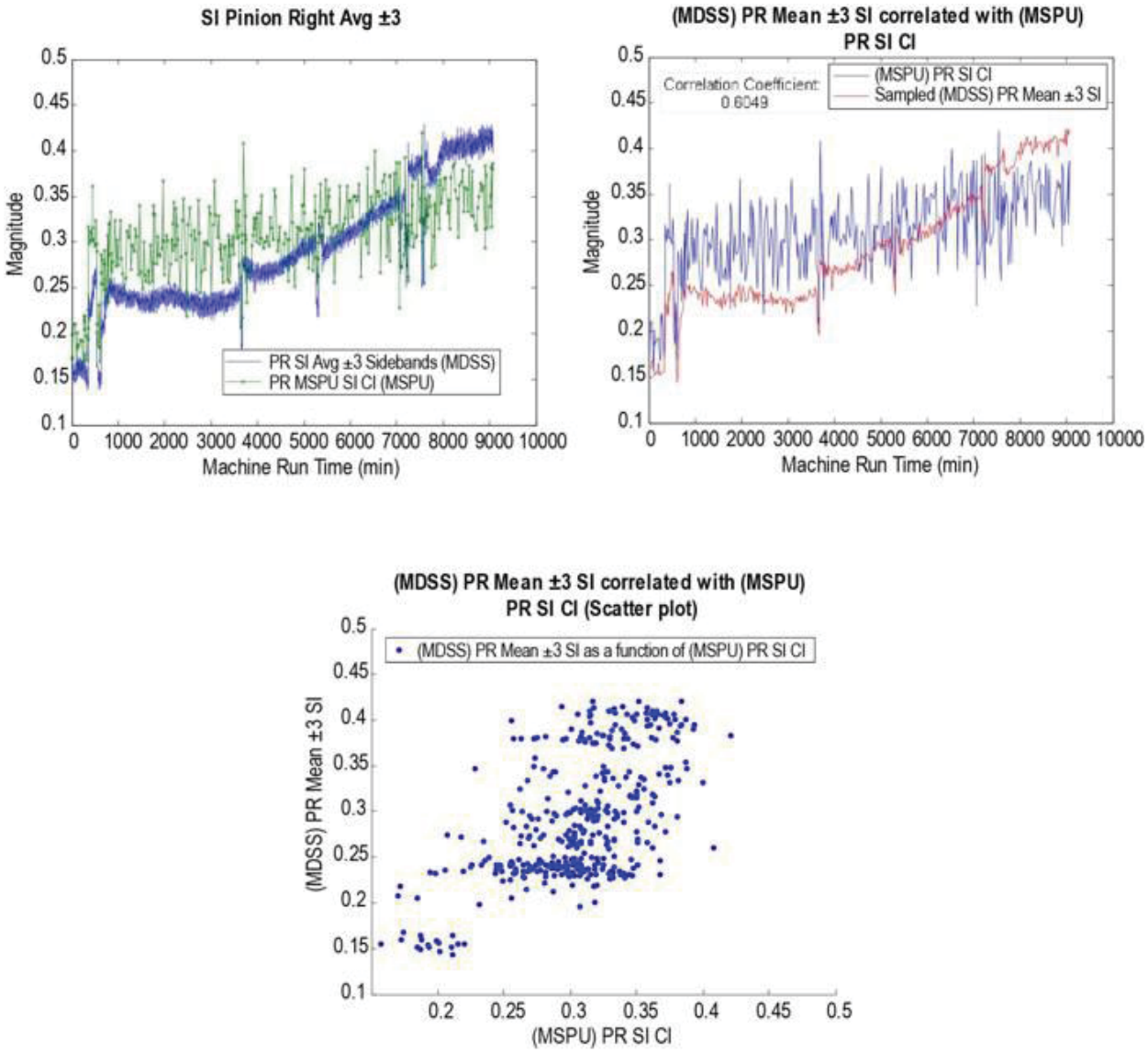

Figure E.5.8.—Compare Test L1818R1616 PR SI3 and SI Nearest Time Correlation Methods.

E.6 L3737R2424

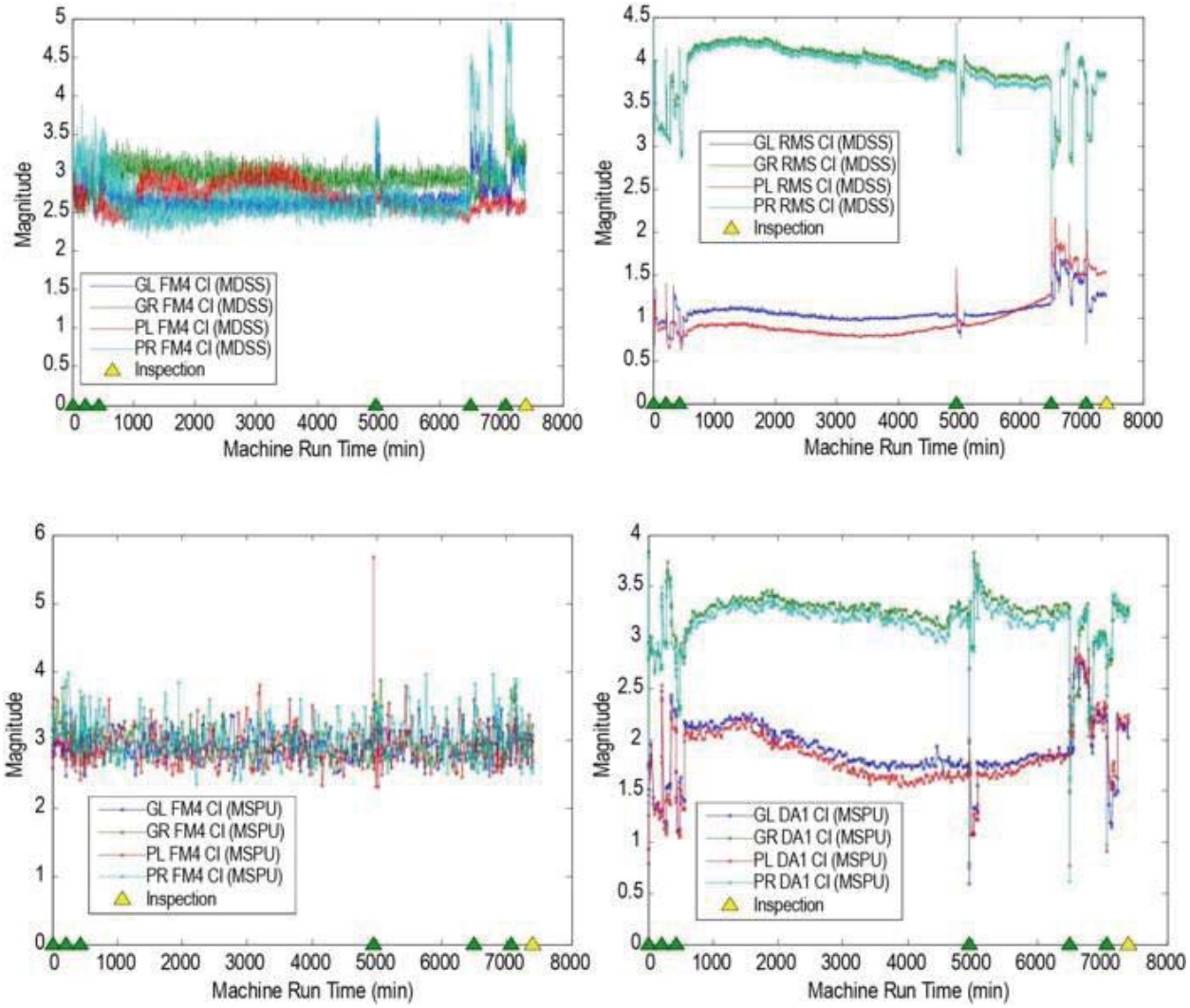

Figure E.6.1.—Compare Test L3737R2424 FM4 and RMS/DA1 for MDSS and MSPU.

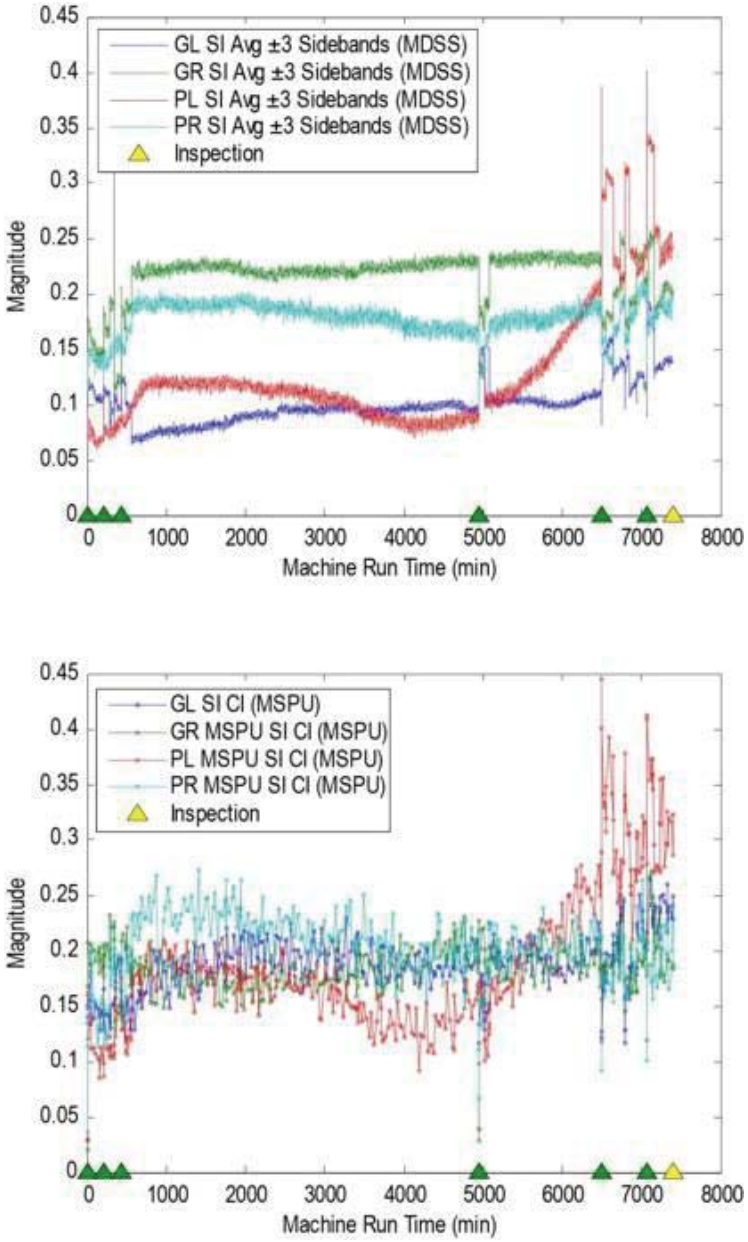

Figure E.6.2.—Compare Test L3737R2424 SI3 for MDSS and MSPU.

E.7 L3737R5036

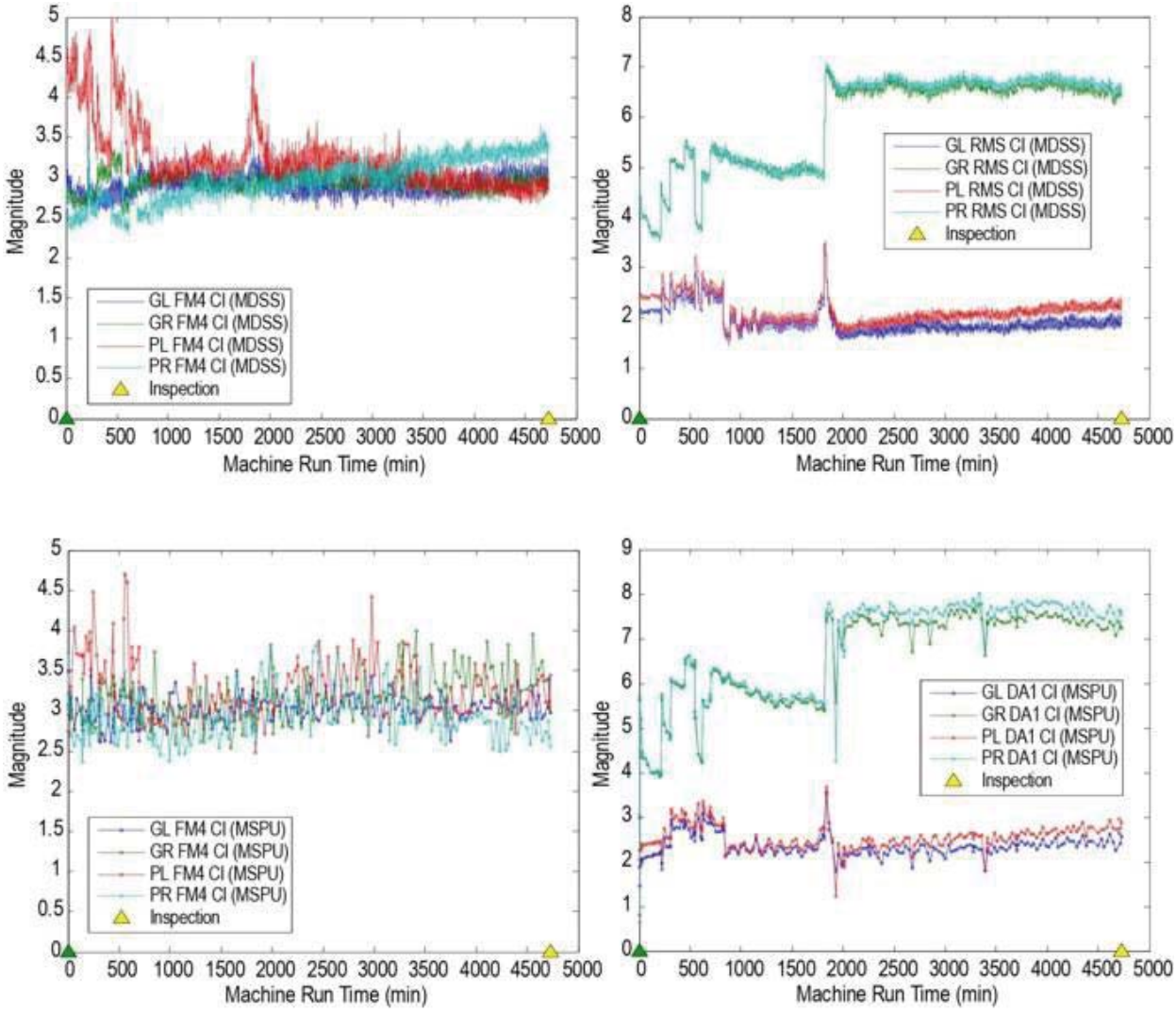

Figure E.7.1.—Compare Test L3737R5036 FM4 and RMS/DA1 for MDSS and MSPU.

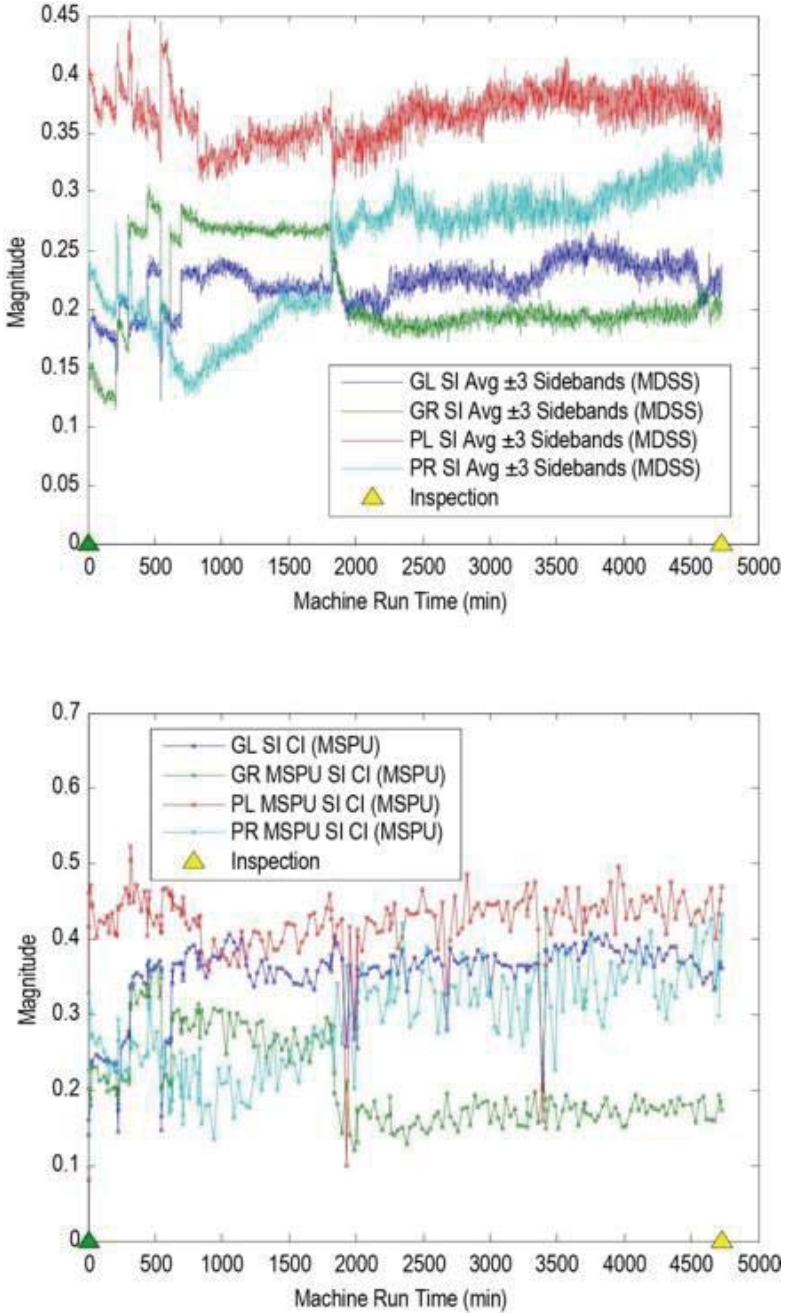

Figure E.7.2.—Compare Test L3737R5036 SI3 for MDSS and MSPU.

References

1. Federal Aviation Administration Advisory Circular (AC) 29–2C, Section MG–15, Airworthiness Approval of RC (HUMS) per Code of Federal Regulations, Title 14-Aeronautics and Space, Chapter I-Federal Aviation Administration, Department of Transportation, Part 29-Airworthiness Standards: Transport Category Rotorcraft.
2. Antolick, L., Wade, D.R. and Brower, N.G.: Application of Advanced Vibration Techniques for Enhancing Bearing Diagnostics on a HUMS-Equipped Fleet. Presented at the American Helicopter Society CBM Specialists Conference, Huntsville, AL, February 11-13, 2013.
3. Civil Aviation Authority: CAP 753, "Helicopter Vibration Health Monitoring (VHM) Guidance Material for Operators Utilizing VHM in Rotor and Rotor Drive Systems of Helicopters," First Edition June 2006. First Edition incorporating amendment 2012/01, August 2012.
4. Delgado, I., Dempsey, P., Antolick, L. and Wade, D.: Continued Evaluation of Gear Condition Indicator Performance on Rotorcraft Fleet. Airworthiness, CBM, and HUMS Specialists' Meeting, February 11-13, 2013, Huntsville, AL.
5. Antolick, L., Branning, J., Dempsey, P. and Wade, D.: Evaluation of Gear Condition Indicator Performance on Rotorcraft Fleet, American Helicopter Society International 66th Annual Forum 2010, Phoenix, AZ, May 11-13, 2010.
6. Dempsey, P.J. and Brandon, E.B.: Validation of Helicopter Gear Condition Indicators Using Seeded Fault Tests. MFPT 2013 Conference, May 13-17, 2013, Cleveland, OH, NASA/TM—2013-217872.
7. Handschuh, R.F.: Thermal Behavior of Spiral Bevel Gears. NASA TM-106518, 1995.
8. Handschuh, R.F.: Testing of Face-Milled Spiral Bevel Gears at High-Speed and Load. NASA/TM—2001-210743, 2001.
9. Dempsey, P., Tuck, R. and Showalter, S.: Comparison of an inductance in-line oil debris sensor and magnetic plug oil debris sensor. AHS International 68th Annual Forum & Technology Display, Fort Worth, TX, May 1-3, 2012.
10. Isom, J. and Dempsey, P.: Performance Evaluation of a Second-Order Indicator of Cyclostationarity for Gear Condition Monitoring. MFPT 2013 Conference, Cleveland, OH, May 13-17, 2013.
11. Siegel, D., Lee, J. and Dempsey, P.: Investigation and Evaluation of Condition Indicators, Variable Selection, and Health Indication Methods and Algorithms For Rotorcraft Gear Components. MFPT 2014 Conference, Virginia Beach, VA, May 20-22, 2014.
12. Chen, Y., Chaudhry, Z. and Dempsey, P.: A Novel Gear Condition Monitoring Method Based on Transient Impulse Response. AHS International 70th Annual Forum & Technology Display, Montréal, Québec, Canada, May 20-22, 2014.
13. Dempsey, P., Handschuh, R. and Delgado, I.: Integrating Condition Indicators and Usage Parameters for Improved Spiral Bevel Gear Health Monitoring. AHS International 69th Annual Forum & Technology Display, Phoenix, AZ, May 21-23, 2013.
14. Dempsey, P.: Investigation of Sideband Index Response on Gear Tooth Contact Fatigue Damage NASA Technical Memorandum NASA/TM—2013-216610, November 2013.
15. Dempsey, P., Islam, A., Feldman, J. and Larsen, C.: Investigation of Gearbox Vibration Transmission Paths on Gear Condition Indicator Performance. NASA TM—2013-216617, December 2013
16. Updated RTAPS Gear Design and Analysis Report. Report No.: L9WE-AR-001. NASA Glenn Task Order NNC10TA71T. The Boeing Company. June 20, 2012.
17. Updated FMECA and Load Rating to Fatigue Life Correlations for AH-64 Legacy and NASA Scaled Nose Gearbox Gears Report. Report No.: L9WE-AR-001. NASA Glenn Task Order NNC10TA71T. The Boeing Company. June 20, 2012.
18. ANSI/AGMA 1010-E95. Appearance of Gear Teeth – Terminology of Wear and Failure.
19. Dempsey, P.J., and Rickmeyer, T.: Processes and Considerations in Extension to Time Between Overhauls and Paths to On-Condition for U.S. Army Rotorcraft Propulsion Systems, American

Helicopter Society 67th Annual Forum and Technology Display, Virginia Beach, VA, May 2-5, 2011.
20. U.S. Army Research, Development & Engineering Command, “Aeronautical Design Standard Handbook for Condition Based Maintenance Systems for US Army Aircraft Systems,” ADS-79B-HDBK, March 7, 2013.
21. Stewart, R.M. 1977. Some useful data analysis techniques for gearbox diagnostics. Machine Health Monitoring Group, Institute of Sound and Vibration Research, University of Southampton, Report MHM/R/10/77, July 1977.
22. Zakrajsek, J.J. 1989. An investigation of gear mesh failure prediction techniques. NASA TM–102340, AVSCOM TM 89–C-005.
23. Zakrajsek, J.J., Handschuh, R.F., and Decker, H.J. 1994. Application of fault detection techniques to spiral bevel gear fatigue data. Proceedings of the 48th Meeting of the Mechanical Failures Prevention Group. Office of Naval Research, Arlington, VA, pp. 93–104.
24. Dempsey, P. J., Antolick, L. J., Branning, J. S., and Thomas, J. (2014). “Data Fusion Tool for Spiral Bevel Gear Condition Indicator Data,” MFPT 2014 Conference, Virginia Beach, VA, May 20-22, 2014.
25. Triola, Mario. Elementary Statistics. 6th edition. Addison-Wesley 1995.
26. Townsend, Dennis P. Dudley’s Gear Handbook. 2nd edition. McGraw-Hill, New York, NY 1991.
27. Wiig, J., and Picard, D. (2006). Optimization of fault diagnosis in helicopter health and usage monitoring systems. S.l.: [s.n.].
28. Drago, R.J., Cunningham, R.J. and Cymbala, S.: The Anatomy of a Micropitting-Induced Tooth Fracture Failure— Its Causation, Initiation, Progression and Prevention. http://www.geartechnology.com/issues/0610x/drago.pdf. Accessed August 8, 2014.